Naval Research Laboratory

Washington, DC 20375-5320

NRL/MR/6180--20-10,145

Environmentally-Friendly Surfactants for Foams with Low Fuel Permeability Needed for Effective Pool Fire Suppression

Ramagopal Ananth
Katherine M. Hinnant
Spencer L. Giles
John P. Farley

Naval Technology Center for Safety and Survivability Branch
Chemistry Division

Arthur W. Snow

Volunteer Emeritus
Chemistry Division

October 5, 2020

REPORT DOCUMENTATION PAGE

Form Approved
OMB No. 0704-0188

1. REPORT DATE *(DD-MM-YYYY)*	**2. REPORT TYPE**	**3. DATES COVERED** *(From - To)*
05-10-2020	NRL Memorandum Report	09-031-2017 – 09-30-2020

4. TITLE AND SUBTITLE

Environmentally-Friendly Surfactants for Foams with Low Fuel Permeability Needed for Effective Pool Fire Suppression

5a. CONTRACT NUMBER

5b. GRANT NUMBER

5c. PROGRAM ELEMENT NUMBER

6. AUTHOR(S)

Ramagopal Ananth, Katherine M. Hinnant, Spencer L. Giles, Arthur W. Snow*, and John P. Farley

5d. PROJECT NUMBER

5e. TASK NUMBER

5f. WORK UNIT NUMBER
6A70/1P02

7. PERFORMING ORGANIZATION NAME(S) AND ADDRESS(ES)

Naval Research Laboratory
4555 Overlook Avenue, SW
Washington, DC 20375-5320

8. PERFORMING ORGANIZATION REPORT NUMBER

NRL/MR/6180--20-10,145

9. SPONSORING / MONITORING AGENCY NAME(S) AND ADDRESS(ES)

Office of Naval Research
One Liberty Center
875 N. Randolph Street, Suite 1425
Arlington, VA 22203-1995

10. SPONSOR / MONITOR'S ACRONYM(S)

ONR

11. SPONSOR / MONITOR'S REPORT NUMBER(S)

12. DISTRIBUTION / AVAILABILITY STATEMENT

DISTRIBUTION STATEMENT A: Approved for public release; distribution is unlimited.

13. SUPPLEMENTARY NOTES

*Volunteer Emeritus

14. ABSTRACT

We conducted bench scale experiments, computational modeling, large scale testing, and collaboration with industry to develop fluorine-free aqueous foam for effective pool fire suppression to replace Aqueous Film Forming Foam (AFFF). We invented a siloxane formulation containing commercial trisiloxanepolyoxyetylene and alkylpolyglycoside (APG) that suppressed heptane fire effectively (60% of AFFF) due to synergistic effects reducing foam degradation by heptane. However, the siloxane is less effective on gasoline fire due to its extraction by the fuel. By performing surfactant synthesis, we varied the oxyethylene size and head and tail sizes of the APG; competition between increased synergism and decreased amphiphilicity might have limited the improvements in foam stability. An understanding of the synergistic mechanisms and a more efficient design of surfactant structures are needed to improve fire suppression involving different fuels.

15. SUBJECT TERMS

Pool fire, Aqueous foam, Siloxane surfactant, Glycoside surfactant, Fire extinction

16. SECURITY CLASSIFICATION OF:			**17. LIMITATION OF ABSTRACT**	**18. NUMBER OF PAGES**	**19a. NAME OF RESPONSIBLE PERSON**
a. REPORT	**b. ABSTRACT**	**c. THIS PAGE**			Ramagopal Ananth
Unclassified Unlimited	Unclassified Unlimited	Unclassified Unlimited	Unclassified Unlimited	145	**19b. TELEPHONE NUMBER** *(include area code)* (202) 767-3197

Standard Form 298 (Rev. 8-98)
Prescribed by ANSI Std. Z39.18

This page intentionally left blank.

CONTENTS

This page intentionally left blank.

EXECUTIVE SUMMARY

AFFF must be replaced due to environmental and human health concerns. But, a fluorine-free foam replacement must maintain AFFF‘s fire suppression performance essential for the DOD applications. We developed a new approach that focused on fuel transport through a foam layer and foam degradation by fuel as targets to design novel fluorine-free surfactants to generate foams.

We conducted bench scale experiments, computational modeling, large scale testing, and collaboration with industry to develop fluorine-free aqueous foams. A custom formulation (ReferenceAFFF) containing fluorocarbon and alkylpolyglycoside (APG: Glucopon215 UP) surfactants, and a solvent in water was developed that had the same fire suppression performance as the commercial AFFF. New fluorine-free formulations replacing the fluorocarbon surfactant with a commercial siloxane or hydrocarbon surfactant were evaluated using bench scale methods. They confirmed our hypothesis that increased foam stability and decreased fuel vapor transport through a foam layer correlated with decreased fire extinction time, and identified a commercial trisiloxanepolyoxyethylene (Dowsil 502W) as a promising surfactant for a replacement foam.

Trisiloxanepolyoxyethylene and APG surfactants were found to interact synergistically, which increased foam stability and heptane pool fire suppression. Even though molecular dynamics (MD) simulations showed that the packing density at an interface is increased by the surfactant mixture, the mechanisms of synergism are not well understood. However, we increased the glycoside head size by using a different commercial APG (Glucopon 225DK) instead of the Glucopon215 UP that resulted in increased heptane fire suppression from 40 to 60% of RefAFFF. The siloxane foams were less effective on a gasoline fire due to the extraction of siloxane by the aromatic components of gasoline, and revealed new surfactant-fuel interactions that were absent in AFFFs. In fact, we reproduced the gasoline fire suppression using trimethylbenzene-heptane mixture, which is simple, well-defined, and non-seasonal unlike gasoline.

To increase the synergisms further, we synthesized twelve trisiloxane surfactants to vary the head size from 0 to 50 oxyethylene units. With the synthesized siloxanes replacing Dowsil 502W in the siloxane formulation containing Glucopon225DK, we showed that both the degree of heptane fire suppression and the fuel transport rate increased and then decreased as the head size was increased; maximum occurred around 10 to 12 oxyethylene units. Similarly, increasing the alkyl tail size of the APG with a fixed glycoside head size (2 units) or increasing the head size of the APG with a fixed alkyl tail size (8 carbons) exhibited maxima in fire suppression. The maximum in fire suppression appears to be due to increased synergism and decreased amphiphilicity as the size is increased. Also, synergisms may depend on controlling the polydispersity for proper geometrical fit between different size siloxane and APG molecules.

A basic understanding of synergism mechanisms is needed to develop new surfactant designs with higher synergism and amphiphilicity. Current modeling tools are not suited for designing surfactants because they cannot predict fire suppression from surfactant structures. Surfactant synthesis/experimentation are too slow to explore a large and diverse number of surfactant. Future works should develop new modeling approaches to design surfactants and use synthesis/experimentation more efficiently to explore a range of surfactant structures.

This page intentionally left blank.

Environmentally-Friendly Surfactants for Foams with Low Fuel Permeability Needed for Effective Pool Fire Suppression

1. INTRODUCTION

Aqueous Film Forming Foams (AFFF) are used worldwide to fight pool fires in military and civilian applications including airports since their invention by the U.S. Naval Research Laboratory (NRL) in the 1960s [1]. They are considered the gold standard for pool fire suppression. The perflorosurfactants contained in AFFF are the key to the high fire suppression performance, which is critical to prevent weapons "cook-off" [2]. The chemical structure of a perfluorosurfactant is shown in Figure 1. Like any surfactant, it has a hydrophilic head and a hydrophobic tail. But, the tail is perfluorinated. The surfactant gets adsorbed at air water and fuel-water interfaces with the head and tail in water and organic or air phases respectively.

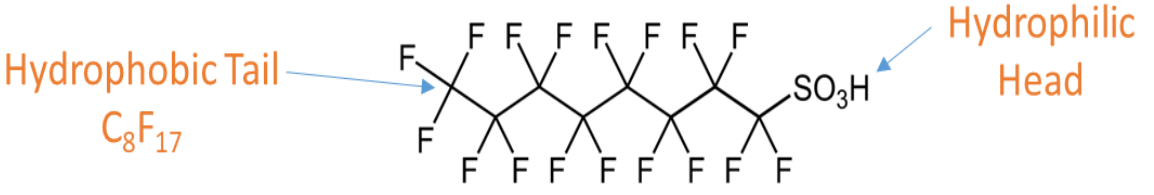

Figure 1. Chemical structure of perfluoro-octonylsulfonic acid

Perfluoro-octanyl based surfactants like the one displayed in Figure 1 were shown to be bio-accumulative, bio-persistent, and toxic [3] due to the extreme stability of the carbon-fluorine bonds in the tail of the chemical structure shown in Figure 1. 3M stopped manufacturing the perfluorooctynyl surfactants in 2002. The U.S. EPA restricted manufacturing the perfluorooctnyl surfactants in 2003. EPA also conducted a voluntary stewardship program with industry to phase out the perfluoroctnyl surfactant products by 2015. There have been media reports of contamination at military bases that resulted in litigation against the DOD and industry. Industry developed surfactants with a shorter tail polyfluoroalkyl surfactants to replace the perfluoro-octanyl using a telomere-based process. However, the long-term environmental fate and routes into the environment of the newly formulated fluorocarbon surfactants are poorly understood. Recently, U.S. Congress mandated that a fluorine-free alternative be available by October 1, 2023 and all use of perfluoro and polyfluoroalkyl substances (PFAS) be phased out by October 1 2024 from the DOD as detailed in the National Defense Authorization Act (NDAA) of 2020. Replacing the fluorocarbon surfactant with a fluorine-free surfactant in AFFF will significantly reduce its environmental impact.

Foam industry introduced fluorine-free firefighting foams that completely eliminate the fluorocarbon surfactants and PFAS from the solution and rely only on the hydrocarbon surfactants and other additives. However, existing commercial fluorine-free alternatives to AFFF are unable to meet the stringent gasoline fire extinction time and viscosity requirements listed in U.S. DOD's Mil-F-24385F [4]. The MilSpec includes 28 ft^2 gasoline pool fire extinction and burnback tests as

Manuscript approved October 1, 2020.

the gateway test before conducting a larger (50 ft^2) fire test. The MilSpec also includes limits on physical properties, such as the viscosity of 3% or 6% concentrates that are within the working limits of the proportioning systems used to generate foams. The U.S. MilSpec was developed based on small (50 ft^2 gasoline pool), large (1200 ft^2 gasoline pool), and field testing and has a proven record as a successful test for qualifying AFFFs for DOD firefighting needs over many decades. It is also one of the most stringent tests for firefighting requiring an extinction time of 30 seconds for a 28 ft^2 pool fire at a low solution application rate of 2 gallons per minute to ensure an adequate safety margin. The extinction time requirement is crucial for preventing weapons "cook-off" because of the presence of weapons on military sites and ships. Therefore, research and development of alternative and novel surfactants to replace the fluorocarbon surfactants in AFFF are crucial for improving the fire suppression performance to meet Mil-F-24385F requirements.

The first step in developing AFFF replacements is to understand the basic mechanisms involved in AFFF fire suppression and the role of surfactants in influencing those mechanisms. AFFF contains a number of components developed over many decades. Tuve et al. [1] developed "light water", which was made by mixing commercial agents (0.25 % L-1083 and 0.25% L-1162 of 3M Co. 1964, and 0.5 % ethylene oxide polymer by weight) with proprietary chemical composition. Tuve et al. [1, 5] demonstrated fire extinction on both bench (20 cm diameter pool) and large-scale (150 ft^2 pool) gasoline and jet fuel fires. It was a forerunner to a category of fire-suppression products known as AFFF formulations. Norman and Regina [6], R.A. Falk [7, 8] reduced the fluorine content of AFFF by adding hydrocarbon surfactants to "light water" in a series of large-scale tests in 1977. The AFFF formulation developed by R.A. Falk contained six components with well-defined composition and identities of molecular structures. Thus, "light water" was developed into modern AFFF by the foam industry by adding numerous proprietary components needed for full MIL-F-24385F qualification. They included fluorocarbon and hydrocarbon surfactants, and other components: organic solvents (viscosity control, storage stabilization at subzero or elevated temperatures); polymers (precipitated barrier formation on polar/alcohol fuels); salts (surfactant shielding); chelating agents (polyvalent ions sequestering); buffers; corrosion inhibitors; and biocides [9].

AFFF suppresses fires by forming a physical barrier between the pool and fire, blocking the fuel vapor transport from the pool surface to the combustion process. The fluorocarbon surfactants play a crucial role in blocking the fuel supply to the fire. The firefighting community believes that when AFFF is applied onto a burning fuel pool, excess perfluoro-surfactant solution drains from the foam and forms a thin "aqueous film" on the burning pool surface because the surface tension of the solution is smaller than the hot fuel pool. They presume the film spreads and forms a major barrier to fuel transport, and the foam itself is a means to form the film and protect the film from the fire. However, the evidence for aqueous film formation is limited to fuel pools at ambient conditions and a limited degree to hot fuel pools.

1.1. Aqueous Film formation

The criterion for film formation is based upon the spreading coefficient given by Harkins and Feldman [10] as

$$S = \gamma_f - (\gamma_s + \gamma_i) \ , \tag{1}$$

where γ_f, γ_s are the surface tensions of the fuel and surfactant solution respectively, γ_i is the interfacial tension between the surfactant solution and fuel, and S is the spreading coefficient. A

zero or negative value for the spreading coefficient indicates an inability to form the aqueous film. Investigators at the Naval Research Laboratory [11] demonstrated that fluorosurfactants reduce the surface tension of water far below the surface tension achieved with conventional hydrocarbon surfactants when a solvent was used to increase the solubility of fluorosurfactants in water. The spreading of the aqueous film was demonstrated on JP-4, JP-5, and gasoline fuel pool surfaces at room temperature and the film spreads due to the reduced surface tension, γ_s, in Eq. (1) [1, 5, 10]. Tuve [1, 5] demonstrated that the JP-4, JP-5, and gasoline pools (covered with the aqueous film) did not ignite when a small flame was held over the pool surface. However, Tuve [1] also showed that the aqueous film did not form on a n-heptane pool which has a smaller surface tension, γ_f, than jet fuels and gasoline, which resulted in a negative spreading coefficient for n-heptane [5].

Pabon and Copart [12], and Clark and Kleiner [13] added hydrocarbon surfactants to the fluorocarbon surfactants to decrease both the surface and interfacial tensions (γ_s, γ_i) in Eq. (1), leading to a higher value of the spreading coefficient on a heptane pool. The higher spreading coefficient for the mixture of surfactants was suggested to result in more rapid film formation relative to fluorocarbon and hydrocarbon surfactants individually [12, 13, 14]. Kissa [15] showed that a mixture of fluorocarbon and hydrocarbon surfactants reduced water surface tension more rapidly with time compared to the surfactants individually. Williams [16] measured dynamic surface tension using a bubble tensiometer with bubbles generated at varying frequencies for commercial fluorocarbon (FORAFAC 1157, DuPont Inc. DE) and hydrocarbon (Triton X100, Dow Chemical Co.) surfactants individually and in a 3:1 mixture by volume. Williams showed that the mixture of fluoro and hydrocarbon surfactants (0.3% FORAFAC 1157, 0.1% Triton X100, 0.5% Butyl Carbitol solvent) had a significantly smaller surface tension (28 mN/m) than the individual surfactant solutions (72 mN/m for 0.3% FORAFAC 1157 and 45 mN/m for 0.1% Triton X100) at a bubble age of 30 ms. The mixture approached the equilibrium surface tension value of the fluorocarbon surfactant solution but at a faster rate. Williams also showed that the spreading coefficient for the mixture was positive (0.8 mN/m) on heptane fuel but negative for the individual surfactants (-1.0 for 0.3% FORAFAC 1157 and -15 for 0.1% Triton X100). The data indicated a lack of film formation on heptane fuel when only FORAFAC was used with the solvent. Williams's data show clearly that hydrocarbon surfactant and fuel type affect aqueous film formation at room temperature. Because commercial AFFFs contain both fluorocarbon and hydrocarbon surfactants, they have a positive spreading coefficient over heptane due to the lower interfacial tension, indicating film formation at room temperature, unlike "light water" which contained fluorocarbon surfactants only. Thus, film formation is considered necessary for rapid fire suppression, so much so that a spreading coefficient of more than 3 mN/m and a "film and seal" test are requirements for military qualification of firefighting foams [4]. To date, a significant emphasis has been placed on film formation and replacement surfactants are screened based on their film forming ability [17, 18]. However, the spreading coefficient is not an indicator of how the foam layer itself may be acting to rapidly suppress a fire. Additionally, past research by Briggs et al. [19] showed that despite a higher spreading coefficient for AFFF over toluene compared to heptane, the toluene flames were more difficult to extinguish with AFFF.

Bernett et al. [20], Moran et al. [21] and Leonard et al. [22] studied the dynamics of aqueous film formation on liquid fuel pools at room temperature by estimating average thickness of the film and measuring the fuel vapor concentration above the film in the absence of a foam and fire. They demonstrated the thinner the film floats longer on a fuel pool by placing the foam solution on an n-octane fuel pool (5 cm diameter) surface. The fuel vapor concentration above the film

was measured in a closed chamber by sweeping the vapors with nitrogen flow and analyzing with gas chromatography. The vapor concentration above the film was suppressed by a maximum of 20 times relative to the vapor pressure on bare fuel pool for films greater than 10 µm thick for 10s of minutes. The concentration was suppressed by 1.7 times for a 7.1 µm thick film for several minutes. Above a critical film thickness of 10 µm, the vapor concentration was not significantly suppressed further but appears to increase the length of time the vapors are suppressed. The critical film thickness was found to increase with increased vapor pressure of the fuels from dodecane to heptane. Thicker than 47 µm films led to breaking and sinking of the films to the bottom of the pool immediately. The foam layer can also suppress the fuel vapors because the vast number of bubble lamellae in the foam can be vapor barriers as illustrated in Figure 2. Studies comparing the relative contributions of the foam and "aqueous film" as barriers to fuel transport through AFFF have been lacking.

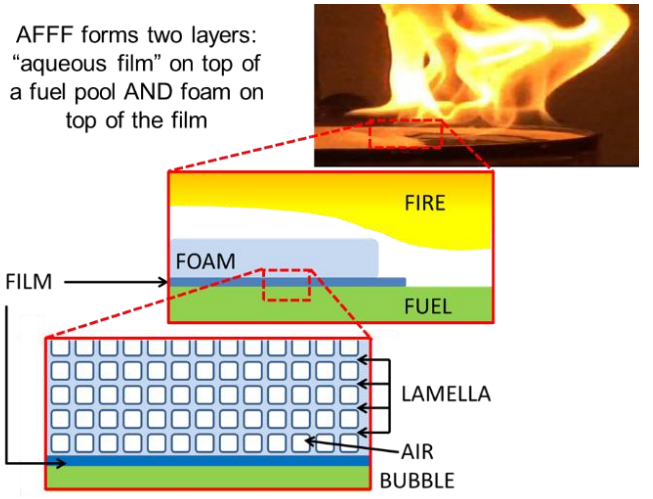

Figure 2. (Top) Fire extinction with foam on liquid heptane, (Middle) "Film" formation with AFFF, (Bottom) many lamellae in foam as fuel diffusion barriers in addition to a "film".

1.2. Foam Dynamics and NRL's Previous Research

The firefighting community developed a flux chamber to characterize a foam's ability to suppress fuel vapors by determining the rate of fuel transport through a specified thickness of foam covering a liquid pool surface over a long time period (steady-state), without the presence of a fire, at ambient, non-combusting, conditions [23-28]. Schaefer et al. [27, 28], relying on previous designs [23-26], designed a flux chamber to compare the performance of fluorinated and fluorine-free foams, which were generated using a food blender. Schaefer et al.'s results revealed that fluorinated foams had a much smaller fuel flux than fluorine-free foams. They attributed this superior performance of fluorinated foams to both the transport resistance of liquid lamellae (bubble wall) separating adjacent bubbles and to the presence of an "aqueous film" [27].

We designed a flux chamber and an experimental method [29] which was an improvement over previous flux chamber designs in its ability to create a uniform foam layer for studying the transient fuel transport characteristics of the foams rather than the steady state flux because foams degraded with time. Figure 3 compares the percent suppression in the concentration of fuel vapor emerging from a pool covered with only the "aqueous film" as reported by Leonard et al. [22]

versus a foam-covered-pool relative to the bare fuel corresponding to 100% on the y-axis (logarithmic scale). The top part of the Figure 3 shows the data collected for the film of different thicknesses [22] and bottom part of the Figure 3 shows our data for the 4-cm thick AFFF foam with the film. It shows that the foam suppresses fuel diffusion by orders of magnitude more than the film despite higher vapor pressure of heptane versus n-octane used by Leonard et al. Figure 3 shows that the vast number of bubble lamellae in a 4-cm thick foam layer are a significant barrier for fuel vapor permeation through the foam layer compared to a single aqueous film covering the pool which could only suppress the fuel vapor pressure by a maximum of 20 times (5%).

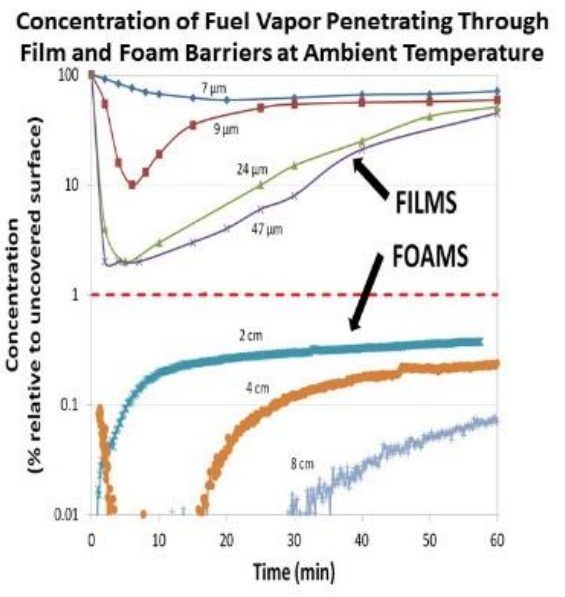

Figure 3. Fuel (% of vapor pressure) above the surface of an "aqueous film"-covered-n-octane fuel (without foam) [21, 22] and above foam-covered-n-heptane fuel, for the indicated film or foam thickness versus time. Even though the n-heptane pool has a higher vapor pressure (5.33 kPa) than the n-octane (1.47 kPa) pool, the foam exhibits orders of magnitude greater suppression compared to film only.

We also quantified fuel flux for AFFF over three fuels: n-heptane, methyl-cyclohexane, and iso-octane [29]. AFFF solution was shown not to form a film on iso-octane unlike n-heptane and methyl-cyclohexane. These three fuels have similar vapor pressures, but differ in surface tension and solubility in water. Figure 4 shows the fuel flux through 4 cm thick foam layers of AFFF and RF6 (a commercial fluorine-free foam, Solberg Inc.) placed on n-heptane liquid pool at 20°C. The fuel flux is much smaller than that (7.5 e-08 mole/cm^{2}s) reported for an uncovered pool. When the foam layer is applied on top of the pool, the fuel concentration at the foam surface rises slowly over time and the fuel flux into the chamber also increases with time. The slow increase in fuel flux as measured by FTIR is shown in Figure 4 for AFFF and RF6 foams of the same thickness. The slow rise in fuel transport is indicative of the transport resistance of the foam.

Figure 4 shows that AFFF has a lower fuel flux than a commercial fluorine free foam (RF6, Solberg Inc.) by an order of magnitude over 2000 seconds for the same foam layer thickness over the same room temperature n-heptane fuel. The AFFF layer suppresses the fuel flux of n-heptane at the pool surface by a factor of 300 from 7.5 e-8 to 2.5e-10 mole/cm^{2}s at 1500 s and the suppression is much greater during the initial 10 min. In comparison, the RF6 layer suppresses the

n-heptane flux by a factor of 42 from 7.5e-8 to 1.8e-9 mole/cm^{2}s at 1500 s. The fuel vapor break-through times are 276 s and 820 s for RF6 and AFFF respectively and are indicated by the "break-through flux" in Figure 4 at a flux of 1.21e-10 mole/cm^{2}s corresponding to 10 ppm of fuel vapor. The large difference in the measured fuel flux between AFFF and RF6 shown in Figure 4 can be due to differences in the composition of surfactant solution and in properties of the foams.

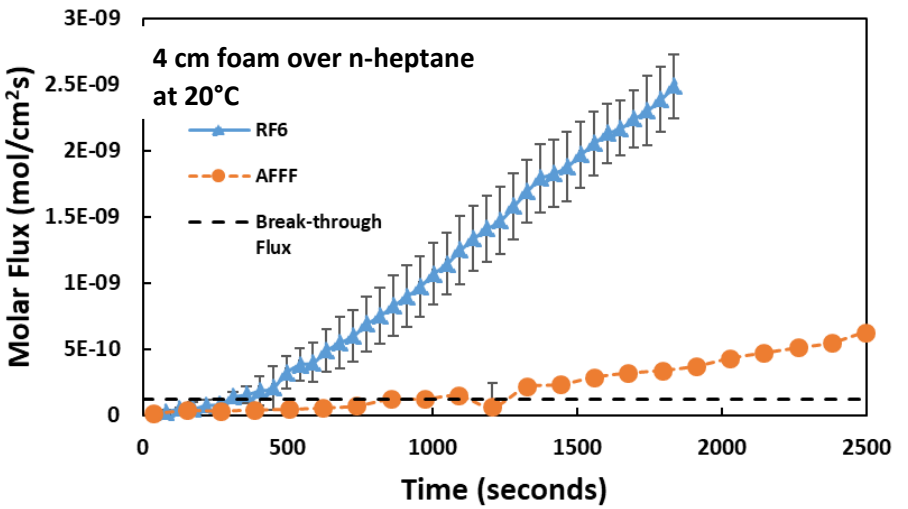

Figure 4. Measured fuel flux with time through 4 cm thick foam layer covering n-heptane pool at 20°C [29].

Figure 5 compares fuel flux through a 4 cm thick AFFF layer over three fuels, n-heptane, iso-octane, and methyl-cyclohexane at 20°C [29]. In Figure 5, AFFF has the smallest fuel flux over iso-octane, slightly greater for n-heptane, and largest for methyl-cyclohexane. The break-through times are greater than 1900 s for iso-octane, 820 s for n-heptane, and less than 80 s for methyl-cyclohexane. At 1500 s, fuel flux is 1e-11 mole/cm^{2}s, 2.5e-10 mole/cm^{2}s, and 2.4e-9 mole/cm^{2}s for iso-octane, n-heptane, and methyl-cyclohexane respectively.

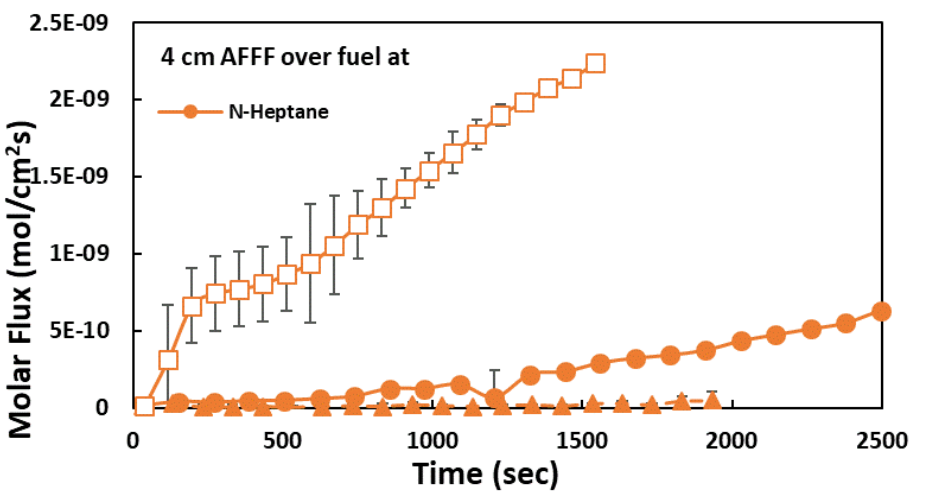

Figure 5. AFFF, 4 cm thick layer covering different fuel pools at 20°C [29].

One of the most interesting observations from the data shown in Figure 5 is that the smallest molar flux through AFFF measured for the fuel iso-octane, which is the most unyielding fuel for AFFF solution to form an "aqueous film" among the three fuels because iso-octane has the lowest surface tension of the three fuels. Moran et al. [21] showed that AFFF solution (6% FC195, 3M Co.) had either very low (0.2 dynes/cm) or negative (-1.3 dynes/cm) spreading coefficient (see Table 3 of [21]) leading to marginal or no "aqueous film" formation on an iso-octane pool. This means the aqueous solution that drains from AFFF foam cannot form a film over an iso-octane pool surface during our experiment. Despite the absence of a film barrier, Figure 5 shows that very small amounts of iso-octane vapor are transported through AFFF foam relative to n-heptane and methyl-cyclohexane, which enables film formation. In comparison to the iso-octane pool, AFFF solution was found to form an "aqueous film" easily on a methyl-cyclohexane pool. Despite the film formation, methyl-cyclohexane pool exhibits the highest steady-state fuel flux and transient fuel flux as shown in Figure 5. Figure 5 suggests that the aqueous film may be less effective than the foam layer as a barrier to fuel vapor transport. The transient fuel transport measurements suggested a mechanism for the surfactant's role in fuel transport through aqueous foams as shown in Figure 6 [29].

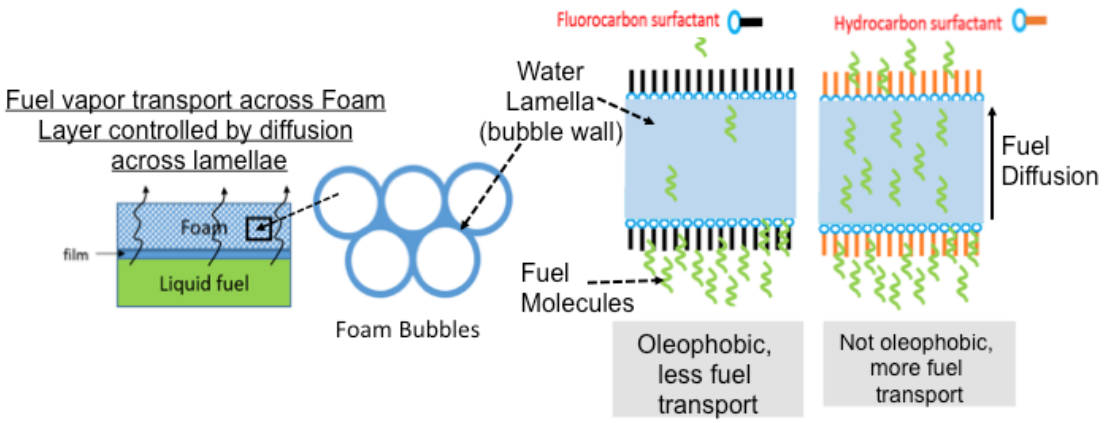

Figure 6. Fuel transport within the bubble structure and the lamellae, and the role of fluorocarbon and hydrocarbon surfactants in the transport across a lamella [29].

A 4 cm foam layer contains a myriad of aqueous lamellae and air, forming a significant barrier to fuel transport relative to a few micrometers thin, single "aqueous film". Fuel transport through the foam layer can occur as the fuel travels through the gas phase contained in the foam bubbles, through the liquid lamella (liquid layer between two adjacent bubbles or bubble wall) surrounding the bubbles, and through the plateau borders (liquid columns formed at the junction of three adjacent bubbles) as shown in Figure 6. The vaporized fuel first dissolves into the liquid lamella. Transport through liquids is much slower than transport through gases due to differences in diffusion coefficients between gases and liquids by four orders of magnitude. Therefore, the dissolved fuel vaporizes from the lamella into a gaseous bubble in the foam. The fuel vapor then re-dissolves into another liquid lamella further up the foam layer and continues this transport until the vapor has reached the foam layer surface as depicted in Figure 6. The foam solution composition may affect fuel transport since AFFF has both fluorocarbon and hydrocarbon surfactants and commercial fluorine-free foam (RF6, Solberg Inc.) has only hydrocarbon surfactants. All surfactants adsorb at the lamella interface (bubble surface) as shown by the individual lamella diagrams in Figure 6, which only shows fluorocarbon surfactant versus

hydrocarbon surfactant absorption at the lamella interface for emphasis. Fluorocarbon surfactants in AFFF are unique in having both hydrophobic and oleophobic repulsions. The surfactant repels a hydrocarbon fuel like n-heptane and suppress fuel dissolution into the liquid lamella as depicted by the lamella diagram in Figure 6. The fluorocarbon surfactant may impede the transport through the foam layer. RF6 contains hydrocarbon surfactants which are also hydrophobic, but the hydrocarbon tails do not repel the hydrocarbon fuel and are not as oleophobic as fluorocarbon surfactants. Fuel vapors can easily dissolve into the liquid lamella and move unimpeded by the hydrocarbon surfactant of RF6 through the foam layer resulting in faster transport in RF6 foam compared to AFFF as shown in Figure 6.

In addition to repulsion towards fuel, foam stability and lamella thickness are also important to reduce fuel flux through the lamellae. Surfactants can affect the thinning dynamics of lamellae and thereby affect foam degradation directly. We discovered that fuel vapors can accelerate the degradation of foam by rupturing bubble lamellae promoting bubble coalescence [30]. Experiments were conducted to quantify foam degradation when placed on top of a hot liquid fuel surface. We quantified foam degradation by measuring the foam layer thickness over time. We did not consider changes in the "quality" of the foam as indicated by its translucency or density. Liquid drainage from the foam can change the foam's density. When the foam was exposed to fuel, we observed the formation of a large bubble near the foam-fuel interface similar to that reported by Osei-Bonsu et al. [31, 32]. In our experiments, foam is exposed to the fuel at the fuel-foam interface and the large bubble grows to cover the entire fuel surface in the container forming a "gap". A single large bubble or "gap" separates the entire foam layer from the fuel surface in the container. We measured both the size of the "gap" and the total foam layer thickness inclusive of the "gap" volume for the circumstances in which a gap formed. Furthermore, in some cases, the foams expand and become translucent; we reported the increase in foam layer thickness as foam expansion rather than degradation.

Figure 7 shows time-lapse images from AFFF and RF6 placed on a hot *n*-heptane at 50°C. About 30-40 mL of foam initially at room temperature is placed over 60 mL of hot (preheated) liquid fuel or water in a 150 mL glass beaker (5.5 cm diameter and 8 cm height). The liquid temperature was maintained to be constant during the experiment by placing the lower part of the beaker (up to the 60 mL mark) in a heated water bath equipped with a thermostat which was set at the desired temperature during the experiment. A clamp used for handling can be seen at the top of the beaker in Figure 7. As time continues, the foam thickness changes. Figure 7 shows that AFFF lasts significantly longer than the commercial fluorine-free foam (Solberg Inc. RF6) as indicated by the average foam height in the beaker. When hot fuel is replaced by hot water, no change in foam height was observed for both the foams in the same period of 4.5 minutes.

Figure 8 and 9 are time-lapse images of the interface between the foams over *n*-heptane (Fig. 8(a-d) and Fig. 9(a-c)) and water (Fig. 8(e-g) and Fig. 9(d-f)) at 50°C for AFFF and RF6 foam respectively. At higher temperatures, the vapor pressure of the fuels increase and a greater amount of fuel vapor escapes from the liquid fuel surface. At higher temperatures, the rate of bubble growth occurs much more rapidly than at room temperature.

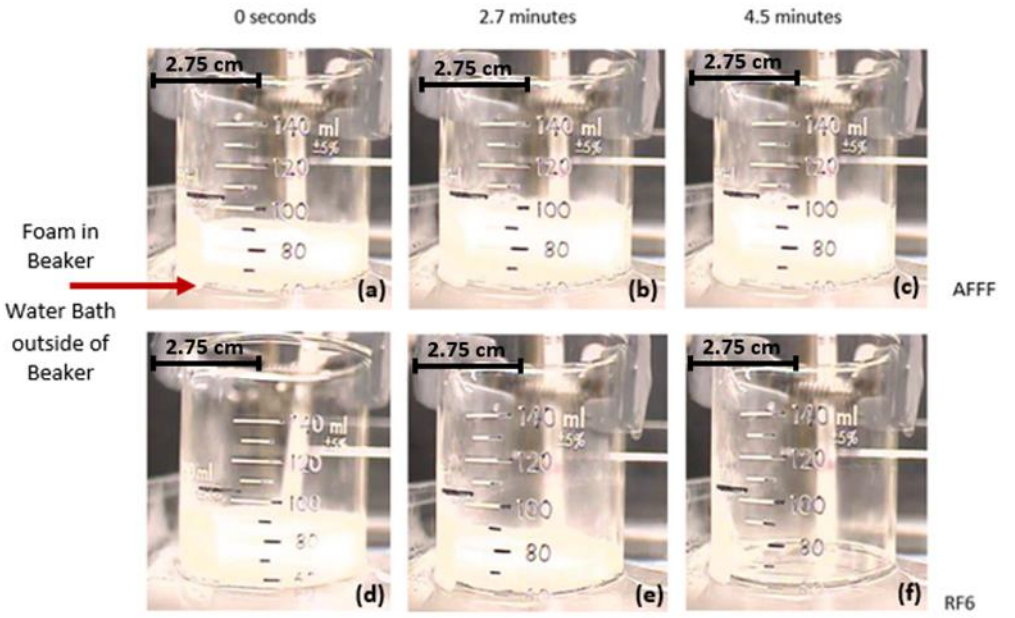

Figure 7. Images taken during experiments with AFFF (a-c) and RF6 (d-f) foam floating on liquid *n*-heptane at an elevated temperature (50°C). Red line indicates the level of the water bath outside of the beaker in (a) to (f). Fuel is inside the beaker at the same height as the water level outside of the beaker. Initial foam layer thickness was 1.8-2 cm above the fuel layer [30].

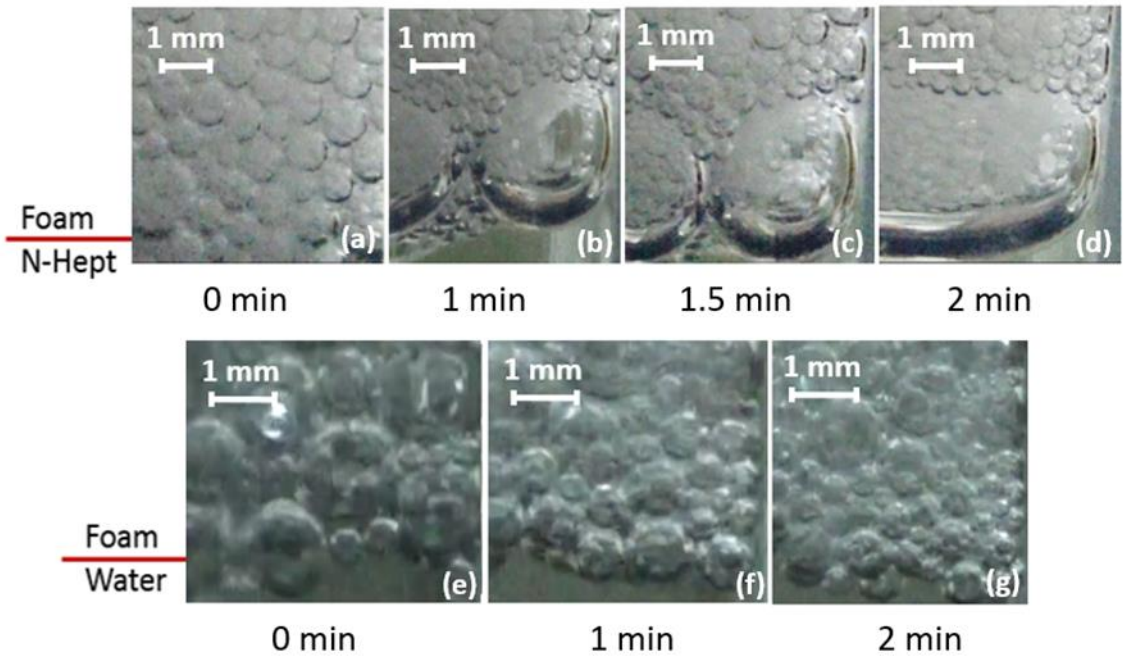

Figure 8. Interfacial images of AFFF foam over *n*-heptane (a-d) and water (e-g) at 50°C; interface position between the liquid and foam is shown by a red line on the left of the images [30].

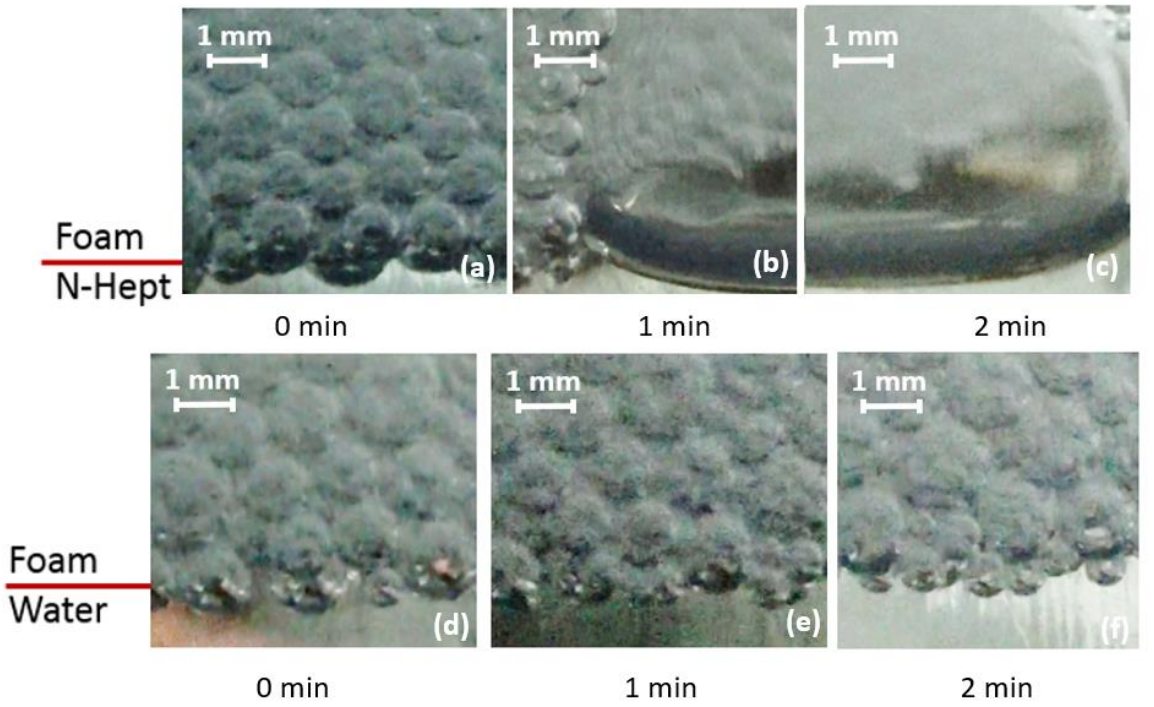

Figure 9. Interfacial images of RF6 foam over *n*-heptane (a-c) and water (d-f) at 50°C; interface position between the liquid and foam is shown by a red line on the left of the images [30].

Focusing closely on bubbles adjacent to the foam-fuel interface, videos showed that all bubbles at the interface, large and small, grew but at different rates. Slightly away from the interface the bubbles remained unaffected during the same time period. The videos showed that at some point during the growth, the lamella separating adjacent bubbles ruptured and bubbles coalesced. This process was more rapid in RF6 foam compared to AFFF foam. This is how degradation is initiated at the interface. This cannot be seen in Figures 8(b) and 9(b) because the growth and coalescence had already taken place adjacent to the interface and other smaller bubbles away from the interface migrated to the interface. Even as the temperature increased, Figures 8 and 9 show that there is no drastic change in bubble diameter when the foams are placed over hot water. In the images of foam placed over hot water, the bubbles at the interface appear to be getting smaller. Because the rapid bubble growth observed for foams placed over *n*-heptane was not observed with hot water, the video observations of bubble growth and the increased rate of foam degradation must be induced by *n*-heptane.

When an aqueous foam is applied on to a burning pool, the hot (at its boiling point) pool surface can be cooled instantly by direct contact with the foam, which is near room temperature. The foam layer absorbs heat from the pool. The decrease in surface temperature can lead to a significant decrease in fuel vapor pressure, which depends exponentially on the temperature. To measure this cooling, we performed experiments using a 19-cm diameter heptane pool with thermocouples distributed at different depths from the pool surface and at different radial positions. The pool was ignited and burned for 60 seconds before the fire was extinguished by placing a metal plate on top [33]. Within 15 seconds after the fire extinction, a foam layer of 2 cm thickness was placed on to the hot pool using a springform pan with removable bottom. The filling of the springform cylindrical container was strategically timed such that it was completed just before the end of the

60 seconds preburn. The measured temperature at the center of the pool and at different depths into the pool versus time are shown in Figure 10. The first figure shows that the measured pool temperature at 1 mm below the surface drops from 85 ºC to 60 ºC within a few seconds after the foam is applied at time=0, and continues to decrease relatively slowly.

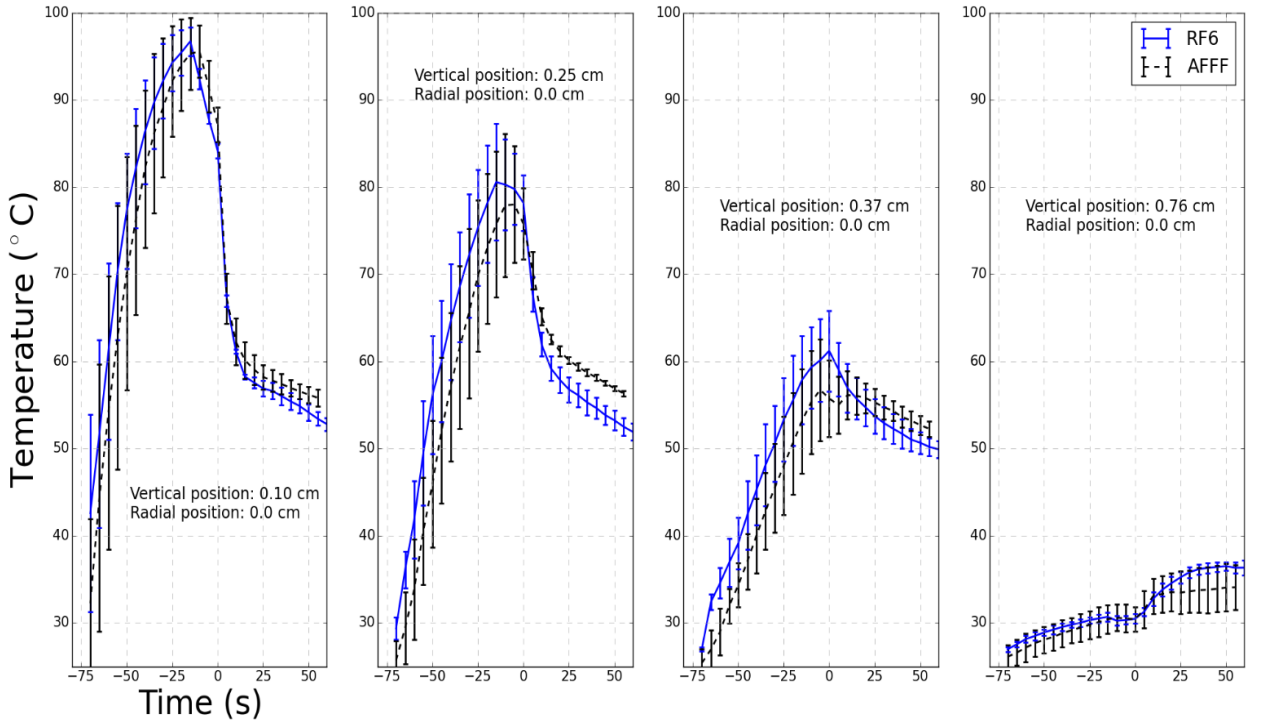

Figure 10. Comparison of measured temperatures versus time for different foams: RF6 and AFFF. Temperature measurements with thermocouples placed at different depths in the fuel at the radial center of the pool. Foam is applied at time=0 following a 60 seconds preburn and fire extinction by placing a metal plate on the burning pool [33].

1.3. Bench Scale Fire Extinction

We developed a 19-cm diameter bench-scale pool fire suppression apparatus to measure time to cover the pool surface by foam and fire extinction time for a heptane pool [34]. It includes a sparging method for foam generation, where air is bubbled through a porous disk immersed at a fixed height in surfactant solution. The foam was applied to the center of a burning pool at a constant volumetric flow rate after a 60 second preburn. Both coverage and extinction times were measured as functions of foam flow rate as shown in Figure 11. Figure 11 shows extinction time decreases as the foam flow rate is increases for commercial AFFF and a fluorine-free foam RF6 (Solberg Inc.) for a heptane fire collected in our laboratory. MilSpec application rates of 2 gallons per minute of liquid flow corresponds to 2.9 kg/m^2/min in Figure 11. It corresponds to 660 mL/min foam flow rate and 82 mL/min liquid flow rate (assuming 8 mL foam contains 1 mL solution, expansion ratio of 8) for the 19-cm bench scale apparatus. For comparison, Figure 11 also shows the data reported for a recently developed siloxane foam collected by Professor Dirk Blunk, University of Cologne, Cologne, Germany for a jet fuel fire. The fluorine-free foams perform poorly with fire extinction times greater than 35 seconds at the highest foam flow rate of 2400 mL/min relative to the 8 to 10 seconds for the fluorinated AFFF because of the differences in foam degradation and fuel transport rates rather than the aqueous film formation discussed above.

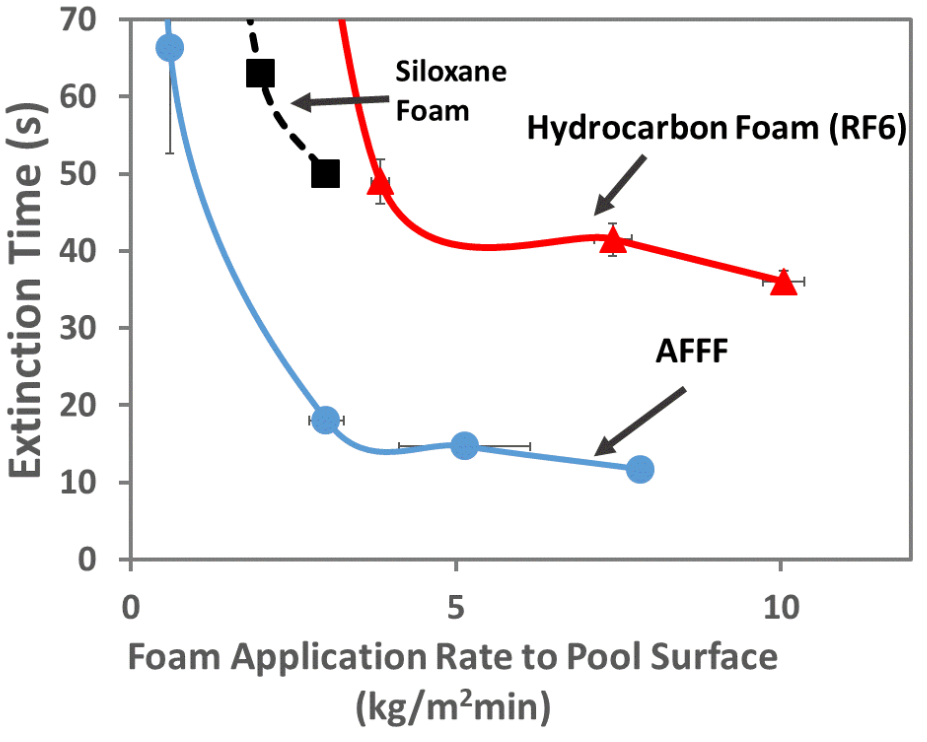

Figure 11. 19-cm diameter heptane pool fire extinction at different foam application rates with fluorinated and fluorine-free foams [34].

1.4. Need for Novel Fluorine-free Surfactants

Drop-in replacements for AFFF can be developed with alternate fluorine-free surfactants. The above discussed findings open a new parametric space (lamella thickness, lamella rupture in the presence of fuel, fuel diffusion rate through lamella, lamella number density in foam) that provide multiple avenues to develop new fluorine-free surfactant formulations for a *drop-in* replacement for AFFF. Novel surfactants can influence the foam dynamics in a focused and new ways to bring about needed improvements in fire extinction for heptane and gasoline fuels. The commercial fluorine-free foam, RF6, was developed using alkyl polyglycoside surfactants with a viscous additive (xanthan gum) to reduce liquid drainage from the foam to improve foam stability. We found that the RF6 flame extinction time was much longer compared to AFFF because of higher fuel flux and foam degradation rate. Despite reduced liquid drainage using the thickeners, degradation of RF6 was high. The high degradation can significantly enhance fuel diffusion and slow the foam spread on the pool surface especially at low foam application rates. Also, the lamellae in the AFFF foam appear to be more fuel resistant than the lamellae inside RF6 foam as indicated by the measured fuel transport and degradation rates. These offer clues to a more fundamental approaches to vary surfactant structure by synthesis and influence foam-fuel interactions depicted in Figure 6 to decrease the fire extinction time.

Although we quantify differences in foam mechanisms between fluorinated and fluorine-free foams, The role of surfactants in fire extinction remains unclear. How do fluorosurfactants and hydrocarbon surfactants in AFFF influence foam dynamics, aqueous film formation, and fire

suppression? We aim to define how surfactant structure and properties effect firefighting foam performance.

2. OBJECTIVE

The objective of our research program is to develop an environmentally-friendly, fluorine-free, firefighting surfactant formulation to replace AFFF by reducing the fuel permeability through foam and foam degradation with increased surfactant oleophobicity as shown in Figure 12. Figure 12 shows that foam acts as a fuel vapor barrier and surfactants adsorbed at bubble surfaces interact with fuel vapors as they permeate through the foam feeding the fire. By increasing the oleophobicity of the fluorine-free surfactants, the fuel vapor permeation could be suppressed quickly to cut-off fuel supply into the fire.

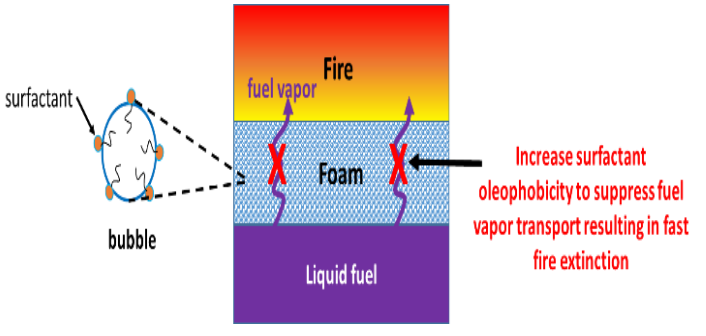

Figure 12. Enhancing fire suppression with surfactants by targeting the foam layer as a fuel vapor barrier rather than the aqueous film formation.

Our overall approach is to build on the research community's understanding and our own research experience on fire suppression mechanisms, laboratory experimental methods, and computational models at the U.S. Naval Research Laboratory (NRL). It will benefit the DOD, government and civilian agencies (particularly airports) that use AFFF.

3. APPROACH

Our first step is to develop a simple, well-defined, three component (two surfactants and a solvent) custom AFFF formulation with known molecular structures, and show its gasoline fire suppression matches that of a commercial AFFF. This is crucial because the compositions of commercial AFFFs are proprietary and subject to continuous changes. Known as the Reference AFFF, the fluorocarbon surfactant can be replaced with an alternative and the alternative's properties and performance can be evaluated against the fluorocarbon surfactant. This enabled us to empirically formulate cause-effect relationships which are used as the basis for changes due to the molecular structure of the alternative surfactants for improved performance.

A broad spectrum of commercially available siloxane and hydrocarbon surfactants are evaluated using bench scale methods as alternatives that are not necessarily designed for firefighting. Using bench scale methods, the surfactants are ranked and promising candidates are identified for large scale fire extinction testing.

Novel surfactants are designed based on chemical intuition for increased oleophobicity and by performing molecular dynamics (MD) simulations to predict monolayer structures for surfactants

at heptane-water and water-air interfaces. The novel surfactants are synthesized by chemical reactions at 10 grams scale using routes that are well established for hydrocarbon surfactants but are established only to a very limited degree for the siloxane surfactants. Characterizations of the synthesized chemical structures are performed using NMR and LC/MS methods.

A number of bench-scale experiments are used. A single lamella is formed with the surfactant solution and its dynamics of rupture was studied; lamella is a representation of a bubble wall. Solution and foam properties, foam degradation, fuel transport through a foam layer, foam spread, and fire extinction are measured at bench scale to evaluate the surfactants. The surfactants are evaluated for heptane, jet fuel (JP-5), and gasoline fire suppression. Bench scale experiments have two purposes; (1) to screen and rank fluorine-free surfactants and the top-ranked surfactants are then subjected to large scale testing, (2) to guide the design of new surfactant molecular structures by varying the experimental parameters under well controlled conditions to establish cause-and-effect relationships. Because, the bench scale tests use tens of grams of surfactant to vary a parameter (e.g., vary foam application rates by a factor of 20, three fuels, many surfactant compositions) rather than 100s of grams needed for a single large scale test, they are the most appropriate tool to understand the effects of surfactants on foam dynamics and fire suppression unlike the large scale tests. The bench scale experiments are the only convenient choice for synthesized surfactants that are available only in small quantities. The bench-scale experiments also allow for more detailed measurements unlike the large scale tests. But, the bench scale experiments are not a replacement for the large scale tests. Therefore, we also conducted large scale, 28 ft^2 heptane and gasoline pool fire extinction and burnback tests at varied foam application rates to a very limited degree (2, 3, 4 gpm of solution flow). The detailed methods used are given below.

We have been collaborating with Dow Silicones Co., Midland, MI on synthesizing and developing novel siloxane structures for firefighting. This started as a request for free samples and contacting one of their chemist for a recommendation on their products. This led to their commercial silicone DOWSIL 502W surfactant, which we identified as promising for fire suppression. After the performance evaluations, discussions began and we received another set of samples of their products. This is a new application for them and they had to be convinced by their market research before jumping into this area for research and development. Their present commercial silicone DOWSIL 502W surfactant which we identified as promising for fire suppression was designed as an intermediate in polyurethane foam synthesis. To make them effective for fire suppression, they are synthesizing new variations of silicone molecular structure to suppress surfactant extraction by gasoline, and down selecting samples by using NRL developed bench-scale methods. We have been evaluating the Dow samples by quantifying foam degradation, fuel transport, foam spread, and fire extinction at bench-scale.

3.1. Selection of Commercial Surfactants

Many commercial surfactants are available and are categorized as hydrocarbon, siloxane, non-ionic, anionic, cationic, and zwitterionic. The first level properties are surface tension and critical micelle concentration (CMC) that are important for foam generation, a prerequisite for fire suppression. We prioritized surfactants with surface tension below 35 mN/m and CMC values less than 0.1 weight%. These are used individually and as part of Reference AFFF formulation replacing the fluorocarbon surfactant.

3.2. Surfactant Design Strategy

Surfactant design is guided by physicochemical interactions between the surfactant molecules and the fuel as shown in Figure 12. Fuel molecules such as alkanes interact through weak induced dipoles with other similar molecules based on the principle of "likes dissolve likes". The strategy is to design surfactants such that they interact by strongly induced diploes and permanent dipoles so that they have less attraction to alkanes by creating surfactants that are different from the alkanes.

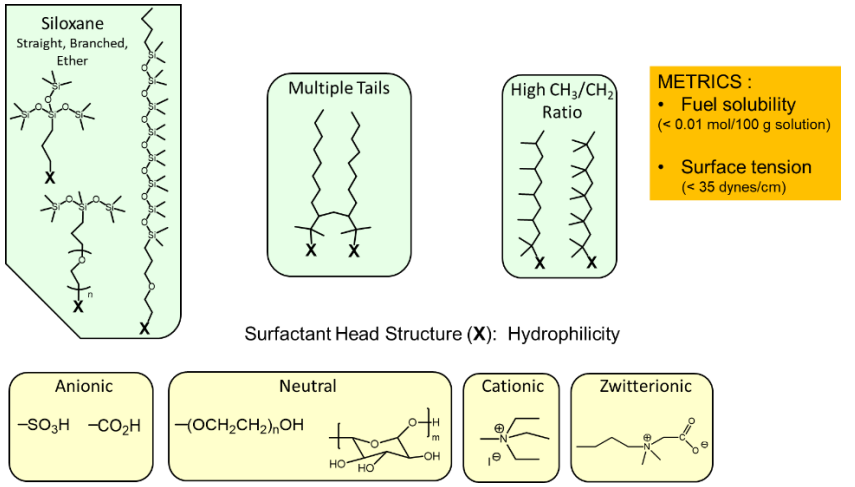

Figure 13. Candidate surfactants to suppress fuel transport through foam

Perfluorosurfactant tails are unique because they are both oleophobic and hydrophobic because fluorine is least polarizable. To mimic this feature of a fluorosurfactant, we attempt to reduce the molecular interactions between surfactants and fuels. Figure 13 shows chemical structures of tails on top and head at the bottom of the figure. Siloxane tails have Si-O bonds with permanent dipoles in linear and branched configurations. Another feature is to take advantage of differences in the degree of polarizabilities. Methyl groups are 25% more polarizable than methylene groups. The diploe moment of dimethyl siloxane is in between that of water and heptane so that it does not like either of them. The branched siloxane packs more methyl groups in a smaller area than the linear siloxane and increases the difference with heptane fuel. It also includes oxyethylene groups to further incorporate dipoles into the tail. The hydrocarbon surfactants shown in Figure 13 use steric crowding of multiple tails that prevent the double tailed hydrocarbon surfactant from interacting with an alkane. Similarly, we vary CH2/CH3 ratio of the pendant groups of a hydrocarbon surfactant tail to vary polarizability and reduce interactions with alkanes. As the tail's oleophobicity is varied, its hydrophobicity varies as well. Ideally the hydrophilicity of head and hydrophobicity of the tail should be in balance to provide optimum amphiphilicity needed for a surfactant to create foam. The head groups at the bottom allow us to vary amphiphilicity of the surfactants so that it is optimally placed at air-water and heptane-water interfaces. The surfactant structure in Figure 13 are only a starting point, the data obtained from them will guide the design of the next set of molecules.

3.3. Molecular Dynamics Modeling (MD) Approach

The surfactant design is also guided by performing MD simulations. MD simulations are performed to study the effect of structure of surfactants on the surfactant monolayer properties at

the air/water and heptane/water interfaces. The model for well-established hydrocarbon surfactant molecules is validated by experimental data [35].

The MD simulations [35] are performed on air-water and heptane-water interface systems with and without a surfactant, some of which are shown in Figure 14. A specified constant number of molecules, volume, and temperature (*NVT*[1]) ensemble was applied for the air-involved systems, such as air/water and air/surfactant-monolayer/water interfaces (Figure 14b). Simulations with *NVT* ensemble predict positions and velocities of atoms, and pressure with time which are used to calculate surface tension and then Gibbs elasticity. A specified constant number of atoms, pressure, and temperature (*NPT*[2]) ensemble was applied for the systems not involving air, such as water, heptane, heptane/water and heptane/surfactant-monolayer/water interfaces (Figure 14a and 14c). Simulations with *NPT* ensemble predict positions and velocities of atoms and volume with time which are used to calculate the densities of the pure water and heptane liquid, and also the interfacial properties related to surfactant packing such as area per molecule, component density, and interfacial thicknesses. More detail descriptions on each of the simulation system are provided in the subsection below.

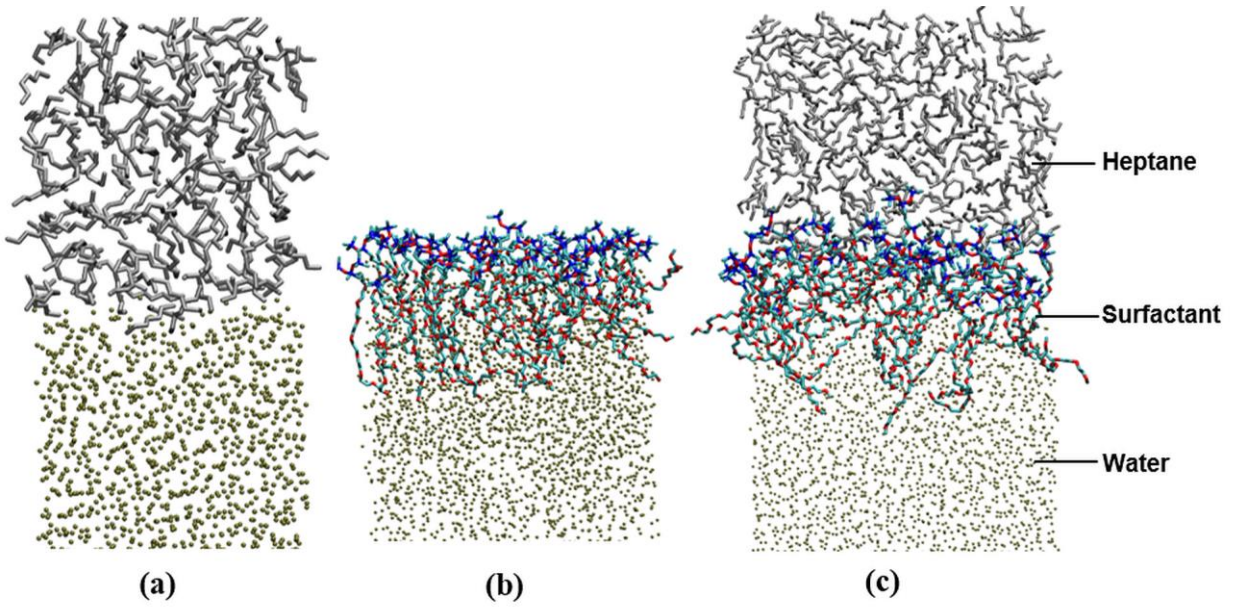

Figure 14. (a) The heptane/water, (b) siloxane surfactant-monolayer/water, and (c) heptane/siloxane surfactant-monolayer/water systems at the end of the MD simulations. Water is shown as tan spheres, heptane as silver lines. Siloxane surfactant L77, C, O, Si atoms are shown in cyan, red, and blue, respectively. Only the top half in the z direction of the simulation setup are shown, the bottom half is a mirror image of top [35].

Nanoscale Molecular dynamics (NAMD) computational program was used to run the MD simulations. Chemistry at HARvard Macromolecular Mechanics (CHARMM) was used to build the models and the property calculations. C36FF [36] was used for hydrocarbon and fluorocarbon surfactants, and also for heptane. CHARMM22 siloxane parameters [37] were used for the siloxane surfactant tail and C36FF was used for the head group. TIP3P water model [38, 39] was

[1] *NVT*: constant number of atoms, volume, and temperature
[2] *NPT*: constant number of atoms, pressure, and temperature

applied. Periodic boundary conditions were applied to avoid edge artifacts and obtain good statistical data. To increase efficiency for van der Waals interactions, a switch function with a switch distance of 10.0 Å was applied so that the interaction was switched off 2.0 Å before the cut-off (12.0 Å). For the electrostatic interactions, the particle mesh Ewald summation was applied which splits the summation into short- and long-range interactions separated by the cut-off. The temperature was set at experimental temperatures. Langevin dynamics was applied to non-hydrogen atoms to maintain constant temperature with a Langevin coupling coefficient of 1.0 ps^{-1}. When *NPT* ensemble was applied, the pressure was set at 1.0 atm, and Nosé-Hoover Langevin-piston algorithm was used to maintain constant pressure with a piston period of 50.0 fs and a piston decay of 25.0 fs. Python modules NumPy and SciPy [40] were used for further data analyses. Visual Molecular Dynamics (VMD) [41] was applied to visualize and plot the simulated systems. Gnuplot [42] was used to plot the result data.

The simulations are also performed for the siloxane surfactants and its mixtures with hydrocarbon surfactants. From the MD simulations, the interfacial properties such as the surface area per molecule (A), interfacial thicknesses of water (d_w) and heptane (d_h), the heptane to surfactant ratio (*hsr*), the heptane surface number density (*hsnd*), the inverse of maximum surfactant volumetric number density ($msnd^{-1}$), the heptane volumetric number density (*hvnd*), hydrogen bond number per molecule (*hbnm*) and hydrogen bond number per $Å^2$ (*hbna*) are calculated. The d_w and *hbnm* are the properties of the hydrophilic head group, and d_h, *hsr*, $msnd^{-1}$, and *hvnd* are the properties of the hydrophobic tail, while the *hsnd* and *hbna* are the additional cross-sectional unit area properties calculated to compare to unit molecule properties (*hsr* and *hbnm*), respectively. The *hbnm* is related to stability of the head group, while the $msnd^{-1}$ and *hvnd* are related to heptane transport rate in the tail. The *hsr* is related to both stability and heptane transport rate in the tail.

MD simulations [43] are performed on the heptane/surfactant-monolayer/water interface (Figure 13) with constant number of molecules, pressure and temperature (*NPT*) ensemble using an orthorhombic box ($\alpha=\beta=\gamma=90.0°$, $L_x \neq L_y \neq L_z$) with a hexagonal close packing as initial conditions. The initial set up is generated from a fixed total number of surfactant molecules, $N_s=36$ (6 by 6 array). The initial values of the area per surfactant molecule A_i are given. (The area per molecule will change with time and reach a steady-state value for A at the end of simulation.) We then take the water and heptane layer from the large pure systems with dimensions the same as the surfactant monolayer (L_x and L_y). We appended the water and heptane layers in such a way that half of the head and tail groups of the surfactants overlapped with the water and heptane layers respectively. The thickness of the water and heptane layers are selected so that the tail end of the surfactant monolayers do not interact with each other. The total thickness L_{Zi} is the summation of the initial water layer thickness L_{wi} and the initial heptane thickness L_{hi}, and the half of the surfactant length, i.e. $Lz_i = Lw_i + 2Lh_i + L_s/2$. For each run, we start with 10000 steps of energy minimization, and then equilibrate with *NVT* ensemble for 0.05 ns with the time step of 1.0 fs, followed by another equilibration with *NPT* ensemble for 0.6 ns with the time step 2.0 fs. Eventually, we run MD simulations with *NPT* ensemble for 100.0 ns with the time step of 2.0 fs at 25°C and 60°C. Each simulation is run with three replicates to obtain average and standard deviation of each properties calculated. For two-component and three-component surfactant monolayer, the distribution of components are random in each replicate to get a good statistics. 1g9 is alkylpolyglycoside having 9 carbon tail length (nonyl) and 1 glycoside head and 2g9 has two glycoside heads.

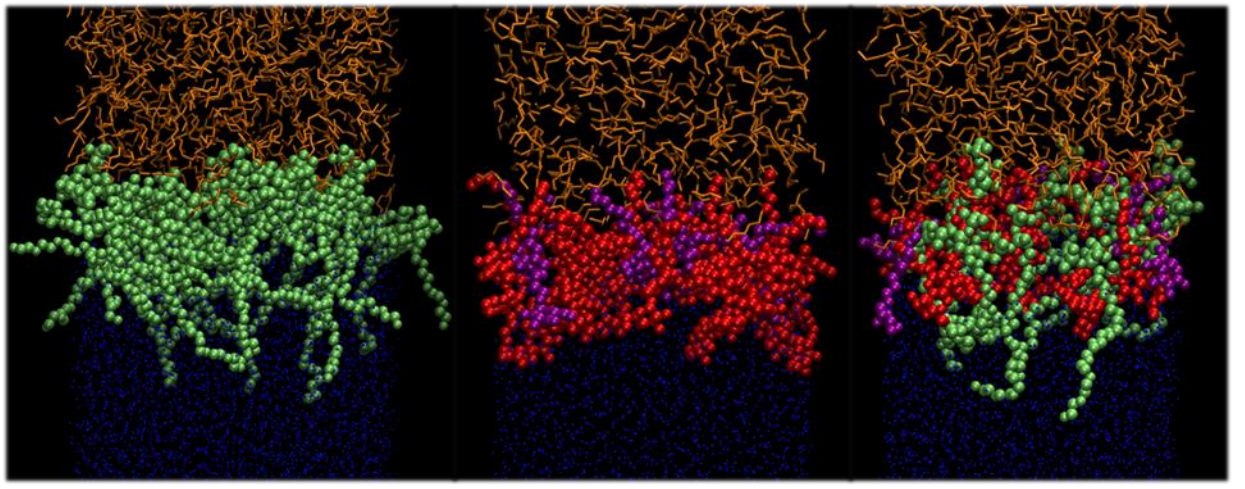

(a) **(b)** **(c)**

Figure 15. (a) The pure polyoxyethylenated trisiloxane (X=OH, *n*=8) (b) the 1g9/2g9 two-component surfactant monolayer with ration 3:7 (c) trisiloxane (X=OH, *n*=8)/1g9/2g9 three-component surfactant monolayer at the heptane/water interface system at the end of the MD simulations, respectively. (Water is not shown for image clarity, heptane as orange lines, and trisiloxane surfactant are shown in cyan spheres.) 1g9 are shown in purple spheres, and 2g9 are shown in red spheres. Only the top half in the z direction of the simulation setup are shown, the bottom half is nearly a mirror image of the top one [43].

3.4. Surfactant Synthesis and Characterization Methods

The initial choice of surfactants for synthesis are continuously informed and refined by using computational models, experimental data on performance, and synthetic accessibility throughout the program. We synthesize selected silicone surfactant structures (Si-O chain) that increase the quantity and density of methyl groups attached to Si. These compounds are not commercially available, but reagents and adaptable literature procedures from other siloxane molecules are available. For the head group and the connecting linkage between the hydrophilic head group and the silicone tail structure, the reagents are readily available and routinely used in the literature to accommodate using a short trimethylene (-$CH_2CH_2CH_2$-) chain as a connecting linkage. Figure 16 shows an example synthesis steps to attach commercially available tail and head to make a surfactant. For small molecules with oxyethylene unit of 1 or 2, distillation can be performed to purify the surfactant product. But for longer molecules, it becomes difficult to purify surfactants by solvent extraction methods because surfactants tend to dissolve in almost every solvent to some degree. So, we focus on finding reaction routes with high yield which often means one or two step synthesis as indicated in Figure 16. We follow the extent of reaction by intermittently analyzing small samples using ^{1}H NMR. It is important to ensure the trisiloxane tail is intact at the end of each step. Reaction is conducted initially at an mg scale and then at a10 g scale. The products are structurally characterized using ^{1}H NMR, ^{13}C NMR, and ^{29}Si-NMR as well as transmission IR, and LC/MS methods.

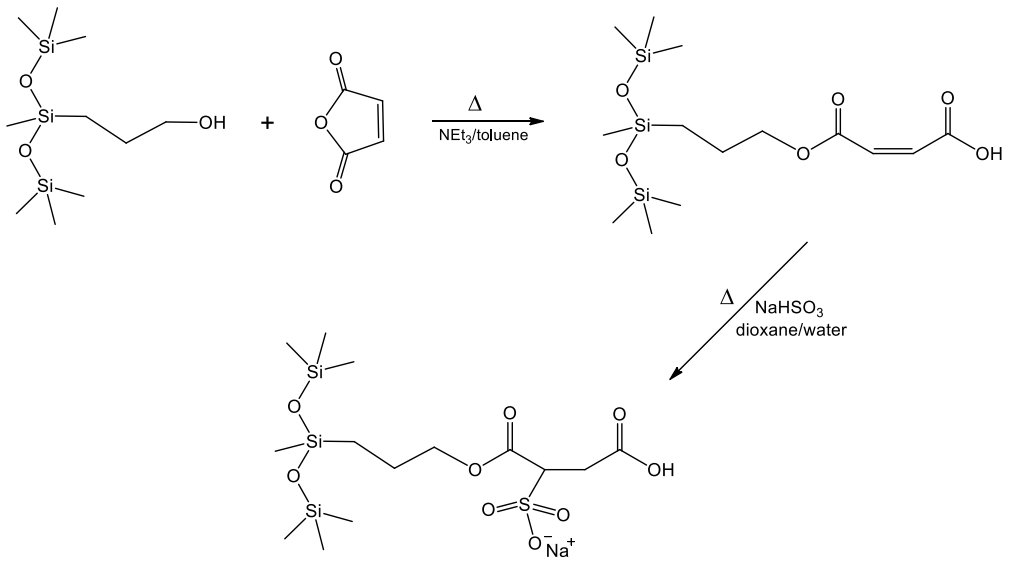

Figure 16. Synthesis routes involving one or two steps for forming a novel siloxane surfactant from commercially available reagents as an example.

3.5. Materials and Preparation

The components of the RefAFFF formulation are: Glucopon® 215 CS UP (an alkyl polyglycoside concentrate contributed by BASF Corporation, Ludwigshafen, Germany and referred to as "Gluc215" [44]; Capstone™ 1157 (fluorotelomer sulfonamide alkylbetaine concentrate contributed by Chemours Inc. , Wilmington, DE and referred to as "Cap") [44]; Butyl Carbitol™ (Dow Chemical Co., Midland, MI purchased as diethyleneglycol butylether, "DGBE", from Sigma Aldrich, St. Louis, MO) [44]. The component chemical structures are depicted in Figure 17.

The Siloxane-Gluc215 formulation was prepared by replacing Cap in RefAFFF with Dow Corning® 502W Additive 502W Additive, which is a silicone polyether copolymer, a 100% by weight concentrate contributed by Dow Corning Co., Midland, MI density 0.97 g cm^{-3} [45]. The Siloxane-Gluc225 and Siloxane-Gluc600 formulations were prepared by replacing the BASF Glucopon® 215 CS UP with Glucopon® 225DK (an alkyl polyglycoside, a 68-72% by weight concentrate in water, contributed by BASF Corporation and referred to as "Gluc225" in this report, density 1.13 g cm^{-3} [46]) and with Glucopon® 600 CS UP [46] (50 to 53 % by weight concentrate) in the Siloxnae-Gluc215 formulation respectively. The resulting solutions were used for generating foams for fire suppression as well as for foam and solution properties' measurements.

U.S. MilSpec compliant commercial AFFF formulations are typically sold as 3% or 6% concentrates, such that the final formulation used for generating the foam should contain 3% or 6% of the concentrates in water respectively. We received 3% concentrates provided by Buckeye Fire Equipment Company, Kings Mountain, NC (BFC-3MS, Lot# 120050**,** 2003) [47] and by Dafo Fomtec AB, Tyreso, Sweden (FOMTEC AFFF 3% M USA, Batch # US-16-07-07, August 4, 2016) [48] and used them as received for the analytical characterization described by Hinnant et al [44]. The Buckeye and Fomtec concentrates were diluted with water at 3% by volume for generating the foams for fire suppression.

The chemical structures of the siloxane surfactant contained in 502W [44], Capstone™ 1157 [44], Glucopon 215 CS UP [46], Glucopon 225 DK [45], Glucopon 600 CS UP [46], and DGBE [44] are depicted in Figure 17. The exact chemical structures of these commercial surfactants are proprietary, but the general features and chemical family are given in published and vendor supplied literature [44, 45]. The details of the chemical structures of Capstone, Glucopon 215 CS UP, and DGBE were confirmed by analytical characterization described in the supporting material provided in the reference [44].

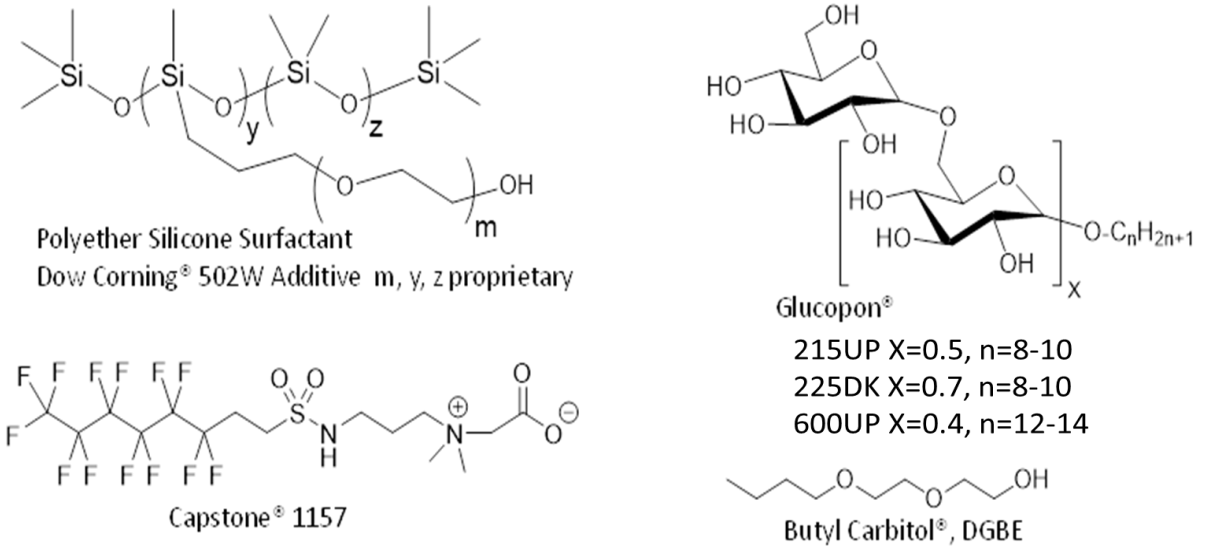

Figure 17. Structures of surfactant components in Siloxane-Glucopon [44-46] and RefAFFF [44] formulations.

The siloxane surfactant in 502W has general structure of siloxane-polyoxyethylene at 100% concentration as shown in Figure 17 [45]. The siloxane surfactant has a hydroxyl functional group (R-OH) and a distribution of polyoxyethylene (OCH_2CH_2) chain lengths represented by the parameters m and y respectively. The distributions and the average values of m, y, and z are proprietary according to Dow Corning Co.'s literature [45]. Glucopon® 600 CS UP, Glucopon® 215 CS UP, and Glucopon® 225 DK are alkyl polyglycoside surfactant products of BASF in concentrate form. All three Glucopons have a distribution in both the number of glycoside structural units and in the number of methylene units in the alkyl tail structure as represented in Figure 17, but differ only in the average number of glycoside units of the head group according to BASF literature [46]. Glucopon® 600 CS UP, Glucopon® 215 CS UP, and Glucopon® 225 DK have x=0.4, 0.5, and 0.7 respectively and have n=8 to 10 except Glucopon® 600 CS UP, which has n=12 to 14. Increased glycoside head size increases the number of OH functional groups on the hydrophilic head. The hydrocarbon surfactant's structures shown in Figure 17 are poly-D-glucopyranose with octyl and decyl alkyl chains [46]. Butyl Carbitol™ is a Dow product available in a relatively pure form of diethylene glycol butyl ether (DGBE) with a molecular weight of 162.2 g $mole^{-1}$ [44]. DGBE has a relatively long history as a component in AFFF formulations [6-9] being a good solvent for fluorocarbon surfactants, hydrocarbon surfactants and water. Capstone™ 1157, also known by its earlier tradename Forafac® 1157 [9], is a Chemours/DuPont product. The fluorosurfactant's structure shown in Figure 17 is tridecafluorooctyl sulfonamide alkylbetaine.

Comparative analytical data of the Capstone™ 1157, Buckeye 3% and the Ref AFFF formulations are displayed in the supporting material provided in Reference [44].

3.6. Methods for Solution Properties

Dynamic surface tension [49] is measured using a bubble pressure tensiometer (Model BP2, KRUSS, Hamburg, Germany) as a function of the bubble's age (frequency^{-1}, 10 ms to 10000 ms). The tensiometer generates bubbles at a capillary tube lip (0.22 mm diameter) continuously at a specified frequency by pushing nitrogen through the capillary immersed in a surfactant solution. Surfactant diffuses from the solution to the bubble surface, where it gets absorbed and suppresses the surface tension. Pressure inside the bubble increases and reaches a maximum when the bubble diameter is equal to the capillary tube diameter before the bubble detaches from the capillary. Surface tension is calculated from the measured maximum pressure using Young's equation. Critical micelle concentrations (CMC) and static surface tensions for the Siloxane-Gluc600, Siloxane-Gluc215 and Siloxane-Gluc225 were measured using a ring (radius 9.58 mm, wire radius 0.185 mm) tensiometer at 20°C (Du Nouy Model Sigma 701, Biolin Scientific Inc., Gothenburg, Sweden). Surface tension was measured at different concentrations of the total surfactant. CMC values were determined from the log plot of surface tension against weight % of the sum of 502W and Gluc surfactant concentrates supplied by the manufacturers. Interfacial tensions were measured with the ring tensiometer between heptane and the siloxane formulations at 20°C. The viscosity was measured at 20°C using a Cannon™-Fenske viscometer (Fisher Model 50 13616B, capillary size #50).

3.7. Single Lamella Apparatus

An experiment was designed to study individual solution lamella, measuring the thickness of a thin lamella, suspended on a horizontal ring, using interferometry with a Filmetrics® LS-DT2 light source and software. A sketch and an image of the setup is seen in Figure 18. The lamella was suspended using a 9.6 mm diameter platinum-iridium ring. This is the ring used for surface tension measurements in a DuNouy ring tensiometer. We found that unless a wire ring was level and flat, film lifetimes would only be a few seconds long due to instabilities of the ring. The flat level formation of the tensiometer ring was a good first-round effort, but the wire can still be easily deformed. A mechanical stage was used to raise a 30 mL beaker containing the surfactant solution, submerging the ring. The stage was then used to remove the beaker, leaving a film suspended on the ring. Film thickness data collection began when the ring was submerged and stopped when the film ruptured. Data at each time was fit using the refractive index, an appropriate wavelength range, an initial thickness estimate, and confidence interval (part of the interferometer internal software). The confidence interval was generally set to 95% to ensure the initial parameters could be used over multiple time steps as the lamella thinned. The initial thickness was taken as the first data point that showed interference patterns, within 1 second of film generation. Thicknesses with time plots were also collected to compare differences between the surfactant solutions. Lamella thickness tests were repeated 3-4 times to improve precision.

Lifetime measurements were recorded from the time when the film completely separated from the liquid in the beaker until film rupture. Lamella lifetimes were taken using a stopwatch. For some tests, the beaker was manually raise and lowered, for others a motorized stage was used. Some variation in lamella lifetime was seen between generating the lamella by hand or with the motorized stage. Two motorized tests were approximately 20s shorter than the eight done by hand.

We suspect shorter lifetimes with the motorized stage are due to the speed of the stage dragging the solution down whereas generating the lamella by hand can more gracefully remove the solution. Continued issues with software fitting and lamella generation have made us reconsider design elements. The experiment design is still being finalized for improved reproducibility as well as the encorporation of fuel transport measurements through the film. Figure 18 represents a new experimental design in a glass cross is used to simultaneously measure lamella thickness with time as well as fuel transport through the lamella.

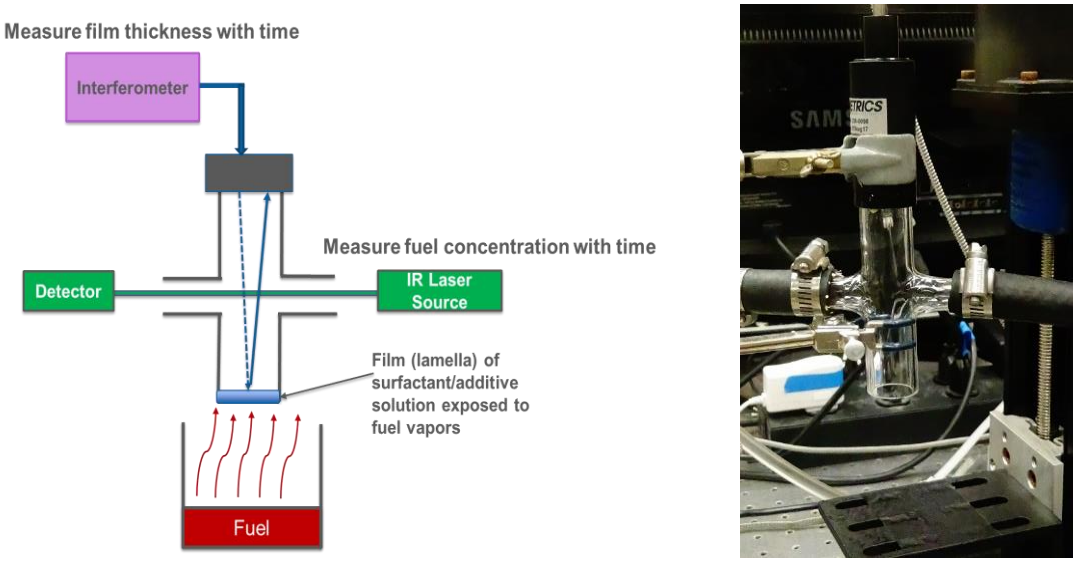

(a) (b)

Figure 18. (a) Diagram of single lamella apparatus for measuring thinning dynamics with an interferometer and fuel vapor diffusion through the lamella with IR, (b) An image of the apparatus.

3.8. Foam Generation and Characterization Methods

Foams are generated from the Siloxane-Glucopon formulations using a sparging method for bench-scale evaluations as detailed by Hinnant et al. [44]. Air flows through a circular sparger disc (2 cm dia., 25-50 μm pore size) placed 3 cm deep in the surfactant solution at a constant rate to generate bubbles as shown in Figure 19. The foam is dispensed through an outlet tube of the generator at a constant foam flow rate. The tabulated foam properties are measured as foam is dispensed at a constant foam flow rate of 1000 mL min^{-1}. A single cup, as shown in Figure 19, is used for generating small volumes of foam needed to characterize the foams by measuring degradation and fuel transport. But for fire extinction experiments where the foam flow rate is varied, a liquid leveling system is used to maintain constant liquid depth above the sparger.

The candidate formulations are also used to generate foams at large-scale by pushing the foam solution from a pressurized tank (689.5 kPa or 100 psi) through an air aspirated nozzle at constant solution flow rate of 7.57 L min^{-1} (2 gallons per minute) as described in MIL-F-24385F [4]. A larger diameter inlet tube is placed in the nozzle to increase the liquid flow rate to 11.36 L min^{-1} (3 gpm) as needed.

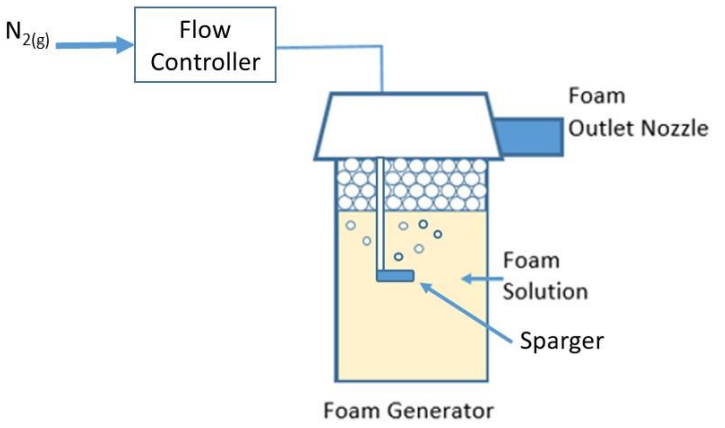

Figure 19. Foam generation by using a porous disc sparger.

The foams are characterized by measurements of initial bubble size, initial expansion ratio, and liquid drainage rate versus time at bench scale and large scale. Expansion ratio is the volume of foam per unit volume of liquid contained in the foam. Expansion ratio is measured by generating a fixed volume of foam into a graduated cylinder and measuring the foam's mass, which is converted to liquid volume using the density of water. Foams are generated with air externally using the extinction apparatus at a constant foam flow rate between 950 to 1000 mL min^{-1} and fed directly to fill the glass container of a Dynamic Foam Analyzer (DFA100, KRUSS GmbH, Matthews, NC) shown in Figure 20 for the bench-scale measurements. The DFA container (40 mm diameter, 25 cm height cylinder) has part of its walls (inner and outer) shaped flat. The flat surface is in contact with the bubbles of the foam. A prism attached to the flat surface reflects light forming a mirror image of the foam-surface bubbles at a video camera's focal plane. The camera is placed 13 cm from the top of the foam column. Starting within one minute of the foam generation, the video images are continuously analyzed by the computer software (ADVANCE) to provide plots of bubble size distributions, average bubble size, and the position of foam-solution (drained solution) interface with time. In additions to the bubble size distributions, the plots provide bubble coarsening and liquid drainage rates from the 25 cm height foam column.

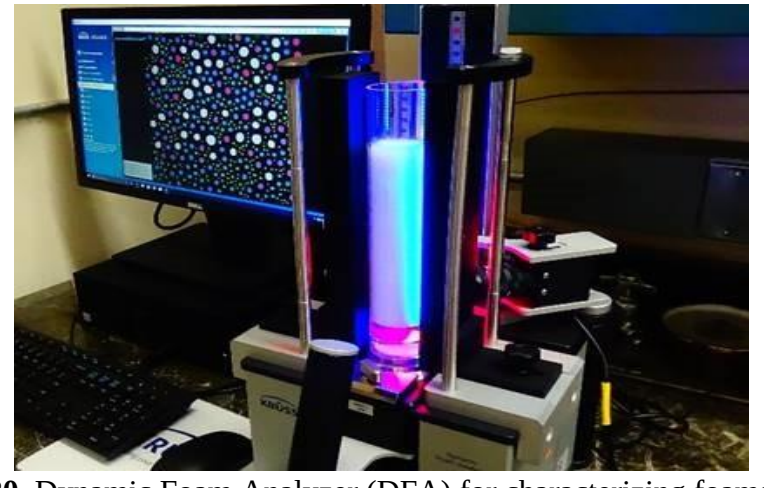

Figure 20. Dynamic Foam Analyzer (DFA) for characterizing foams.

Foam generated at large-scale is measured differently than foam collected for characterization at bench-scale. As prescribed in MilSpec [4], foam is sprayed on to an aluminum plate and the foam is collected into a rectangular container for characterization. The foam fills a rectangular glass container (4.2 cm x 4.2 cm x 30.5 cm) affixed with a millimeter ruler positioned in front of a digital camera (Nikon DSLR) placed at 13 cm height of the 30.5 cm foam column. Images of the foam in the column with the ruler were taken within two minutes of the foam being collected. The diameter of 50 to 100 bubbles for three independent images (150 to 300 total bubbles) were measured using open source software (ImageJ). The liquid drainage rate was measured by collecting a 28 cm height column of foam into a 500 mL graduated glass cylinder (5 cm diameter) and measuring the change in liquid level at the base of the container with respect to time.

3.9. Foam Degradation and Fuel Transport Methods

We measured foam degradation following a procedure similar to those described elsewhere [30] and shown in Figure 21. Figure 21 depicts foam degradation rate. The foam height is measured as a function of time in a 100 mL glass beaker (5.0 cm diameter) in a water bath (150 mL) controlled by using a heating tape and a thermostat set at 60^{o}C, based on our previous measurements of the foam-pool interface temperature during fire extinction [33]. We then poured 50 mL of preheated heptane liquid into the beaker using a funnel, leaving a head space of 4 cm height to accommodate the foam layer. Foam was generated at a constant foam flow rate between 950 to 1000 mL min^{-1} using nitrogen gas flow of 900 mL min^{-1}. Foams were generated a by the sparging method and fed directly into the beaker. A spatula was used to scrape excess foam from the top of the beaker, forming an even 4 cm foam layer on top of the preheated liquid fuel. We were careful to keep the water bath level just below the foam-fuel interface in the beaker so that the foam is not heated by the water bath directly. A video camera monitored the foam height over time. We determined the thickness of foam by measuring the height of the top surface of the foam layer and the liquid fuel surface seen in the recorded video. In the cases where a gas bubble or “gap” lifted the entire foam layer from the liquid fuel surface, the volume of the gap was excluded from the total foam height. The “gap” is a result of foam bubbles bursting and coalescing to form a single bubble that spans the width of the container when in contact with the liquid fuel [30]. Thus, the gap contains the nitrogen that was inside the foam bubbles along with warm fuel vapor.

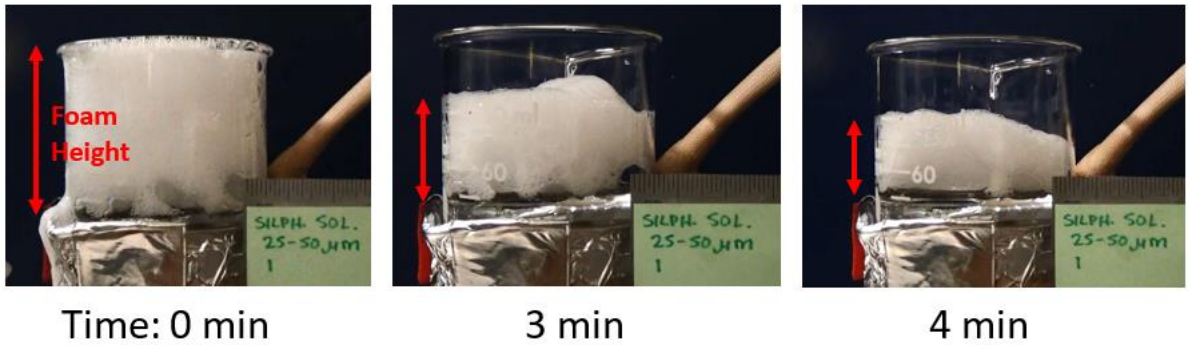

Figure 21. Measuring change in the height of 4 cm thick foam layer placed on a heptane pool maintained at a constant temperature of 60^{o}C versus time [30].

Schaefer et al. [27, 28] used a flux chamber to measure fuel vapor suppression by AFFF and a fluorine-free foam (RF6) in the absence of a fire. They also measured times for ignition of vapors

permeating through a foam layer on top of heptane and gasoline fuel pools at room temperature. We designed new flux chambers to capture new phenomena that had not been monitored before in flux chamber designs. The chambers were designed to measure fuel vapor permeation rates at small times through foams covering hot fuel pools [50]. We monitor fuel transport over a heated fuel to emulate aspects of a flame environment. We also monitor changes in foam height with time during the fuel transport experiment to understand how differences in collected flux data may be related to differences in foam lifetime versus fuel vapor diffusion effects within the foam.

Our chamber designs consisted of a two piece flux chamber initially as described in detail in reference [29]. However, challenges with hot fuel led to the need for an updated chamber material. Glass was chosen as an initial material to minimize effects and data was successfully collected over heated fuel in this apparatus [50]. A water bath was used to heat fuel contained in the bottom piece, foam was then generated above the fuel. A top piece was then secured to the bottom which contained a sparger and outlet to sweep fuel vapors above the foam out to an FTIR for gas analysis. This glass flux chamber was roughly 5 cm in diameter and cylindrical. The curved sides of the container and large clamping mechanism (described and shown in reference [50]) made it difficult to monitor changes in foam height with time and a new chamber was designed.

A new fuel transport apparatus was made using a 250 mL thin-walled, transparent, PET (polyethylene terephthalate) rectangular plastic bottle, shown in Figure 22 on the right. The flat shape enables an undistorted photographing of foam thickness during the test. The PET bottle was cut horizontally to create a top and bottom piece. The top piece had a 1/8" pipe fitting hole drilled and tapped into it to feed gases from the fuel transport container into an infrared spectrometer (FTIR). A ¾" pipe fitting hole was drilled and tapped into the screw cap of the bottle to hold a nitrogen sparger (frit 3 cm diameter, 25-50 µm pore size). The glass tubing of the nitrogen sparger was held in place with a compression fitting (Cajon) in union with a bored through ¾" pipe fitting. Two Plexiglas plates were milled out to fit snuggly over the cut ends of the PET bottles and sealed to the bottle with plastic adhesive (Weld-On). Guide holes were also drilled on two sides of the plates to hold small screws, ensuring the top and bottom piece were directly on top of each other while closing. To close the top and the bottom piece, a flexible 1/8" neoprene gasket was placed in between the top and bottom layer. Four spring clamps were used to seal the two pieces together in a closed, air-tight configuration.

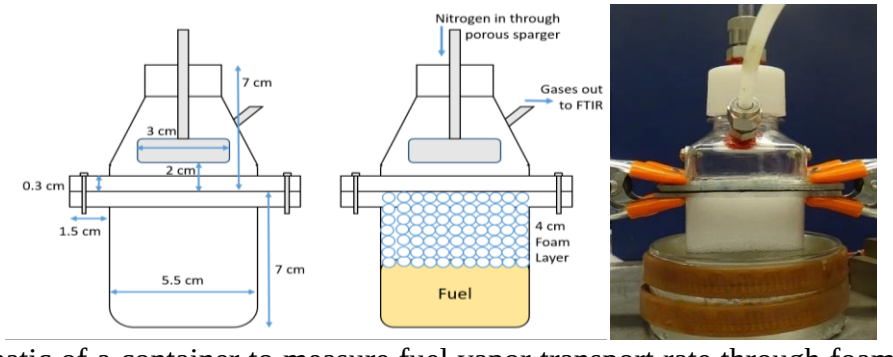

Figure 22. Schematic of a container to measure fuel vapor transport rate through foam laid on a heated fuel pool with nitrogen gas fed through a porous disc to sweep the fuel vapors emanating from the foam surface in a stagnation flow (left), schematic of assembled test (center), image of actual container with a 4 cm (initial thickness) foam layer and the bottom piece placed in a hot water bath to maintain constant pool temperature (right).

Fuel transport was meausred by pouring 90 mL of heptane into the bottom piece. The bottom piece was then placed in a water bath, thermostated with heating tape to ensure a fuel temperature of 60°C. The water bath only extended to the height of the fuel layer, actively heating the fuel pool, but not the foam. Foam solution was then poured into a foam generator that generated foam using a 25-50 µm sparger. Foam was generated into the bottom piece above the fuel layer and a timer was started, indicating time 0 for foam lifetime. Foam filled the headspace of the bottom piece and was levled with a spatula, creating a flat 4 cm layer. The neoprene gasket and top piece were then lowered onto the bottom and sealed with 4 spring clamps on the 4 corners of the container. The sparger in the top piece fed nitrogen into the container at a flow rate of 500 mL/min. The stream was then opened to the FTIR and the time between when foam entered the container and when the FTIR began collecting data was recorded. This value was then added to the initial time of the FTIR data (40-100 seconds). The FTIR had an additional by-pass of nitrogen, 100 mL/min, resulting in a total flow of 600 mL/min into the FTIR. The FTIR measured fuel concentration by collecting vapors in a 10 cm long heated gas cell (50°C), comparing observed signal to a reference standard of n-heptane, 1000 ppm, 50°C, 10 cm pathlength. The measured concentration of fuel by FTIR was converted to molar flux by multiplying the heptane vapor concentration (volume fraction, # ppm/1000000) with molar flow rate (4.45×10^{-4} mole sec^{-1}) of total nitrogen flowing (600 mL min^{-1}) through the FTIR and dividing by the pool surface area.

Foam height was measured using a camera oriented perpendicular to a rectangular face of the container. A ruler was placed in the same plane as the rectangluar face in order to have a pixel to distance ratio for all images collected. Foam lifetimes in the fuel transport container are not expected to mimic foam degradation measurments collected in a beaker. The closed container creates a moist environment around the foam and provides vertical wall space above the foam. Foam can cling to this space creating a large physical gap between itself and the fuel pool. The gap would not be sustained as long as it is in the absence of the excess wall space or a moistened environment. We therefore only use the degradation data to better understand fuel transport rates rather than for determing its relationship to fire suppression which is in open space. The measurement of foam height with time while simultaneously collecting fuel transport data will allow for the derivation of intrinsic fuel transport profile for a given fuel-surfactant system. This will ultimately separate effects of surfactant structure that may be related to foam stability or fuel transport, allowing surfactant structural optimization for either mechanism of foam fire suppression.

3.10. Bench Scale Fire Extinction Apparatus

To measure the extinction performance of multiple formulations in a cost-effective manner, a benchtop pool fire apparatus was developed at NRL as described in detail elsewhere [33,34,44,50], and discussed only briefly here as shown in Figure 23.

A 19 cm diameter, 11 cm deep Borosilicate glass container with an outlet at the bottom was used to contain a fuel pool. A heptane fuel layer (1 cm thick) was formed on top of a water layer (9 cm deep) with a 1 cm lip above the fuel layer to accommodate the foam. Foam was generated and applied onto the center of the pool at a constant foam flow rate. The constant foam flow rate was achieved by maintaining constant air flow and by the liquid leveling system that continuously transfers additional solution from the leveling vessel to the foam generation vessel. The liquid level was maintained at 3 cm above the sparger disc. Extinction experiments consisted of a pre-burn of the heptane pool for 60 seconds followed by the foam application at a constant flow rate

until fire extinguishment. In cases, when no extinction event was observed at low foam flow rates, foam flow was turned off after 180 seconds to prevent overflow of the foam. As the foam drained liquid into the fuel, fuel overflow from the extinction vessel was prevented by lowering the tygon tube connected to the bottom of the extinction vessel to a specified height as shown in Figure 23.

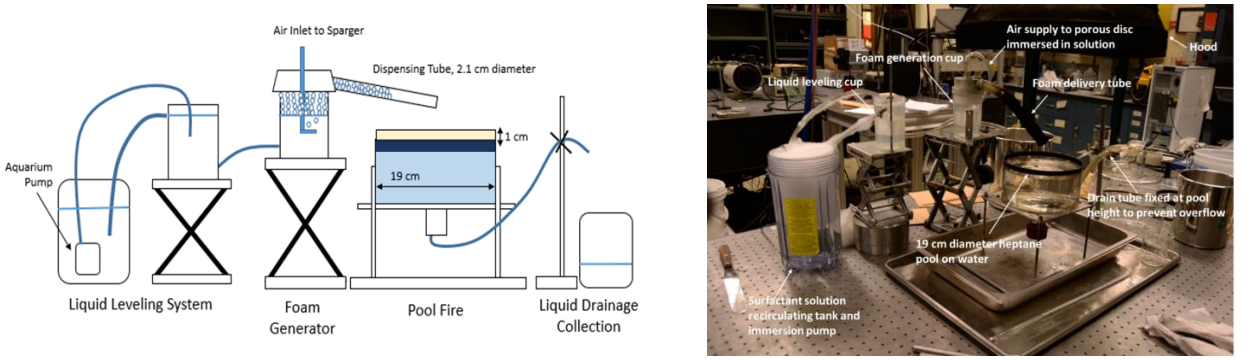

(a) (b)

Figure 23. (a) Diagram of a bench-scale extinction apparatus; 1 cm heptane layer placed on top of water layer and 1 cm lip to accommodate the foam layer [44], (b) Picture showing foam generation, leveling system, and pool fire [50].

Centar vesus Edge Deposition of Foam:

Foams were deposited at a fixed position on the pool at a constant rate. At the beginning of the project, the galss delivery tube was placed at the center of the pool and the foam was deposited until the fire was extinguished. It worked fine except at very low foam application rates. At the low foam flow rates, the galss tube got very hot and foam disintegrated to mostly solution emerging from the glass tube. Therefore, we changed the protocol to depositing the foam at the edge (about 1" inside from the lip of the container). These extinctions are labled as EDGE in the extinction time versus foam application rate plots.

3.11. Large Scale Testing

Six foot diameter pool fire tests outlined in MIL-F-24385F [4] are performed as shown Figure 24. Both gasoline and heptane are used at different solution application rates. Only tests related to fire extinction performance are performed. An active firefighter is involved in spraying the foam on to the pool surface unlike in the bench-scale tests. Fire extinction tests are performed on the candidate formulations following tests with AFFF for comparison using fresh water at full strength [4]. The extinction time is measured from the time of initiating deposition of the foam onto the 2.6 m^2 (28 ft^2) heptane pool fire, which has been burning 10 sec (pre-burn) before starting the foam application, until the time of extinguishment. The burnback test involves a reignition of the extinguished pool fire after 90 sec of total foam application (includes time to extinguish fire). The foam covered pool is reignited by lowering a 30.5 cm diameter pan of burning heptane-fuel into the center of the pool and recording the time for fire re-involving 25% of the pool surface. The film and seal test is conducted by covering the cyclohexane fuel surface in a small container with foam, then inserting a wire screen to scoop out the residual foam, waiting 60 sec then placing a small butane lighter flame approximately 1.27 cm (½ inch) above the surface to ignite the fuel vapors permeating through the water-surfactant film on the fuel surface. If the cyclohexane fuel does not ignite, it receives a pass [4].

Figure 24. 28 ft^2 pool fire extinction test

4. RESULTS AND DISCUSSION

4.1. Development of Reference AFFF

Commercial AFFF solutions contain numerous proprietary components preventing us from isolating the effect of a surfactant on fire extinction from other components in the solution. We need a simple, well-characterized, and known chemical structures to constitute a Reference AFFF formulation to establish baseline properties and performance. We demonstrated that a simple four-component Ref AFFF formulation matches the small and the large-scale fire extinction performance of a commercial AFFF [44]. This Ref AFFF formulation is prepared by mixing 0.2 % Glucopon 215 CS UP (poly-D-glucopyranose with octyl and decyl alkyl chains), 0.3% Capstone 1125 (tridecafluorooctyl sulfonamide alkylbetaine), 0.5% DGBE (diethyleneglycol monobutyl ether) by volume in distilled water. All chemicals are used as supplied. Based on the analytical characterizations of the individual components and the molecular structures of the surfactants contained in the concentrates are shown in Figure 17. The composition of Ref AFFF corresponds to 3.7 mMole/L of the hydrocarbon surfactant, 1.6 mMole/L of the fluorosurfactant, and 29.3 mMole/L of the solvent in distilled water. We examined two other candidate formulations where Triton X-100 (4-{1,1,3,3-Tetramethylbutyl}-phenyl-polyethylene glycol) was used as the hydrocarbon surfactant at two different ratios. A bench-scale fire extinction apparatus using n-heptane as the fuel enabled us to rank the candidate AFFF formulations, which were qualitatively consistent with the ranking exhibited in the large-scale (Milspec 28 ft^2 gasoline pool fire) test despite the differences in foam generation methods and fuels used. Use of a bench-scale foam generation method more similar to the large-scale may improve quantitative comparison of fire extinction at different scales. Both bench and large scale fire extinction tests showed that replacing Triton X-100 with Glucopon 215 CSUP as the hydrocarbon surfactant in the candidate AFFF formulations resulted in the reduction of fire extinction time. The Ref AFFF passed a subset of Milspec criteria relevant to fire extinction.

The Ref AFFF formulation may be used for basic research in the study of foam properties and mechanisms important to fire suppression. Also, the development of simple analytical and small scale inexpensive extinction performance apparatus can be used to more effectively

screencandidate formulations prior to large scale testing. As to the very difficult challenge of replacing fluorocarbon surfactants in AFFF formulations by fluorine-free surfactants, a simple substitution of a fluorine-free surfactant for the Capstone in the Ref AFFF formulation may not rapidly solve this problem. Progress will require more scientific insight as interactions and synergies between candidate surfactants and other formulation components may play a major role in determining foam formation and properties. However, the Ref AFFF formulation can serve as reference point of known composition with MilSpec extinction qualification.

4.1.1. Composition of RefAFFF

Table 1 shows the compositions of three candidate formulations used for making the foams. For a proper comparison of the three candidate formulations, we prepared candidate formulations at concentrations significantly higher (two to five times) than their respective CMC values, which are measured. Based on the above analysis of the individual components, we calculated the actual surfactants' mole ratios and molar concentrations as shown in Table 2, which correspond to the volumetric compositions of the candidate AFFF formulations shown in Table 1. Table 2 defines the Ref AFFF's composition in column four; commercial AFFF's surfactants' contents are proprietary preventing calculation of molar ratios for proper substitution of the fluorosurfactant with alternate surfactant.

Table 1. Candidate AFFF Formulations[1] containing Capstone concentrate (27.5 weight % surfactant), Glucopon concentrate (63.6 weight % surfactant), TritonX-100, and DGBE. The values shown under each column are volume percentages of the individual components (uded as supplied by manufacturers) in distilled water [44].

3:1 Cap/Trit	3:2 Cap/Trit	3:2 Cap/Gluc (Ref AFFF)
0.15 % Capstone	0.3% Capstone	0.3% Capstone
0.05% TritonX100	0.2% TritonX100	0.2% Glucopon
1.0% DGBE	0.5% DGBE	0.5% DGBE

[1]The formulation compositions shown are used for generating foams and for measuring foam and solution properties.

Table 2. Surfactant mole ratios and molar concentrations for the compositions of candidate AFFF formulations shown in Table 1 [44].

Surfactant or solvent	3:1 Cap/Trit	3:2 Cap/Trit	3:2 Cap/Gluc (Ref AFFF)
fluorocarbon/hydrocarbon surfactants (mole ratio)	1:1	1:2	1:2
tridecafluorooctyl sulfonamide alkylbetaine (mMole/L)	0.8	1.6	1.6
4-(1,1,3,3-Tetramethylbutyl)-phenyl-polyethylene glycol (mMole/L)	0.8	3.3	0

poly-D-glucopyranose (mMole/L)	0	0	3.7
diethylene glycol monobutyl ether (mMole/L)	58.7	29.3	29.3

4.1.2. Bench-Scale Fire Suppression Evaluation of RefAFFF

Fire extinction time measurements using the benchtop pool fire extinction apparatus was described in the previous section to compare commercial AFFF and fluorine-free foams. Here, we present fire suppression data for the candidate surfactant formulations and a commercial AFFF, Buckeye. Figure 25 presents time-lapse images of this fire suppression over a 19-cm diameter n-heptane pool fire using a foam application rate of 1500 mL/min for 3:2 Cap/Trit and 3:2 Cap/Gluc formulations and Buckeye. At 0 seconds, the foam is introduced to the pool fire surface after the pool has been burning for 60 seconds. After 12 seconds, Figures 25c, 25k, and 25g show that the 3:2 Cap/Gluc formulation extinguished the fire similar to Buckeye, while the 3:2 Cap/Trit formulation could not completely extinguish the fire even at the highest foam flow rate (1500 ml/min) studied. We noticed fire above the Cap/Trit foam even in the regions of the pool covered with the foam as shown in Figure 25(g). The fire above the foam covered surface of the pool is indicative of fuel leakage through the foam. The fire was extinguished in 25 s using 3:2 Cap/Trit formulation at 1500 ml/min foam flow rate.

Figure 26 compares fire extinction times for the candidate surfactant formulations and Buckeye foams at low and high foam flow rates. Figure 26a and 26b show that the extinction times of 3:2 Cap/Gluc formulation are closest to those for the commercial AFFF, Buckeye. But, the two formulations of Cap/Trit have significantly higher fire extinction times. Only one foam flow rate was tested for the 3:1 Cap/Trit formulation. Figure 26 shows that replacing the hydrocarbon surfactant Triton -100 with Glucopon has reduced the extinction times.

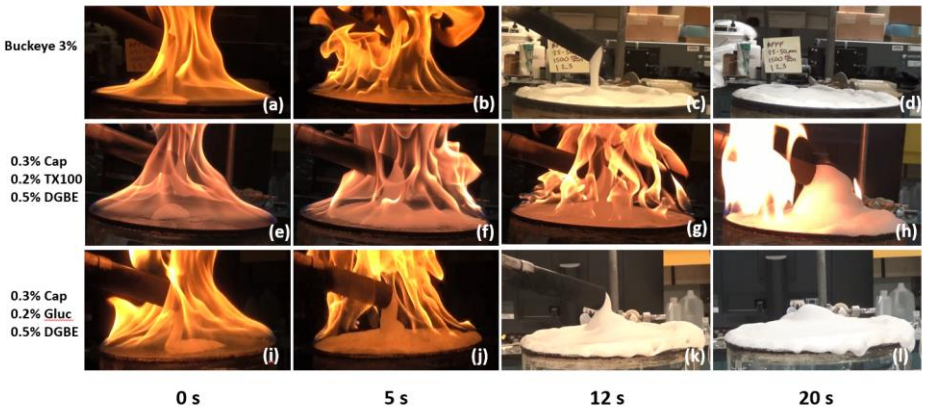

Figure 25. Time-lapse images of Buckeye (a-d), 3:2 Cap/Trit (e-h), and 3:2 Cap/Gluc (i-l) foams extinguishing an n-heptane pool fire at a foam application rate of 1500 mL/min. Images are taken at times 0, 5, 12, and 20 s during extinction [44].

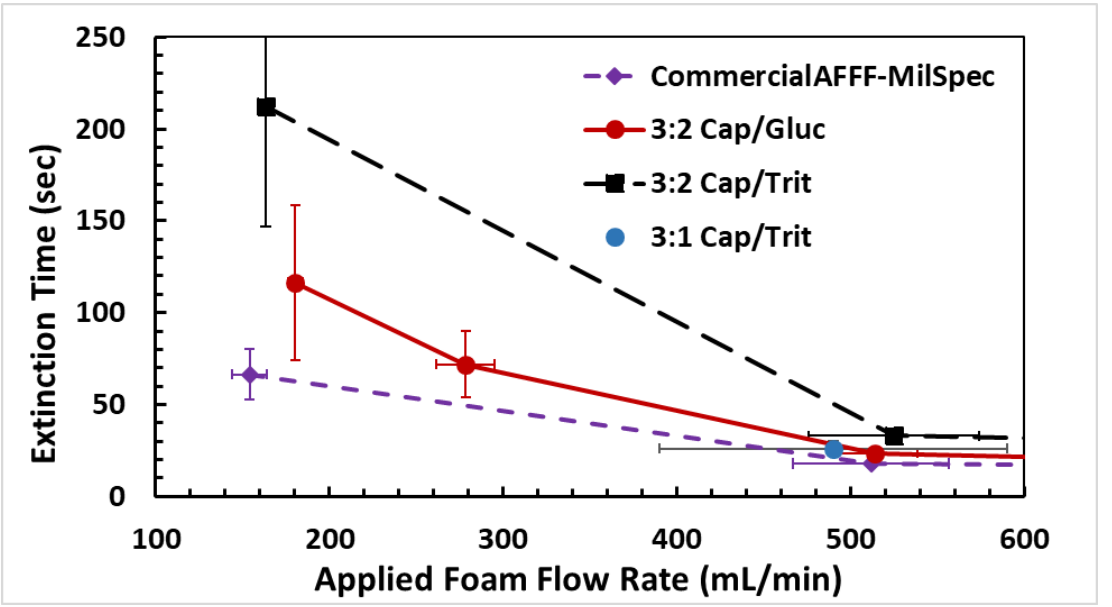

(a)

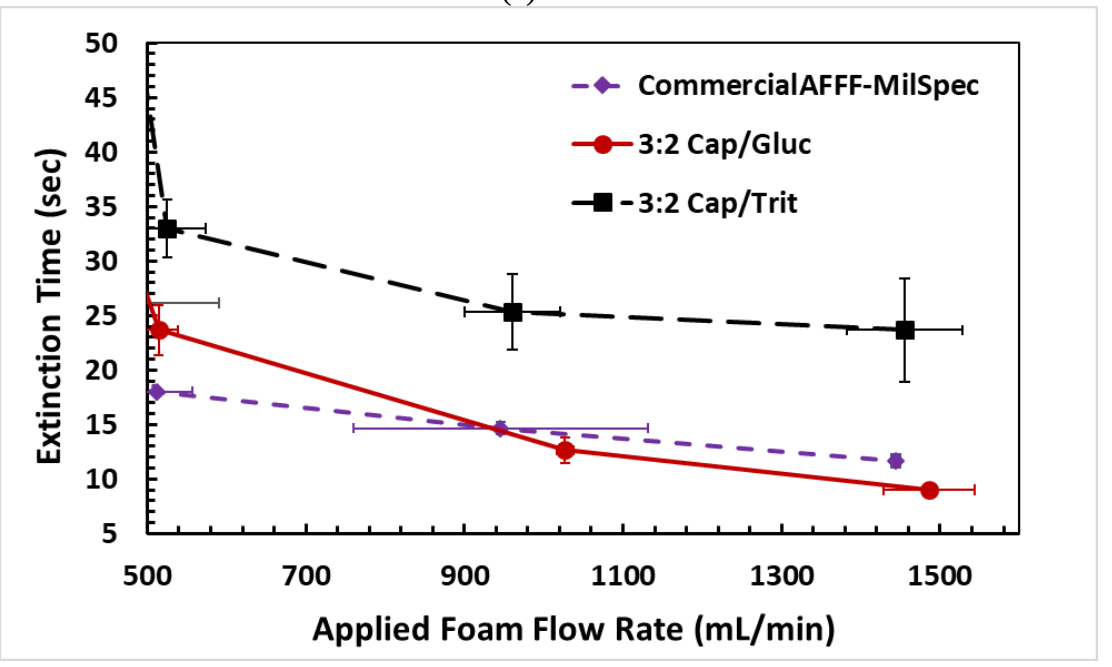

(b)

Figure 26. Bench-scale fire extinction of n-heptane pool fire showing extinction time of candidate surfactant formulations relative to the commercial formulation (Buckeye) (a) at low foam application rates, (b) at high foam application rates [44].

4.1.3. Large-Scale MilSpec Fire Suppression Evaluation of RefAFFF

To further develop the Ref AFFF we progressed from the 0.4 ft^2 bench-scale apparatus with a sparged foam delivery system to the 28 ft^2 MilSpec standard pool fire [4]. We focused on a subset of five required metrics in the MilSpec standard MIL-F-24385 to evaluate the candidate AFFF and a commercial AFFF (Fomtec) formulations wherein we measured five parameters and compared with passing metrics. The parameters measured were (1) 28 ft^2 gasoline pool fire extinction time,

(2) burnback time, (3) film and seal, (4) expansion ratio, and (5) 25% drainage time, and are described in MilSpec standard MIL-F-24385. Results are presented in Table 3.

Both the 3:2 Cap/Gluc and the Fomtec formulations passed all five criteria. Both 3:1 Cap/Trit and 3:2 Cap/Trit failed fire extinction and burn back tests. The results are a liitle surprising in that the commercial AFFF formulations contain 10 to 12 components, but a four component 3:2 Cap/Gluc formulation successfully extinguished a pool fire in under 30 seconds; some of the components in the commercial AFFF are needed to meet all aspects of the MilSpec while the Ref AFFF is designed to meet mainly the fire extinction metrics. This work gives insight into the role of hydrocarbon surfactants in fire suppression in that extinction performance appears to be directly related to the surfactant type.

Table 3. Comparison of candidate AFFF formulations with a commercial AFFF (Fomtec) and MilSpec criteria [44].

MilSpec Test	**Criteria**	**3:1 Cap/Trit**	**3:2 Cap/Trit**	**3:2 Cap/Gluc**	**Fomtec**
Extinction (s)	< 30	54	37	26	23
Burnback (s)	>360	295	358	562	496
Film and Seal	PASS	PASS	FAIL	PASS	PASS
Expansion Ratio	5-10	7.35	7.41	7.46	7.6
25% Liquid Drainage (s)	>150	238	295	317	281

Based on measured fire extinction times, Table 3 shows a ranking of the candidate surfactant formulations that is similar to that found using the bench-scale extinction apparatus, when the full range (150 ml/min to 1500 ml/min) of foam flow rates are considered. The bench-scale apparatus is a qualitative tool able to identify the superior performing surfactant consistent with the large scale test. However, it is unclear as to the ability of the bench-scale test to show quantitative agreement with the large scale test at a fixedfoam application rate per unit area of the pool because of significant differences in foam generation and foam properties relative to the large scale..

Table 4 lists arithmetic average bubble sizes, which show that the air-aspirated foams have 2 to 2.5 times smaller average bubble sizes than the sparged foams for all of the surfactant formulations examined. The initial bubble size distributions at large-scale are likely even smaller than shown in Table 4 because of significant coarsening that could have occurred during the 5 minutes after their generation. Due to issues collecting foam and filming at large-scale, data collection could not begin until 5 minutes into foam lifetime. Among different formulations examined, Table 4 shows that the arithmetic average bubble sizes differ by less than 35% for the sparged and 19% for the air-aspirated nozzle foams, respectively. Table 4 suggests that the differences in surfactant formulations examined in this report have a smaller effect on the bubble size relative to the generation methods. It is also possible that the hydrocarbon surfactant effect on bubble size is small compared to the effect of the fluorosurfactant, whose replacement with a fluorine-free surfactant is the ultimate research goal. Both commercial foams Buckeye and Fomtec were MilSpec qualified and the differences in average bubble sizes are expected to be small.

Table 4. Measured foam properties for the three candidate and commercial AFFFs at bench and large-scales respectively [44].

Scale	Property	3:1 Cap/Trit	3:2 Cap/Trit	3:2 Cap/Gluc	Commercial AFFF[1]
Bench scale	Expansion ratio	10.63 ± 0.44	14.67 ± 2.47	8.19 ± 0.82	6.68 ± 0.92
	Bubble Diameter (mm)	0.35 ± 0.08	0.47 ± 0.03	0.36 ± 0.02	0.37 ± 0.03
	25% liquid Drainage (s)	108 ± 3	55 ± 2	53 ± 2	68 ± 1
Large Scale	Expansion ratio	7.35	7.41	7.46	7.6
	Bubble Diameter (mm)	0.17	0.19	0.16	0.18
	25% liquid drainage	238	295	317	281

[1]Commercial AFFF was Buckeye for bench-scale measurements and Fomtec was used in large-scale measurements. Both Buckeye and Fomtec were MilSpec qualified; MilSpec testing of Buckeye gave expansion ratio of 9.4, 360 s for 25% liquid drainage, 30 s extinction time for 28 ft^2 gasoline pool fire, 500 s for 25% burnback time, and pass for film and seal test.

4.2. Role of Surfactants in AFFF Fire Extinction

In this report, we evaluated fire suppression performance of a fluorocarbon surfactant and two hydrocarbon surfactants, both individually and as mixturesto quantify the role of a surfactant in fire suppression [51]. The fire suppression performance was also evaluated on a large-scale gasoline fire (28 ft^2 US MilSpec), which showed trends consistent with the bench-scale evaluations. To understand how a surfactant affects fire extinction, we examined the surfactant's effect on three different contributing mechanisms; (1) aqueous film formation by measuring the spreading coefficients, (2) fuel-foam layer interactions by measuring foam spread rates, fuel transport rate through a foam layer, and foam layer degradation rate by fuel, and (3) foam structure by measuring bubble diameters, bubble coarsening, and liquid drainage from the foam in the

absence of a fuel [51]. The three contributions are quantified independently in the absence of a fire; it is very difficult to quantify them during the fire extinction measurements. Based on these independent measurements, we found that trends in fire extinction performance among different surfactants can be explained by trends in fuel-foam layer interactions as measured by foam spread rates, fuel transport rates, and foam degradation rates [51]. The measurements for the six formulations show that surfactants that reduce foam degradation and fuel transport through a foam layer covering a hot pool can lead to more rapid extinction of heptane pool fires. A fluorocarbon surfactant is especially effective in suppressing foam degradation and fuel transport rates through a foam by quickly covering the pool, extinguishing the fire rapidly by blocking the fuel supply to the fire. Furthermore, for the surfactants and conditions employed in this work, trends in fire extinction performance among different surfactants did not directly follow trends in aqueous film formation or foam properties [51]. The molecular mechanisms by which a surfactant affects fuel-foam interactions remain unclear and their understanding is needed to design effective fluorine-free replacement surfactants.

4.2.1. RefAFFF Components versus Mixtures

Table 5 shows the five compositions of surfactant solutions contained RefAFFF and their mixtures. The component surfactant solutions were made with 0.5 weight % total surfactant concentrate supplied by the manufacturer, 0.5 weight % DGBE, and the remainder distilled water. The surfactants evaluated individually and as mixtures had critical micelle concentrations well below the 0.5 weight % concentrations in the surfactant solutions. Five formulations were made to compare the fire extinction performance of fluorocarbon, hydrocarbon, and mixtures of the two surfactants. The five-surfactant formulations along with a commercial AFFF, Buckeye 3%, were characterized through foam and solution properties [51].

Table 5. Surfactant formulations; Cap+Gluc215 formulation is also referred to as RefAFFF [51].

Cap+TX100	Cap+Gluc215	Cap	Gluc215	TX100
0.3% Capstone	0.3% Capstone	0.5% Capstone	0.5% Gluc 215UP	0.5% Triton X100
0.2% Triton X100	0.2% Gluc 215UP	0.5% DGBE	0.5% DGBE	0.5% DGBE
0.5% DGBE	0.5% DGBE	distilled water	distilled water	distilled water
distilled water	distilled water			

4.2.2. Bench Scale Fire Suppression with Components of RefAFFF

Figure 27 compares interesting fire suppression behavior between the Cap solution, the RefAFFF, and the Gluc215 solution. At foam application rates less than 500 mL/min, Figure 27(a) shows that the Cap foam suppresses the fire faster than a mixture of Cap with Gluc215 or TX100.. This does not correlate with aqueous film formation being the key player; Capstone alone does not form an “aqueous film” on heptane [5, 12, 14] unlike Cap+Gluc215. For example, at 250 mL/min foam flow rate, Cap foam extinguishes the fire in 40 seconds compared to the 70 to 100 seconds for the surfactant formulations that include TX100 or Gluc215. A similar inconsistency is found in the large-scale results on gasoline discussed later. Furthermore, at a fixed foam flow rate, Figure 27(a) shows that the extinction time increases in the order Cap, Buckeye, Cap+Gluc215 or Cap+TX100, TX100, and Gluc215. There is a significant variation (e.g., up to 75 s at 100 mL/min foam flow rate) in extinction time as indicated by a cluster of three points at low foam flow rates, and the error decreases with increasing foam flow.

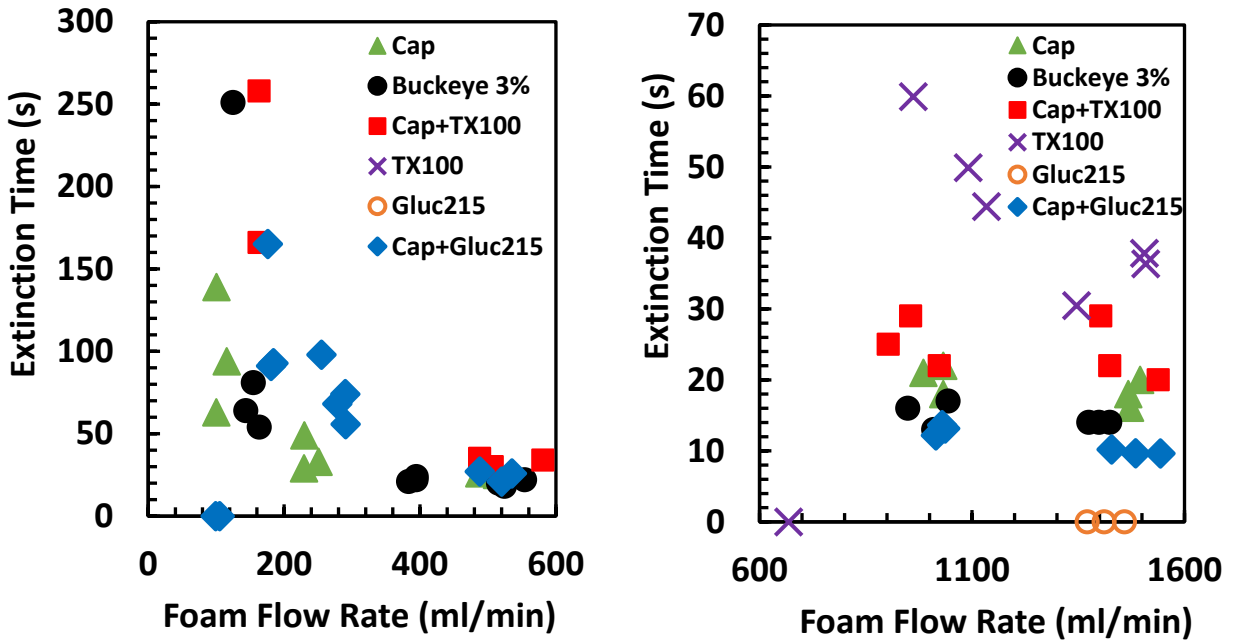

(a) (b)

Figure 27. Bench-scale heptane-pool fire extinction results for foam formulations shown in Table 5 and a commercial AFFF at (a) low foam application rates, and (b) high foam application rates. Points along the x-axis indicate a foam flow rate at which extinction did not occur in 5 minutes. Even though three extinction time data points were collected at each airflow rate, they are presented as individual points in the figure because of the variability in the measured foam flow rates [51].

Above 500 mL/min foam application rates, the fire extinction times for Cap+Gluc215 are slightly smaller by 5 to 10 s than those for the Cap only solution as shown in Figure 27(b); the error in extinction time was 5 s at 1400 mL/min. The surfactant mixture containing TX100 took longer to extinguish the fire than the fluorosurfactant alone at all foam application rates shown in Figure 27. At a fixed foam flow rate, the fire extinction time increases in the order Cap+Gluc215, Buckeye, Cap, Cap+TX100, TX100, and Gluc215. The data in Figure 27 show that the effect of hydrocarbon surfactant on extinction performance depends on the foam application rate. The extinction times in Figure 27 vary nonlinearly with the foam flow rates, and are sensitive to small variations in foam flow rate especially below 500 mL/min. Small variations (< 100 mL/min) in foam flow rate occur despite accurately fixing the air flow rate (to the sparger generating the foams, 1% error) across three repeated measurements. Therefore, we decided to display three repeated experiments at a fixed air flow as individual points in Figure 27 rather than averaging.

One may expect the fire extinction times for the surfactant mixture containing Gluc215 and Cap to be in between the extinction times for the individual surfactants following the law of averages. But, there is a slight synergistic effect between Cap and Gluc215 on fire extinction. Figure 27(b) shows that the mixture (Cap+Gluc215) foam has slightly more rapid extinction than Cap and very rapid extinction relative to Gluc215 for foam application rates greater than 500 mL/min. Also, one may expect a mixture of Cap and TX100 to exhibit more rapid fire extinction than the Cap+Gluc215 solution. This would be because TX100 can extinguish the fire at some

foam flow rates whereas Gluc215 cannot as shown by the open circle along the x-axis in Fig. 2(b). Figure 27 shows the opposite behavior because of slight synergism between Cap and Gluc215 and no apparent synergism with TX100. Although slight synergism between Cap and Gluc215 can be seen at high flow rates, at foam application rates below 500 mL/min the Cap solution extinguishes faster than the Cap+Gluc215 solution. This is because Cap foam is very wet and the foam spreads faster as will be discussed in more detail later in the report.

4.2.3. Large Scale Fire Suppression with Components of RefAFFF

Fire extinction time of a 28 ft^2 gasoline pool fire, burnback time, aqueous film formation by film and seal test, expansion ratio, and 25% liquid drainage time are recorded in Table 6 [51]. The first row lists the necessary criteria for a foam to pass MIL-F-24385F and the other rows list the measurements made for different formulations. The film and seal test was measured with cyclohexane. Only one test per surfactant formulation was performed in view of the limited resources and materials required for the large-scale.

Table 6. Large-scale pool fire data collected over a 28 ft^2 gasoline pool fire, with foams generated from some of the surfactant formulations listed in Table 1 using an aspirated nozzle at 2 gpm solution flow rate as detailed by MIL-F-24385F.

Foam	**28 ft^2 Ext Time (s)**	**Burnback Time (s)**	**Film and Seal**	**Expansion Ratio**	**25% Liquid Drainage Time (s)**
MilSpec Criteria	*< 30*	*> 360*	*No flame*	*5-10*	*> 150*
Cap+TX100	37	358	Flame	7.41	295
Cap+Gluc215	26	562	No flame	7.46	317
Cap	24	505	No flame	7.80	695
Buckeye 3% (2003)	30	500	No flame	9.40	360

Large-scale extinction results given in Table 6 show similar fire extinction times for the fluorocarbon surfactant (Cap, 24 s) without and with a glycoside hydrocarbon surfactant (Cap+Gluc215 , 26 s), and the commercial AFFF (Buckeye 3%, 30 s). The fluorosurfactant (Cap) solution also shows a burnback time similar to the commercial AFFF, and the longest drainage time of the four formulations. This limited test series shows that the fluorosurfactant solution, without a hydrocarbon surfactant, rapidly suppresses a gasoline pool fire, passing the MilSpec requirements shown in row 1 of Table 6 and is consistent with the tests performed by Tuve et al. [1, 5]. This is inconsistent with spreading coefficient values; the Cap solution has a smaller spreading coefficient than Cap+Gluc215 by 2.3 mN/m on cyclohexane (0.9 mN/m smaller for gasoline, as will be shown later in the paper). The measurements also show that the fire extinction time increases and burnback time decreases when the hydrocarbon surfactant is switched from Gluc215 to TX100. The effect of the identity of the hydrocarbon surfactant on fire extinction is significant. Clearly, a surfactant's effect on fire extinction is critical and the fluorocarbon

surfactant is so effective that a simple mixture with a solvent can meet one of the most stringent MilSpec fire performance for a 28 ft^2 gasoline pool.

4.2.4. Foam Degradation, Fuel Transport, and Foam Spread for Components of RefAFFF

To explain the fire extinction results, foam degradation by heptane and fuel permeation through a foam layer (4 cm thick) covering a hot (60°C) fuel pool were measured in the absence of a fire [51]. Foam degradation is defined as the decrease in foam layer thickness. Change in foam layer thickness due to degradation versus time is plotted in Figure 28. The foam lifetimes at 100% degradation increase in the order Cap+Gluc215, Cap, Buckeye, Cap+TX100, Gluc215 or TX100. Foam degradation data show long foam lifetimes for fluorinated foams, including the commercial AFFF, Buckeye 3%, but rapid foam degradation for foams without fluorocarbon surfactants (Gluc215 and TX100). The hydrocarbon only foams degrade in under 3 minutes. The Cap solution, the Cap+TX100 solution, and Buckeye 3% degrade in a similar time around 35-45 minutes, whereas the Cap+Gluc215 solution degrades in 60 minutes over a heated heptane pool. The rapid foam degradation of hydrocarbon-only solutions provides insight into their limited use as fire suppressing foams unlike the fluorocarbon surfactant containing foams.

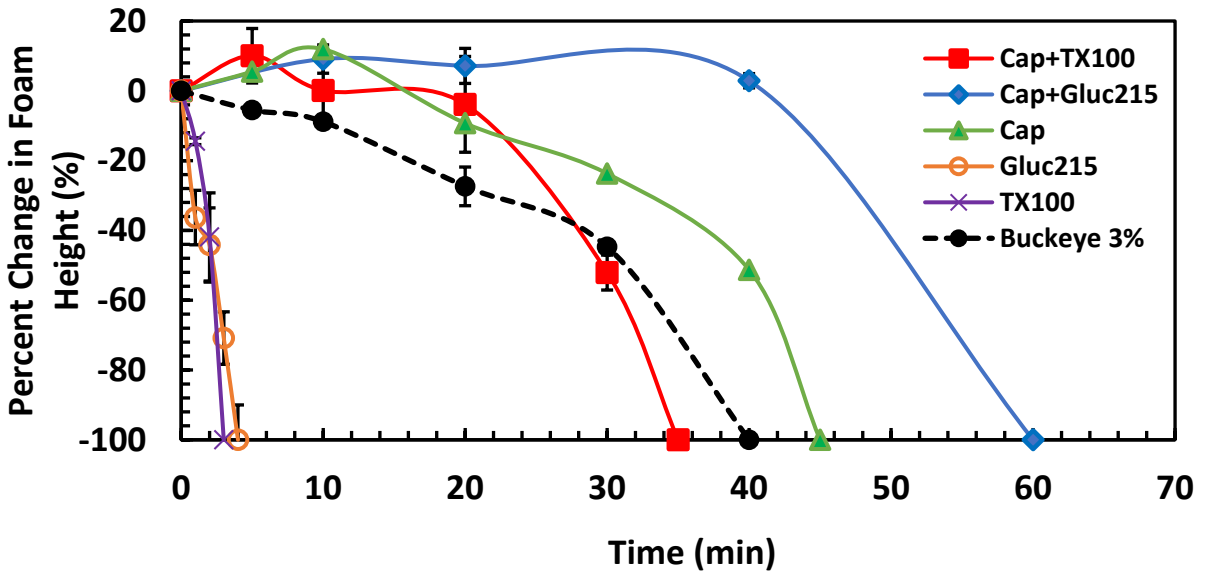

Figure 28. Percent change in foam layer thickness versus time over 60°C heptane for five foam formulations listed in Table 5 and a commercial AFFF, Buckeye 3%. The error bars represent one standard deviation from the averaged value of three trials for each foam [51].

Fuel vapor flux through foams were also quantified for the six foams as shown in Figure 29. The fuel fluxes increase in the order of Cap+Gluc215, Cap or Buckeye, Cap+TX100, Gluc215, and TX100 at ten minutes time. The measured fuel flux for the Cap foam was found to be comparable to that of a commercial AFFF. Synergism between Capstone and Glucopon 215 UP is seen in fuel transport in Figure 29; the Cap+Gluc215 foam had about half the fuel flux of the Cap foam and more than 10 times smaller flux than the fuel flux of the Gluc215 foam after 6.7 min. This synergism is not seen between Capstone and Triton X100, similar to the lack of synergism in foam degradation between the two individual surfactants. The measured fuel flux for the Cap+TX100 foam is in between the fuel flux for the TX100 and Cap foams. The addition of Triton

X100 to Cap increases the fuel flux by a factor of 2 but has only a small effect on foam degradation. Even though synergism between fluorocarbon surfactants and hydrocarbon surfactants has been shown in spreading and wetting [28], to our knowledge, Figure 29 is the first report of synergistic enhancement in fuel transport.

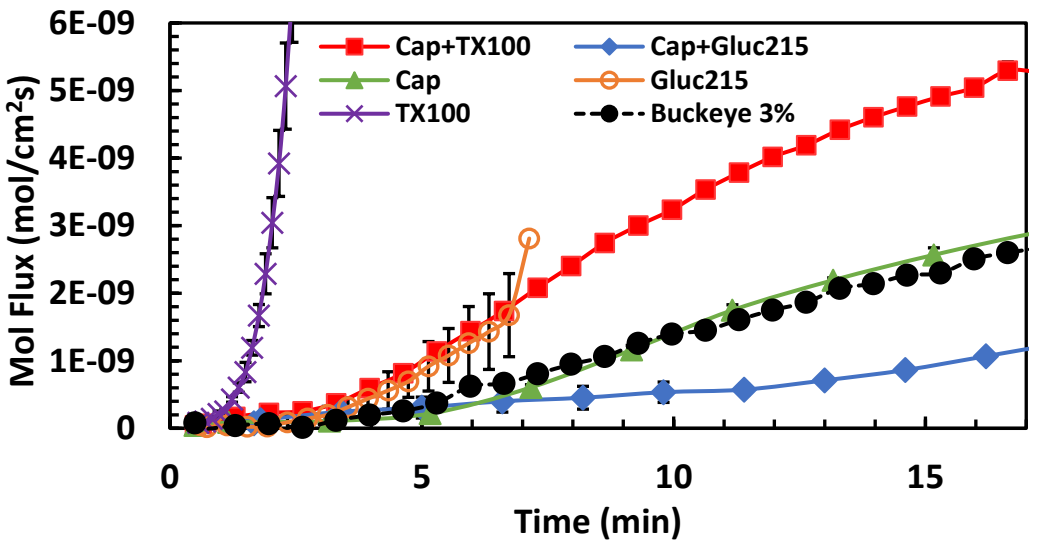

Figure 29. Fuel flux over time through a foam layer (4 cm initial thickness) covering a heptane pool at 60°C for the five formulations shown in Table 5 and Buckeye 3%. The error bars represent one standard deviation from the averaged value of three trials for each foam [51].

During an extinction experiment, foam is applied at the center of a burning heptane pool at a constant rate. For some surfactant formulations, typically a thin layer of foam spreads initially and covers the entire pool, coverage time is noted based on visual observation. However, the pool continues to burn after complete coverage. As the foam application continues, the foam layer builds up and thickens (visually) near the center where the fire is extinguished. But, the edges of the pool continue to burn until a thicker foam layer builds and extinguishes the edge flames, and the extinction time is noted. Figure 30 plots pool coverage and extinction times versus foam flow rates for the individual surfactant solutions in Figure 30(a) and for the mixtures as well as Buckeye 3% solutions in Figure 30(b).

Figures 30(a) and (b) demonstrate that the foam spreading time (not aqueous film spread time) decreases as the foam application rate increases. At low foam flow rates, Cap foam spreads faster on the pool compared to Cap+Gluc215 and the other four formulations; Cap spreads in 25-70 s compared to other formulations, which could not cover the pool surface at 100 mL/min foam flow rate in Figure 30. The reasons are due to unique foam properties of Cap at very low foam flow rates that are used in the sparging method. For Cap only formulation, we found that the expansion ratio decreases from 8 to 4 as the foam flow rate is decreased. For most surfactant formulations, the expansion ratio typically increases from 7 to 12 as the foam flow rate is decreased because foam accumulated in the foam generation cup drains liquid for a longer time before exiting on to the burning pool. We also found that the expansion ratio of Cap+TX100 foam remains high (13) as the foam flow rate decreased.

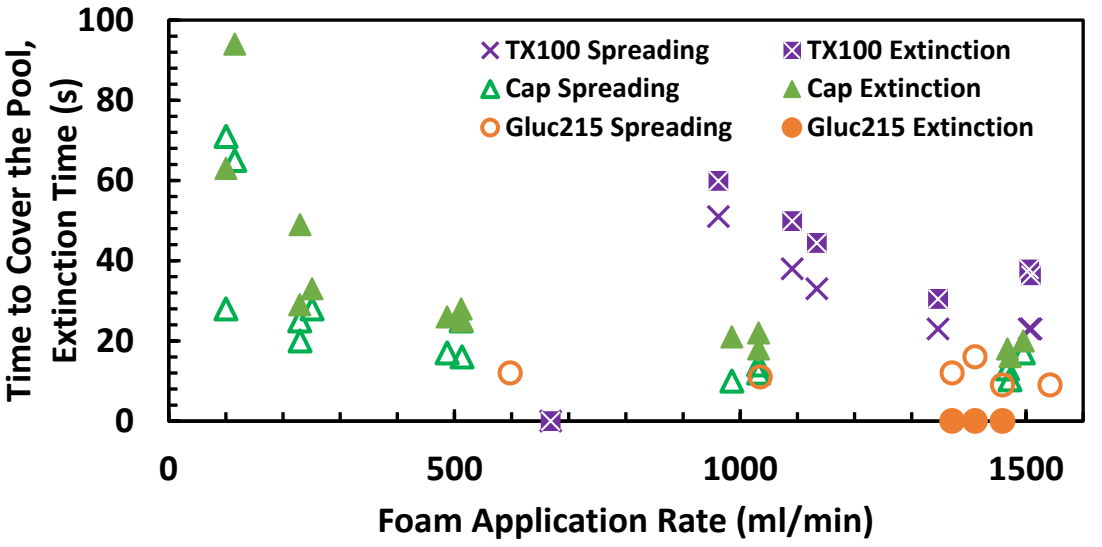

(a)

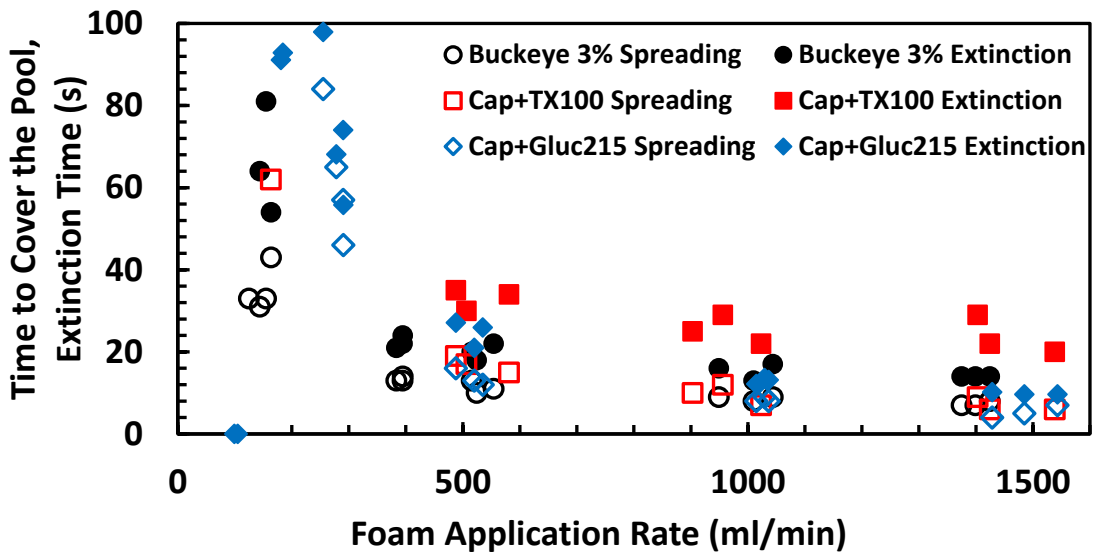

(b)

Figure 30. Time for full coverage of a 19 cm heptane pool surface and extinction times for foams generated from the (a) individual surfactants and (b) the surfactant mixture solutions at various foam flow rates. Three extinction-time and coverage-time data points were collected at each airflow rate and are presented as individual points in the figure due to variability in the measured foam flow rates. Data points shown along x-axis indicate foam flow rates where no extinction occurred; the figures show all pool coverage data but not all of the corresponding foam flow rates where extinction did not occur [51].

Trends in fire extinction among the surfactant formulations can be related to the trends in foam degradation, fuel transport, and foam spread rates. A surfactant can affect foam degradation by fuel and fuel vapor transport through foam, which can affect the foam spread rate and fire extinction time depending on the foam application rates. Figure 31(a) shows fuel transport times

as functions of foam lifetimes for different surfactant formulations. The fuel transport times are defined as times to reach the lower flammability limit of 1.1 volume % at the foam surface and is obtained from Figure 29 as time to reach a corresponding fuel flux of 5.4 x 10^{-9} mol/cm^{2}s. The fuel concentration of 1.1 volume % is 28 times smaller than the vapor pressure (28 volume %) of heptane at 60ºC. An increase in foam lifetime increases the fuel transport time or decreases the fuel flux through a foam covering a pool. As the foam degradation is decreased, foam can better maintain the barrier to fuel vapor transport through the foam layer, and surfactants that decrease foam degradation decrease fuel vapor transport rate or increase the fuel transport time. Figure 31(b) shows the foam flow rates needed to achieve a 30 s fire extinction time as function of fuel transport times for different surfactant formulations; the foam flow-rate values are obtained from Figure 27 that shows extinction time as a function of foam flow rate. The smaller the foam flow rate at 30 s extinction, the better fire extinction performance as the foam can rapidly suppress the fire with minimal amount of foam. As the fuel transport time is increased, fuel transport rate through the foam layer is decreased. As the rate at which fuel feeds the fire is decreased, the fire is extinguished faster and the foam flow rate needed to achieve 30 s extinction decreases. Figure 31(b) shows that the surfactants that decrease fuel transport rates decrease fire extinction time.

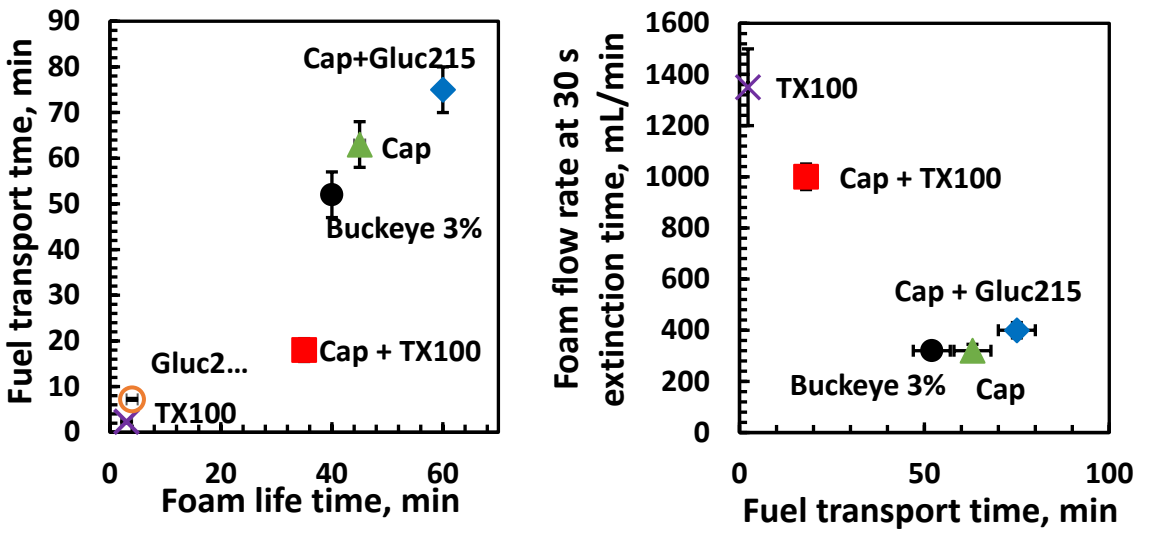

(a) (b)

Figure 31. (a) Foam transport time for heptane vapor concentration to reach the lower flammability limit 1.1 volume % (or flux 5.4 x 10^{-9}mole/cm^{2}s in Fig. 4) on a foam surface versus foam lifetime, (b) foam application rate needed to achieve 30 s heptane-fire extinction time versus fuel transport time. Fuel transport times are longer than foam life times because foams lasted longer in the closed chamber used in the transport measurements than in the open beaker used for foam life time measurements [51].

When foam application rate is much larger than foam degradation rate, foams spread quickly to cover the pool, and the trends in fire extinction time are qualitatively consistent with the trends in fuel transport. The extinction times increase as the fuel transport rates increase in the order

Cap+Gluc215, Buckeye, Cap, Cap+TX100 at foam application rates greater than 500 mL/min in Figures 27 and 29. Synergistic effects between Cap and Gluc215 lead to half the fuel flux for the mixture Cap+Gluc215 compared to Cap and resulted in small synergistic effects in fire extinction times for the mixture. When the foam application rate is comparable to or smaller than the foam degradation rate, foam spread is affected by foam degradation. The trends in pool coverage times are largely consistent with measured foam lifetimes, and the coverage times increase in the order Cap or Buckeye, Cap+TX100, Cap+Gluc215, TX100, and Gluc215 at a foam flow rate of 300 mL/min in Figures 28 and 30. At very low foam flow rates (100 mL/min), Cap foam has low expansion ratio (4.5) and spreads faster than Cap+Gluc215 mixture as shown in Figure 30, despite the slightly longer (by 30%) foam lifetime of the mixture. Fire extinction times follow the same trends as in pool coverage times in Figure 30. They can be influenced by both foam degradation and fuel transport, which vary significantly among the surfactant formulations.

In general, foam degradation rates, fuel transport rates, foam spread rates, and fire extinction times for surfactant mixtures, Cap+TX100, Cap+Gluc215, are closer to the values measured for the fluorocarbon surfactant, Cap, than to the individual hydrocarbon surfactants (TX100, Gluc215). The two hydrocarbon foams degrade so rapidly by heptane, that their pool coverage times are influenced greatly by foam degradation even at high foam application rates (1500 mL/min). The fire extinction times for TX100 are not completely consistent with its similar foam lifetime and higher fuel transport rate than those for Gluc215. This could be due to the influence of slow spreading dynamics of TX100. At 1400 mL/min foam flow rate, we noticed that the TX100 foam forms a thick layer that spreads slowly exposing a smaller area of the foam to the fuel pool, which could result in reduced degradation by the fuel, unlike Gluc215 foam, which spreads as a relatively thin layer covering the entire pool area relatively quickly. For a quantitative relationship, one must investigate the dynamics of foam application, foam spread, fuel transport, foam degradation, and fire suppression. Also, heat transfer from fire to the foam can increase foam degradation and fuel transport rates during the fire extinction process. Heat effects on foam degradation and fuel transport should be included in the above analysis in future works.

4.2.5. Aqueous Film Formation with Fluorocarbon Surfactant Formulations

Aqueous film formation is thought to be essential for forming an effective barrier to block the flow of fuel vapors from the pool surface to the fire, leading to rapid fire suppression. Tuve [5] reported that a fluorosurfactant only solution did not form an aqueous film on a n-heptane pool. However, Figure 27(a) shows that the Cap foam suppresses a heptane fire more rapidly than the rest of the formulations without the aqueous film formation on heptane. In an effort to correlate aqueous film formation to the bench-scale extinction results, spreading coefficient data were collected over heptanes (mixture of isomers, Tilley Chemical Co., Middle River, MD). Even though the film and seal test discussed under MilSpec tests in Table 6 shows the formation of an aqueous film on cyclohexane (except for Cap+TX100), one must measure the spreading coefficient for the same fuel used in extinction experiments. Because heptane is used in the bench-scale tests and gasoline in large-scale tests described in this paper, the film spreading coefficients were calculated for heptane and gasoline fuels.

The measured surface tension data in Table 7 show that the formulations containing a fluorocarbon surfactant have lower surface tensions than the individual hydrocarbon surfactants (Gluc215 and TX100) consistent with the values reported in the literature [28]. Also, mixtures of

hydrocarbon and fluorocarbon (Cap) surfactants have a lower interfacial tension with heptane (1-3 mN/m) than Cap, which has an interfacial tension above 5 mN/m consistent with previous reports. More importantly, the fluorocarbon solution (Cap) has a negative spreading coefficient on heptane indicating a lack of aqueous film formation and is consistent with the observation of the lack of a film on an n-heptane pool surface reported by Tuve [5]. In contrast, Cap+Gluc215 has a positive spreading coefficient on heptane indicating aqueous film formation on a heptane pool. Regardless of the spreading coefficients, both Cap and Cap+Gluc215 formulations extinguished a heptane pool fire effectively as shown in Figure 27. For gasoline, Table 8 shows positive spreading coefficient data for the Cap and Cap+Gluc215 solutions consistent with the film and seal test results reported in Table 6. However, Cap has a smaller spreading coefficient than Cap+Gluc215 and yet, Cap and Cap+Gluc215 extinguished the fire in 23 and 26 seconds respectively as shown in Table 6. Therefore, there appears to be no direct or consistent correlation between spreading coefficients and fire extinction for the six formulations listed in Table 5. However, direct measurements of aqueous film under fire conditions are needed to quantify its contribution to fire extinction and are very difficult to perform.

Table 7. Measured surface tensions and interfacial tensions between heptane and different surfactant formulations, and Buckeye 3% at 16°C. The film-spreading coefficient given by Eq. (1) was calculated using the measured surface tension of heptane, 20.4 mN/m at 16°C [51].

Foam	Surface Tension (mN/m)	Interfacial with Heptane (mN/m)	Spreading Coefficient (calculated, heptane)
Cap+TX100	16.8 ± 0.5	2.9	0.7
Cap+Gluc215	16.7 ± 0.5	1.9	1.8
Cap	15.3 ± 0.5	5.2	-0.1
Gluc215	31.1 ± 0.5	2.9	-13.6
TX100	27.8 ± 0.5	2.4	-9.8
Buckeye 3%	16.4 ± 0.5	1.5	2.5

Table 8. Measured interfacial tensions between cyclohexane, gasoline, and two formulations: Cap and Cap+Gluc215. The film spreading coefficient given by Eq. (1) was calculated using the measured surface tension of cyclohexane and gasoline: 23.9 and 21.5 mN/m respectively at 18°C [51].

Foam	Interfacial with Cyclohexane (mN/m)	Interfacial with Gasoline (mN/m)	Spreading Coefficient (calc, cyclo)	Spreading Coefficient (calc, gasoline)
Cap+Gluc215	1.9	1.0	5.3	3.8
Cap	5.6	3.3	3.0	2.9

4.3. Evaluations of Commercial Surfactants

Commercial surfactants were chosen for two purposes; (1) to rank and identify top performing surfactants based on the foam degradation by fuel, fuel transport through foam, foam spread, and

fire extinction time, (2) to establish a correlation among foam degradation, fuel transport, and fire extinction and examine the hypothesis that reducing fuel transport reduces fire extinction time.

We selected non-fluorocarbon surfactants that are reported or advertised to have good foam-forming properties and that may group into structurally related sets of surfactants, even if they were not designed for firefighting purpose. This enabled us to look for structure-property correlation for guidance toward the more effective surfactant candidates. We selected two categories of hydrocarbon and siloxane surfactant systems. Siloxane surfactants are more promising category on the basis of a lower surface tension but more challenging as the chemical structures of the commercial siloxane surfactants are complex and generally proprietary. We performed a broad literature search and developed contacts with surfactant industry over a period of time to identify structurally related surfactants to the extent the industry is willing. Specifically, we conducted a number of consultations with a chemists at Dow-Corning Inc., SilTech Inc., and Colonial Chemical Co., who provided some of their silicone surfactants and related technical information. We chose surfactant structures because of varying number of hydrocarbon, siloxane, and oxy-ethylene units.

By their nature, commercial surfactants can only allow a broader variation in chemical structure. We can explore the molecular structure effects semi-quantitatively within a given type (siloxane or hydrocarbon surfactants); linear versus branched tails, single versus multiple tails, ionic versus non-ionic head groups, etc. Head group is polar or hydrophilic and gets adsorbed on the water side of an air bubble in the foam. The tail is relatively non-polar or hydrophobic and gets adsorbed on the air side of the bubble.

4.3.1. Commercial Fluorine-free Surfactants

We selected a group of five non-ionic siloxane surfactants with identical trisiloxane tails and closely related head groups of different average length (a distribution of lengths exist) as shown in Figure 32. They are Silwet L77 from Momentive Inc., GelestSiH6185 from Gelest Inc., and 67A, 501W, and 502W from Dow-Corning Inc. as shown in Figure 32. 67A and 502W have poly oxy-ethylene head groups with hydroxyl terminal unit. Silwet L77 and 501W also have poly oxy-ethylene head group but have methyl terminal unit as shown in Figure 32. The other three are grafted siloxane surfactants, and have multiple siloxane tails and heads as shown in Figure 32. They are 193A from Dow-Corning Inc. and SilsurfJ208 from Siltec Inc. The eighth surfactant, SilphosJ208, is similar to SilsurfJ208 but is anionic as shown in Figure 32.

Similarly, Figure 33 shows three hydrocarbon surfactants with an alkane tail of similar lengths (six to twelve carbons) but different polar head groups; Alpha Foamer (Stepan Inc.) has an oxy-ethylene connected to the sulfonate head group unlike sodium dodecyl sulfonate (SDS, Aldrich Co.), and Glucopon215UP (BASF) has a glucoside head group having numerous hydroxyl units, which are non-ionic. The other hydrocarbon surfactants have different number of oxyethylene head groups and different hydrocarbon tails; Tergitol 15-S-7 (Dow Chemical) has two alkane tails and Tergitol TMN6 (Dow Chemical) has pendant methyl groups on the two tails as shown in Figure 33.

We also conducted measurements on commercial fluorine-free foam, RF6 (Rehealing Foam 6%, Lot#506166, August 2005, Solberg Inc.), which is ICAO certified and sold in Europe. RF6 failed the 28 ft^2 pool fire extinction test of U.S. Milspec, and the 6% concentrate is highly viscous

to adapt to Navy's existing hardware [4]. It contains multiple surfactants and additives with a proprietry composition.

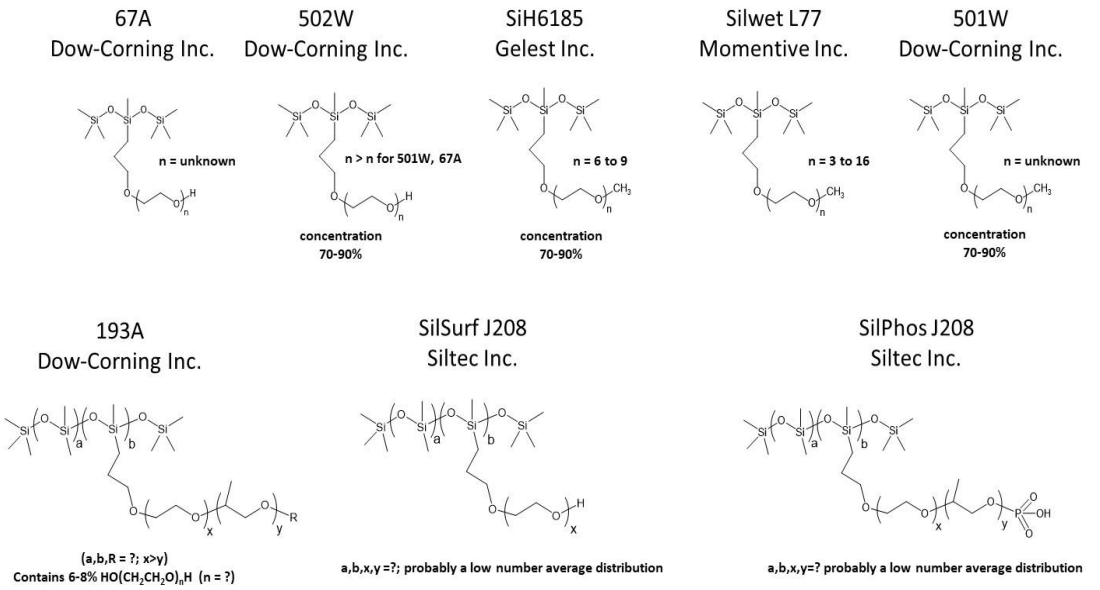

Figure 32. Top row: All have identical trisiloxane tails with unspecified distribution of oxy-ethylene units in the head group terminated with a hydroxyl unit. 502W has larger head than 501W and 67A. Other three are similar but have head groups terminated with a methyl unit. **Bottom row**: Grafted surfactants with multiple tails and heads, but differ in the number of siloxane, oxy-ethylene and oxy-propylene units, non-ionic. Silphos is similar but has an anionic head group.

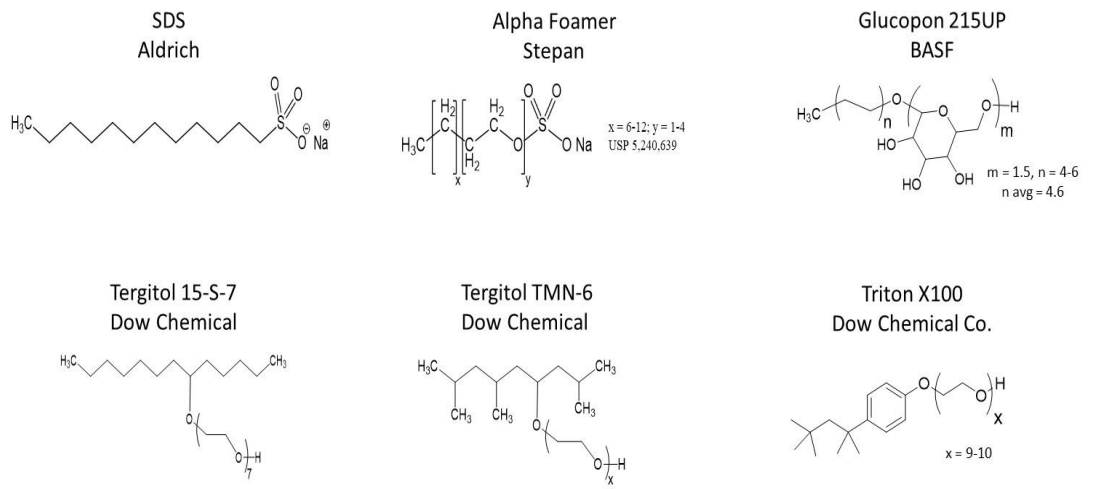

Figure 33. Top row: SDS and Alpha Foamer differ by an oxy-ethylene unit in the head group; Alpha Foamer has a distribution of chain lengths including the dodecyl similar to SDS's tail. Glucopon has slightly smaller length (octane) tail and a glucoside head group. **Bottom row**: Tergitols have twin hydrocarbon tails and similar head groups containing different length poly

oxy-ethylene units. Tergitol TMN6 also has pendant methyl units. Triton is branched with phenyl linker.

4.3.2. Preparation of Commercial Surfactant Solutions and Properties

Aqueous solutions of surfactants only and surfactant mixtures (formulations) were prepared. The formulations were prepared by replacing Capstone1157 in the RefAFFF composition shown in Table 1. We measured surface tensions for these solutions to determine the critical micelle concentration (CMC). We typically used well above the CMC values to prepare the solutions for foam degradation, fuel transport, and fire extinction testing.

The surface tension of aqueous solutions of commercial surfactants were measured using DuNoy ring apparatus at different dilutions of a stock solution containing 2 weight % surfactant. In the case of formulations, stock solution was prepared using 2 weight % of the total surfactant (1.2 % candidate + 0.8 % Glucopon + 2% DGBE by volume). Figure 34 shows the measured surface tension values from which CMC values were determined by fitting two straight lines at small and large values of the concentration, and finding the intersection of the two lines.

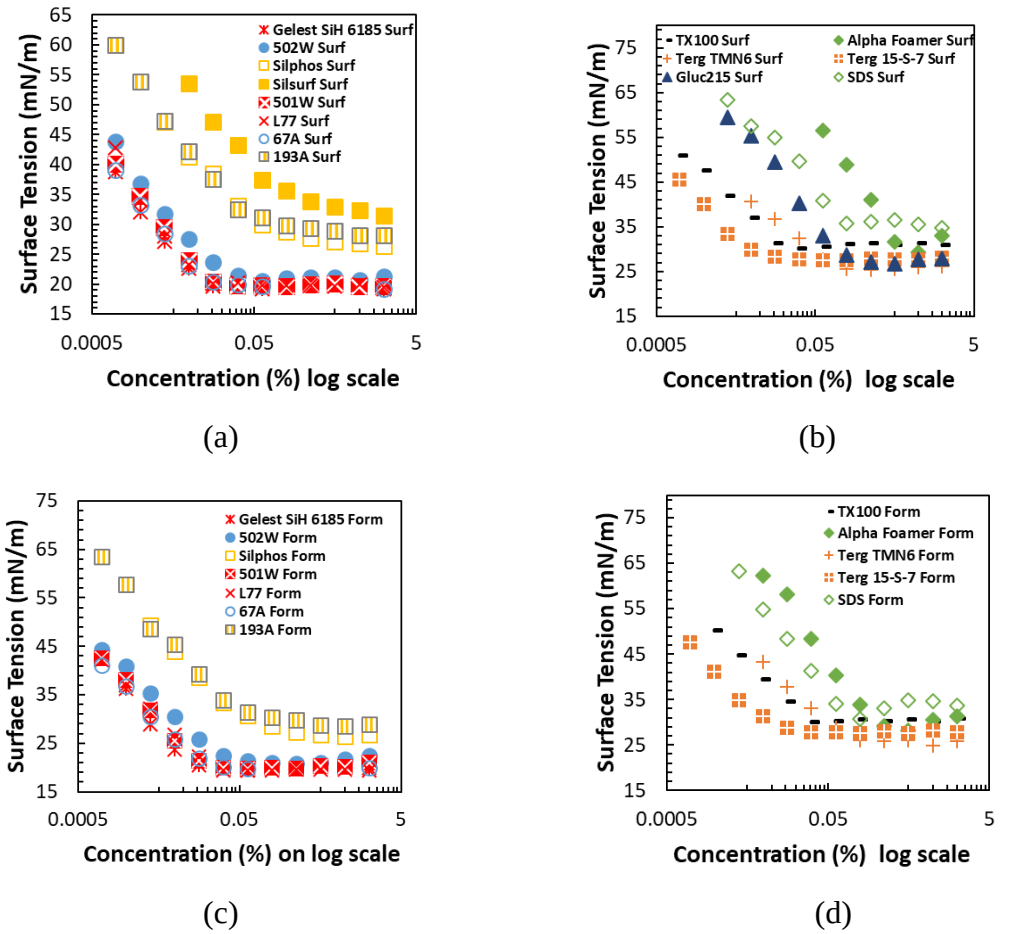

Figure 34. Surface tension versus concentration plots for commercial (a) individual siloxane surfactant solutions, (b) individual hydrocarbon surfactant solutions, (c) siloxane formulations with Gluc215, and (d) hydrocarbon formulations with Gluc215.

The surface tensions are 35 mN/m or less above CMC, which are a fraction of 1 volume %. As one might expect, the formulations have CMC values typically less than that of individual surfactant solutions. We prepared most solutions 2 to 10 times greater than their CMC values.

4.3.3. Foam Degradation and Fuel Transport for Commercial Surfactants

Figures 35 and 36 show percent change in foam height with time for foams generated with a surfactant by itself in water and with the surfactant replacing the fluorocarbon surfactant, Capstone 1157, in the RefAFFF formulation in Table 1. A more detailed data are shown in Appendix A. The foams were generated and allowed to flow directly on to a heptane pool to an initial thickness of 4-cm at 1000 mL/min foam generation rate. The heptane pool was heated by a water bath to maintain a temperature of 60 ^{o}C, but the foam itself was not heated externally. Degradation time is the time for complete disappearance of the foam layer (lifetime).

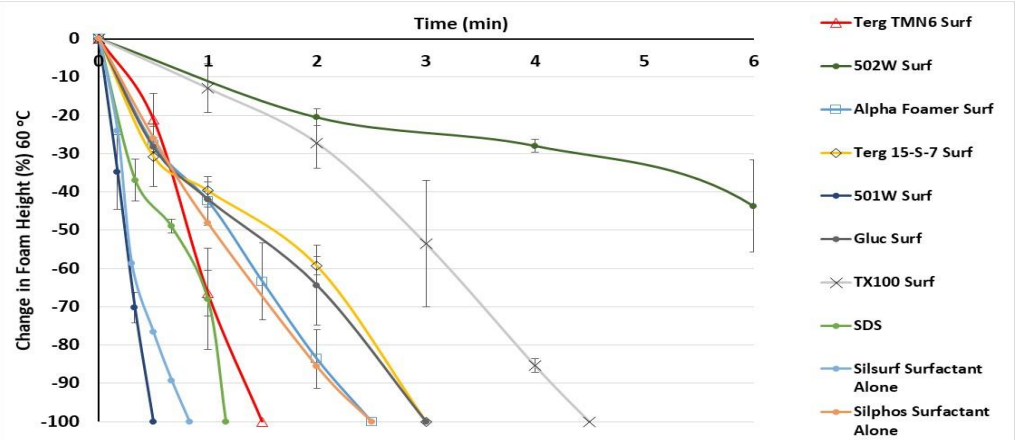

Figure 35. Percent change in foam height for foams generated using different surfactants.

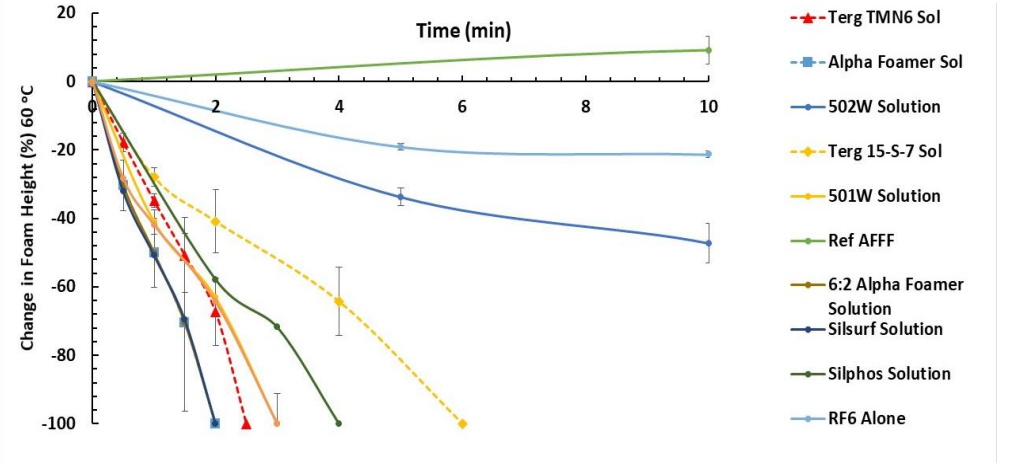

Figure 36. Percent change in foam height for foams generated using different surfactant formulations. Alphafomer was prepared as 6:2 ratio with Glucopon215 CS UP unlike the rest of the formulations which are 3:2 ratio.

Figures 35 and 36 show that surfactant formulations have longer life times than the individual surfactant solutions. The surfactant 502W siloxane from Dow Silicones Inc. has the longest lifetime among the foams examined. Even though RF6 has even longer lifetime, its high viscosity prevents it from being a drop-in surfactant formulation.

Figures 37 and 38 show mole flux of heptane vapor transported through a foam layer for foams generated with a surfactant by itself in water and with the surfactant replacing the fluorocarbon surfactant, Capstone 1157, in the RefeAFFF. A more detailed data are shown in Appendix A. The foams undergo degradation during the measurement inside a closed flux chamber because the foams were placed on hot (60 ^{o}C) heptane pool. The foam lifetimes are typically higher than in the degradation measurements shown above, which are in an open beaker. The humidity is expected to be higher in a closed flux container. Pool area was 19.6 cm^2 and initial foam layer thickness was 4 cm, total nitrogen flow of 600 mL/min (500 mL/min through the flux chamber and 100 mL/min by-pass flow) to FTIR. Transport time is defined as the time at which fuel flux is 4.4 x 10^{-9} mole/cm^2/s corresponding to 193 ppm heptane measured by FTIR. A fuel concentration of 193 ppm in the nitrogen flow through FTIR corresponds to the lower flammability limit (1 vol. %) at the pool surface as calculated based on 29 vol% vapor pressure on bare heptane that resulted in 5675 ppm in the nitrogen flow through the FTIR.

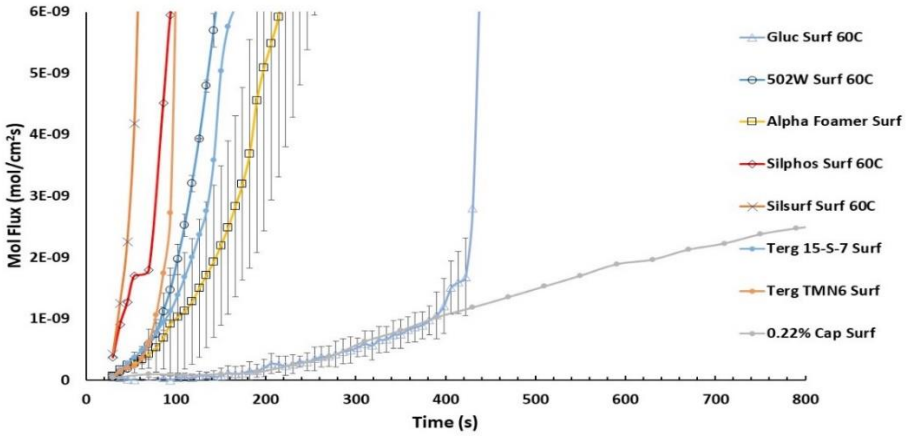

Figure 37. Fuel vapor flux with time for foams generated with different surfactants.

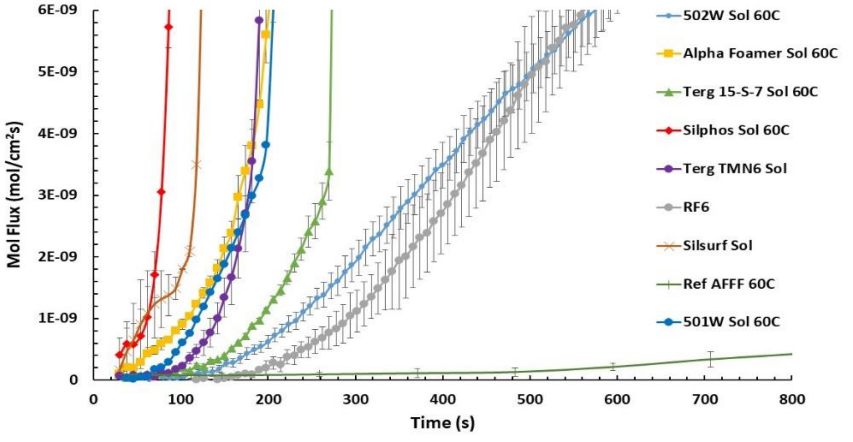

Figure 38. Fuel vapor flux with time for foams generated with different surfactant formulations.

Figures 37 shows that Glucopon 215 CS UP of BASF has the smallest fuel transport rate among the commercial foams including 502W.But, Figure 38 shows that the 502W formulation and RF6 have the smallest transport rates. The 502W formulation's transport flux is even smaller than the Glucopon surfactant by itself. It is possible that combining Glucopon 215 CS UP with 502W in the 502W formulation reduced the fuel flux further due to increased foam stability shown in Figure 36. A similar effect can be seen between Capstone1157 surfactant by itself shown in Figure 37 and RefAFFF shown in Figure 38.

4.3.4. Heptane Pool (12-cm diameter) Fire Extinction with Commercial Surfactants

Figure 39. A pool (12-cm diameter, n-heptane liquid, 2-cm lip) fire extinction by foam applied at the center at a constant flow rate; from 30-sec pre-burn to extinction.

We initially conducted fire extinction on a 19-cm diameter heptane pool fire and found that most commercial surfactants could not extinguish the fire and no quantitative measurements could be made. We conducted fire extinction experiments for the surfactants shown in Figure 34 to 38 on a 12-cm diameter heptane pool fire. Most of them are expected to perform poorly compared to the RefAFFF, but the interest here is to see if a correlation develops in Figure 39 so that new surfactants could be developed based on the knowledge gained from the commercial surfactants. Figure 39 shows a 12-cm diameter heptane pool fire with a constant foam flow rate, from 30 s pre-burn to extinction. The foam spread from the center to the edges covering the entire pool. During and after spreading, a foam layer of increasing thickness continues to build eventually causing extinction. When the foam flow rate was too low, the foam was unable to cover the pool completely, and in some cases the foam receded after covering the pool initially. This is especially true for foams that have higher degradation rates in Figure 35 and 36. Also, we noticed fire on top of the foam covered regions of the pool because the foam layer was not thick enough to block the fuel vapor supply to the fire above the foam surface. As the foam flow rate was increased, spreading occurred faster and fire extinction time decreased depending on the surfactant system employed. Some surfactants, with very high foam degradation rates in Figure 35, did not extinguish the fire in a reasonable time (90 s to 150 s) even when the foam flow was increased. Typically, foam supply was continued up to 150 s, if the foam layer appeared to be spreading or growing. But, if there appeared to be a steady state in the pool coverage by the foam layer or foam was receding, the foam supply was stopped at 60 to 90 s.

Figures 40 and 41 show measured fire extinction time with foam flow rate applied at the center of heptane pool at a constant foam flow rate. Fire extinction time increased as the foam flow rate is decreased. The foam flow rates, where the fire did not extinguish in 120 s are shown as symbols placed along the x-axis in Figures 40 and 41. We found that 501W and SilsurfJ208 surfactant solutions were unable to cover the 12-cm diameter pool even at a high foam flow rate (2500 mL/min), but the Silsurf covered a larger area of the pool consistent with the fuel transport and

degradation rates shown in Figure 35 to 38. We also found that Tergitol 15-S-7 and TMN6 were unable to extinguish the fires at foam flow rates from 1000 to 3300 mL/min as shown above. The extinction with Tergitol TMN6 was inconclusive because we noticed extinction only at a foam flow rate of 1440 mL/min. The results for Tergitol TMN6 were complicated by the fact that the drained solution from the foam formed a whitish emulsion layer that settled just below the fuel layer. These results appear to be not consistent with the foam properties shown in Figure 35-38, and may need further investigation.

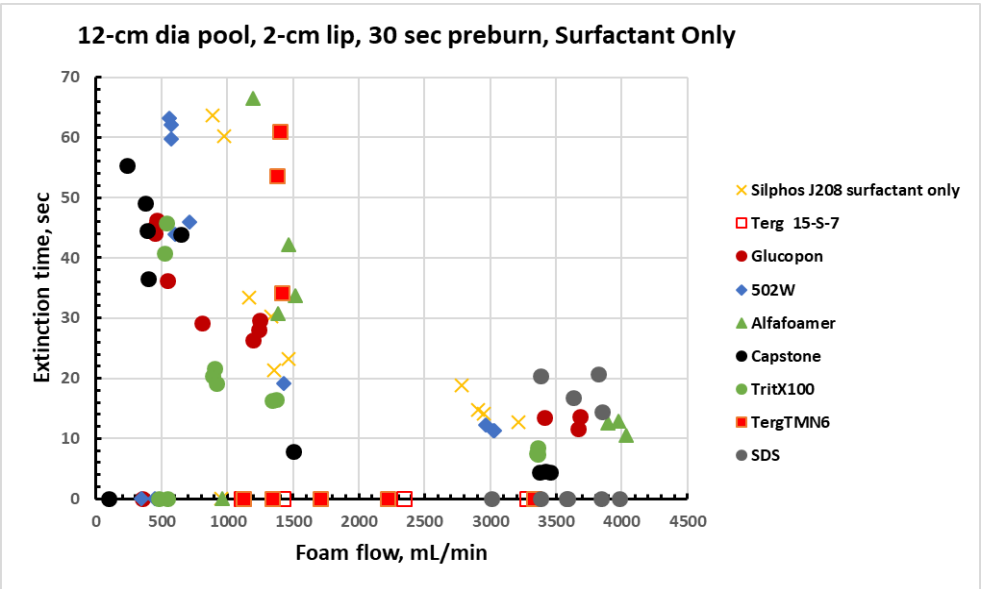

Figure 40. Extinction time with foam flow rate for foams generated with different surfactants. A 6:2 Alpha Foamer to Glucopon ratio was used for extinction while 3:2 ratio was used in Figures 36 and 38.

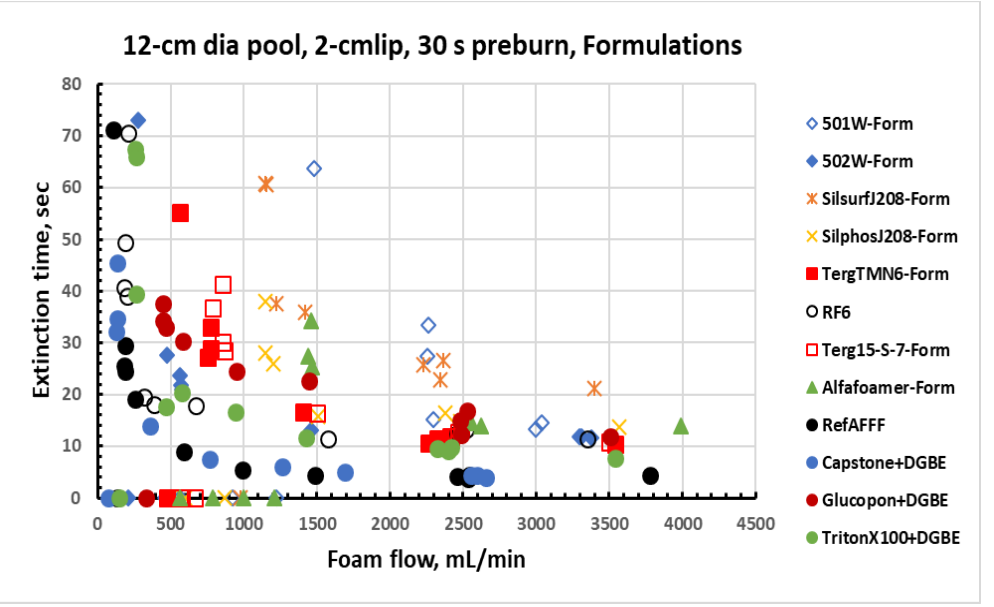

Figure 41. Extinction time with foam flow rate for foams generated with different surfactant formulations.

Figures 40 and 41 show that extinction time decreases as the foam flow rate is increased and the surfactant's effectiveness at suppressing the fire depends on foam application rate. Figure 40 shows TritonX100 and 502W are relatively more effective than the other surfactants in suppressing the fire especially at low foam flow rates. RF6 is more effective at low flow rates than at high foam flow rates. Surprisingly, TritonX100 with DGBE solvent has comparable effectiveness with RF6 and 502W formulation. The 501W formulation has the highest fire extinction time.

4.3.6. Relationships among Foam Degradation, Fuel Transport, and Fire Extinction

Table 9 shows relative degradation and transport times and extinction times at 500 mL/min foam flow rate calculated from the data shown in Figures 35 to 41.

Table 9. Fire extinction time for foams generated by different surfactant solutions.

Surfactant	Extinction time, s	Transport time, s	Degradation time, s	CMC, g/L	Concentration/CMC
RefAFFF	12	3619	3800	0.05	10
Capstone1157+DGBE	12	2790	2700	0.033	7.3
RF6	17	478	1620	N/A	N/A
502WForm	25	448	840	0.018	6.7
Capstone1157	38	2710	2100	0.031	7.3
Glucopon215UP	40	433	190	0.072	2.8
TritonX100	44	138	270	0.012	42
Tergitol TMN6Form	70	182	150	0.07	7.1
502W	70	126	500	0.016	6.0
Tergitol 15-S-7Form	No extinction	272	360	0.0086	6.0
501WForm	No extinction	198	195	0.01	6.8
AlfafoamerForm	No extinction	190	195	0.13	13.9
Alfafoamer	No extinction	190	150	0.38	3.4
Tergitol 15-S-7	No extinction	142	195	0.009	6.0
SilsurfForm	No extinction	122	115	0.1	7.0
Tergitol TMN6	No extinction	94	90	0.07	6.0
SilphosJ208	No extinction	86	135	0.04	7.5
SilphosForm	No extinction	78	250	0.125	2.0
SDS	No extinction	67	67	0.04	10.6
SilsurfJ208	No extinction	57	45	0.07	0.2
501W	No extinction	20	20	0.09	6.0
67A (0.5%)	N/A	76	120	--	--
Glucopon215UP+DGBE	N/A	470	260	0.072	6.3
TritonX100+DGBE	N/A	130	180	0.012	42
Angus 3%	N/A	158	780	N/A	N/A

Figures 35 and 36 showed foam lifetimes when a 4-cm thick foam layer degraded completely for fluorinated and fluorine-free surfactants and their formulation mixtures. Relative degradation rate is calculated by dividing the lifetime for RefAFFF with that of a fluorine-free surfactant candidate. Fuel transport time is defined as the time taken for the surface concentration to reach 1 vol %, which is just below the lower flammability limit for heptane and is calculated from Figures 37 and 38,. The concentration of 1 vol. % at the surface corresponded to 193 ppm concentration in the nitrogen gas flow carrying the fuel vapors to FTIR because of the nitrogen dilution. Relative transport rate is defined as the transport time for RefAFFF divided by the transport time for a candidate fluorine-free surfactant.

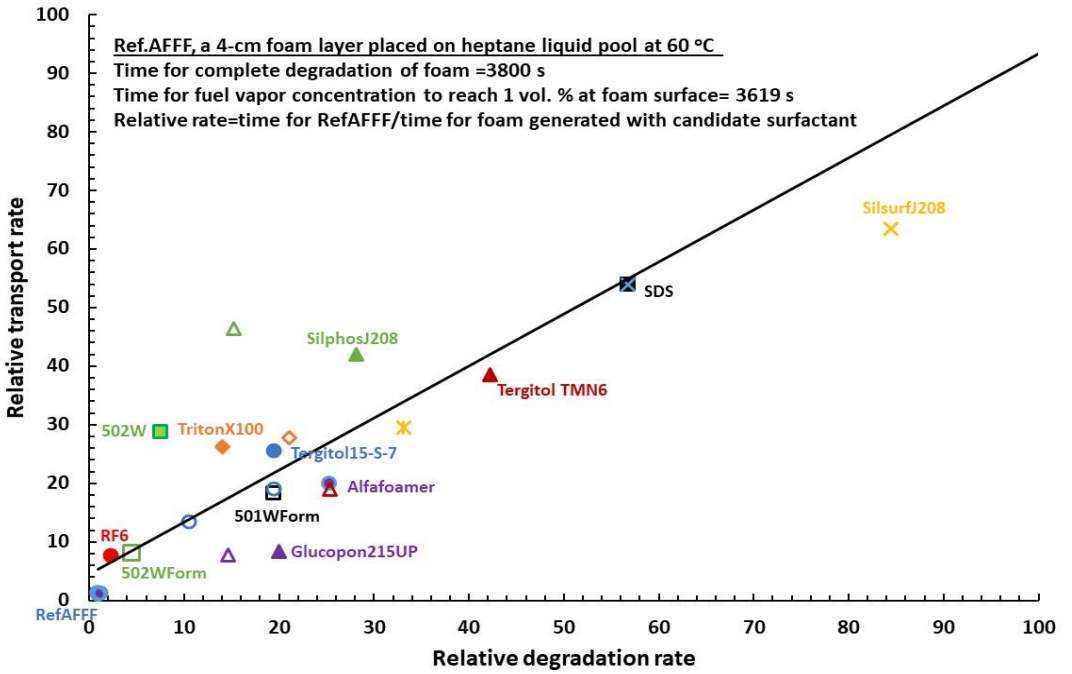

Figure 42. Fuel transport rate versus degradation rate relative to RefAFFF. Open and solid symbols represent data taken for foams generated with surfactant as a part of the formulation (e.g. 502WForm) and surfactant alone (e.g. 502W); same color symbol is used for a given surfactant.

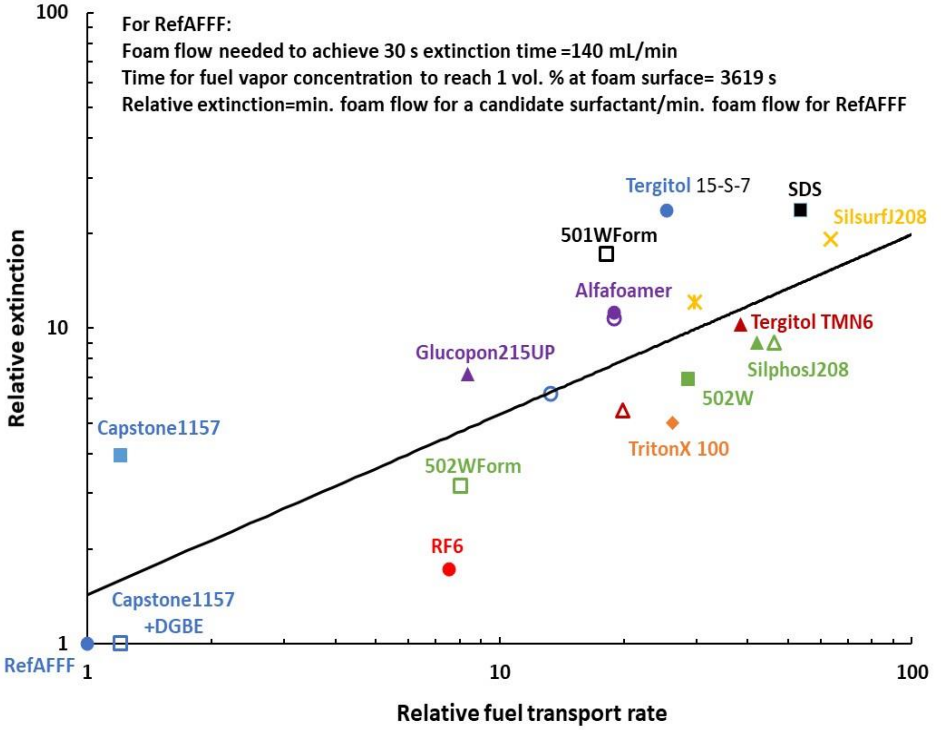

Figure 43. Fire extinction for 12-cm diameter heptane pool versus fuel transport rate. Open and solid symbols for formulations and surfactants only respectively.

Figure 42 shows the relative transport rate against the relative degradation rate for surfactants by themselves and as part of the reference formulation. By definition, a value of 1 corresponds to the measured rates for RefAFFF, whose values are given in Table 9. The data for different surfactants fall at different distances away from the origin and represent increasing rates of fuel transport and foam degradation. Figure 42 shows that the siloxane surfactant based 502W formulation (502WForm) is the closest to RefAFFF among the surfactants examined to date. The 502W formulation has transport and degradation rates comparable to that of a commercial fluorine-free foam, RF6, which is an important milestone to achieve; 502W is not viscous unlike RF6 concentrate. Figure 42 also shows that the fuel transport rate and degradation rates for 502WForm are 8 and 4.5 times higher than those for RefAFFF respectively.

Figure 42 enables comparison of the effects of variations in chemical structures shown in Figures 32 and 33 and ranking of the surfactants. Figure 35 shows a dramatic difference between 502W and 501W (surfactant only measurements), which degraded so quickly (< 30 s) that repeatable measurements could not be made. As formulations, 502W and 501W also show significant difference in fuel transport rate and degradation rate. These differences in foam properties suggest that the differences in surfactants' structures shown in Figure 32, namely the larger length oxy-ethylene head of 502W compared to that of 501W, could be one of the causes (we also found that foam generated using 67A surfactant with a hydroxyl terminal group was unable to extinguish the bench-top fire, further measurements on 67A are in progress) in addition to the differences in polydispersity and purity . Silphos had smaller transport and degradation rates compared to Silsurf. This could be due to Silphos's anionic head group and a different length oxy-ethylene and ox-propylene units compared to Silsurf. In general, the data suggest that polarity and structural differences in the head group of the siloxane surfactants appear to have significant effect on foam's properties.

Among the hydrocarbon surfactants shown in Figure 33, Alpha Foamer has a distribution of oxy-ethylene units ranging from 1 to 4 in the head group unlike SDS. Figure 42 shows significant reduction in foam's fuel transport and degradation rates over SDS, again confirming the positive effect of oxy-ethylene units in the head group similar to the silicone surfactants discussed above. Glucopon 215UP has larger head having numerous hydroxyl units, which might have led to further reduction in both fuel transport and foam degradation properties over those with Alpha Foamer surfactant. The Tegitols shown in Figure 33 appear to be somewhat unique. Figure 42 shows that Tergitol 15-S-7 had significantly smaller degradation and transport rates for the foam than Tergitol TMN6. But, it is difficult to separate the effects of the pendant methyl groups from the effects of different number of oxy-ethylene units in Tergitol TMN6's structure relative to the structure of Tergitol 15-S-7.

The surfactants can be ranked based on the values of foam flow rate at which the extinction time becomes relatively long. Figure 43 shows the foam flow rate needed for fire extinction time of 30 s (12-cm dia. pool) relative to that for RefAFFF versus the relative transport rate. The smaller the foam flow rate needed for a 30 s extinction time, the more efficient is extinction. Figure 43 shows a power law correlation between relative foam extinction and the relative transport rate with an exponent of 0.6. The scatter among the data points is partially attributed to significant and uneven degradation of the foam layer by the heptane fuel during the fuel flux measurements; some of the foams degraded quickly before fuel flux could be measured reliably.

In general, the surfactants in Figure 43 follow the trends shown in Figure 42. Extinction was not observed with 501W, but 502W extinguished the fire, as expected from Figure 42. Similarly, SilphosJ208 had superior extinction performance to SisurfJ208 as shown in Figure 42. Also, Alpha Foamer had faster extinction than SDS. Glucopon 215UP performed better than Alpha Foamer. In Figure 43, 501W, SilsurfJ208, SDS are farther from RefAFFF (at origin) similar to those in Figure 42. RF6, Capstone, 502WFormulation are closest to RefAFFF as in Figure 42. Rest of the surfactants fall between the two groups in Figure 43 as in Figure 42. Alpha Foamer formulation's extinction performance is comparable to Alpha Foamer surfactant solution as expected, because 6:2 Alpha Foamer to Glucopon was used for extinction while 3:2 was used in Figure 42. Capstone 1157 appears to have synergism with DGBE that makes it an exception to the general trend. The combined solution extinguished the fire as fast as the RefAFFF. The transport rate for 502WForm and RF6 are close but the extinction times are significantly different because of slower foam spread rate for 502W.

4.4. Invention of a Siloxane Formulation

Figures 42 and 43 identified siloxane surfactants, especially 502W formulation, as a potential fluorine-free surfactant formulation for further development. We developed a formulation by substituting the fluorocarbon surfactant in the RefAFFF formulation described in Table 10 with a commercial siloxane-polyoxyethylene surfactant [50]. The siloxane surfactant has large siloxane tail and slender polyoxyethylene head while the alkylpolyglycoside surfactant has a large glycoside head and a slender alkane tail. The interactions between siloxane's and glycoside's head and tail structures in the surfactants mixture can affect foam stability in the presence of fuel, fuel diffusion through a foam layer, foam properties and fire suppression. We investigated synergistic effects due to such interactions and the effects of polyglycoside head size of the hydrocarbon surfactant on foam stability and heptane fire suppression [50].

Aqueous foams generated from commercial Siloxane-polyoxyethylene and alkyl polyglycoside surfactants were characterized individually and as mixtures in a formulation. The results showed significantly smaller fire extinction times for the surfactant mixtures than for either of the individual components exhibiting a synergistic fire extinction rather than following the law of averages; 5 times enhancement in extinction performance. The measured foam degradation rate with the foam exposed to a hot heptane pool also showed a similar synergism. The reduced foam degradation rate resulted in a reduced fuel vapor transport for longer times and a more rapid fire extinction for the siloxane-glycoside mixture. By increasing the hydrophilicity with increased size of the polyglycoside head, the synergistic effect was enhanced. Both benchtop (19 cm diameter) and large scale (6 ft diameter) heptane pool fire extinction with the siloxane-glycoside surfactant mixture showed that the extinction time was 1.5 times that of an equivalent AFFF formulation containing a fluorosurfactant in place of the Siloxane surfactant at a fixed foam application rate (22 L m^{-2} min^{-1}). An understanding of the molecular interactions at the interface causing the synergistic effects may lead to improved siloxane-glycoside systems and other novel surfactant systems with performance matching that of fluorocarbon surfactants.

4.4.1. Compositions of Siloxane Formulations

It is crucial to have a complete sets of data for the same formulations because it allows us to relate the solution and foam properties to the extinction performance and determine those properties that have a significant impact on fire extinction. Table 10 shows the compositions of three Siloxane-Gluc formulations and the RefAFFF formulation used for making the foams. The

percentages of surfactants and DGBE refer to the amounts of the surfactant concentrates and DGBE supplied by the respective manufacturers. The surfactant concentrations shown in Table 10 for the Siloxane formulations are two and half (3:2 Siloxane-Gluc215) to ten times (2:3 Siloxane-Gluc225 and 2:3 Siloxane-Gluc600) the respective CMC values, and the RefAFFF is 5 times the CMC value. CMC values are described later in the paper. Increasing the concentrations of the siloxane and glycoside surfactants to 0.3% and 0.2% respectively in 3:2 Siloxane-Gluc215 formulation shown in Table 10 did not result in a significant change (< 10%) in fire extinction, degradation, and transport properties in the bench scale measurements possibly because they are significantly higher than CMC.

Table 10. Fluorine-free Siloxane surfactant formulations and fluorinated RefAFFF formulation. The values shown under each column are volume percentages of the individual components (or concentrates) in distilled water. The formulations were used for foam generation, property and fire performance measurements [50].

2:3 Siloxane-Gluc225	**2:3 Siloxane-Gluc600**	**3:2 Siloxane-Gluc215**	**3:2 Cap-Gluc215 (RefAFFF)**
0.2 % 502W	0.2 % 502W	0.075% 502W	0.3% Capstone
0.3% Glucopon 225 DK	0.3% Glucopon 600 CS UP	0.05% Glucopon 215 CS UP	0.2% Glucopon 215 CS UP
0.5% DGBE	0.5% DGBE	0.5% DGBE	0.5% DGBE

4.4.2. 19-cm Diameter Heptane Pool Fire Extinction with Siloxane-Glycoside

Figure 44 presents time-lapse images of this fire suppression over a 19 cm diameter heptane pool fire using a foam application rate of 1000 mL min^{-1}[50]. At 0 seconds, the foam is introduced to the pool fire surface after the pool has been burning for 60 seconds. Within the first 5 seconds of foam application, a significant suppression is not observed in all cases in Figure 44b, 44g, and 44l. After 10 seconds of foam application, Figures 44c and 44h show that the 3:2 Cap-Gluc215 (RefAFFF) formulation extinguished most of the fire (knockdown) similar to a commercial AFFF (Buckeye), while the Siloxane-Gluc225 formulation did not suppress the fire to the same degree as shown in Figure 44m. After 15 seconds, Figures 44d and 44i show complete extinction while Figure 44n shows that Siloxane-Gluc225 suppressed most of the fire (knockdown). Finally, Figure 44o shows that Siloxane-Gluc225 took longer (20 seconds) to completely extinguish the fire unlike the other two fluorinated foams, 3:2 Cap-Gluc215 and Buckeye 3%, which took 12 and 16 seconds respectively for complete extinction. For the two fluorinated foams and the fluorine-free foam, we noticed fire persisting for a few seconds above the foam even in the regions of the pool covered with the foam and also subsequent to complete coverage of the pool by the foams. In the case of the two fluorinated foams, we found that the fire persists above the foam layer for as long as 50% of the extinction time and may underscore the significant role the foam layer plays in fire extinction relative to any “aqueous film” layers that may exist underneath the foams. Also, the persistent fire above the foam layer may be indicative of that the fuel vapor emanating from the hot pool surface permeates through the foam layer feeding the fire above. The fuel transport through the foam

ceases as the foam layer thickens due to continued application of the foam, resulting in fire extinction due to lack of the fuel supply. During the extinction process, foam also degrades and delays building a thick foam layer. This can be noticed at very slow foam application rates, where the foam was unable to cover the pool despite continuous application of the foam for a long time (up to 6 min) because foam was degraded by the hot fuel and the fire. At high flow foam application rates subsequent to the fire extinction, we also noticed that the residual foam layer disappeared quickly with time especially for the fluorine-free foams. Thus, high fuel transport and high foam degradation can increase the minimum volume of foam (or minimum foam layer thickness) needed to extinguish a fire, which is a performance measurement of a given formulation (For example, MilSpec requires a 2.6 m^2 (28 ft^2) fire to be put out in 30 s using less than 7.57 L (1 gallon) of surfactant solution, which translates to 37.85 to 75.7 L (5 to 10 gallons) of foam depending on the expansion ratio).

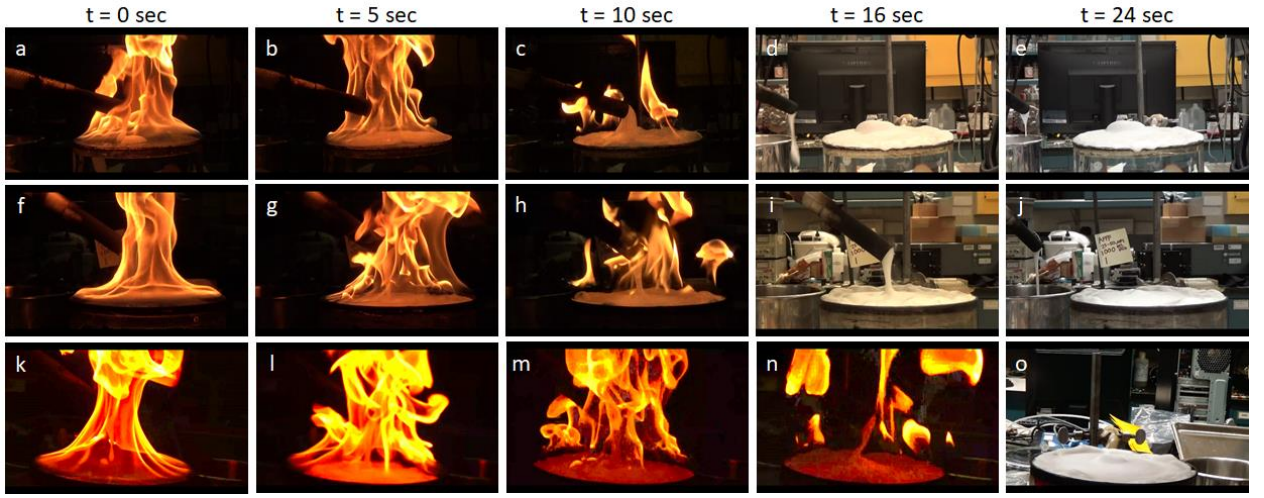

Figure 44. Time-lapse images of Buckeye (a-e), RefAFFF or 3:2 Cap-Gluc215 (f-j), and Siloxane-Gluc225 (k-o) foams extinguishing a benchtop (19 cm diameter) heptane pool fire at a foam application rate of 1000 mL min^{-1}. Images are taken at times 0, 5, 10, 16, and 24 s during extinction.

In Figure 45, we show extinction times measured for 19-cm diameter bench top and 1.83 m (6 ft) diameter large scale heptane pool fires as functions of foam application rate per unit area (flux) of the pool. The 1.83 m (6 ft) pool fire test is same as the MilSpec MIL-F-24365F [4] but with heptane fuel instead of gasoline. For the benchtop, we compare fire extinction times for the Siloxane-Gluc225 surfactants formulation (red solid square), RefAFFF (black solid circle), and the commercial AFFF (Buckeye 3%, black solid diamond) foams. As the foam application rate is decreased, the extinction time increases and reaches extinction times greater than 180 seconds when the foam application is stopped and the fire is extinguished by placing a tray over the pool. The RefAFFF and the Siloxane-Gluc225 formulations could not extinguish the flame within 180 seconds at foam application rate below 5.9 and 9.7 L m^{-2} min^{-1} respectively. The extinction times for the siloxane formulation are closer (< 1.5 times that of RefAFFF) to the AFFFs at large foam application rates. For the 1.83 m (6 ft) diameter heptane pool fire, we compare the extinction times for the Siloxane-Gluc225 formulation at fixed solution flow rates of 7.6 and 11.4 L min^{-1} (2 and 3 gallons per minute) which correspond to 18.6 and 22.2 L m^{-2} min^{-1} of foam flow rates respectively. The foam flow rates are calculated by multiplying the measured liquid flow rates with the measured expansion ratio values. We also compare the extinction times for the Siloxane-

Gluc225 formulation with that of RefAFFF formulation for the 1.83 m (6 ft) diameter heptane fire in Figure 45. The extinction times are 45 and 30 seconds for the Siloxane-Gluc225 and RefAFFF respectively at a fixed foam flux of about 22 L m^{-2} min^{-1}. Thus the extinction times for the siloxane formulation are within 1.5 times those for the RefAFFF, consistent with the bench-scale data for the same foam flux. Despite significant differences in the foam generation and foam properties between the bench and large scales, the fire extinction data are surprisingly consistent possibly because the surfactant-fuel interactions and the foam application rate per unit area have more significant effects. Although the foam application rate 22 L m^{-2} min^{-1} is about the same for the two formulations, the solution application rate 11.4 L min^{-1} (3 gallon/min, expansion ratio 5.1) is higher for the Siloxane-Gluc225 than 7.57 L min^{-1} (2 gallon per min, expansion ratio 7.5) for the RefAFFF because of the differences in the foam expansion ratio in the large scale testing. The foam expansion ratio of Siloxane-Gluc225 decreases from 6.4 to 5.1 as the solution flow rate increases from 7.57 to 11.36 L min^{-1} (2 gpm to 3 gpm) during the large scale foam generation.

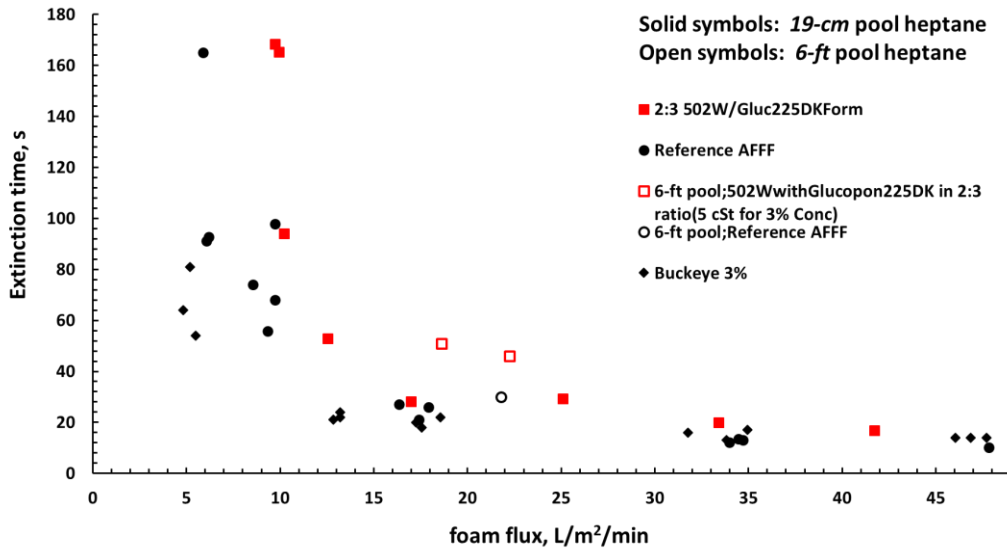

Figure 45. Bench-scale (19 cm dia.) and large scale (1.83 m or 6 ft dia.) extinction of heptane pool fire showing extinction times of Siloxane-Gluc225 surfactant formulation relative to the RefAFFF and commercial formulation (Buckeye 3%) at different measured foam application rates; For the 1.83 m (6 ft) fire, the foam and liquid flux values correspond to 7.57 to 11.36 L min^{-1} (2 and 3 gallons per min) solution flow rates [50].

4.4.3. 28 ft^2 Heptane Pool Fire Extinction with Siloxane-Glycoside

We focused on a subset of five metrics in the MilSpec standard MIL-F-24385 to evaluate the Siloxane-Gluc225 and the RefAFFF formulations [50]. We measured five parameters and compared with passing criteria, which are based on gasoline fuel rather than the heptane. The parameters measured were (1) 2.6 m^2 (28 ft^2) pool fire extinction time, (2) burnback time, (3) film and seal, (4) expansion ratio, and (5) 25% drainage time, and are described in MilSpec standard MIL-F-24385. The results are shown in Table 11.

Both 90% and 100% extinction times decrease as the foam flow rate is increased as shown in Table 11. At a fixed foam flow rate of about 56.8 L min^{-1} (15 gpm) shown in row 3 and columns 3 and 4 of Table 11, the 90 and 100% extinction times for the Siloxane-Gluc225 are less than or

equal to a factor of 1.5 times those for RefAFFF. However, at a fixed solution flow rate of 7.57 L min^{-1} (2 gpm), the extinction times differ by as much as a factor of two as shown in columns 2 and 4. The factor 1.5 times is consistent with the bench-scale data as shown in Figure 45. One reason

Table 11. Comparison of Siloxane-Gluc225 formulation at 7.57 and 11.36 L min^{-1} (2 and 3 gpm) and with RefAFFF at 11.36 L min^{-1} (2 gpm) liquid application rate for 6-ft diameter MilSpec pool fire using heptane as the fuel instead of gasoline[1][50].

MilSpec Test with Heptane fuel	**2:3 Siloxane-Gluc225**		**RefAFFF 3:2 Cap/Gluc215**	**Criteria (based on gasoline)**
Liquid flow rate L min^{-1} (gpm)	7.57 (2)	11.36 (3)	7.57 (2)	7.57 (2)
Foam flow rate[2] L min^{-1} (gpm)	48.4 (12.8)	57.9 (15.3)	56.8 (15)	N/A
90% extinction (s)	43	26	21	N/A
Extinction (s)	51	45	30	<30
Burnback (s)	338	424	981	>360
Film and seal	N/A	N/A	PASS	PASS
Expansion ratio	6.4	5.1	7.5	5-10
25% Liquid Drainage (s)	198	198	251	>150
Average bubble size (μm)	220±111	140±30	170±30	N/A
3% concentrate viscosity, 20°C (cP)	5.3	5.3	3.2	>2
3% concentrate viscosity, 5°C (cP)	7.4	7.4	4.7	<20
Solution viscosity, 20°C (cP)	1.14	1.14	1.12	N/A
Spreading coefficient on cyclohexane[3], (mN m^{-1}) at 20°C	-0.4	-0.4	6.4	>3
Interfacial tension on cyclohexane, (mN m^{-1}) at 20°C	2.2	2.2	1.9	N/A
Surface tension (mN m^{-1}) at 20°C	22.4	22.4	16.7	N/A
3% concentrate refractive index	1.371	1.371	1.362	>1.363
CMC (% volume of total surfactant concentrates)	0.05	0.05	0.1	N/A
3% concentrate pH	6-8	6-8	6-8	7-8.5

[1]The MilSpec typically requires unleaded, alcohol-free, gasoline fire suppression rather than heptane fire.
[2]Foam flow rate is the specified liquid flow rate multiplied by the measured foam expansion ratio.
[3]Surface tension of cyclohexane is 25 mN m^{-1} at 20°C.

for the longer extinction time for Siloxane-Gluc225 is the larger foam degradation rate, as indicated by the smaller burnback time of 338 s for the siloxane formulation compared to 981 s for the RefAFFF as shown in columns 2 and 4. Foam is applied for a total of 90 s including extinction, therefore the expected burnback time for the siloxane formulation is 544 s, after correcting for the shorter foam application time following fire extinction and for the difference in the expansion ratios. The measured burnback time of 338 s for the siloxane-Gluc225 is significantly smaller than the expected 544 s indicating significantly greater foam degradation. The data in Table 11 show that the increased foam flow rate decreases the extinction time. The foam flow rate can be increased by increasing the foamability or the expansion ratio as well as by increasing the solution flow rate. Other properties especially the viscosity of the concentrate are within MilSpec criteria. This is important because many commercial fluorine free concentrates to date have viscosities well above the MilSpec criteria.

4.4.4. Synergistic Effects with Siloxane-Glycoside

The reason for relatively good fire suppression performance of the Siloxane-Gluc225 formulation is the synergism between the Siloxane and Glycoside surfactants indicated by the smallest foam flow rate at which the formulation can extinguish the fire in a given time (e.g., 180 seconds) [50]. Figure 46 depicts the synergism where the surfactant mixture can extinguish the fire at a much smaller foam application rate than the individual surfactant solutions rather than an intermediate foam flow rate, which is expected following the law of averages. Figure 46 shows the bench scale heptane pool fire extinction data for 3:2 Siloxane-Gluc215 formulation composition listed in Table 10 and for the three individual surfactant solutions (0.45% Glucopon 215 CS UP, 0.1% siloxane 502W, 0.5% siloxane 502W, 0.5% Glucopon 225 DK, 0.5% Glucopon 600 CS UP all with 0.5% DGBE in distilled water). Gluc215 could not extinguish the fire even at a very high foam flow rate (2100 mL min^{-1} or 74 L m^{-2} min^{-1} within 180 s) as shown by the data points (open squares) on the x-axis, which represent no extinction. Similarly, 502W siloxane surfactant solution also could not extinguish the fire below a high value of the foam flow rate (1550 mL min^{-1} or 54.7 L m^{-2} min^{-1}) as represented by the data points (solid green circles) on the x-axis. But, when both the surfactants are combined in a 3:2 ratio the foam extinguished the fire at significantly smaller foam flow rate (in 197 s at 453 mL min^{-1} or 16 L m^{-2} min^{-1}) as indicated by the data (red solid squares) for Siloxane-Gluc215 (composition 0.075% 502W, 0.05% Gluc215, and 0.5% DGBE) exhibiting synergism. Similar results are shown for Siloxane-Gluc225DK and Siloxane-Glucopon600UP mixtures.

Figure 46 also shows the effect of varying Glucopon surfactant's head size and the number of OH functional groups on heptane pool fire extinction because of the synergistic effects. The head size is varied from x=0.4, 0.5, and 0.7 using commercially available Glucopon 600 CS UP, Glucopon 215 CS UP, and Glucopon 225 DK respectively while keeping the composition fixed (0.2% 502W, 0.3% Glucopon, and 0.5% DGBE). Gluc600 has slightly longer alkyl tail than Gluc215 and Gluc225. Increasing the hydrophilicity of the hydrocarbon surfactant increases the synergistic effect, and reduces the foam flow rate where the extinction time is 180 s in Figure 46. The synergistic extinction between 502W and Glucopon surfactants is unique because for most other commercial surfactants that we examined, the extinction times fell between the extinction times of the individual surfactant following the law of averages. The synergism is responsible for the high extinction performance of the siloxane formulation.

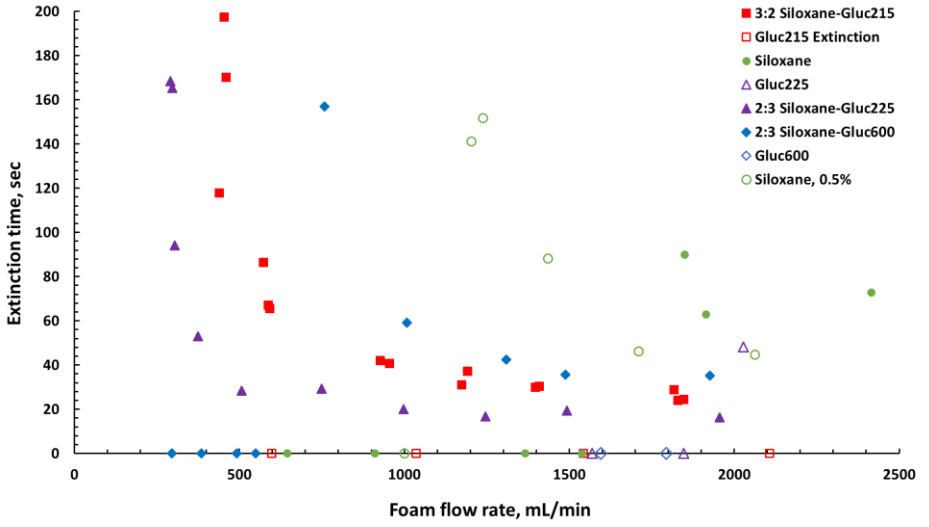

Figure 46. Bench-scale (19-cm dia.) extinction of heptane pool fire showing extinction time of Siloxane-Gluc mixtures listed in Table 10 relative to the solutions of individual components, which also contain 0.5% DGBE. The data points shown along the x-axis represent no extinction data after 180 s of foam application [50].

The synergistic extinction between 502W siloxane and Glucopons relates to the synergistic foam degradation, which is shown in Figure 47a. Again, Figure 47a shows that the surfactant mixture exhibits smaller foam degradation rate than the rates for the individual surfactants rather than an intermediate value, which is expected following the law of averages. Figure 47a shows percent change in foam layer thickness (initial thickness of 4-cm) on top of a hot heptane pool with time due to fuel vapor induced degradation. The foams generated from 0.5% Glucopon 215 CS UP with 0.5% DGBE and 0.1% 502W with 0.5% DGBE degraded in 240 and 480 s respectively. The foam generated from Siloxane-Gluc215 (0.075% 502W, 0.05% Glucopon 215 CS UP, and 0.5% DGBE) degraded completely in a much longer time (900 s) compared to the degradation times of the individual surfactants. Figure 47a also shows degradation data for the individual surfactant solutions of Gluc600 and Gluc225 and their mixtures with 502W. They also show synergistic effects like those described for Siloxane-Gluc215. Furthermore, as the glycoside head size of the Glucopon is increased, the degradation rate is reduced for the glycoside mixtures with the siloxane surfactant. The synergism is increased by increasing the hydrophilicity of Glucopon's head group as shown by the foam degradation for Siloxane-Gluc600, Siloxane-Gluc215, and Siloxane-Gluc225 formulations in Figure 47a. The number of OH functional groups increased from x=0.4, 0.5 to 0.7 by switching from Gluc600, Gluc215 to Gluc225 as shown in Figure 1; Gluc600 has slightly longer alkyl tail. The exact mechanisms for the increased foam stability are not well understood. However, it is possible that the increased hydrophilic interactions between the polyoxyethylene and glycoside head groups may have reduced the surfactant solubility in heptane resulting in increased foam stability over the individual surfactants. Figure 47a shows that the foam generated from Siloxane-Gluc225 formulation degraded completely in 1380 s versus 900 s for the foam generated from Siloxane-Gluc215 (in a 3:2 ratio), and 500 s for Siloxane-Gluc600. Siloxane-Gluc225 has the smallest degradation rate but is still significantly higher than the RefAFFF as shown in Figure 47a. For comparison, commercial AFFF (Buckeye 3%) and RefAFFF degrade completely in time periods that are 1.7 (2400 s) and 2.6 times (3600 s) longer respectively than the time (1400 s) for Siloxane-Gluc225.

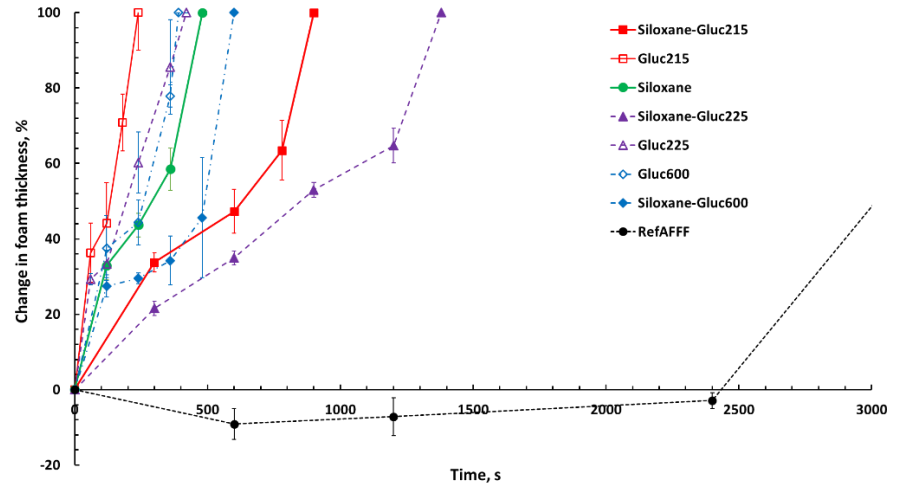

(a)

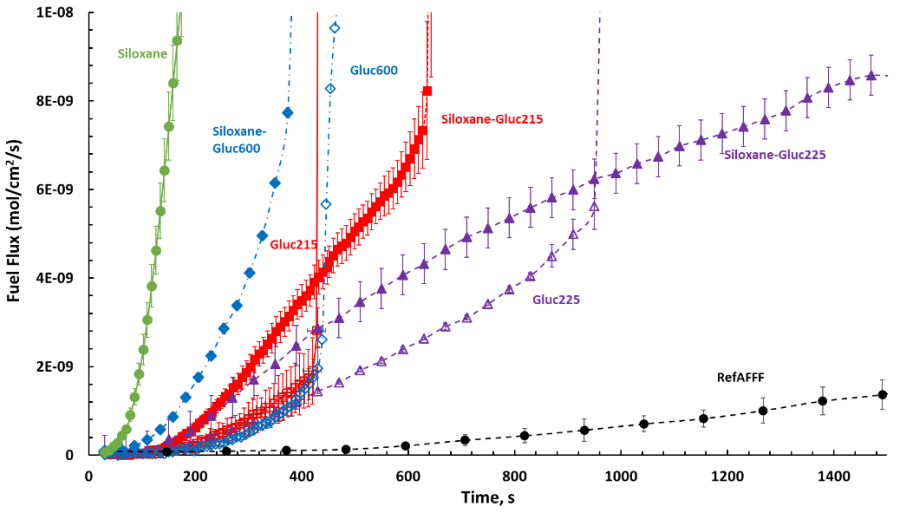

(b)

Figure 47. Measured rates for a 4 cm thick (initial thickness) foam layer covering heptane pool at 60°C with time for the Siloxane-Gluc225, Siloxane-Gluc600, and Siloxane-Gluc215 listed in Table 10, and for the individual surfactant components (0.5% Gluc215, 0.5% Gluc225, 0.5% Gluc600, and 0.1% 502W. All four solutions contain 0.5% DGBE.): (a) foam degradation, (b) heptane vapor permeation rate through the foam. Error bars represent one standard deviation calculated between three trials [50].

Figure 47b shows that the fuel permeation rate through foam follows roughly the law of averages and does not show the synergistic effects observed in foam degradation at small times for all three Siloxane-Gluc surfactant combinations. For example, below 450 s, the fuel flux for foam generated from Siloxane-Gluc215 lies between those for foams generated from the individual surfactants. However, the synergism exhibited in foam degradation in Figure 47a prolongs the foam life time and suppresses the fuel flux shown in Figure 47b at long times. At longer than 450 s, the surfactant mixture Siloxane-Gluc215 has a smaller fuel flux than the individual surfactants, which exhibit a steep rise in fuel flux because of differences in the foam degradation rate. Thus, the synergism in degradation leads to a dramatic reduction in fuel transport rate for the three surfactant mixtures compared to foams generated with individual surfactants because of the increased lifetimes of the foams for the mixtures. Even though the fuel flux is smaller for Gluc225

than for Siloxane-Gluc225 mixture at short times, Siloxane-Gluc225 lasts longer (>1750 s) than Gluc225 (980 s) and the trend reverses. For comparison, commercial AFFF (Buckeye 3%) and RefAFFF have a heptane flux of 0.4 (2.7×10^{-9} mole cm^{-2} s^{-1}) and 0.1 (7×10^{-10} mole cm^{-2} s^{-1}) times that of Siloxane-Gluc225 (6.6×10^{-9} mole cm^{-2} s^{-1}) respectively at 1000 s. The reduction in degradation and fuel transport rates decreases the fire extinction times for the mixtures over the individual surfactants shown in Figure 46. The foams lasts longer in the fuel transport apparatus because it is closed and the water vapor is relatively more contained than in the open degradation apparatus. This is especially true for Gluc225 which lasts greater than 980 s in the transport apparatus but less than 400 s in the degradation apparatus. But, Figure 47b shows a steep rise in fuel flux to $1x10^{-8}$ mole cm^{-2} s^{-1} in less than 200 s for the Siloxane foam. It take much longer than 200 s for the foam to degrade completely and for the fuel flux to reach that of bare heptane's fuel flux (not shown in Figure 47b). The reason the Siloxane foam's fuel transport curve rises rapidly in Figure 47b is that the heptane vapors travel through the foam very quickly and not because of a significant reduction in foam layer thickness. Thus, the Siloxane foam seems to have significantly higher fuel transport than Gluc225 foam and the Gluc225 foam has only a slightly higher degradation rate than the Siloxane foam. However, the combination of Siloxane with Gluc225 suppresses the foam degradation dramatically and as a result the fuel transport is also suppressed at long times. It is also interesting that the three Glucopons have very similar fuel transport rate profiles at small times (<400 seconds). The fuel transport rate depends on the fuel concentration in surfactant solution which may depend on the micelle size and number density because most of the fuel is expected to reside inside the micelles. Micelle size can affect the diffusion rate. The exact mechanisms of fuel and micelle transport in the presence of a surfactant remain unclear. During fire extinction, as the foam is applied continuously on to a burning fire, the foam spreads and foam layer thickness increases with time. The thickness (foam volume) needed to extinguish the fire varies between 0.5 to 2 cm depending on the foam application rate, rate of foam degradation by the fuel vapor, fuel vapor permeation rate, and foam spread rate. Foam's ability to resist fuel vapors from coalescing and permeating through the bubbles plays a crucial role in foam degradation, fuel permeation, and foam spread.

If a foam spreads too slowly, it can increase the extinction time because complete coverage of the pool surface is necessary, but not sufficient, to extinguishing a fire. Figure 48 shows the time to cover a burning heptane pool with foam, which is delivered at the center of the bench-scale pool at a constant flow rate for the Siloxane-Gluc225 and the RefAFFF formulations listed in Table 10. As the foam flow decreases the foam spread time increases as expected. Also shown are the fire extinction times for comparison. The foam spread times are about half the extinction times at high foam flow rates for both the formulations. As the foam flow rate is decreased, the foam spread times become greater than half, but still remain smaller than, the fire extinction times likely because foam degrades significantly due to longer exposure to the hot pool and fire. In addition to foam degradation, foam spread also depends on the rheological properties and the expansion ratio, which increases as the foam flow rate decreases in our foam generation apparatus as discussed later.

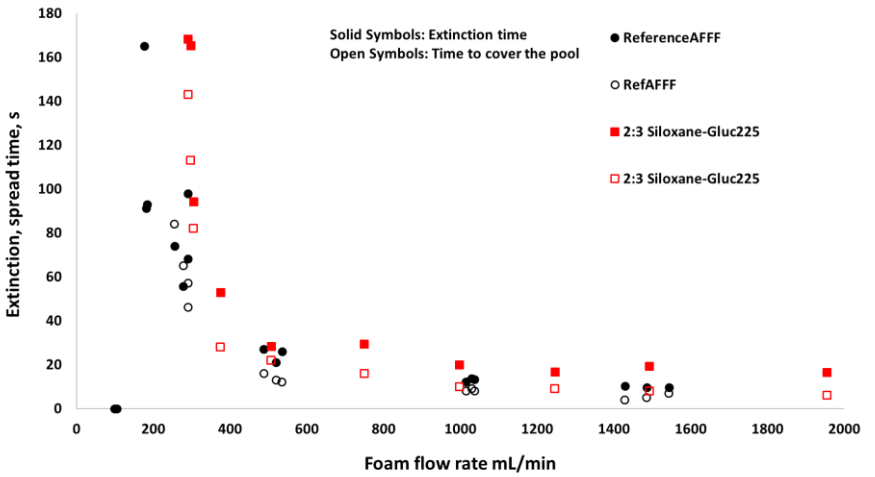

Figure 48. Comparison of foam spread time to cover the pool surface during the heptane pool fire suppression with the fire extinction time at different foam application rates for the bench-scale pool. Foam is delivered at the center of the pool at a constant flow rate and allowed to spread. Spread times (open symbols) and extinction times (closed symbols) are shown for Siloxane-Gluc225 and RefAFFF listed in Table 10. Data points on x-axis (y=0) show flow rates where fire was not extinguished in 180 s [50].

Fluorocarbon surfactants differ significantly from the fluorine-free surfactants in their hydrophobic and oleophobic interactions with water and fuel leading to superior foam properties and fire performance. However, combining two fluorine-free non-ionic surfactant structures in a mixture can exhibit synergistic effects leading to superior performance over the individual components. We showed that a commercial siloxane surfactant with a polyoxyethylene head group when combined with a certain commercial alkane surfactant with polyglycoside head group exhibited quicker (4.7 times smaller extinction time at 1200 mL min^{-1} foam flow rate) fire extinction of a heptane pool fire than the individual components. This was due to synergistic reduction in foam degradation rate (3.5 times longer time at 100% foam degradation caused by the heptane vapors generated by the hot fuel pool for the mixed surfactant formulation over the individual surfactants. Despite the lack of a similar synergism in fuel transport rates through a foam layer, the fuel transport rates are suppressed for longer time for foams generated with the surfactant mixture because of the enahanced foam stabiliy. The molecular intercations between the two surfactants' hydrophilic head groups (poly oxyethylene and poly glycoside) and precise mechanisms of the synergism are unclear. However, increasing the number of –OH functional groups by increasing the size of the polyglycoside head, reduced the foam degradation and the fire extinction time further. Indeed, small differences in the size (x=0.4, 0.5, and 0.7) of polyglycoside head had a significant effect on foam stability. Similarly, we hypothesize that varying the size of oxyethylene head of siloxane surfactant can also affect the degree of synergism. It is possible that the stronger interaction between the two head groups may have suppressed the surfactant solubility in heptane resulting in increased foam stability near the foam-fuel interface. Previuosly, we showed that the fuel destabilizes the foam near the foam-fuel interface causing coalescence of bubbles in a cascading effect leading to rapid degrdation. Similarly, the micelle size and micelle number density can affect the fuel concentration and diffusivity, which may affect the fuel transport. The large tail and slender head of the branched-trisiloxane surfactant and vice-versa for

the glycoside surfactant may enable bilayer vesicle formation providing stability to the bubble lamellae and resistance to the fuel. The mechanisms of transport for the individual versus combined surfactants are unclear and may not be limited to trisiloxane-glycoside systems. The synergism between siloxane and glycoside structures resulted in a factor of 5 enhnacement in foam stability and fire extinction performance demonstarting the key role played by the interactions between the surfactant structures and fuel in extinction. A basic understanding of the mechanisms of synergism can lead to an approach based on synthesizing synergistic molecules, which can result in performance matching that of fluorocarbon surfactants.

We found that the fire extinction time for NRL's siloxane surfactant formulation to be less than 1.5 times that of an equivalent AFFF formulation containing a flurocarbon surfactant for both the bench (19 cm diameter) and 1.83 m (6 ft) diameter heptane pool-fires at a fixed foam application rate (22 L m^{-2} min^{-1}). The viscosity of NRL's siloxane-formulation concentrate is within the MilSpec criteria unlike many commerical fluorine-free firefighting-foam concentrates. Foam's resistance to fuel vapors from hot pool play crucial role in designing firefighting surfactants and foams. Foam's resistance depends on specific surfactants and their interactions with a specific fuel at air-water and fuel-water interfaces, and micelles. The difference in fire extinction between the Siloxane-Glycoside and RefAFFF formulations was due to differences in foam degradation and fuel vapor transport rates rather than the differences in surface tension (dynamic and static) or aqueous film formation, bubble size distributions and coarsening, foam spread rates, and liquid drainage rates for the foam appliaction rates studied. However, fluorocarbon and fluorine-free surfactants can have very different effects on bubble sizes, coarsening, and liquid drainage when hot fuel is present and need to be studied further. Single lamella studies are needed to directly relate surfactant and fuel effects to a bubble lamella stability. Solution and foam properties measured especially in the presence of hot fuel cannot be ignored because they may become the controlling factors for fire extinction depending on the specific surfactant system and the fuel under consideration, and the foam generation methods used.

4.5. Siloxane-Glycoside Surfactant Monolayers at Heptane-Water Interface

We aim to study surfactant monolayers to facilitate the process of searching new surfactant in order to replace the toxic fluorocarbon surfactants contained in firefighting foams using molecular dynamics (MD) simulation. MD simulations mimic the physical movements of atoms (position and velocity) by numerically solving Newton's equations of motion subject to interatomic potentials (i.e. force field) on tens of nano-seconds scale. We developed experimentally validated MD models for a few examples of siloxane and hydrocarbon surfactants and developed an understanding of the differences with a fluorocarbon surfactant in air/water and heptane/water interfacial structures [35]. The validated MD models are used to develop new understanding of how variations in chemical structure impact interface structure and may give rise to new surfactant designs.

We examine the interfacial properties of a few commercially available hydrocarbon (sodium dodecyl sulfate, SDS, and hexadecyltrimethylammonium bromide, CTAB (or C_{16}TAB)) and siloxane (2,2,4-trimethyl-4-[(trimethylsilyl)oxy]-3,8,11,14,17,20,23,26,29,32-decaoxa-2,4-disilatritrilacontane used to represent Silwet L77) surfactants and compare them with a commercial perfluorosurfactant (2,2,3,3,4,4,5,5,6,6,7,7,8,8,8-pentadecafluorooctanoic acid, PFOA) [35]. The simulation results demonstrate that the predicted values of surface area and surface tension agree reasonably well with experimental data and validate the methods including the CHARMM36 lipid

force field used to simulate the surfactant molecules in foams. Moreover, the simulation results show that the Gibbs elasticity of perfluorocarbon and siloxane surfactants at air-water interface are greater than the two hydrocarbon surfactants considered in this study. High Gibbs elasticity and low surface tension may suggest higher stability of bubble surfaces packed with the fluorocarbon and siloxane surfactants to dilatation of the lamellae than those with the hydrocarbon surfactants. The heptane penetration distance into the heptane-water interface is also smaller for the fluorocarbon and siloxane surfactants compared to the two hydrocarbon surfactants [35].

Using the experimentally validated MD model, we varied the structure of surfactants and compare the interfacial properties in order to search possible good candidate that can be effective enough for fire suppression and be MilSpec-qualified [43]. From the MD simulations, the interfacial properties such as the surface area per molecule (*A*), interfacial thicknesses of water (d_w) and heptane (d_h), the heptane to surfactant ratio (*hsr*), the heptane surface number density (*hsnd*), the inverse of maximum surfactant number density ($msnd^{-1}$), the heptane volumetric number density (*hvnd*), hydrogen bond number per molecule (*hbnm*) and hydrogen bond number per Å^2 (*hbna*) are calculated [43]. The d_w and *hbnm* are the properties of the hydrophilic head group, and d_h, *hsr*, $msnd^{-1}$, and *hvnd* are the properties of the hydrophobic tail. The *hbnm* is related to stability of the head group, while the *hsr*, $msnd^{-1}$ and *hvnd* are related to heptane transport rate in the tail.

The key aspects of variation of structures that we are interested are tested, and the detail results are presented [43]. The key conclusions are that hydroxyl-capped trisiloxane have smaller heptane to surfactant ratio (*hsr*) and inverse of maximum surfactants number density ($msnd^{-1}$) than methoxyl-capped trisiloxane, which suggests that hydroxyl-capped trisiloxane is a better candidate. By varying the alkyl glucoside length *n*, the result that the alkyl glucoside with $n \geq 9$ would have lower $msnd^{-1}$ and *hvnd*, and also higher *hbnm*, which make $n \geq 9$ good candidate. The β- and (α,β-1→4)-alkylglucoside have significantly smaller *hsr*, *hvnd* , thus better candidate than the ones with α- and (α,β-1→6) linkage. The 2k3s and 2k3t have smaller *hvnd* and greater *hbnm* than other siloxanes which make them good candidate. The neutral charged or zwitterionic hydrocarbon surfactants have lower heptane number density than that of the charged ones. By studying the commercial surfactants, we conclude that two Glucopon-based hydrocarbon surfactants g215 and g225 have very similar interface properties. Among the commercial surfactant, capstone and capstone/g215e have the minimum *hvnd* which agrees with the experimental heptane diffusion rate of AFFF. Among the pure trisiloxane and trisiloxane/alkylglucoside studied, the H8 and H8/g225 have the minimum d_h, *hsr* and also $msnd^{-1}$ and *hvnd*.

4.5.1. Development and Validation of MD Model

For developing and validating the MD model, we chose the chemical structures of the surfactants shown in Figure 49 [35]. The firefighting surfactants are chosen partly because experimental data for the interfacial properties are available or can be measured. The hydrocarbon surfactants SDS and CTAB at an air-water interface were simulated using MD previously [52] and serve as references to compare against the siloxane and the fluorocarbon surfactants. A validated model can be used to understand the effects of surfactant's structural changes on interface and film stability in future works.

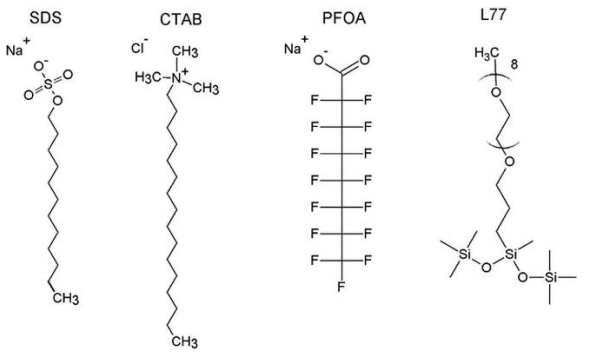

Figure 49. The chemical structures of hydrocarbon surfactants SDS and CTAB, perfluorocarbon surfactant PFOA, and siloxane surfactant L77. For CTAB (or C_{16}TAB), as the parameter for the free bromide ion is not available in CHARMM force field, the bromide is replaced by chloride in our MD simulations [35].

Figure 50e-h show a comparison of MD predictions with the experimental data using Gibbs-equation (GE_2). The results show good agreement between MD and GE_2 for the hydrocarbon and fluorocarbon surfactants SDS (Figure 50e) and PFOA (Figure 50g) respectively. Figure 50e-h also show good agreement between MD predictions and direct experimental measurements (labeled EXP) of surface area per molecule at saturation and surface tension reported in the literature [53, 54, 55-58]. However, there are quantitative differences between MD predictions and GE_2 for the hydrocarbon and trisiloxane surfactants CTAB and L77 (Figure 50f and 50g respectively) possibly due to high sensitivity to the calculation of slope using a polynomial fit of the experimental data.

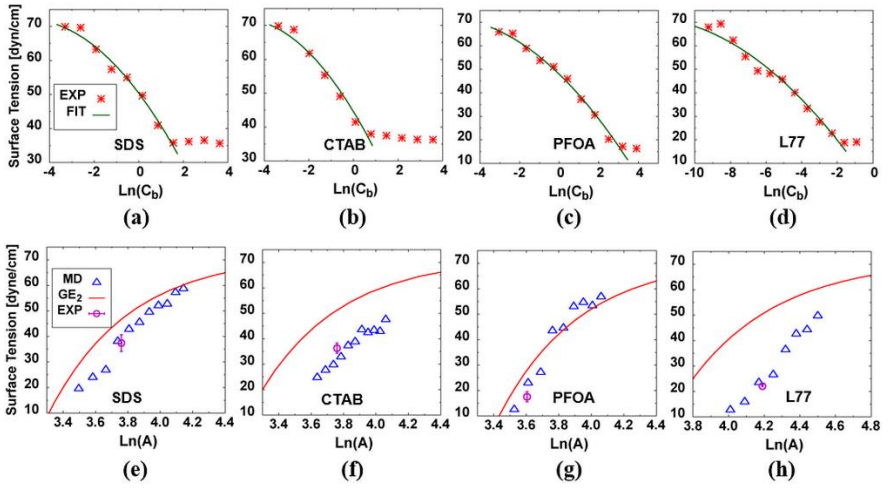

Figure 50. (a)-(d) Experimental measurements of surface tension versus concentration (mole/m^3) of surfactant in the bulk solution and 2nd order polynomial fit to the experimental data to calculate area per molecule *A* using Gibbs-equation. The uncertainty for each experimental surface tension measurement is 0.5 dyne/cm. (e)-(h) Comparison of surface tension versus surface area per molecule calculated from Gibbs equation (GE_2) with MD-predictions. The purple data indicate the direct measurement of surface area per molecule and surface tension at saturation for SDS [55], CTAB [56], PFOA [53, 57], and L77 [58]. For consistency, all MD predicted surface tension values including that of pure water are adjusted by 19.0 dyne/cm higher to correct for the TIP3P water model [35].

4.5.1.1. Gibbs Elasticity (E) and Most Probable Surface Area per Molecule (A_m)

The Gibbs elasticity E of a film describes the strength of the intermolecular interactions between surfactant molecules at an interface. It is an indication of the capability of a monolayer to resist change in surfactant packing or area per molecule due to stretching of the interface, which is a measure of the film stability. E is given by

$$E = d\gamma/d(lnA)\ , \qquad (2)$$

where γ is the surface tension and A is the surface area per molecule of surfactant. E can be determined from MD simulations, which are shown in Figure 51. Figure 51a shows the MD predictions for surface tensions of different surfactants that were already shown in Figure 50e-h. Figure 51a also shows a third order polynomial (with the negative coefficient of the highest order) fitted to the MD predictions of surface tension by

$$y = -|a|x^3 + bx^2 + cx + d \quad , \qquad (3)$$

where x is the natural logarithm of surface area per molecule A, y is the surface tension, and a, b, and c are the parameters obtained from fitting.

The trisiloxane has large A values because of its branched tail as one may expect. The surface tension curve is very steep for PFOA among the surfactants studied. As the logarithm of surface area increases, the surface tension increases, trending in an "S" shape. Then by taking the derivative of the fitted polynomial, E was obtained as a function of $ln(A)$ as shown in Figure 51b. Figure 51b shows downward opening parabolas with maxima for different surfactants. The A value corresponding to the maximum Gibbs elasticity (E_m) is defined as the most probable surface area per molecule A_m. The maximum E indicates an interface's capacity to increase surface tension in response to imposed surface dilatation, therefore at this point the surfactant is most stable and resists surface dilatation or surfactant concentration fluctuations by retaining a uniform packing. The E_m and A_m values obtained from Figure 51b are shown in Figure 51c. Figure 51c shows that the E_m value predicted by MD simulation for CTAB monolayer was 64.6 dyne/cm at 25.0 °C, and agrees well with experimental value of 61.0 dyne/cm measured at 23.0 °C [56]. Experimental measurements of E_m for the other three surfactants were not available to our knowledge. The MD simulations show that the fluorocarbon surfactant PFOA has the greatest E_m (119.4 dyne/cm) and thus it is most stable, the siloxane surfactant L77 has an intermediate E_m value (90.9 dyne/cm), while hydrocarbons SDS (75.5 dyne/cm) and CTAB have the lowest values of E_m among the four surfactants. A surfactant is adsorbed on lamellae of bubbles within the foam structure. In foam stability experiments, foams are generated from different surfactants and degradation rates of a foam layer are measured with time. The order of the Gibbs elasticity values predicted by MD for different surfactant monolayers are qualitatively consistent with the foam stability measurements for SDS, perfluorocarbon surfactants and hydrocarbon surfactants.

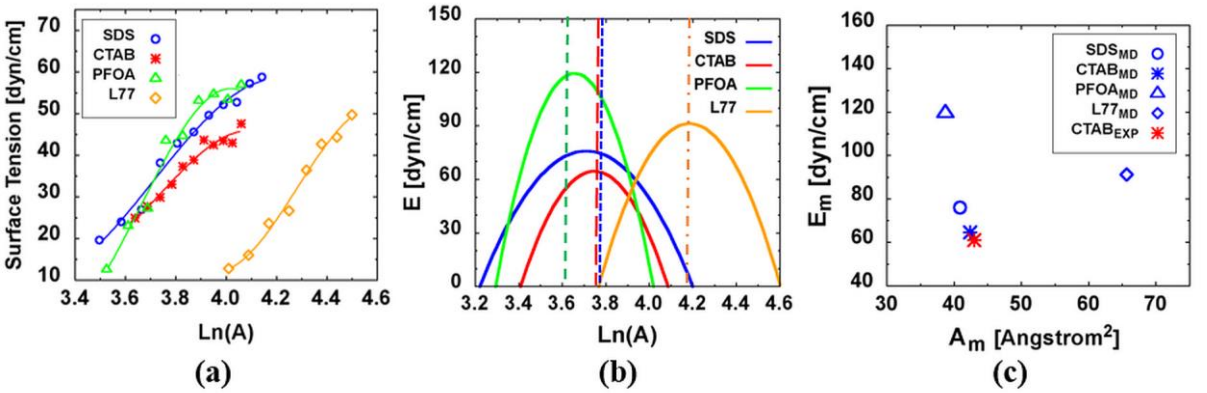

Figure 51. (a) The MD predictions for surface tension as functions of surface area per molecule, A, along with 3rd order polynomial fits (solid lines) for calculating maximum Gibbs elasticity, E_m. The uncertainty for each experimental surface tension measurement is 0.5 dyne/cm. (b) The MD-predicted Gibbs elasticity as functions of $ln(A)$. The vertical lines indicate the experimental values for surface area per molecule [53, 54, 56, 58]. (c) The most probable surface area at maximum Gibbs elasticity of surfactant monolayer obtained from MD simulations compared with experimental values of E_m and A_m for CTAB surfactant monolayer [35].

4.5.1.2. Comparison of MD-based A_m and γ_m with Experiments

The MD predictions of A_m were compared with experimental data [53, 54, 56, 58-60] and the MD simulation results of Jang et al. [52] in Figure 52a [35]. The results show that the A_m obtained from simulations agree reasonably well with experiments, with deviations less than 3.0 Å^2 for all four surfactants. The area of siloxane surfactant L77 is significantly larger than both the hydrocarbons, SDS and CTAB, and the fluorocarbon PFOA due to the long oxyethylene chain in the head group and also the bulky tri-siloxane group in the tail. PFOA has the smallest area due to its small head group (Figure 49). Zhuang et al. [61] showed that with the same tail, the surface area increases as the size of the head group increases; with the same head group, the surface area decreases as the hydrocarbon chain length increases due to stronger hydrophobic interaction of the tails. Therefore, the surface areas of SDS and CTAB are close because CTAB has a larger head group (trimethylamine) and longer hydrocarbon tail than SDS.

Figure 52b shows that the surface tension at saturation (γ_m) corresponds to E_m and A_m in Figure 51c. Small differences in the most stable surface area per molecule A_m can lead to rather large differences in the surface tension especially for PFOA which has the steepest curve as shown in Figure 51a. For PFOA, the predicted surface tension is noticeably higher than experimental values (Figure 52b). Nevertheless, the good agreement between the MD predictions for A_m and γ_m with the experimental data shows that our method based on the maximum in E_m for determining A_m and γ_m works well for the surfactants studied in this work. The A_m values from our calculations of the air-water interface using C36FF agree well with previous calculations of Newton black films by Jang and Goddard [52] for SDS and CTAB using DREIDING force-field as shown by blue bars in Figure 52a. Rusanov et al. [62] developed a thermodynamic model for thin and thick films relating Gibbs elasticity and disjoining pressure. The model predicts a peak in elasticity as the surfactant concentration approaches CMC. Their model predictions suggest that E_m corresponds to CMC consistent with the comparisons shown in Figure 52b. The A_m we defined represents the most stable packing, and requires the highest energy and force and it corresponds to E_m.

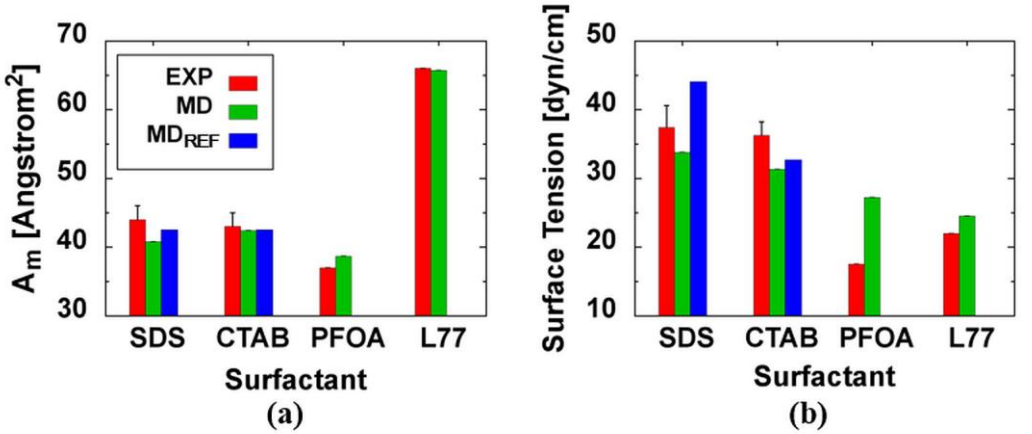

Figure 52. Comparisons of (a) the most stable surface area per molecule A_m, (b) surface tensions at saturation γ_m, MD predicted with the experimental data (EXP) for SDS [54], CTAB [54], PFOA [53], and L77 [56], and MD simulation results reported in the literature [52] (MD_{REF}) [35].

4.5.2. MD Simulations of Trisiloxane-Polyoxyethylenated and Alkylpolyglycosides

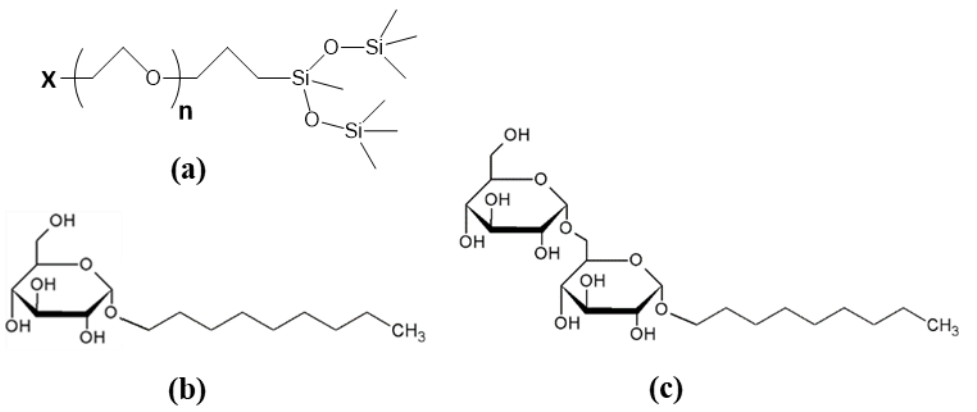

Figure 53. (a) Chemical Structure of polyoxyethylenated trisiloxane (existing in commercial trisiloxane 502W), X is OH, *n* is oxyethylene length in the range between 2 to 20 (b) alkylglucoside 1g9 with one glucoside head group and hydrocarbon length of 9 and (c) alkyl glucoside 2g9 with two glucosides head group 1→6 glucoside linkage and hydrocarbon length of 9 [43].

The chemical structure of polyoxyethylenated trisiloxane surfactant and hydrocarbon surfactant with one and two glucoside head group are shown in Figure 53. Three types of monolayer systems with total of 36 molecules per monolayer are simulated; (1) a pure trisiloxane with a terminal hydroxyl (OH) group and varied oxyethylene length (*n*=3~20 at 25 °C, and *n*=4~20 at 60 °C), (2) a two-component trisiloxane/1g9 and trisiloxane/2g9 systems with varied oxyethylene length of trisiloxane (*n*=2~20 at 25 °C), (3) a three-component trisiloxane/1g9/2g9 systems with varied oxyethylene length of trisiloxane (*n*=2~20 at 60 °C). The experimental measurement shows that the fire suppression performance is best when the ratio of trisiloxane to Glucopon is 2:3, which is applied in the simulations. In the two-component systems, the molecular number ratio of trisiloxane:1g9 and trisiloxane:2g9 is 2:3, i.e. in each monolayer, there are 14 trisiloxane, and 22 1g9 or 22 2g9. Glucopon 225 is a commercial Glucopon with one and two glucoside head, and hydrocarbon tail ranges from 8~10, the averaged value 9 is used in our

simulation. The average number of glucosides in Glucopon 225 is 1.7, which gives ratio of 1g9:2g9=3:7. Therefore, to mimic Glucopon 225 behavior in the three-component systems, in each monolayer, the numbers of trisiloxane, 1g9, and 2g9 are 14, 7, and 15, respectively. Also, 1g9:2g9=1:1 for Glucopon 215, in each monolayer of the three-component systems, the numbers of trisiloxane, 1g9, and 2g9 are 14, 11, and 11, respectively.

4.5.2.1. Surface Area per Molecule (*A*)

The surface area per molecule is calculated by dividing total cross-sectional area by the total number of surfactant 36, i.e. $A = A_{tot}/36$ [43]. Previous studies reported that the ratio of surface area per molecule of polyoxyethylenated surfactant (A) and the square root of oxyethylene unit number ($\sqrt{n}$) is constant, i.e., there is the correlation $A = k \times \sqrt{n}$ for specific type of surfactant at air/water interface [63, 64]. For example, the value of k for a polyoxyethylenated hydrocarbon surfactant $C_{12}H_{25}(OC_2H_4)_nOH$ is between 21.7-24.8 at 25 °C. As shown in Figure 54a, for hydroxyl-capped polyoxyethylenated trisiloxane at heptane/water interface, there is a similar linear correlation that $A = k \times \sqrt{n} + b$, where k and b values are 9.2±0.1 and 48.4±0.5 at 25 °C, and they are 10.6±0.3 and 47.3±1.0 at 60 °C, respectively. Moreover, with the same oxyethylene unit number n, the surface areas of pure trisiloxane at 60 ° C are generally greater than the values at 25 °C due to more atomic movement at higher temperature. The differences are slightly greater at high oxyethylene length. The surface area per molecule A of pure trisiloxane increases as n increases, while for trisiloxane/1g9 and trisiloxane/2g9, the A increase slightly and then level off. The A of pure trisiloxane are much greater than the values of trisiloxane/1g9 and trisiloxane/2g9, and the difference is greater at large n at 25 °C (Figure 54b). Similar trend is observed in pure trisiloxane and three-component trisiloxane/1g9/2g9 systems at 60 °C. It suggests that pure trisiloxane is much more sensitive to oxyethylene length than the mixture systems when n is large.

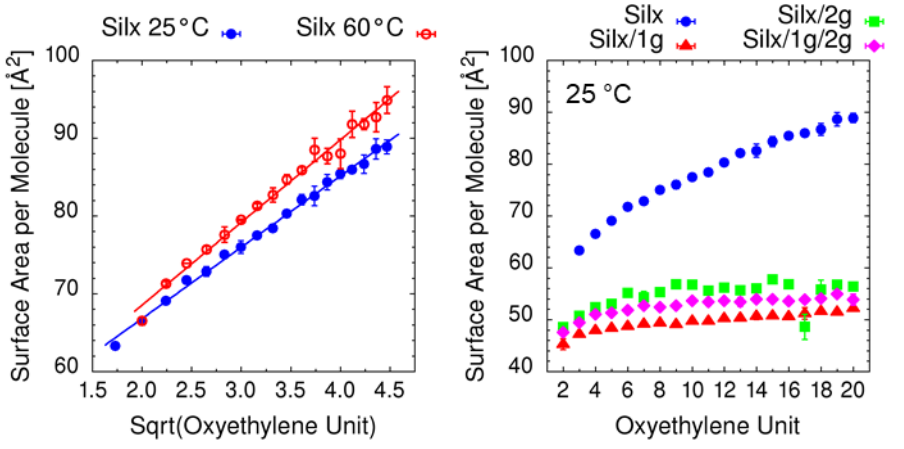

(a) (b)

Figure 54. (a) The surface area per molecule of pure trisiloxane at 25 °C and 60 °C as function of square root of oxyethylene length. (b) The surface area per molecule of pure trisiloxane, trisiloxane/1g9, trisiloxane/2g9, and trisiloxane/1g9/2g9 at the heptane/surfactant-monolayer/water interface at 25 °C as function of trisiloxane oxyethylene length [43].

4.5.2.2. Interfacial Thickness of Water (d_w) and Heptane (d_h)

Mass density profile of each component (trisilxoane, alkylglucoside, water, and heptane) is calculated based on atomic number density of each individual atoms [43]. The heptane/surfactant-monolayer/water system in the normal *z* direction are divided into small bins with bin size 0.2 Å, and then add up the bins of same molecule to obtain the atomic number density of each component. Based on atomic mass, the mass density profile for each component are obtained as shown in Figure 55a. Then, the interfacial thicknesses of water (d_w) and heptane (d_h), and also the heptane to surfactant ratio in the interface (*hsr*) are calculated based on the mass density profile. Interfacial thickness of water d_w is defined as the distance between the 10% to 90% mass density of water. Interfacial thickness of heptane d_h is defined as the distance between the 10% to 90% mass density of heptane, as shown in Figure 55b. The *hsr* is the ratio of number of heptane molecule to number of surfactant molecule in the interface, which is the region between 90% and 90 % of the bulk heptane density.

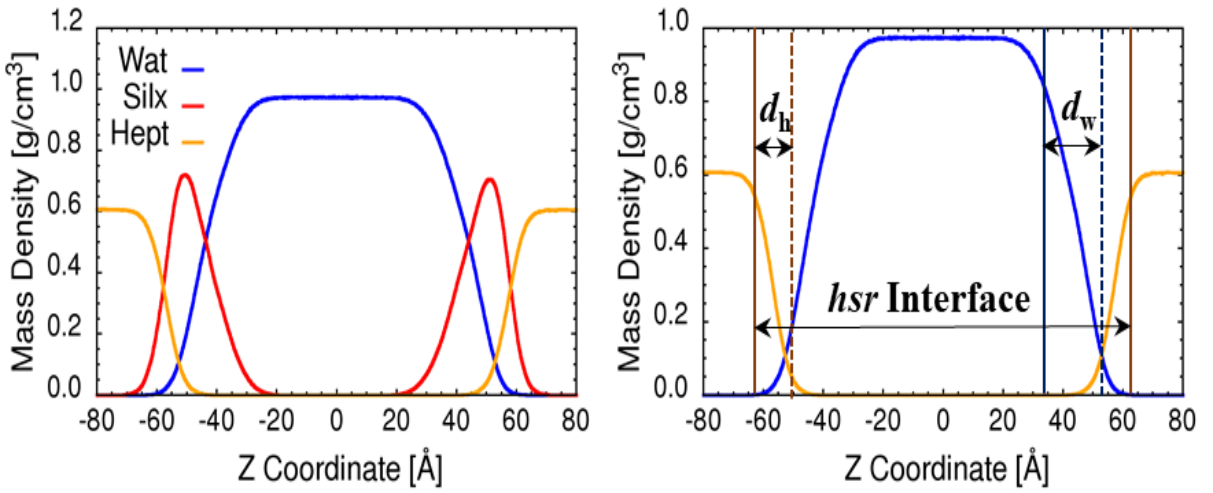

(a) (b)

Figure 55. (a) Mass density profile, and the interface used to calculate interfacial thicknesses and heptane to surfactant ratio (*hsr*) of trisiloxane H8 at 60 °C (b) Schematic plots indicating the definition of interfacial thicknesses of water, heptane and *hsr* interface, respectively [43].

The interfacial thickness of water d_w increases as trisiloxane oxyethylene *n* increases as expected at both 25 °C (Figure 56a) and 60 °C. The d_w of pure trisiloxane are very similar at 25 °C and 60 °C which indicate weak temperature dependence. The pure trisiloxane have the greatest d_w, while the two-component trisiloxane/1g9 and trisiloxane/2g9 and the three-component trisiloxane/1g9/2g9 have similar and smaller d_w. Generally, the interfacial thickness of heptane d_h of all systems increases slightly with *n* when $n \geq 9$, but the *n* dependence is weak. Unlike the d_w, the d_h of pure trisiloxane are smaller at 25 °C than 60 °C which indicate strong temperature dependence. The pure trisiloxane have generally smaller d_h than trisiloxane/1g9, trisiloxane/2g9, and trisiloxane/1g9/2g9 at large *n* (Figure 56b), the difference is greater at 2g9 at 60 °C.

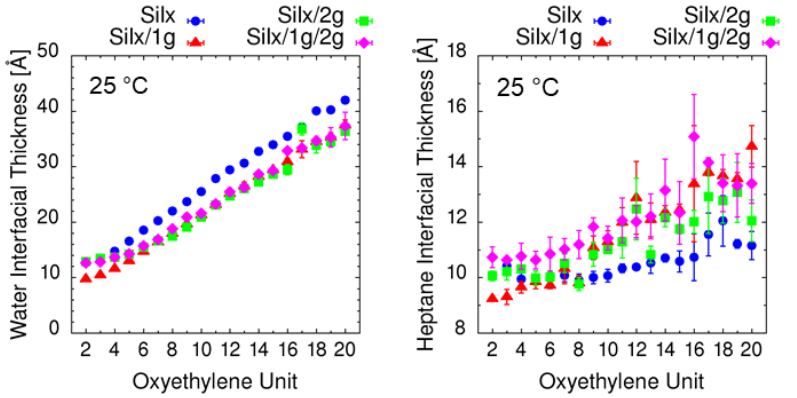

Figure 56. The interfacial thickness of (a) water (b) heptane of pure trisiloxane, trisiloxane/1g9, trisiloxane/2g9, and trisiloxane/1g9/2g9 at 25 °C as function of trisiloxane oxyethylene length.

4.5.2.3. Heptane to Surfactant Ratio (*hsr*) and Heptane Surface Number Density (*hsnd*)

The region between 90% and 90 % of the bulk heptane density is used to calculate heptane to the surfactant ratio (*hsr*) [43]. The *hsr* is the ratio of number of heptane molecule to number of surfactant molecule (72 for all systems in this report) in the interface, i.e. it is the number of heptane molecule per surfactant molecule. The heptane surface number density (*hsnd*) is the number of heptane molecule per unit area (Angstrom^2), and it is calculated by $hsnd = hsr/A$, where A is the surface area per surfactant molecule.

As shown in Figure 57a, generally, the *hsr* increases as *n* increase for all systems. The *hsr* of pure trisiloxane is greater than two- and three-component mixtures. The *hsr* of pure trisiloxane at 60 °C is significantly greater than the value of 25 °C, which suggests strong temperature dependence of *hsr*. The *hsnd* values of trisiloxane/1g9 and trisiloxane/2g9 are slightly higher when $n \geq 9$ at 25 °C (Figure 57b), while the *hsnd* of pure trisiloxane are nearly *n* independent, and trisiloxane/1g9/2g9 are slightly increases when $n \geq 4$ at 60 °C,

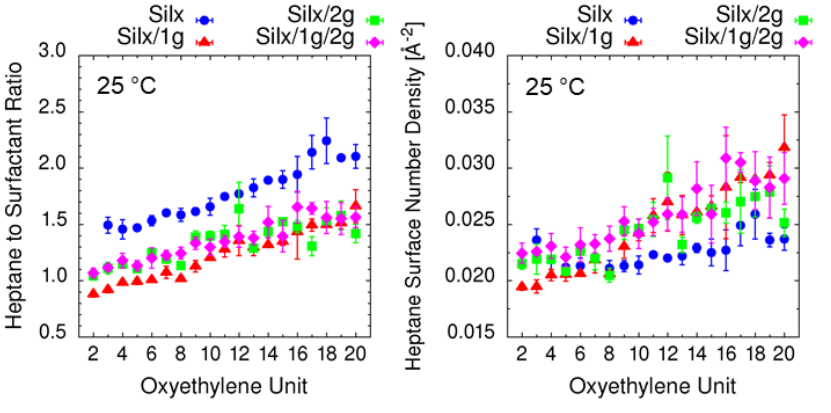

Figure 57. (a) Heptane to surfactant ratio of pure trisiloxane, trisiloxane/1g9, trisiloxane/2g9, and trisiloxane/1g9/2g9 at the interface and (b) the heptane surface number density at 25 °C as function of trisiloxane oxyethylene length [43].

4.5.2.4. Volumetric Number Densities (*msnd*$^{-1}$ and *hvnd*)

Atomic number density profile of each component (type of molecule) can also be calculated based on atomic number density of each individual atoms [43]. Then the maximum surfactant volumetric number density (*msnd*) and the heptane volumetric number density (*hvnd*) at *msnd* are calculated based on molecular/group number density. The *msnd* is the atomic number density of surfactant is at its maximum, and the *hvnd* is the atomic number density of heptane where the atomic number density of surfactant is at its maximum, as shown in Figure 58. The *msnd* and *hvnd* are calculated because they can be used to describe the smallest channel size and the minimum (limit) heptane concentration that can pass through the surfactant monolayer. In this report, the inverse of *msnd*, i.e. *msnd*$^{-1}$ is used instead of *msnd* in order to correlate it to *hvnd* trend directly. The *msnd*$^{-1}$ is the channel size of the narrowest region in the surfactant monolayer. Generally we expect high *hvnd* when *msnd*$^{-1}$ is high.

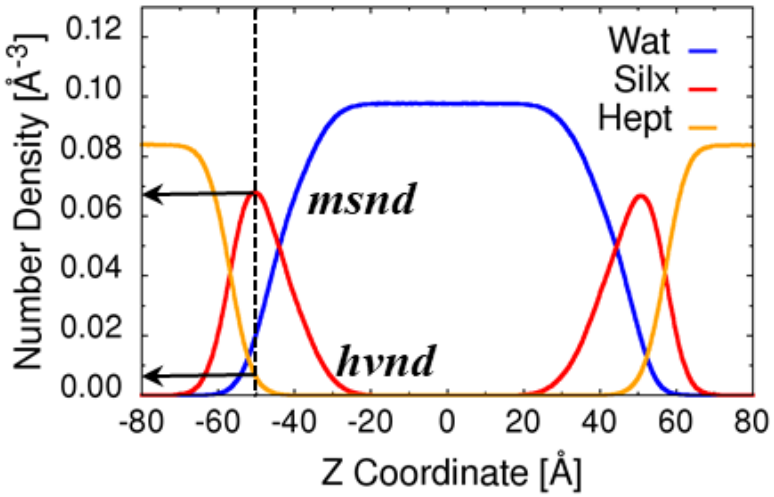

Figure 58. Atomic number density profile of each component in trisiloxane H8 system. The lines indicates the definition of the maximum surfactant volumetric number density (*msnd*) and the heptane volumetric number density (*hvnd*) at the *msnd* [43].

As shown in Figure 59a, the *msnd* of pure trisiloxane at 25 °C is slightly greater than the values at 60 °C. The *msnd*$^{-1}$ of trisiloxane/1g9 and trisiloxane/2g9 are smaller than pure trisiloxane, and the trisiloxane/1g9/2g9 have the smallest *msnd*$^{-1}$ values. As *n* increase, *msnd*$^{-1}$ of trisiloxane/1g9, trisiloxane/2g9 and trisiloxane/1g9/2g9 do not show *n* dependence. As *n* increase, the *hvnd* of pure trisiloxane increases slightly, while the *hvnd* of all mixtures increases more significantly. The *hvnd* of pure trisiloxane are greater than trisiloxane/1g9 and trisiloxane/2g9 when *n* is small ($n \leq 11$). However, the *hvnd* of trisiloxane/1g9 increases so fast that the values get very close to pure trisiloxane at 25 °C (Figure 59b), similar trend is also observed in the *hvnd* of trisiloxane/1g9/2g9 which is likely due to the presence of 1g9.

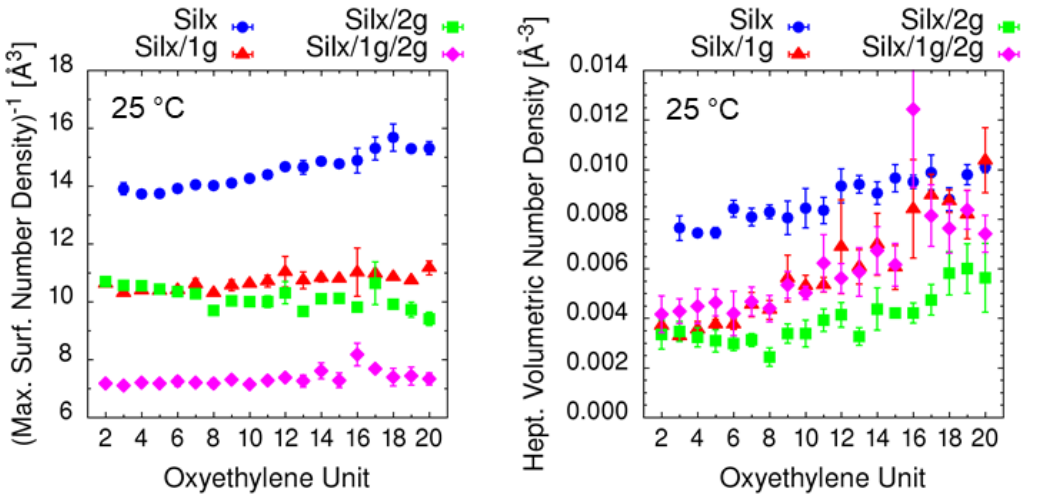

(a) (b)

Figure 59. (a) Inverse of the maximum surfactant volumetric number density (*msnd*$^{-1}$) and (b) the heptane volumetric number density (*hvnd*) at *msnd* at 25 °C as function of trisiloxane oxyethylene length [43].

4.5.2.5. Intermolecular Hydrogen Bonds

The number of hydrogen bond is calculated based on the condition that the distance of proton-donor and proton-acceptor pair is less than 2.4 Å, and the angle between them is greater than 150° [43].The intermolecular hydrogen bond is the hydrogen bond formed between different surfactant molecules, while the intramolecular hydrogen bond is the hydrogen bond formed within the same molecule, which involves bending of proton-donor and proton-acceptor group. The more the intermolecular hydrogen bond, and the less intramolecular hydrogen bond, the more stable the surfactant monolayer head group region. The intramolecular hydrogen bond numbers are generally very small, therefore, the data are not presented in this report. However, it is considered in the intermolecular hydrogen bond calculation for higher accuracy. The number of the intermolecular hydrogen bond is calculated by subtracting the number of intramolecular hydrogen bond from the total number of hydrogen bond, i.e. $N_{inter} = N_{tot} - N_{intra}$.

The (intermolecular) hydrogen bond number per molecule (*hbnm*) of pure trisiloxane at 60 °C are slightly smaller than the ones at 25 °C (Figure 60a**)**, which agree with the slightly greater surface area at 60 °C. As *n* increases, the *hbna* of pure trisiloxane decreases (Figure 60b) while the *hbna* of mixture decrease and level off (and may have a minimum between $9 \leq n \leq 12$) (Figure 60d). The opposite trend of *hbnm* and *hbna* indicate that besides the stability of the monolayer, the *hbna* as a cross-sectional unit area properties, may be related to the heptane transport rate. The *hbnm* of trisiloxane/2g9 are much greater trisiloxane/1g9, and the pure trisiloxane have the least *hbnm* and *hbna* due to the number of glucoside in the system (Figure 60c, 60d**)**. As *n* increases, the *hbnm* of trisiloxane/1g9 increases when $n \leq 11$, and then level off. The *hbnm* of trisiloxane/2g9 when $n \geq 13$ are generally greater than smaller *n*. However, both the *hbnm* and *hbna* of trisiloxane/2g9 data are quite scattered at 25 °C.

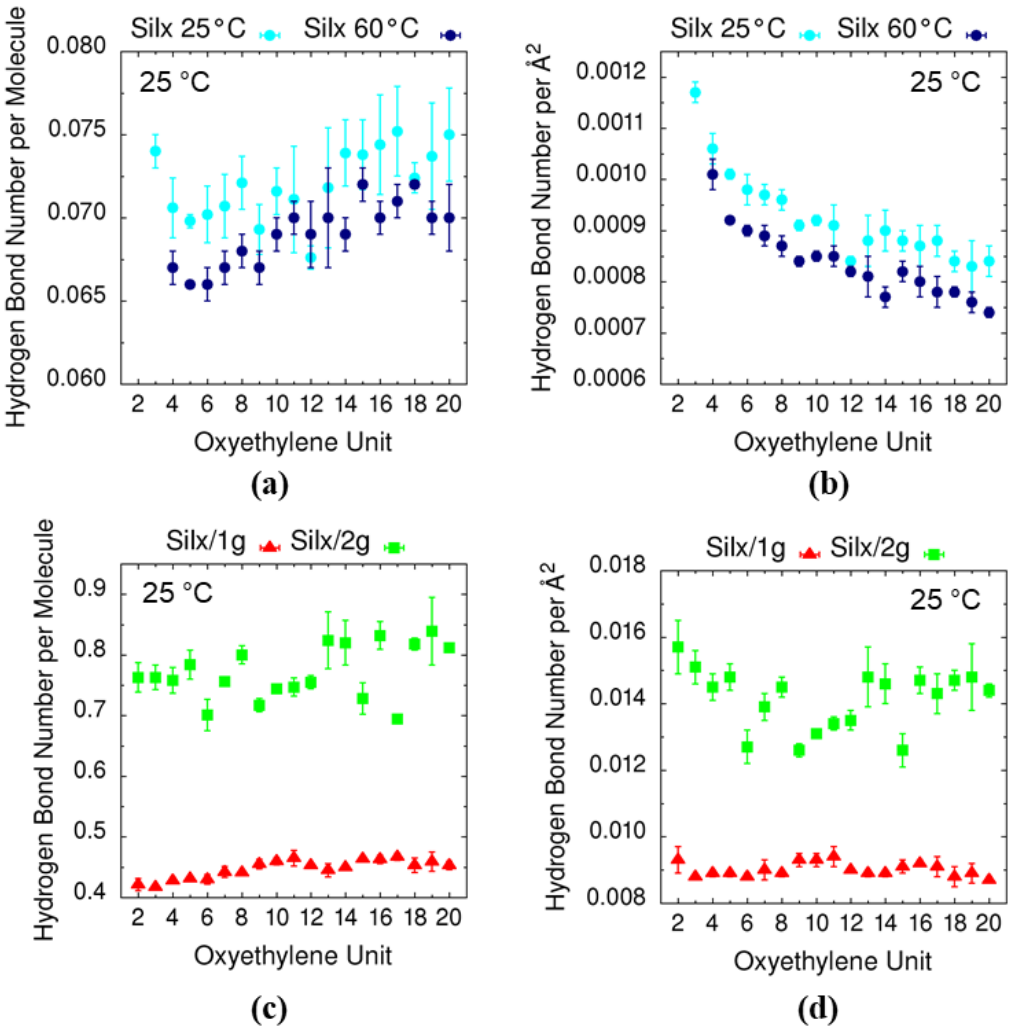

Figure 60. Intermolecular hydrogen bond number per molecule and intermolecular hydrogen bond number per $Å^2$ of (a-b) pure trisiloxane at 25 °C and 60 °C, and (c-d) mixed trisiloxane/1g9, and trisiloxane/2g9 at 25 °C as function of trisiloxane oxyethylene length [43].

4.5.2.6. Comparison of Surfactants Packing

As shown in Figure 61, the packing of pure capstone is tightest and most ordered, and the 1g9 is packed tighter and more ordered than 2g9, while pure trisiloxane H10 has the loosest packing and it is much less ordered, which agree with the surface area per molecule *A* that the *A* of capstone is smallest, followed by 1g9 and 2g9, and trisiloxane H10 has the highest *A* [43]. The pure capstone has the least penetration of heptane into the monolayer, followed by 1g9 and 2g9, while pure trisiloxane H10 has the most heptane penetration, which agree with *hsr* values. By mixing capstone with 1g9 with ratio 3:2, the Ca/1g9 and Ca/2g9 pack tighter and also have less heptane penetration than both pure capstone and 1g9. The packing of H10/1g9 and H10/2g9 and the heptane penetration is between pure H10 and 1g9, however, the heptane penetration is closer to 1g9 and 2g9, which agree with *hsr* values.

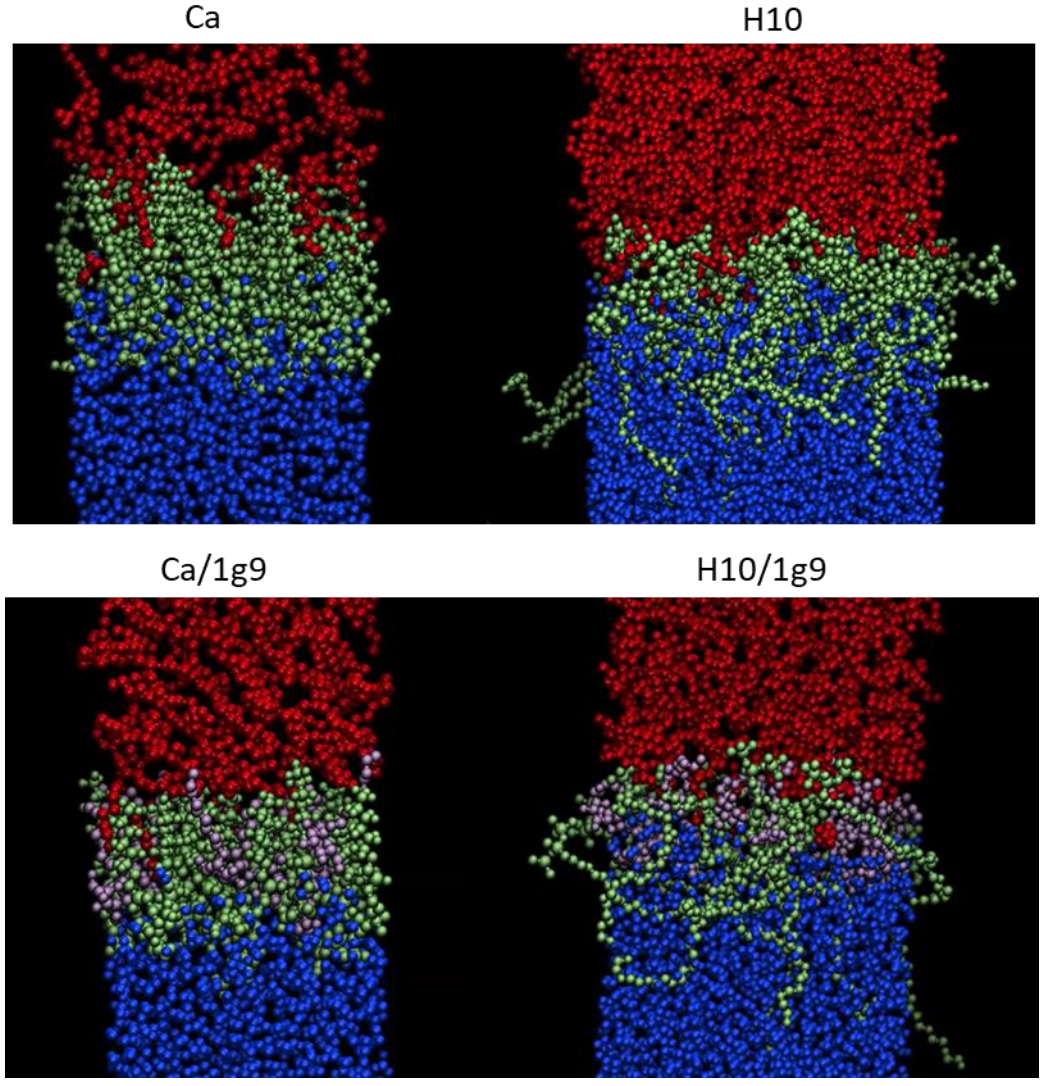

Figure 61. The pure capstone, polyoxyethylenated trisiloxane H10 (X=OH, *n*=10), and two-component capstone/1g9 (with ratio 3:2), and H10/1g9 (with ratio 2:3) surfactant monolayer at the heptane/water interface system at the end of the MD simulations at 25 °C, respectively. (Water is shown in blue spheres, heptane is shown in red, capstone and trisiloxane surfactant are shown in green, and 1g9 is shown in pink spheres.) Only the top half in the *z* direction of the simulation setup are shown, the bottom half is a mirror image of top one [43].

4.5.2.7. Summary of Findings from the MD Simulations

For trisiloxane/1g9, trisiloxane/2g9, and trisiloxane/1g9/2g9, as trisiloxane oxyethylene length *n* increases, the surface area per molecule *A* increase and then level off when $n \geq 8$ [43]. The *hsr* of the mixtures at $n \leq 8$ are smaller than the ones at $n \geq 9$. The *hvnd* of the mixtures increases dramatically when $n \geq 8$. Therefore, to minimize fuel transport rate, the good trisiloxane candidate is to use $n \leq 8$. However, the *hbnm* of trisiloxane/2g9 are mostly higher when $n \geq 13$, which suggest that the monolayer may be more stable. Therefore, when using trisiloxane with single oxyethylene unit length, fuel transport rate and stability are trade off, and the optimization based on *n* is limited. One possible solution to mix the short and long oxyethylene length ($n \leq 8$ and $n \geq 13$).

By comparing the hydroxyl-capped (H) and methoxyl-capped (M) trisiloxane, the results show that hydroxyl-capped trisiloxane have smaller heptane interfacial thickness (d_h), heptane to surfactant ratio (*hsr*), and $msnd^{-1}$ than and methoxyl-capped trisiloxane. Therefore, the hydroxyl-capped trisiloxane would be better choice.

For trisiloxane/alkylglucoside H11/1g and H11/2g, as alkyl glucoside hydrocarbon length *n* increases, the heptane surface number density *hsnd* for $n \leq 6$ are greater than the values for $n \geq 7$ and it shows a possible minimum at *n* around 8 for 25 °C. As the alkyl glucoside hydrocarbon length *n* increases, the maximum surfactants number density *msnd* increase first and then level off at $n=9$, and the heptane volumetric number density (*hvnd*) at *msnd* decrease and level off as expected. The alkyl glucoside with hydrocarbon length $n \geq 8$ have high *hbnm* and *hbna*, thus high monolayer stability. Therefore, the alkyl glucoside with hydrocarbon length $n>=8$ would be better choice.

With the same hydrocarbon length, the β- and (α,β-1→4)alkyl glucoside (represented by *mkn*) have significantly smaller surface area per molecule *A*, heptane to surfactant ratio *hsr*, *hvnd* than the α- and (α,α-1→6)-alkylglucoside (represented by *mgn*). Moreover, for *mkn*, the smaller hydrocarbon length have the slightly lower *hsr*, but also higher $msnd^{-1}$ and *hvnd*. Therefore, intermediate value $n=10$ may be best option.

Siloxane with 1g or *cn* head group with 3u or 6s tail have the smallest *A*. 1k3u have the smallest *hsr* and 2g3t have the smallest *hsnd* at 60 °C. 2k6s have the greatest *msnd*, followed by 2k3s and 2k3t at both 25 °C and 60 °C. 2k6s, 2k3s and 2k3t also have the smallest *hvnd*, which make these three surfactant good candidate surfactant to minimize heptane transport rate. The siloxane 2k6s have the greatest hydrogen bond number per molecule (*hbnm*) and the hydrogen bond number per angstrom (*hbna*), followed by 2k3s and 2k3t, which make them form more stable in the surfactant monolayer, and better surfactant candidate for fire suppression. (Or maybe we can try cn6s, cn3u if it is feasible to prepare them experimentally).

The surfactants 1k10 and dmg have the smaller *hsr*, smaller *hsnd* than the rest surfactants. The 2k10 and 2k12 have much greater *msnd*, and much smaller *hvnd* than the charged hydrocarbon surfactants s310, lau, s312, sds, and dtab, which may suggest a neutral charged hydrocarbon surfactants have lower heptane transport rate than that of the charged ones.

By comparing the interfacial properties with varied capstone or trisiloxane H10 to alkylglucoside (1g9, 2g9) fraction, we conclude that capstone/alkylglucoside has minimum d_h and minimum $msnd^{-1}$ when capstone fraction $f=0.5$, and capstone/1g9 has maximum *hbnm* when $f=0.2$. The H10/alkylglucoside has minimum $msnd^{-1}$ when trisiloxane H10 fraction $f=0.2$.

By studying the commercial surfactants, we conclude that two Glucopon-based hydrocarbon surfactants (g215 and g225) have very similar interface properties. Among the commercial surfactant, capstone and capstone/g215e have the minimum *hvnd* which agree with the experimental heptane diffusion rate of AFFF. Among the pure trisiloxane and trisiloxane/alkylglucoside studied, the H8 and H8/g225 have the minimum d_h, *hsr* and also $msnd^{-1}$ and *hvnd*, which agree with the experimental results that pure H8 has the minimum heptane diffusion coefficient.

4.6. Fuel-Surfactant Effects

We conducted large scale pool fire testing of NRL's drop-in siloxane502W formulation, which is the 2:3 Siloxane-Gluc225 composition listed in Table 10. Tables 12a and 12b compare 28 ft^2

pool fire extinction performance for heptane and gasoline fuels. They show the the siloxane formulation much more effective on heptane than on gasoline fire.

Table 12a. Large scale heptane fire extinction

	Drop-in Requirement	28 ft² Heptane Pool Fire	
	3% concentrate viscosity cP	Extinction Time (s)	Burnback Time (s)
Ref AFFF	4.7	30	981
NRL's Drop-In Siloxane Formulation	7.4	51	338
Commercial Fluorine-Free Foam	16,120	42	778

*28 ft² heptane pool fire at 2 gpm foam solution application rate

Table 12b. Large scale gasoline fire extinction

	28 ft² Gasoline Pool Fire	
	Extinction Time (s)	Burnback Time (s)
MilSpec Criteria	< 30	> 360
Ref AFFF	24	759
Drop-in 502W Formulation	> 60, no extinction	N/A

To understand the causes for this difference among fuels, we studied the composition of gasoline that differentiates it from heptane, and conducted a series of bench scale experiments with siloxane formulation as well as other commercial fluorine-free formulations [65]. We found that the AFFF formulations are relative insensitive to the identity of the fuel, but the fluorine-free formulations display a significant divergence in extinction capability between these two fuels with the gasoline fire being the more difficult to extinguish. Using the NRL's siloxane formulation, twelve major components of gasoline from the *n*-alkane, *iso*-alkane, *cyclo*-alkane, aromatic and olefin categories were examined to determine a source for this difference in extinction capability. We found that it is the aromatic components category that caused the divergence in performance. Within the aromatic components this effect substantially increased with the number of methyl substituents (trimethylbenzene > xylenes > toluene > benzene). The mechanism involved was investigated by an experiment monitoring the aqueous surfactant solution – fuel interface for the crossing of surfactants and fuel with the finding that the surfactant was extracted by the fuel. The degree of extraction of surfactant into the fuel correlated with the effect of the fuel component on extinction, particularly within the aromatic components (trimethylbenzene > xylenes > toluene > benzene). As a simple two-component simulant for gasoline, a trimethylbenzene/heptane mixture is proposed and supported by foam degradation and fuel vapor transport through the foam characterization [65].

We digress a little in the next figure to remind 502W formulation's heptane-fire suppression before getting back to the discussion of fuel-surfactant effects. The 19 cm diameter heptane pool fire extinction times as a function foam flow rate are plotted in Figure 62 for the RefAFFF and an evolution of siloxane-glycoside formulations. The RefAFFF extinction time – foam flow rate profile represents a performance goal which is derived from this formulation's passing the MilSpec pool fire extinction time requirement [50]. As indicated above, the screening of many commercial siloxane and hydrocarbon surfactants by substituting them for the Capstone 1157 surfactant in the RefAFFF formulation produced only one candidate that displayed an extinction profile remotely comparable to that of RefAFFF. The 502W substitution for Capstone at the 3:2 ratio with Glucopon® 215UP is plotted in Figure 62 (Siloxane #1). The surfactant ratio was then systematically varied from 3:1 to 1:3 with the finding that the best improvement occurred at the 2:3 ratio (Siloxane #2). Next, a series of four alkyl polyglycoside surfactants were tested with the finding that the 2:3 502W:Glucopon® 225DK (Siloxane #3) with its larger glycoside head group closely approached the RefAFFF profile on the heptane pool fire.

To further evaluate this Siloxane #3 formulation, the MilSpec extinction test on the 28 ft² gasoline pool at NRL Chesapeake Bay Detachment (CBD) showed neither an extinction nor a fire

knockdown. As a control experiment, the RefAFFF formulation was retested, and it again extinguished the pool fire in less than the 30 sec MilSpec requirement. Sources suspected for this divergent behavior included fuel identity (heptane vs ethanol-free gasoline), foam generation method (near ambient pressure bubbling through a glass frit vs 100 psi passage through an aspirating nozzle, and pool size (correlation with heat intensity).

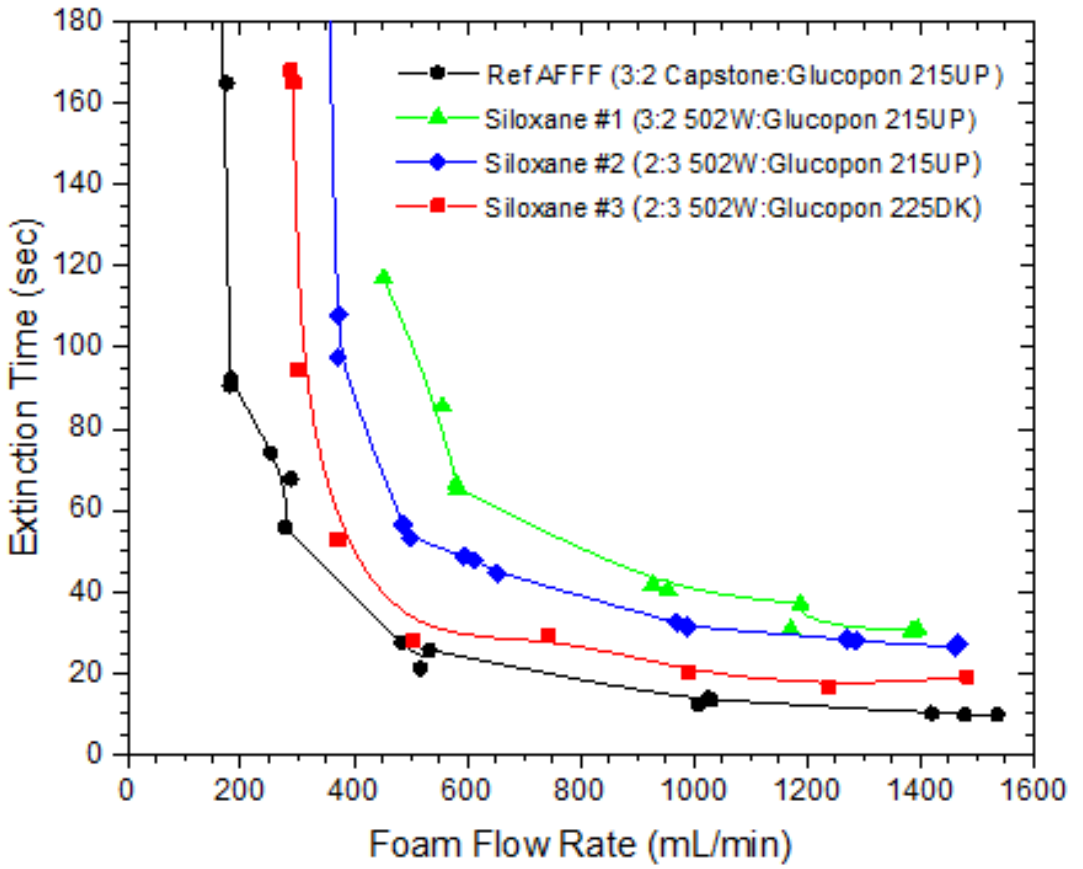

Figure 62. 19 cm diameter heptane pool fire extinction time vs foam flow rate for the RefAFFF formulation and an evolution of siloxane-glycoside formulations based on 502W siloxane surfactant and the alkyl polyglycoside surfactants Glucopon 215UP and Glucopon 225DK.

The alcohol-free gasoline used for the CBD MilSpec pool-fire testing was first item to be investigated. It was used as the fuel in the 19 cm pool fire, and gasoline vs heptane comparative data were obtained (Figure 63). For the Ref AFFF the difference between extinction profiles is small with the gasoline pool-fire being slightly more difficult to suppress although both fuels could be extinguished in less than 20 sec at the 1200 mL/min foam flow rate. However, for the NRL's Siloxane502W formulation the gasoline-heptane extinction profile difference is quite large with no extinction being observed at and below the 1200 mL/min foam flow rate. This remarkable difference is clearly attributable to the identity of the fuel and more particularly to the interaction of gasoline with components of the Siloxane formulation.

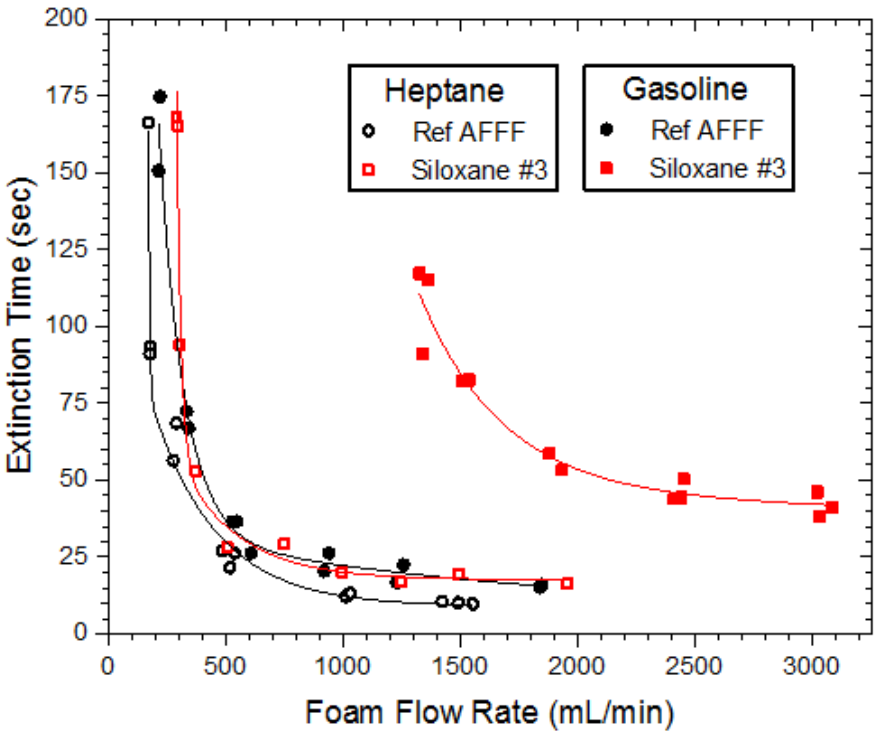

Figure 63. Comparative gasoline vs heptane pool-fire extinction profiles of RefAFFF and Siloxane #3 formulations on a 19 cm diameter pool.

Gasoline is a complex mixture of hydrocarbon components, and its composition varies depending on petroleum source, refining process and formulation for season of intended use. A simple ^{1}H NMR analysis was conducted on the gasoline used in the CBD testing and compared with the heptane fuel used in the benchtop testing and with *n*-heptane as well. Spectra of each fuel are presented in Figure 64. In the gasoline spectrum there are two groups of resonances: one in the 0.5-2.3 ppm range associated with protons bonded to aliphatic carbon structures and the other in the 6.8-7.2 ppm range associated with protons bonded to unsaturated carbon structures. Integration of these two groupings of resonances indicate that a significant quantity of aromatic and olefinic components reside in the gasoline. Within the aliphatic group, the resonances within the 2.0-2.3 ppm range correlate with methyl groups bonded to aromatic or olefinic structures. Examination of the heptane and *n*-heptane spectra provides further insight. Neither of these spectra display resonances corresponding to unsaturation in hydrocarbon structures. The heptane (or "heptanes" as commercial heptane is frequently termed) is a mixture of C7 alkane isomers and closely related cyclic hydrocarbons. The inset in the Figure 64 heptane spectrum is a typical composition of commercial heptane [65] and identifies the numbers of methyl, methylene and methane groups in each major component. The branched chain isomers accentuate the number of $–CH_3$ groups per molecule and result in an integration ratio of methyl to methylene/methane that approaches 1. In the single component *n*-heptane this ratio is 6:10 which is reasonably well approached by the experimental 1.00:1.58. The extra methyl groups in heptane do cause a small depression of its surface tension (19.8 mN/m at 19 ºC) compared with that for *n*-heptane (20.0 mN/m at 19 ºC) which can make a difference with respect to film formation on the fuel surface as calculated by spreading coefficient. With respect to gasoline, the non-aliphatic components appear to cause an increase in the surface tension (22.7 mN/m at 19 ºC). However, as to be presented in

a later section, the prevalent identified aromatic components in gasoline can cause a significant and negative effect in pool fire suppression by F3 formulations.

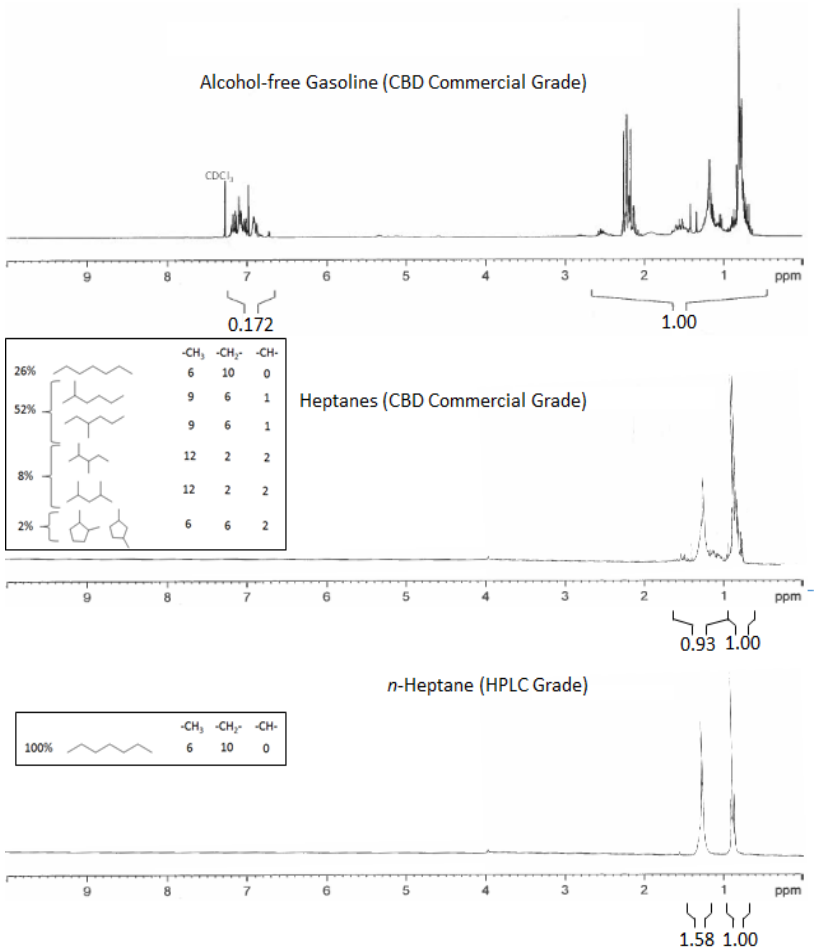

Figure 64. ^{1}H NMR spectra of alcohol-free gasoline, heptanes and *n*-heptane used in 28 ft^2 and benchtop pool-fire extinction testing. Integrations are discussed in the text. The inserts on the heptanes and *n*-heptane spectra identify quantities of major components [65] and the number of methyl, methylene and methane structural units in each component.

Two diagnostics that relate valuable information about foam-fuel interaction are a foam degradation test and a fuel-vapor transport test. Foam degradation was evaluated by monitoring the disappearance of a 4 cm thick layer of laboratory generated foam deposited over 60 ml of 35ºC heptane or gasoline in a 100 ml beaker (Figure 65). There is an increase in bubble size followed by a shrinking of the foam volume. A plot of foam height vs time depicts significant foam degradation differences between the heptane and gasoline fuels for the RefAFFF and Siloxane #3 formulations (Figure 66(a)). This plot indicates the stronger degrading character of the gasoline on the stability of the RefAFFF and siloxane #3 foams. Fuel vapor transport through a foam layer is measured by a similar but closed apparatus where the headspace air above the foam is transported through an FTIR gas cell and monitored for fuel vapor content. These data are plotted in Figure 66(b). This vapor permeation occurs on a shorter time scale than that of the foam degradation experiment. The results indicate that the Siloxane #3 foam is more susceptible to

hydrocarbon vapor permeation and that gasoline is the more permeable vapor through both foams. These diagnostics are conducted under conditions significantly different from fire suppression.

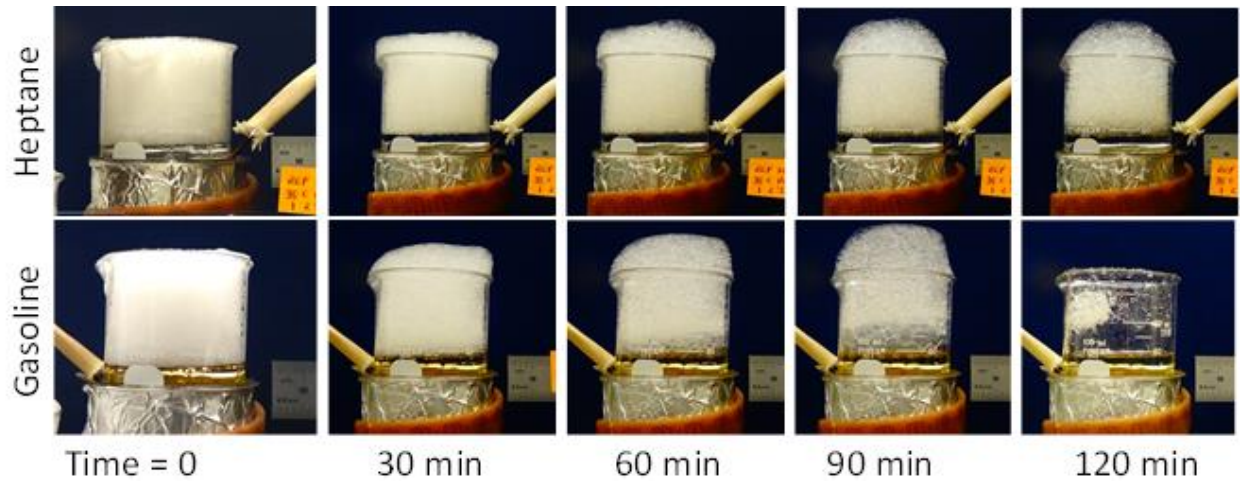

Figure 65. Photographic images of RefAFFF foam degradation over heptane and gasoline at 35ºC.

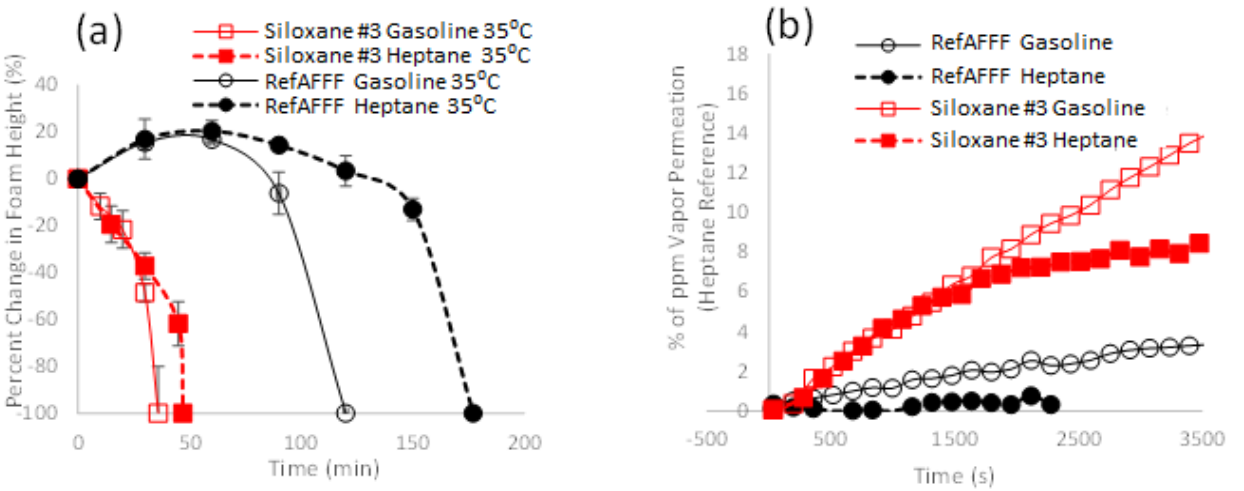

Figure 66. (a) Plot of RefAFFF and siloxane #3 foam degradations over heptane and gasoline at 35ºC; (b) Plot of heptane and gasoline vapor concentration increase in the purged headspace following deposition of a 4 cm layer of foam over a pool of fuel.

4.6.1. Gasoline vs Heptane Fire Suppression

As described above and depicted in Figure 63, the use of gasoline or heptane as a pool fire fuel causes a large divergence in fire suppression behavior for an experimental F3 formulation based on a siloxane-glycoside surfactant formulation. This observation raises the question as to whether this may be a general characteristic of F3 formulations and whether there may even be a significant difference in AFFF extinction performance on pool fires of gasoline vs heptane. In the introduction literature references are cited appeared to indicate this issue to be unresolved. In this section this issue is addressed for both AFFF and F3 formulations by conducting comparative extinction

profile experiments with a benchtop 19 cm diameter pool fire apparatus under controlled conditions using gasoline and heptane as fuels.

Three AFFF formulation concentrates were evaluated, the first being the RefAFFF [65] described above and the second and third being commercial formulations, Buckeye 3% MIL SPEC AFFF and FireStopper PFE-FR(FFC) Green. These concentrates are characterized by non-volatiles component content determined by evaporation under stepped application of vacuum and by fluorine content determined by ^{19}F NMR.[65] The RefAFFF concentrate has a non-volatiles content of 7.3 wt% and a fluorine content of 1.7 wt%. The Buckeye and FireStopper commercial concentrates have respective non-volatiles contents of 15 and 67 wt% and fluorine contents of 0.77 and 1.2 wt%. These concentrates were diluted at a proportionating rate of 3% and fire extinction profile data obtained using benchtop apparatus. The gasoline vs heptane pool fire extinction profile data are presented in Figure 67. The extinction time correlates with foam flow rates being rapid at rates >500 mL/min progressing to a non-extinction at rates <200 mL/min. The fire extinction dependence on the fuel identity is small. All three of these formulations extinguished the MilSpec 28 ft^2 gasoline pool fire in less than the required 30 sec.

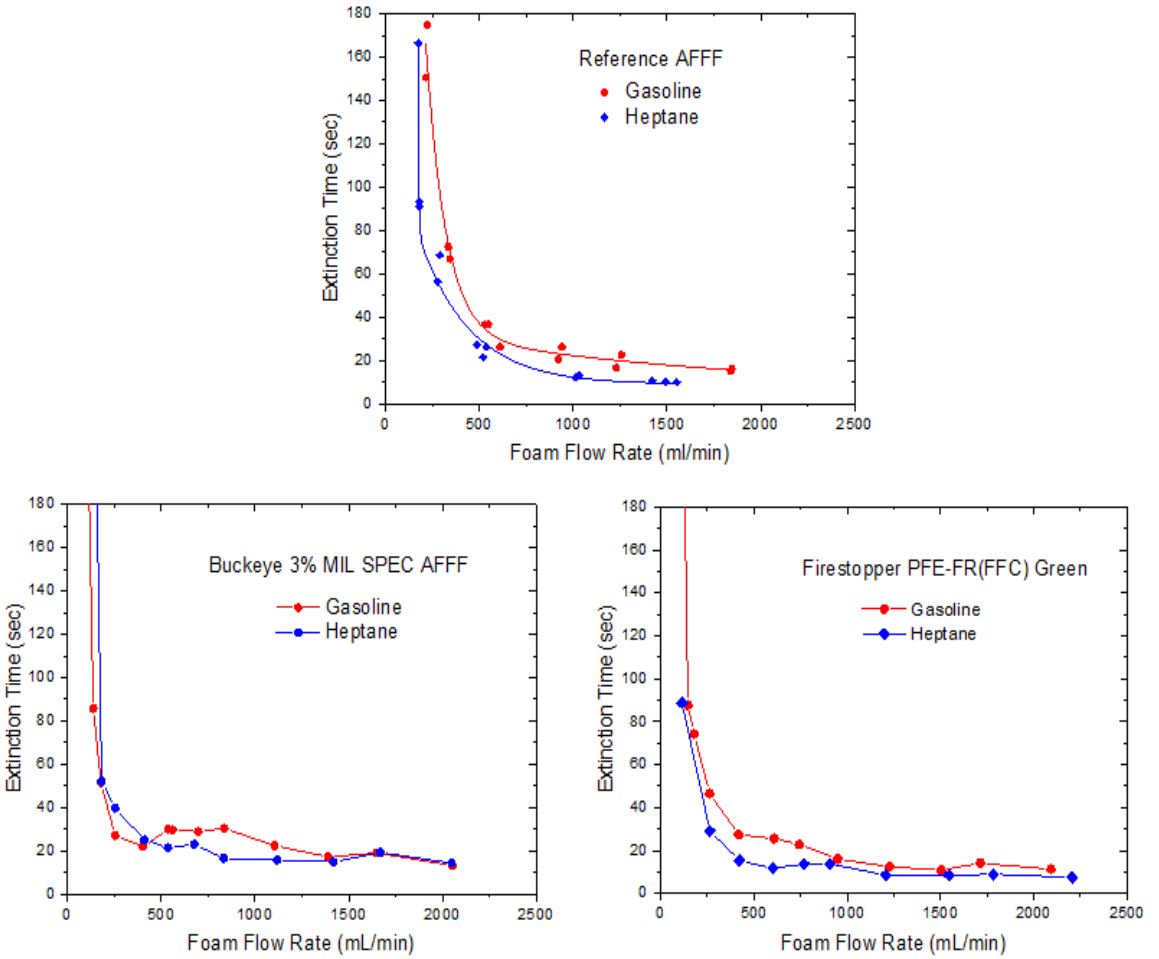

Figure 67. Comparative extinction time profiles of AFFF formulations for gasoline and heptane 19 cm pool fires.

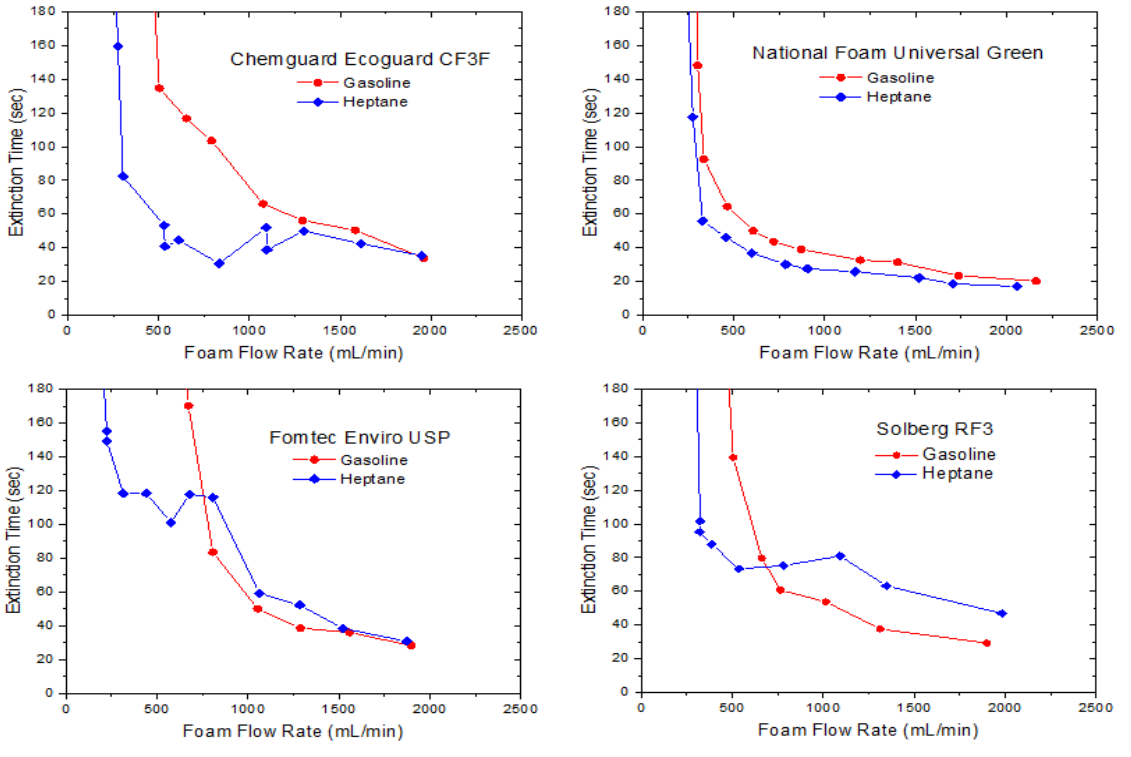

Figure 68. Comparative time extinction profiles of four commercial F3 formulations for gasoline and heptane 19 cm pool fires.

The issue of specific interest here is to determine whether the of gasoline vs heptane as the pool fire fuel causes a significant difference in fire extinction when using commercial F3 formulations as was the case with the experimental Siloxane #3 formulation. Four commercial F3 formulation concentrates were evaluated. These were purchased from the manufacturer/distributor and include: Chemguard (Ecoguard 3%F3); Fomtec (Enviro ARC 3x6); National Foam (Universal Green 3-3%); and Solberg (Re-Healing Foam RF3). General composition information from SDS is presented in Table 3, but specific compositions are proprietary. The gasoline vs heptane pool fire extinction profile data are plotted in Figure 68.

The extinction profile results for these F3 products display considerable variation in effectiveness on both the gasoline and heptane pool fires and are considerably different from the profile of the Siloxane #3 experimental formulation presented in Figure 63. Unlike the AFFF formulations, none of the F3 formulations have an extinction time of less than 20 seconds at the high foam flow rate limit. The region of practical importance is the <1000 mL/min flow rate, and only the National Foam product shows an attractive performance in this region. With respect to the gasoline vs heptane issue, the extinction behavior is quite varied with two products displaying a crossover in effectiveness. In the <1000 mL/min flow region gasoline is the predominantly more difficult fuel fire to extinguish with the differences becoming quite large at the 500 mL/min.

While the intent here is not to analyze failures and limitations of the F3 formulations, there are some other properties of these formulations that are readily measured and have importance with respect to MilSpec requirements. These include non-volatiles and viscosity of the concentrate, surface and fuel-interface tensions of the premix and expansion ratio of the foam, and they are reported for the AFFF and F3 formulations in Table 13. The variation in concentrate non-volatile

component quantities and viscosity cover a substantial range. The AFFF formulations appear to reflect extremes with the three-component RefAFFF being composed of what is minimally necessary to generate foams and suppress pool fires without addressing other requirements and the FireStopper being heavily loaded with components for maximum versatility. The four commercial F3 formulations have variations in non-volatile content consistent with proprietary compositions, and the NRL experimental Siloxane #3 formulation has a relatively low non-volatiles content reflecting a minimal composition to investigation extinction similar to that for the RefAFFF formulation. The viscosity of the concentrate is typically low for AFFF formulations and can be quite high for F3 formulations approaching that of a gel. Its importance is in compatibility with the equipment needed to rapidly dilute the concentrate (3 or 6%) to the premix concentration immediately prior to foam generation. In this regard MilSpec requires a concentrate viscosity range of 2-20 cP. High viscosity can enhance slow drainage of water from foam which many F3 formulations rely upon for fire extinction. Surface and fuel interface tensions of the AFFF and F3 formulations at their premix concentrations is an important difference between these groups. The higher surface tension of the F3 solutions cause a negative spreading coefficient condition, and a continuous aqueous-surfactant film is not formed by drainage from a foam applied to the fuel surface. The lower surface tension AFFF solution drained from its foam can form a continuous film barrier and, along with the oleophobic character of the fluorinated surfactant foam above, can more effectively retard fuel vapor transport to the fire above the foam. Finally, the expansion ratio parameter should pass the MilSpec threshold of >5 such that the foam's dryness results in an efficient consumption of the concentrate. F3 formulations that utilize very wet foams (expansion ratio <5) and slow drainage can increase fire suppression effectiveness but at a high rate of consumption of the concentrate supply.

Table 13. AFFF and F3 formulation concentrate, premix and foam properties

F3 Manufacturer (Product)	Non-Volatiles Content (wt%)	Viscosity (cP)	Surface Tension (mN/N)	Gasoline Interfacial Tension (mN/N)	Heptane Interfacial Tension (mN/N)	Expansion Ratio
AFFF						
NRL (RefAFFF)	7.3	3.19	15.2	1.05	1.00	9.4
Buckeye Buckeye BFC-3MS	15.0	6.97	16.4	1.63	1.50	6.7
FireStopper (FireStopper PFE-FR)	67.4	9.84	14.1	2.74	3.36	6.0
F3						
Chemguard (Ecoguard 3%F3)	36.2	22	27.0	0.64	1.98	9.0
Fomtec (Enviro ARC 3x6)	21.2	150	24.0	1.00	2.74	6.5
National Foam (Universal Green 3-3%)	14.6	????	23.1	3.61	5.11	4.4
Solberg (Re-Healing Foam RF3)	30.1	4900	26.1	0.56	2.40	7.7
NRL (Siloxane #3)	13.6	5.3	22.4	2.20	2.29	8.2

In addition to pool fire suppression, the AFFF and F3 formulations have differing concentrate, premix and foam properties and can be thought of as separate groups having related but different capabilities due to the uniqueness of the fluorocarbon surfactant in AFFF compared with the hydrocarbon surfactants in F3. These formulations have a different mechanisms for fire suppression, and improving on this capability results in the respective formulations developing different properties in their forms as a concentrate, a premix solution and a foam. These will be discussed in more detail in a later section. The main issue of interest is the divergent behavior of the F3 formulation in extinguishing of gasoline and heptane pool fires. What may be the underlying cause for divergence is undertaken in the following section.

4.6.2. Gasoline vs Heptane Divergent FFF Extinction Behavior Analysis

A comparison of the extinction profiles shows that the Siloxane #3 formulation exhibits greatest divergence in gasoline vs heptane pool fires. For the heptane pool fire, its extinction profile approaches that of an AFFF formulation, while for the gasoline pool fire its profile if far less effective than the other F3 formulations. The underlying cause for this divergence has been correlated with the content of gasoline having non-aliphatic components. To uncover a reason why F3 formulations exhibit this divergence in varying degrees, the Siloxane #3 formulation is examined for a deeper analysis of this phenomenon. In this section the isolated effects these gasoline and surfactant formulation components will be examined to learn how these components interact causing a degradation of extinction performance.

The composition of gasoline is variable depending on the season of the year and its source. Its content consists of over a hundred components, and analyses of gasoline composition is usually divided into various classes of compounds. The results of a recent analysis of four commercial gasolines is depicted in Table 14 [65]. These individual compounds along with their content in each gasoline were selected as the predominant members of a particular class and are inserted into the columns of Table 14 in indented format. With respect to quantity, the main compound classes and content ranges are: parafins (10-22%); isoparafins (20-40%); cycloparafins (3-4%); aromatics (20-40%); and alkenes (5-7%). It was hypothesized that the observed gasoline-heptane difference in pool fire suppression would correlate with the presence of the non-alkane compound groups in gasoline, particularly the aromatics. A pool fire suppression experiment was designed where representative compounds from the main classes cited above were selected for 19 cm pool fire extinction evaluation. With the exceptions of *n*-butane and *iso*-pentane the individual compounds in Table 14 were tested as individual fuels and as mixtures ranging from 0 to 40 vol% in heptane for fire suppression with the 19 cm pool fire apparatus using the Siloxane #3 formulation.

The fire extinction – flow rate profile results are plotted in Figure 69. The results for the aromatic set of compounds (benzene, toluene, xylenes, trimethylbenzene) are remarkable in that 3 of the 4 compounds were not extinguishable as 100% fuels by the Siloxane #3 foam. It had further been hypothesized that that the vapor pressure of these aromatic compounds would correlate with the time and with foam flow rate needed for extinction (i.e. benzene with its higher vapor pressure would have a larger degrading effect on the foam and a greater permeation through the foam to feed the fire). Just the opposite trend was observed: the difficulty to extinguish is in the order trimethylbenzene > xylenes > toluene > benzene.

Table 14. Compositions of four gasoline fuels based on chemical groups

Component Class	Fuel A (%)	Fuel B (%)	Fuel C (%)	Fuel D (%)
Parafins	11.084	14.638	15.568	12.765
n-butane	1.175	1.220	0.887	0.996
n-pentane	0.958	5.173	6.223	6.346
n-hexane	6.557	6.271	6.375	4.646
n-heptane	0.265	0.296	0.220	0.227
n-octane	0.351	0.393	0.249	0.228
n-nonane	0.833	0.668	0.747	0.183
n-decane	0.648	0.319	0.343	0.088
Isoparafins	44.317	28.497	18.535	23.343
i-pentane	5.758	1.892	3.150	2.885
i-octane	13.499	7.108	2.174	9.038
Cycloparafins	4.329	4.527	5.285	3.311
methylcyclopentane	3.226	3.087	3.125	2.291
methylcyclohexane	0.103	0.114	0.085	0.089
Mono-aromatics	18.436	31.428	41.375	41.376
benzene	0.879	0.768	0.804	0.828
toluene	4.362	7.240	10.539	9.366
xylenes	3.762	5.990	7.651	9.516
1,2,4-trimethylbenzene	1.786	4.199	6.355	6.097
Naphthalenes	0.225	0.295	0.225	0.230
Naphthaleon/olefin-benzene	0.319	0.503	0.396	0.402
Indenes	0.538	0.785	0.806	0.697
Mono-naphthalenes	5.231	5.087	5.325	3.310
n-Olefins	6.354	6.214	5.273	6.583
1-hexene	5.548	5.348	4.611	5.930
Isoolefins	0.793	0.761	0.747	0.521
Naphthaleno-olefins	0.099	0.134	0.131	0.089
Oxygenates	11.032	10.504	10.276	10.422

This unexpected result is further probed by experiments described below. A less pronounced but similarly unexpected trend for difficulty in extinction was observed was observed for the *n*-alkane series: *n*-decane, *n*-nonane > *n*-octane > *n*-heptane > *n*-pentane. It is further noteworthy that within the pair of octanes (*iso*-octane and *n*-octane), *n*-octane was the more difficult fuel fire to extinguish. Finally, the cycloalkanes (methyl cyclopentane and methyl cyclohexane) and alkene (*1*-hexene) pool fires proved to be not significantly more difficult to extinguish than that of heptane. The remarkable features in this series of gasoline-component experiments are the large effects and systematic trend of the aromatic compounds and the effects of *n*-alkane chain length as fuel composition approaches 100%.

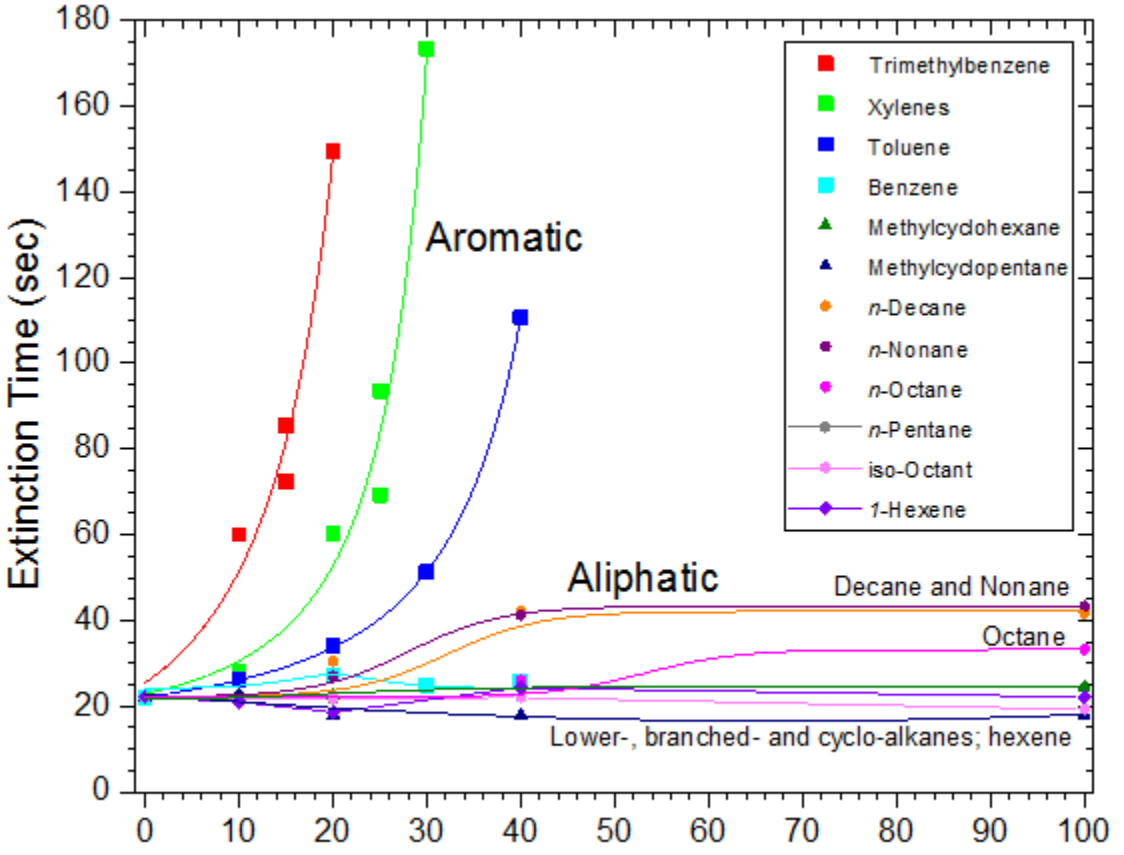

Figure 69. Effect of varying amounts of aromatic and aliphatic gasoline components added to heptane in 19cm pool fire extinction time testing of Siloxane #3 formulation at a constant foam flow rate of 1000 ml/min.

As to causes of this aromatic component induced behavior and to the order of its effectiveness being opposite to vapor pressure, a hypothesis was directed at the interface between the aqueous surfactant solution and the hydrocarbon fuel with speculation that the fuel component might be crossing the interface to reside in aqueous micelles and thereby reduce the foam stability, or that perhaps one of the surfactants is transporting across the interface to dissolve in the fuel leaving the other surfactant unable to stabilize the foam at this interface. A relatively simple experiment was designed to diagnose such behavior and is illustrated in the Figure 70. It involves ^{1}H NMR spectra to detect transport across the interface between an aqueous solution of the Siloxane #3 surfactants and a hydrocarbon fuel component before and after a short time of contact. A stock solution of 0.5 wt% surfactant(s) in D_2O with a comparable small quantity of DMSO reference was prepared. A 2.0 ml quantity of the stock solution was placed in the vial; a 670-700 mg sample is withdrawn for a control spectrum; a gasoline component is gently added for a 1-2 mm upper phase thickness with minimum perturbation of the interface; the aqueous phase is slowly stirred (no vortex formation) for 5.0 min; and a second 670-700 mg sample of the aqueous phase is collected via syringe from the bottom of the vial for NMR analysis. The experiments include stock solutions of 502W, Glucopon 225DK and a 1:1 502W:Glucopon 225DK surfactant mixture and gasoline components of 1,2,4-trimethylbenzene (TMB), xylenes (Xyls), toluene (Tol), benzene (Bz), n-

decane ($C_{10}H_{22}$), n-heptane (C_7H_{16}) and n-pentane (C_5H_{12}). Some spectral features are unique to a surfactant (e.g. Si-CH_3) or to a gasoline component (e.g. Ar-H) and other features have two or more contributors (e.g. –O-CH_2- from both surfactants). In the spectrum these features or resonances are integrated and normalized to the DMSO resonance. In the Table 15 below is a correlation of spectral features with the chemical shift range, general structural assignment and the corresponding components. Spectra of the individual surfactants and gasoline components and the resonance assignments used are presented in reference [65] along with a table of integrated values.

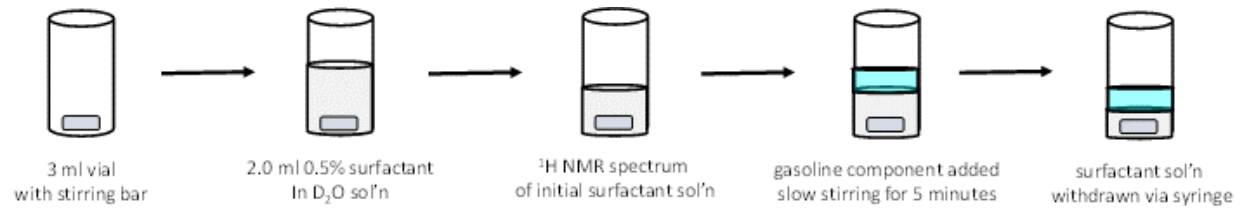

Figure 70. Depiction of simple NMR experiment to probe transport across the aqueous surfactant solution – hydrocarbon interface.

Table 15. NMR Resonance chemical shift – structure correlation

Chem Shift	Assisgnment	Corresponding Component
0.0 – 0.2 ppm	Si-CH3	502W
3.2 – 4.0 ppm	-O-CH2-	502W, Glucopon
1.5 – 1.7 ppm	-O-CH2-CH2-	502W, Glucopon
1.2 – 1.4 ppm	C-CH2-CH2-C	Glucopon, Aliphatic Gas Component
0.8 – 1.0 ppm	Aliph-CH3	Glucopon, Aliphatic Gas Component
0.4 – 0.5 ppm	Si-CH2-	502W
1.8 – 2.1 ppm	Ar-CH3	Aromatic Gas Component
6.5 – 6..8 ppm	Ar-H	Aromatic Gas Component

In Table 15, there is a color and pattern code which is used in a bar graph depiction (Figure 71) of surfactants and gasoline components transporting across the aqueous-organic interface. The solid colors without pattern denote surfactant only resonances; the parallel line pattern denotes overlapping resonances from a surfactant and a gasoline component; and the cross-hatched pattern denotes gasoline component resonances only. All of the transport experiments are summarized in the form of bar graphs in Figure 71. There are six bar graphs arranged in two columns and three rows. For comparative purposes the column on the left represents the aromatic gasoline component experiments, and that on the right represents the aliphatic gasoline component experiments. The three rows correspond to different surfactant solutions; the top row is 502W only, the middle row is Glucopon 225DK only and the bottom row is the 1:1 502W:Glucopon 225DK surfactant combination. Within an individual series of bar graphs, the control experiment is on the left representing the surfactant solution prior to interface contact with the gasoline component, and the subsequent groupings to the right progress from least volatile to most volatile gasoline component. The intent in this design is to identify systematic trends for surfactant and gasoline component interface crossing.

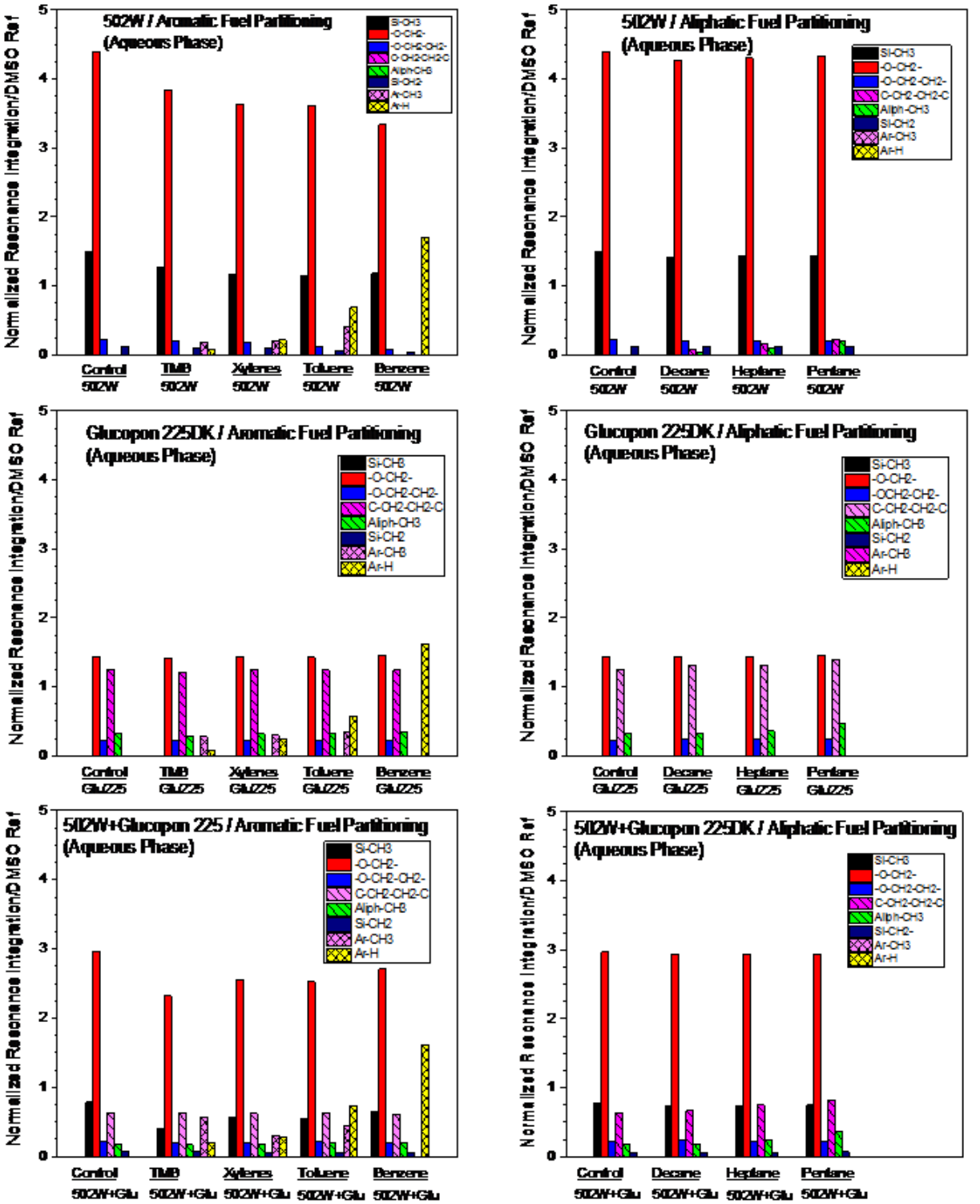

Figure 71. Synopsis of ^{1}H NMR results of surfactant and gasoline component diffusion across the aqueous-organic interface.

One way to interpret the data in Figure 71 is to start with the relatively simple aromatic and aliphatic gasoline components. In the left column of bar graphs there is a progression of yellow (Ar-H) and pink (Ar-CH3) that increase in height as one proceeds from TMB to Bz indicating an increasing quantity of aromatic component crossing the interface into the aqueous phase. There is a parallel with these components' solubility in water: Bz (0.178%) > Tol (0.0515%) > Xyls (0.0187%) > TMB (0.0057%). By comparison in the right column of bar graphs, the aliphatic components (purple parallel line pattern (C-CH2CH2-C) and green parallel line pattern (Aliph-CH3)) display a low transport into the aqueous phase. This is particularly visible in the top right bar graph where there is no Glucopon to contribute to these aliphatic component column heights. The relative amounts of aliphatic component in the aqueous phase also parallels these components' solubility in water: C5H12 (0.0038%) > C7H16 (0.00029%) > C10H22 (0.0000052%). While the amount of aromatic components transferring to the aqueous phase is substantially greater than that for the aliphatic components and the aromatic component also has a pronounced increasing effect on extinction time compared to the aliphatic component, the order of this increased extinction time (TMB > Xyls > Tol > Bz) is opposite to that for aqueous transfer (Bz > Tol > Xyls > TMB). This appears to indicate that diffusion of aromatic components into the aqueous phase does not have a retarding effect on the 502W-Glucopon 225DK formulation's pool fire extinguishing activity.

The data in Figure 71 provide an interesting insight into diffusion of the surfactant from the aqueous into the organic phase. Comparing the 502W data (particularly black and red bars relative to the controls) in the first row, the amount of diffusion into an aromatic phase is much higher than into an aliphatic phase. Within the aromatic components, 502W displays more interface diffusion for Bz than for TMB. In the second row the interface diffusion behavior for Glucopon 225DK is noteworthy for its lack of diffusion as indicated by the constant height of its red bar. However for the 1:1 502W:Glucopon 225DK in the third row, the aromatic phase diffusion activity of the 502 surfactant is altered with the amount now for TMB greater than that for Bz as is evident from comparison of the 502W exclusive black bar data. Surfactant diffusion toward the aliphatic phase is nominal as is the case for the individual surfactants in the upper rows.

The result of significance from these interface transfer experiments is that diffusion of the 502W surfactant from the aqueous to the aromatic organic phase is substantial. When 502W is combined with Glucopon 225DK in a 1:1 formulation, its diffusion out of the aqueous phase is the greatest for TMB in the aromatic component series. This result correlates with the pool fire extinction results in Figure 69. A speculated scenario is that 502W when combined with Glucopon 225DK at the aqueous-organic interface is more prone to cross this interface into the receptive aromatic environment. Its departure from the 502W-Glucopon aqueous foam structure at the foam-fuel interface destabilizes the foam and thus diminishes the ability of this formulation to extinguish pool fires. This speculation can lead to hypothesizing about doing something to 502W that would make it less prone to cross an aqueous interface into an aromatic-hydrocarbon medium. This speculation may also be applied to the hydrocarbon surfactants in the other F3 formulations although their proprietary identities impede experimental verifications.

4.6.3. Two-Component Simulant for Gasoline

From the foregoing results, it is clear that the aromatic components in gasoline are responsible for a pool fire suppression behavior that diverges from that of heptane when foams generated from F3 formulations are used. Of the aromatic components investigated, 1,2,4-trimethyl-benzene is

the most effective. In this section data are presented to support the possibility of designating a two-component simulant for commercial alcohol-free unleaded gasoline. As indicated in the previous section, gasoline is a very complex mixture of over 100 hydrocarbon components with seasonal and source variations. If it is possible to formulate a two component mixture from heptane and an aromatic counterpart that will effectively simulate a general F3 formulation's extinction performance with the gasoline pool fire, it could be a very useful and simple reference fuel for a testing protocol. A substantial body of data is needed to validate the concept of a gasoline simulate. Presented below are foam degradation and extinction data for the fluorine-free Siloxane #3 formulation and for the RefAFFF formulation to represent this concept's initial viability.

Foam degradation data were obtained by monitoring the time-dependent reduction of a 4 cm layer of foam deposited onto a 60 mL volume of 60ºC preheated fuel in a 150 mL beaker. For the Siloxane #3 foam, its degradation over heptane, gasoline and the comparative effects of adding 15 and 25% TMB to heptane are depicted in Figure 72. The 15% TMB data represent intermediate behavior in the foam height vs time plot for the 4 cm layer of foam to disappear. Increasing the TMB content to 25% results in a foam degradation time coincident with that for gasoline. The degradation effect of this 25% TMB/heptane fuel on RefAFFF foam is presented in Figure 73. The rapid decrease in foam height occurs at an intermediate time (130-140 sec) compared with that for the heptane (160-180 sec) and the gasoline (100-120 sec). In this case the foam degradation is accelerated by the 25% TMB but does not match that produced by the gasoline.

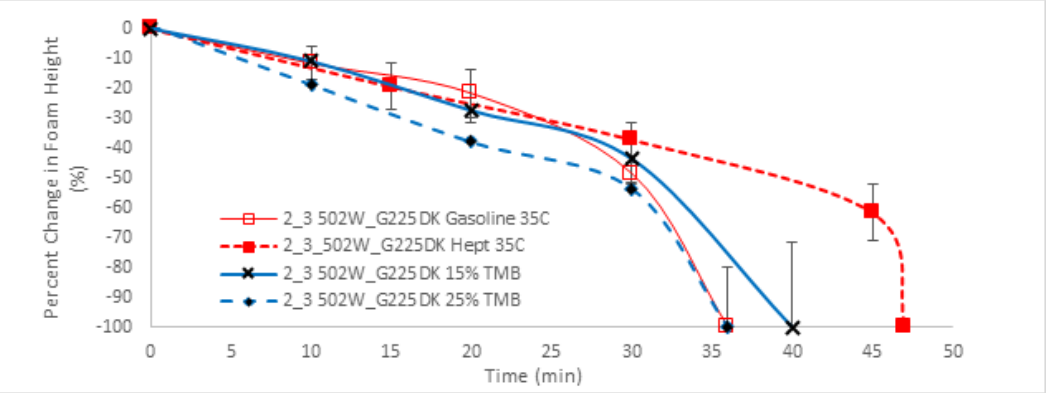

Figure 72. Degradation of a 4 cm Siloxane #3 foam layer over gasoline, heptane and combinations of 15 and 25% TMB/heptane at 35°C.

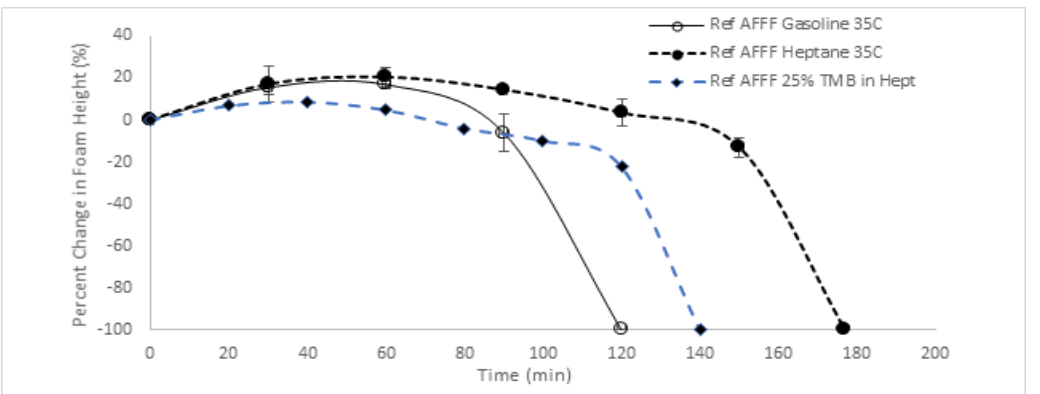

Figure 73. Degradation of a 4 cm RefAFFF foam layer over gasoline, heptane and a 25% TMB/heptane fuels at 35°C.

The 25% TMB/heptane fuel composition's effect on the Siloxane #3 formulation's pool fire extinction time compared with the gasoline and heptane fuels is presented in Figure 74. As previously indicated, this F3 silicone formulation's ability to extinguish gasoline fires is much diminished compared with heptane fires, and the data presented in were obtained at a foam flow rate where extinction was accomplished on both fuels. The 25% TMB/heptane fuel fire extinction by the Siloxane #3 formulation is in reasonably close proximity (about 90 sec) to that for gasoline (average 110 sec) and significantly removed from that for heptane (17 sec). As a two-component simulant for gasoline, these data indicate the 25% TMB/heptane is a good candidate for further benchtop and large scale testing.

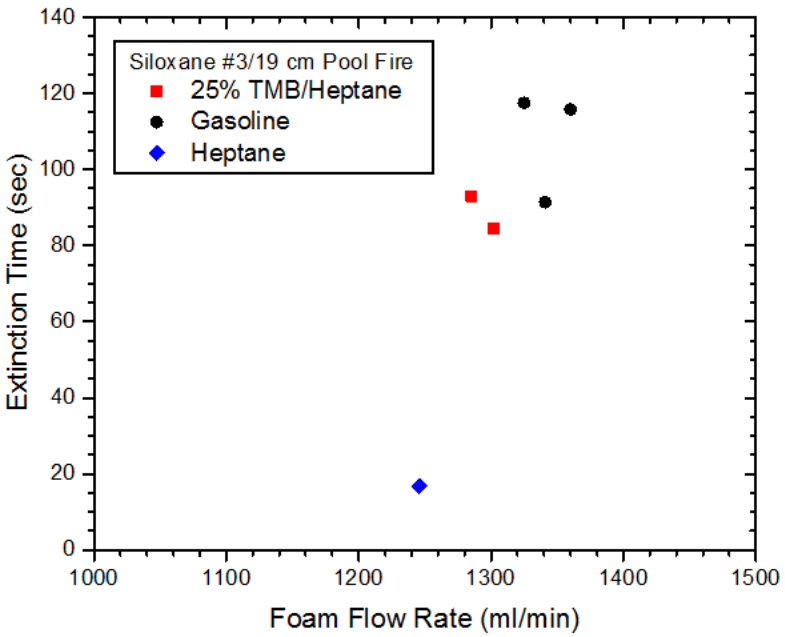

Figure 74. Comparison of extinction times for 25% trimethylbenzene/heptane fuel vs gasoline and heptane fuels using the Siloxane #3 formulation and the benchtop 19 cm pool.

4.7. Varying Siloxane Surfactant Head Size

We focused on increasing the synergistic foam stability and heptane-fire extinction that we discovered between commercial silocone-polyether copolymer and alkyl polyglycoside surfactants (Figure 17) in the NRL's siloxane formulation; synergistic surfactants in combination exhibit performance above that of the individual surfactants. Even though the exact mechanisms of synergism are not well understood, the interactions between the oxyethylene and glycoside head groups shown in Figure 17 are crucial for the synergism in decreasing the foam degradation by heptane. The commercial siloxane surfactant in Dowsil 502W (Dow Silicones Inc.) has general structure of siloxane-polyoxyethylene at 100% concentration [45]. The siloxane surfactant has a hydroxyl functional group (R=OH) and a distribution of polyoxyethylene (OCH_2CH_2) chain lengths represented by the parameters m and y as shown in Figure 17. The distributions and the average values of m.y, and z are proprietary according to Dow Corning Co.'s literature [45]. We varied the glycoside head size to a limited extent possible by using commercial materials and increased synergism and fire suppression effectiveness up to 60% of AFFF at bench scale as shown in Figures 46 and 47.

In this section, we discuss the results from varying the oxyethylene head size using siloxane surfactant synthesis. To improve fire suppression performance, we synthesized siloxanes with a distribution of m and y=1, z=1 as shown in Figure 75. We prepared 12 synthesized siloxanes with an average value of m varying from 0 to 50 characterized by the precursor sources, NMR, and Gel Permeation Chromatography (GPC). These are substituted for Dowsil 502W in the formulation listed in the first column of Table 10 (NRL's siloxane formulation) and evaluated. The results show that the extinction performance exhibited a maximum with increasing oxyethylene head size and is consistent with the molecular dynamics models, which predicted a maximum in interface stability. However, the maximum extinction effectiveness obtained by varying the siloxane head size still remained at 60% of AFFF like the NRL's siloxane502W formulation as described in detail below.

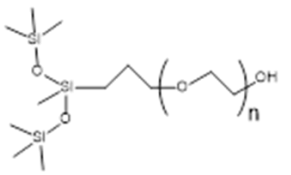

Average n = 0 to 50

Figure 75. Synthesized branched heptamethyl-trisiloxane poly(oxyethylene) (BHMTS-OEn) where n is the number of oxyethylene units.

4.7.1. Surfactant Synthesis and Characterization

We synthesized half a gram to multi-gram, synthesis of a homologous series of trisiloxane-poly(oxyethylene) surfactants with known and analytically defined chain lengths. A single step hydrosilylation reaction between bis(trimethylsiloxy)methylsilane and the allyloxy-poly(oxyethylene) reagent catalyzed by chloroplatinic acid in isopropanol as depicted in Figure 76. The catalyst reactivity is sensitive to the oxyethylene chain length. Initial reactions were conducted on a 0.5g scale to establish conditions (catalyst quantity, ratio of reagents and reaction temperature and time prior to scaling up to a 15-20g quantity needed for further characterization and benchtop fire extinction testing. Reaction conversion was monitored by ^{1}H NMR.

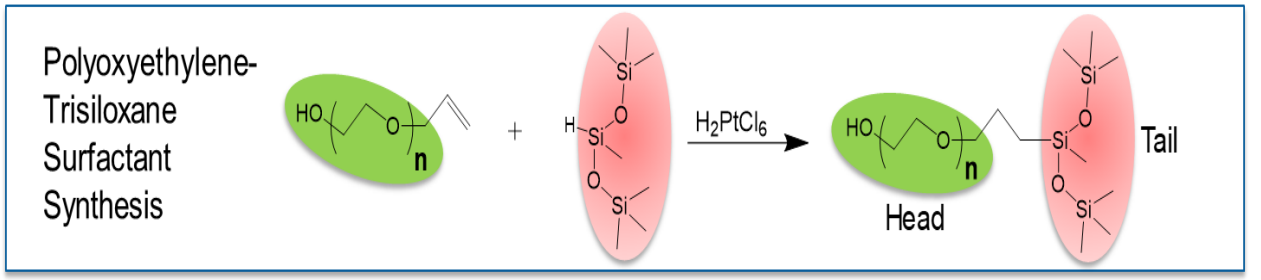

Figure 76. Singlestep synthesis of trisiloxane poly(oxyethylene) (BHMTS-OEn) surfactants with homologous head lengths, average n.

The synthesized surfactant products were evaluated for their foamability and fire extinction. The results are summarized in Table 16. The NMR, surface tension, and the critical micelle concentration (CMC) are reported for the siloxane surfactant solution in water, not formulation containing glycoside surfactant. The fire extinction times (at 1000 mL/min foam application rate)

and foam expansion ratios listed are for the siloxane formulation containing the glycoside surfactant and DGBE solvent in distilled water.

There are two general issues that complicate the synthesis: (1) reactivity/specificity of the catalyst and (2) purification of the surfactant product. Several platinum hydrosilylation catalysts are known and their degree of reactivity and product specificity is much dependent on identities of the reagents. The catalyst is used in 1-100 ppm amounts, and the reaction is frequently characterized by an induction period followed by a rapid exotherm. Side reactions can also occur. These involve the coupling of the Si-H group to the –OH to generate a Si-O-C linkage which is hydrolytically unstable, the isomerization of the C=C bond from the terminal to an internal position in the allyl group and condensation of the trisiloxane structure to a higher polysiloxane. Use of an excess allyloxy reagent helps to lower the amount of side reaction products. Volatile surfactant products ($n \leq 3$) may be purified by distillation but the excess allyloxy reagent complicates the distillation. If the excess allyloxy poly(ethylene) reagent does not affect the application, commercial surfactant concentrates frequently contain such components. In other cases solvent extraction procedures are developed for purification. Also, for $n > 3$ the oxyethylene chain length is usually polydisperse. Having purified monodisperse series of trisiloxane-poly(oxyethylene) surfactants is a very useful analytical tool to interpret important differences in fire suppression properties between seemingly similar commercial surfactants.

Synthesis of the trisiloxane-poly(oxyethylene) or BHMTS-OEn was performed by adding a 20% excess allyloxy reagent to a solution of 100 ppm H2PtCl6 in heptamethyl-trisiloxane and gradually stepping the temperature from 30 to 125°C over an 8 hour period while monitoring by NMR. The 1,1,1,3,5,5,5-heptamethyl-trisiloxane tail group has a characteristic signature in the ^{1}H, ^{13}C and ^{29}Si NMR spectra that is useful for identifying the category of siloxane surfactant. Further, the oxyethylene tail has a relatively simple ^{1}H NMR spectral feature where in most of these proton resonances are closely grouped or overlap as the oxyethylene chain becomes longer. The NMR spectra for some of the synthesized and commercial surfactants used for fire extinction are presented in Figure 77 and 78.

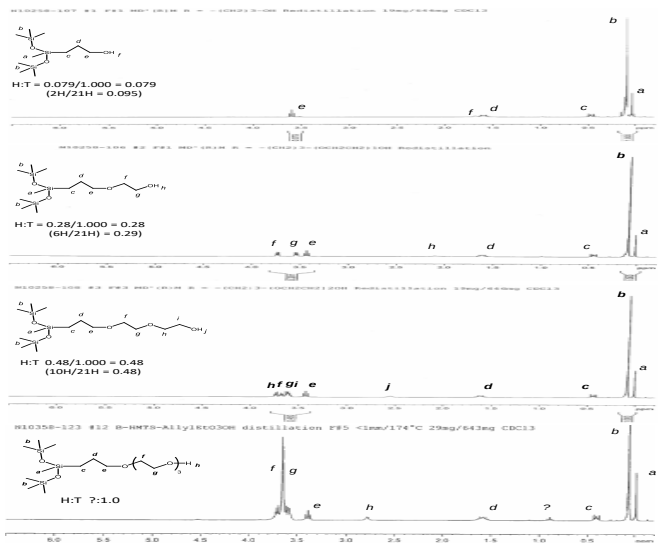

Figure 77. ^{1}H NMR spectra of $(Si(CH_3)_3)_2Si(CH_3)(CH_2)_3(OCH_2CH_2)_nOH$ or BHMTS-OEn illustrating assignments and integration for head:tail (H:T) ratio.

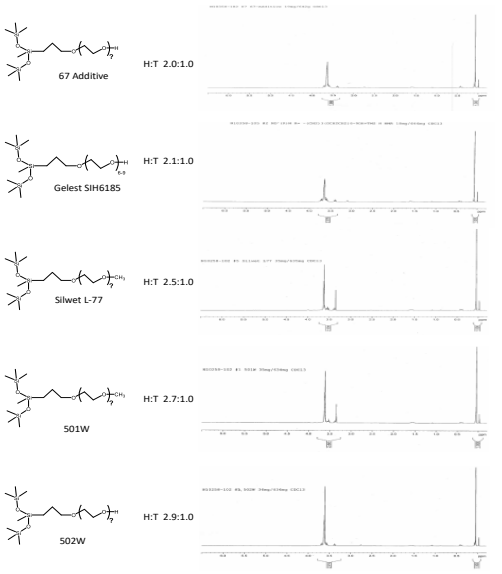

Figure 78. ^{1}H NMR spectra of commercial trisiloxane-poly(oxyethylene) surfactants depicting the H:T integration ratio comparable to the synthesized surfactants.

The 1H NMR spectra of Figure 77 are comparable to spectra of the commercial trisiloxane-poly(oxyethylene) surfactants (67A, Gelest SIH6185, Silwet L-77, 501W and 502W) which were evaluated for fire suppression properties. These spectra are depicted in Figure 78 along with their corresponding H:T integration ratio. Figure 79 shows integrated NMR analyses of the ratio of head to tail protons as a function of chain length for the synthesized trisiloxane surfactants. The dashed red line corresponds to theoretical calibration derived from chemical structure with head and tail proton counts. The 502W near the ordinate are the experimental results assuming 100% surfactant purity.

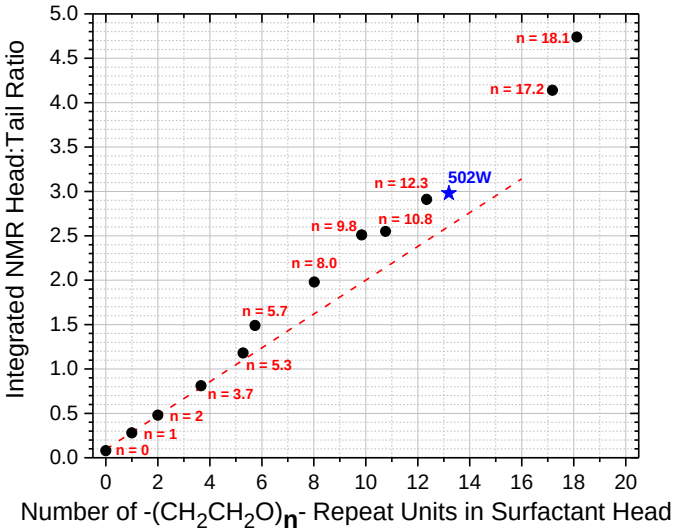

Figure 79. Calibration plot of ^{1}H NMR measurement of integrated H:T proton ratio as a function of oxyethylene chain length (n) in synthesized and commercial trisiloxane surfactants (BHMTS-OEn).

4.7.2. Solution Properties of Synthesized Trisiloxane Surfactants

Figure 80 shows the surface tension measurements for the synthesized trisiloxane BHMTS-OEn surfactants for different values of n. The surface tension of aqueous surfactant solutions were measured using DuNoy ring apparatus at different dilutions of a stock solution containing 2 volume % surfactant. Above the critical micelle concentration, the surface tension becomes independent of the surfactant concentration. CMC is determined by a standard method of fitting two lines to the data as shown in Figure 80(a). Figures 80(b) shows that the equilibrium surface tension reaches a minimum between n=6 to 10 as the oxyethylene length n increases. It shows n=12-20 has slightly higher equilibrium surface tension than BHMTS-OEn with n=9-12 (24 mN/m versus 20 mN/m). For comparison 502W solution has a surface tension of 20.5 mN/m. The CMC also decreases and then increases with n before reaching a constant value as shown in Figure 80 (c). Figures 81(a) and (b) show that the solubility in water and cloud point increase rapidly above n=10. Figures 81(c) and (d) show that the excess surfactant concentration and area per molecule change rapidly up to n=10 and then change only slightly at larger values of n. These data suggest oxyethylene units of 10 appear to be a transition point in head length for many physical and interfacial properties.

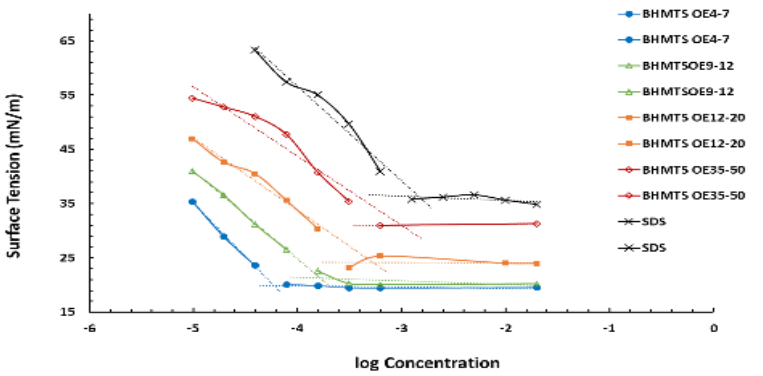

(a)

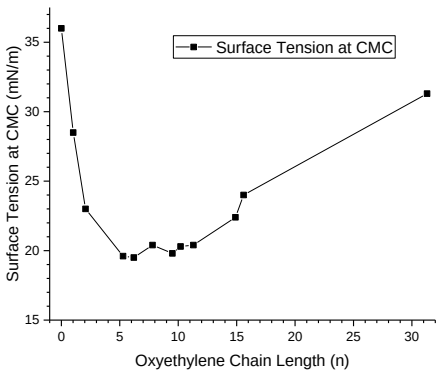

(b)

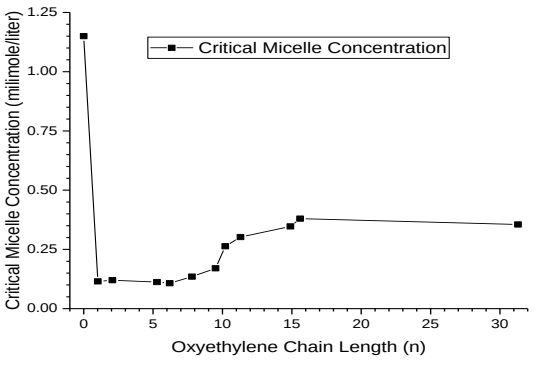

(c)

Figure 80. (a) Surface tension versus surfactant concentration, (b) surface tension at CMC, (c) CMC versus oxyethylene length n of the synthesized trisiloxane poly(oxyethylene) (BHMTS-OEn) as the only component in water.

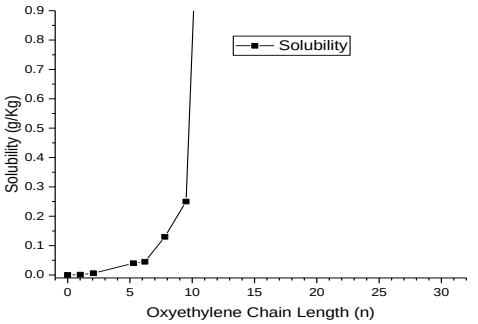

(a)

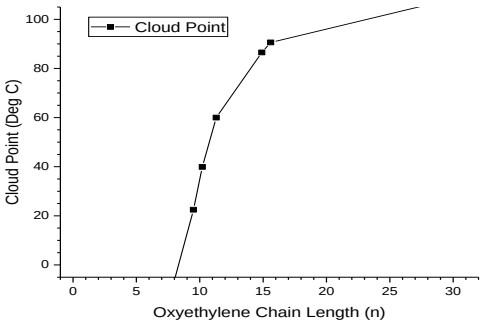

(b)

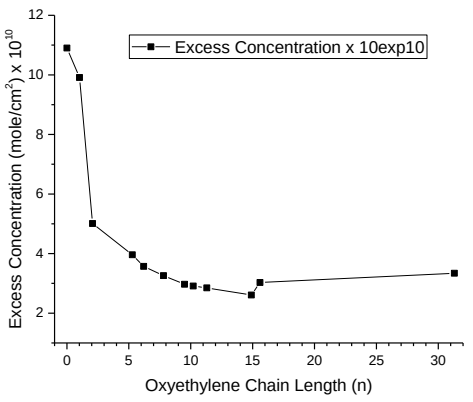

(c)

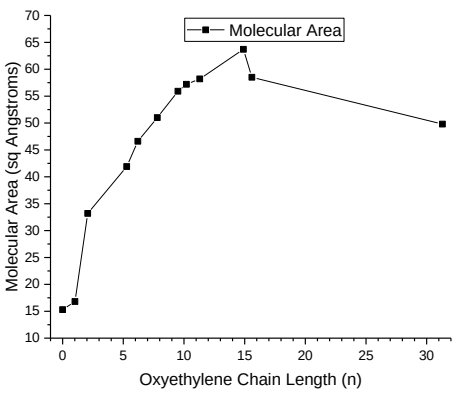

(d)

Figure 81. (a) Solubility in water, (b) cloud point, (c) excess concentration, and (d) area per molecule at air/water interface versus oxyethylene length n of the synthesized trisiloxane poly(oxyethylene) (BHMTS-OEn) as the only component in water.

4.7.3. Foam Properties of Synthesized Trisiloxane Surfactants

Figure 82 shows the foam-fuel interaction effects. Figure 82(a) shows a decrease in foam layer thickness (initially 4-cm thick) on a hot (60 ^{o}C) heptane pool with time, measured in an open beaker, for the synthesized siloxane surfactants with varying oxyethylene length, n. As the fuel vapors diffuse through the foam the lamellae between the bubbles rupture and the bubbles coalesce to form larger bubbles near the pool surface. As the time progresses, the large bubbles move up the foam driven by buoyancy force and rupture to release the fuel vapor from the top of the foam layer. That decreases the foam layer thickness. The coalescence most rapid within the first layer of bubbles at the pool surface and decreases progressively in the bubble layers above the first layer. The foam lifetime (100% degradation) is significantly affected by n. The lifetimes increase with increasing n. Assuming fuel diffusion through foams, the time is expected to be proportional to the square of the foam thickness. So, 1400 s lifetime for a 4-cm thick foam will be reduced to 22 s for a 0.5 cm thick foam layer, which is more typical in a fire extinction scenario; although extinction occurs under very dynamic conditions unlike the degradation measurements.

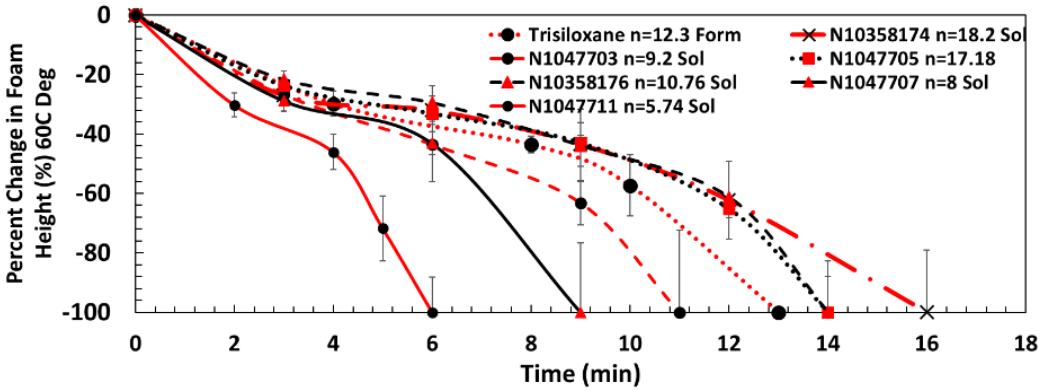

(a)

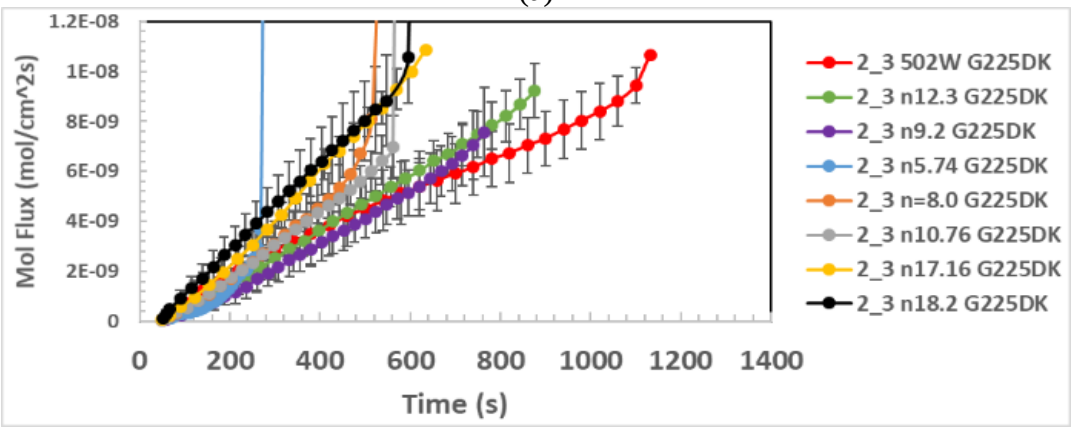

(b)

Figure 82. (a) Foam degradation in an open beaker, (b) Fuel vapor transport through an initially 4-cm thick foam layer covering a hot heptane pool (60 ^{o}C), (c) Foam degradation lifetime inside the closed transport chamber for formulations containing 0.2% synthesized trisiloxane poly(oxyethylene) (BHMTS-OEn), 0.3 % Glucopon 225DK, and 0.5 % DGBE by weight.

Figure 82(b) shows the rate of fuel vapors permeating through a foam layer (initially 4-cm thick) on top of a hot (60 ^{o}C) heptane pool in a closed chamber. It is measured by sweeping the vapors emerging from the foam surface with nitrogen flow into FTIR, which measures the fuel concentration with time. The foams degrade in the closed chamber also during the fuel transport measurements, but more slowly than in the open beaker measurements shown in Figure 82(a). The fuel mass must balance between rate fuel emerging from the foam surface and the rate of fuel passing through FTIR cell; fuel flux is calculated by multiplying the molar concentration with gas flow rate and dividing with pool surface area. Figure 82(b) shows that the fuel flux is affected significantly by the oxyethylene length, n. The measured concentration of 6150 ppm or 1.4×10^{-7} mole/cm^{2}s by FTIR corresponds to 29 mole% vapor concentration (0.29 atm vapor pressure) above a bare heptane pool at 60 ^{o}C. The lower flammability limit of 1.1 mole% corresponds to 5.3×10^{-9} mole/cm^{2}s that can support spontaneous combustion in air at ambient conditions. Figure 83(a) shows the foam degradation measured inside the fuel flux chamber and are different from those shown in Figure 82 (a) which are open beaker measurements. Figure 83(b) shows a maximum in foam lifetime versus n unlike that exhibited in Figure 82(a), which shows monotonically increasing lifetimes with the increasing n.

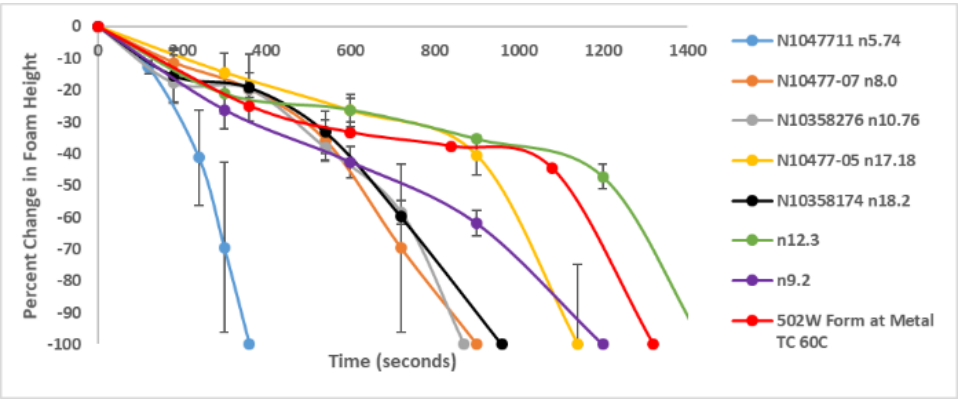

(a)

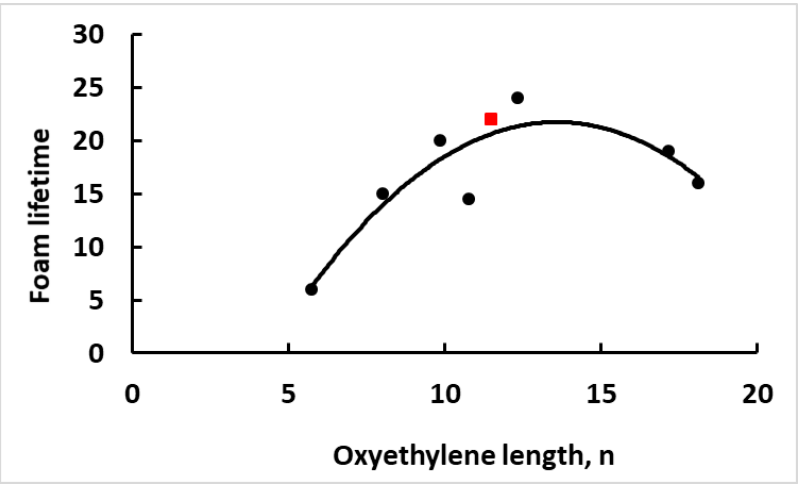

(b)

Figure 83. (a) Foam degradation measured inside the closed fuel flux chamber versus time, (b) Foam life time versus oxyethylene length, n.

4.7.4. Fire Extinction with Synthesized Trisiloxane Surfactants

Figure 84 shows fire suppression by foams generated from the formulations containing the synthesized siloxanes that replaced the 502W in column 1 of Table 10. Figure 84(a) shows the time taken for the foam to fully cover the 19-cm diameter burning heptane pool and Figure 84(b) shows the fire extinction time versus foam application rate in the same experiment where the foams are applied at a fixed position at the center of the pool at a constant rate. Figure 84(a) clearly shows that the foams spread faster as the oxyethylene length n is increased. At n greater than 12, the foams spread faster than 502W and RefAFFF. Figure 84 (b) shows that the extinction time is affected significantly by n and the effect depends on the foam application rate. At high foam application rates and n greater than 12, the extinction times are higher than 502W. We noticed, that the foams cover the pool quickly and the vapors rapidly escape from the pool edges and burn vigorously. The edge flames subside slowly and prolong the fire extinction. At low foam application rates and n greater than 12, the extinction times are lower than that for 502W formulation despite fast degradation and fuel transport shown in Figure 82(a) and (b) respectively.

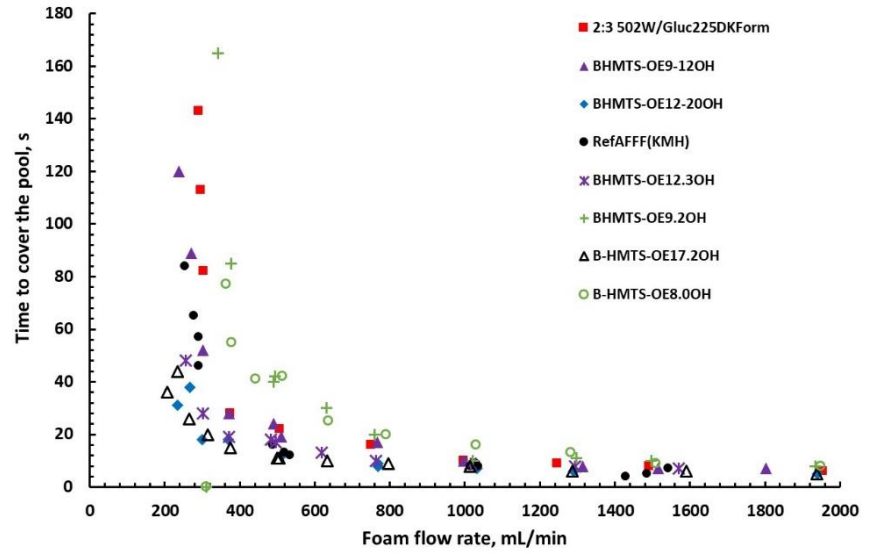

(a)

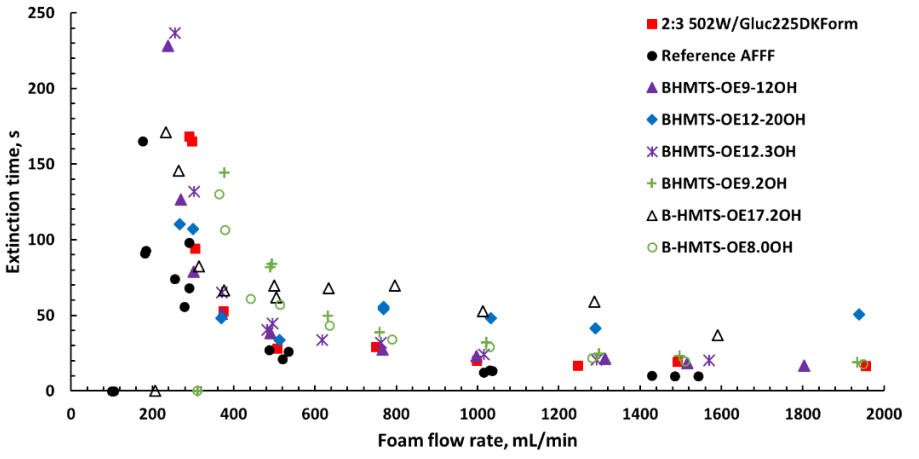

(b)

Figure 84. (a) time for foam to cover the burning pool surface, (b) fire extinction time for a 19-cm diameter heptane pool versus foam application rate for foams generated from formulations containing 0.2% synthesized trisiloxane surfactant (BHMTS-OEn), 0.3 % Glucopon225DK, and 0.5 % DGBE by weight.

4.7.5. Effects of Oxyethylene Length on Foams and Fire Extinction

Figure 85 shows foam expansion ratio, foam lifetime, fuel transport time at 5.3 x 10^{-9} mole/cm^{2}s, and fire extinction time at 1000 mL/min foam application rate as functions of the oxyethylene length, n. While the change in expansion ratio is relatively small, the lifetime, transport time, and extinction times are very much affected by n. While the lifetime increases monotonically with increasing n, the transport and extinction times exhibit maximum and a minimum near n = 10 to 12, respectively. At small oxyethylene chain lengths, foams seem to degrade and unable to block the fuel vapors quickly. Clearly, n=10 to 12 are close to the optimum oxyethylene lengths. However, it is the edge effects that prolonged extinction in Figure 84 (b) may

also play a role in causing the parabolic behavior in Figure 85 (d). It is unclear to what extent the edge effects transfer to the large scale Milspec pool firefighting, where an active firefighter moves around the edges of the pool applying the foam. The synthesized trisiloxane fire performance for n=9-12 and 12.3 are comparable to that of 502W fire performance. Unlike the commercial 502W surfactant, the synthesized surfactant structure is characterized by known reagents, chemical history and spectroscopic analysis. These synthesized surfactants can be modified with additional synthesis in a systematic way to improve the performance further.

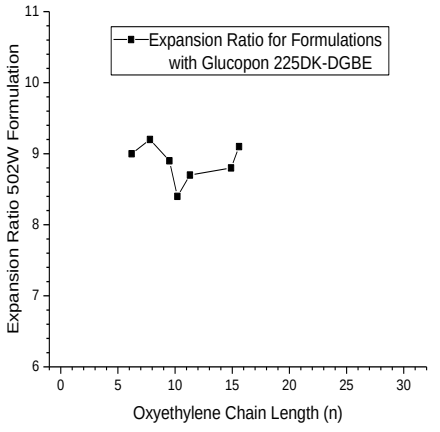

(a)

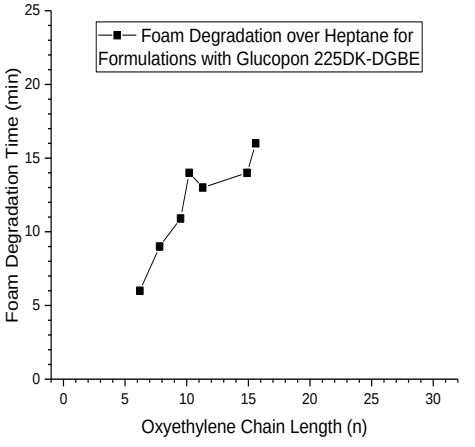

(b)

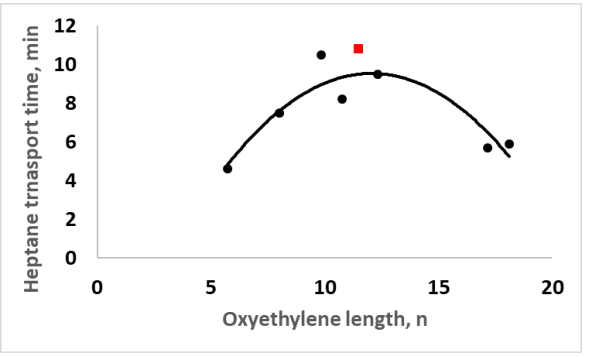

(c)

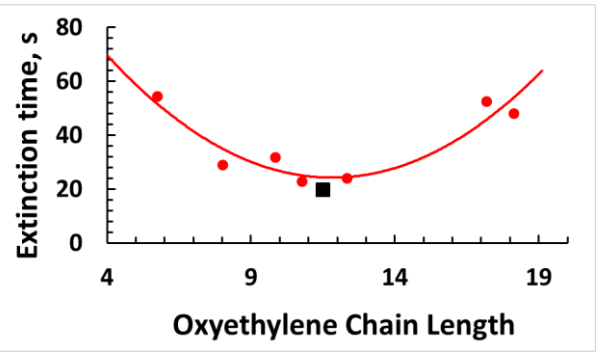

(d)

Figure 85. Foam-fuel interaction dynamics. (a) expansion ratio, (b) foam degradation lifetime, (c) fuel transport time, (d) heptane fire extinction time versus oxyethylene length, n. The transport time is obtained from Figure 82 (b) at a fixed fuel flux of 5.3 x 10^{-9} mole/cm^{2}s corresponding to the lower flammability limit (1.1 mole%). Square symbol is the data for 502W formulation shown in column 1, Table 10.

Table 16 lists the foam properties and fire extinction properties at different oxyethylene lengths along with the analytical characterizations and specific identities of the precursor materials. The Ross-Miles tests shows initial and after 5 min foam heights in the absence of any fuel effects. Table 16 shows that n=10.8, based on NMR of the precursor material, is the optimum length for properties of interest for firefighting.

Table 16. Synthesized trisiloxane (BHMTS-OEn) surfactants and their properties

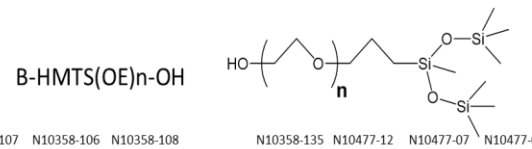

NRL Notebook Ref	N10358-107	N10358-106	N10358-108		N10358-135	N10477-12	N10477-07	N10477-03	N10358-176	N10477-01	N10477-05	N10358-174	N10358-169
n (precursor NMR)	0	1.02	2.07	3.56	5.28	5.74	8.02	9.84	10.76	12.34	17.18	18.12	45.13
n (precursor source)	0(Acos)	1(Acos)	2(Glst)	3.2(NOF)	3.0(Glst)	4-7(Glst)	7.8(NOF)	8-9(NOF)	9-12(Glst)	11.9(NOF)	15.7(NOF)	12-20(Glst)	35-50(Glst)
n (precursor GPC)	_	_	_	_	_	6.2	7.8	9.5	10.2	11.3	14.9	15.6	31.3
MWprecursor (g/mole)	58.08	103.0	149.3	_	290.7	331	402	477	507	556	714	745	1437
MWsurfactant (g/mole)	280.6	325.5	372	_	513	554	624	699	730	778	937	968	1659
Solubility (g/Kg)	<0.001	0.001	0.006	_	0.040	0.045	0.13	0.25	miscible	miscible	miscible	miscible	miscible
Cloud Point (°C)	_	_	_	_	_	_	<0	22.5	39.9	60.0	86.5	90.6	>100
CMC (%)	0.2	0.0062	0.004	_	0.005	0.0059	0.0085	0.010	0.017	0.025	0.035	0.053	0.099
CMC (g/Kg)	0.309	0.0398	0.0457	_	0.0676	0.0617	0.0912	0.115	0.191	0.240	0.316	0.372	0.575
CMC (mM)	1.15	0.115	0.120	_	0.112	0.107	0.135	0.170	0.263	0.302	0.347	0.380	0.355
γ_{CMC} (mN/m)	36.0	28.5	23.0	_	19.6	19.5	20.4	19.8	20.3	20.4	22.4	24.0	31.3
Excess, Γ (mol./cm^2 x10^{10}	10.9	9.91	0/0	_	3.96	3.57	3.26	2.97	2.91	2.85	2.61	3.03	151/121
Area/molecule A (Å^2)	15.3	16.8	5.01	_	41.9	46.6	51.0	55.9	57.2	58.2	63.7	54.8	3.34
Ross Miles (H_0mm/H_5mm)	_	_	33.2	_	_	8/1	64/45	78/64	151/140	188/137	200/163	219/150	49.8
19cm Pool (hepts/1000)	_	_	_	_	_	√	√	√	√	√	√	√	_
ext time (sec)	_	_	_	_	_	55	31	32	23	24	60	65	_
exp ratio	_	_	_	_	_	9.0	9.2	8.9	8.4	8.7	8.8	9.1	_
Degradation (min)	_	_	_		_	6.0	9.0	10.9	14.0	13.0	14.0	16.0	_
Transport	_	_	_		_	4.6	7.5	10.5	8.2	9.5	5.7	5.9	_

4.8. Varying Glycoside Surfactant Head and Tail Sizes

We quantified the effect of variations to alkylpolyglycoside (APG) co-surfactant's head and tail sizes shown in Figure 17 on heptane pool fire suppression performance, foam dynamic and physical properties, and solution properties. As mentioned earlier, our approach is to focus on the roles of surfactants in a multi-component formulation to increase oleophobicity and synergisms between siloxane and glycoside surfactants in the NRL siloxane formulation. The glycoside co-surfactant is one of the two surfactants in NRL's siloxane formulation, which contains polydispersed commercial glycoside (Glucopon225DK) with a head size of x=0.7 and tail size n=8 to 10 as shown in Figure 17, polydispersed commercial siloxane surfactant (502W), and diethyleneglycol butylether (DGBE) as shown in column 1, Table 10. To vary the glycoside surfactant's head size with the tail size fixed and vary the tail size with the head size fixed, we used two approaches: (1) fractionation of polydispersed commercial Glucopon225DK to enrich the fraction with average glycoside head size greater than 0.7, (2) used commercially available monodispersed alkyl glycosides with head size ranging up to 2 and tail sizes ranging from carbon backbone lengths of C6 to C12. We evaluated foams generated from by these glycosides replacing the Glucopn225DK in the formulation containing Dowsil 502W as listed in column 1, Table 10. We measured replaced the effects of varying the glycoside head and tail sizes on solution and foam properties, and heptane fire suppression. The results showed a minima in extinction time and foam degradation lifetimes as the head size and tail sizes are varied one at a time. The extinction time changed by a factor of 2 due to the head or tail variation. Thus, both tail size and head size have significant effect on the degree of fire suppression. Even though, the minimum extinction time did not fall below that of Dowsil 502W siloxane formulation, the results suggest that the head and tail sizes need to be increased simultaneously, rather than one at a time, to maintain amphiphilicity of the surfactant mixture while increasing the synergism. Also, instead of using monodispersed alkylglycosides in NRL's siloxane formulation, polydispersed glycosides with an average head size greater than 0.7 need to be used to increase synergism with the polydispersed siloxane 502W; the polydispersed glycosides may be created from mixing commercially available monodispersed alkylglycosides.

4.8.1. Compositions of Glycoside Formulations

We prepared formulations listed in Table 17 for generating foams, where the enriched fractions of Glucopon225DK as well as the monodispersed glycosides with different head and tail sizes are substituted for Glucopon225DK in a formulation containing 502W siloxane surfactant.

Table 17. Siloxane (502W-Glycoside) surfactant formulations and fluorinated RefAFFF formulation. The values shown under each column are weight percentages of the individual components (or concentrates) in distilled water. The formulations were used for foam generation, property and fire performance measurements**.**

2:3 Siloxane-Gluc225 (NRL Siloxane Formulation)	**2:3 Siloxane-Fractionated Gluc225DK**	**2:3 Siloxane-Glycosides**	**3:2 Cap-Gluc215 (RefAFFF** [14]**)**
0.2 % 502W, polydispersed	0.2 % 502W, polydispersed	0.2% 502W, polydispersed	0.3% Capstone
0.3% Glucopon 225 DK, polydispersed	0.3% Fractions of Glucopon 225DK, polydispersed	0.3% Glycosides of different head/tail sizes, monodispersed	0.2% Glucopon 215 CS UP, polydispersed
0.5% DGBE	0.5% DGBE	0.5% DGBE	0.5% DGBE

4.8.2. Fractionation of Glucopon225DK and Characterizations

Glucopon 225DK is a BASF alkyl polyglycoside surfactant product is polydispersed [46] and is a very important component of the NRL siloxane (502w-Glucopon 225DK-DGBE) formulation [32]. It out-performed other glycoside surfactants (Glucopon 215UP, Glucopon 600UP, Triton CG425) in combination with 502W as a foam formulation for fire suppression. Commercial APG surfactant preparation is usually done via Fischer synthesis from glucose and fatty alcohols. The reaction yields products which are complex mixtures of mono-, di-, and higher glycosides with a variation in geometric and stereo isomer structures along with a range in alkyl chain length of 8-10. APG surfactants are schematically represented by the structure shown in Figure 17 accompanied by numerical averages and ranges for the polyglycoside and alkyl chain lengths [46]. The structure, however, over simplifies the complexity in that glycosides moieties bond to each other at variable positions and with different stereochemistry is addition to that illustrated by the structure.

We found a correlation of higher degree of fire suppression with the higher polyglycoside content of Glucopons and with TritonCG-425 (x=0-2 and n=8-14). The correlation appears to indicate that improvement may be obtained by increasing the glycoside content. Unable to obtain commercial APGs with higher glycoside content, the approaches of fraction of Glucopon 224DK, purchasing analytical APG compounds and of synthesis of a monodispersed triglycoside were adopted as hypotheses for fire suppression improvement over that for the NRL's 502W-Glucopon 225DK-DGBE formulation shown in Column 1 of Table 17.

The solubility of APG compounds is dependent on the quantities of glycoside head and alkane tail in the surfactant. Solubility testing of Glucopon 225DK in a range of solvents produced an interesting pattern of degree of solubility (Table 18).

Table 18. Solubilities of Glucopon225DK in different solvents

Glucopon 225DK Solubilities

Solvent	% PPT Fraction	% Sol Fraction
DMSO	0%	100%
CHCl3	0%	100%
MeOH	3.0%	97.0%
EtOH	13.3%	86.7%
iPrOH	22.7%	77.3%
THF	29.8%	70.2%
Acetone	38.4%	61.6%
EtOAc	53.6%	46.4%
CH3CN	60.8%	39.2%
Toluene	97.4%	2.6%

With the exception of chloroform, there appears to be a correlation of solubility with solvent polarity. Chemical intuition would expect the glycoside structure with its multi-hydroxyl functionality to favor water, DMSO and alcohol solubility with molecules having higher hydroxyl contents requiring higher degrees solvent polarity for solubility. This behavior is the basis Glucopon 225DK fractionation based on solubility. Solubility based fractionation is a practical technique as it can be readily adapted to 100g quantities of surfactant. The fractionation approach developed involved starting with the acetone solvent, and collecting acetone-soluble and acetone-precipitated fractions. The acetone-soluble fraction is then subjected to acetonitrile dissolution and results in acetonitrile-soluble and acetonitrile-precipitated fractions. Finally, noting that ethanol dissolves almost 90% of the Glucopon 225DK, an ethanol-precipitated fraction was collected by dropwise addition of the Glucopon 225DK concentrate into stirred ethanol. Figure 86 illustrates this overall fractionation scheme below.

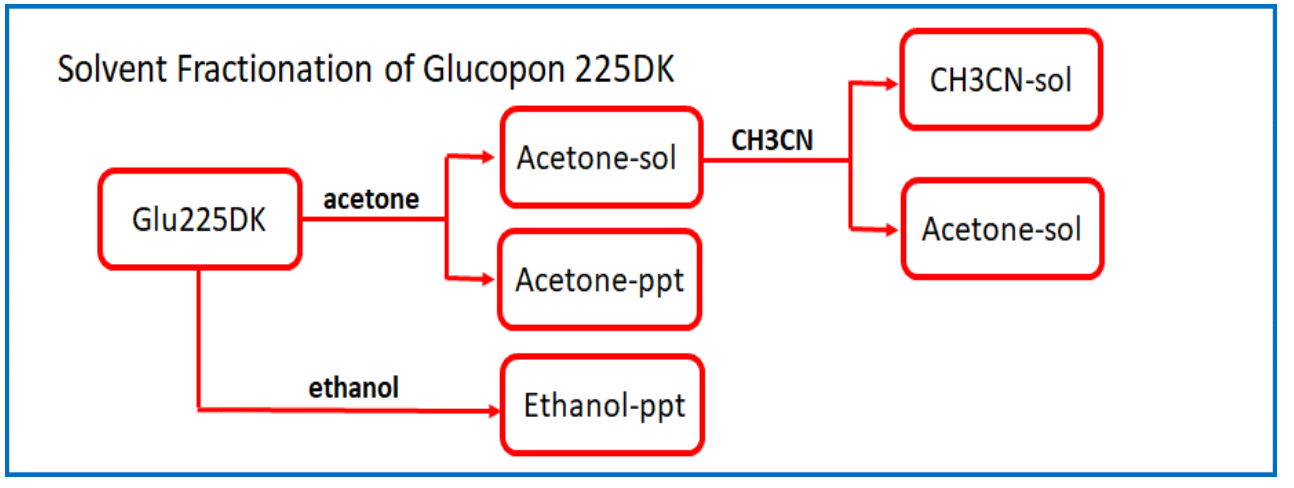

Figure 86. Fractionation scheme for Glucopon225DK with acetone, ethanol, and acetonitrile.

4.8.2.1. Procedure for Fractionation of Glucopon225DK

The commercial BASF surfactant concentrate Glucopon 225DK was analyzed by thin-layered chromatography on silica gel plates. Although there were no UV-active components of the product, the plates could be visualized by staining with 10 wt% phosphomolybdic acid in ethanol. The best solvent system for elution was 20 vol% methanol in chloroform. By this method, the 225DK was separated and was found to be mostly a single spot of Rf = 0.6, along with a streaking material from the origin and a strong spot at the origin. A 5 g sample of 225DK was then separated by silica gel chromatography, and a sample of the upper spot at Rf = 0.6 was obtained pure. Proton and carbon-13 NMR showed that the purified material was the C8/C10 mono-glucoside.

Next, 225DK was separated into various fractions with organic solvents. First, it was found that 225DK (6.5 g) would yield a precipitate when dissolved in both ethanol and acetone (100 mL of either solvent). For expediency, all later further separation employed acetone as the starting point. The granular solid that precipitated from acetone could be collected on a medium porosity glass filter frit and then dried under vacuum. In one such run, 6.5 g 225DK yielded 1.89 g of a light tan precipitate (~29%). The acetone filtrate could then be evaporated down to a gummy residue. TLC analysis of the two fraction showed that the mono-glucoside spot at Rf = 0.6 was nearly completely gone from the acetone-insoluble fraction, while the acetone-soluble fraction appeared to be enriched with it, the latter also having less of the lower running components. The acetone-soluble fraction was further fractionated by dissolving into warm acetonitrile. Allowing the acetonitrile solution to cool to RT and a precipitate formed. The precipitate from the acetonitrile was not a well-behaved solid but stuck well to the sides of the flask. Thus, the acetonitrile solution could be decanted away from the precipitate. However, there was not a great amount of acetonitrile-insoluble material, most of the material was soluble in acetonitrile. In fact, after repeating the acetonitrile fractionation a second time, the resulting acetonitrile-soluble material was almost completely clean mono-glucosides by TLC analysis. Three samples from this fractionation process were available for pool fire extinction testing: 1) ~60 g of acetone-insoluble 225DK; 2) ~40 g of acetone-soluble 225DK; and 3) ~20 g of acetonitrile-soluble 225DK.

The EtOH-ppt fraction of Glucopon 225DK was prepared as described in NRL Notebook N10477-77 and is described as follows. BASF Glucopon 225DK is a concentrate with a non-volatiles content of 70wt%. It was prepared in two batches by dropwise addition of 50.0 g 225DK concentrate into 2000 ml absolute ethanol and 40.0 g 225DK concentrate into 1600 ml absolute ethanol while stirred (vortex of 2/3) over a 1 hr period. These suspensions were stirred for an additional hr. The finely divided precipitate was collected by slow filtration through a 15cm Whatman #41 filter paper supported by a large conical funnel. The soft paste filtrate was transferred by spatula to a large petri dish and placed in a vacuum desiccator and covered by a large watch glass. Vacuum was gradually increased at a rate where spattering of ethanol was avoided. After six hours a maximum mechanical pump vacuum (<1mm) was obtained. The <1mm vacuum was maintained for 3 days. Product yield was 7.395g (90.3% based on 70% 225DK non-volatiles and 225DK solubility in ethanol of 13.3%). ^{1}H NMR showed trace of residual EtOH which 3 additional days <1mm vacuum treatment could not remove.

4.8.2.2. Characterization of Glucopon225DK Fractions

The four fractions (CH3CN-sol; Acetone-sol; Acetone-ppt and EtOH-ppt) were collected in 8-20g quantities and were characterized by ^{1}H NMR spectroscopy and gel permeation chromatography. The NMR spectra somewhat complicated by the mixed-isomer structure of the

polyglycoside moiety. An oversimplified APG structural representation is provided Figure 87 with ppm chemical shift assignments for various proton resonances indicated, and the spectra of the unfractionated Glucopon 225DK and its series of fractions are presented in Figure 88. In viewing the APG structural representation it should be kept in mind that, in addition to the 6 position illustrated, polyglycoside linkages can occur at the 2, 3 and 4 positions and that stereochemistry can vary at the 1 position.

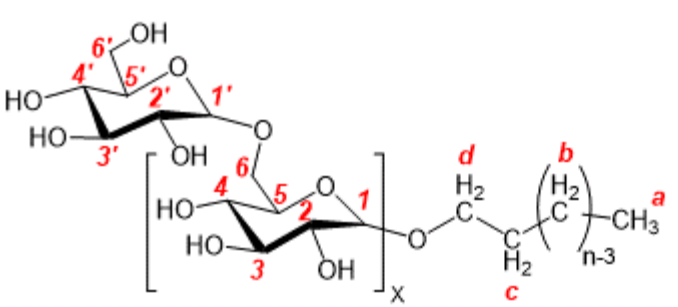

Position	ppm
a	0.87
b	1.25
c	1.52
d	3.3
1	4.6
2	3.1-3.4
3	3.1-3.4
4	3.1-3.4
5	3.4-3.5
6	3.6
-OH	4.4-4.8

Figure 87. Structural representation of a glycoside surfactant with identification of chemical shift assignments.

In the spectra shown in Figure 88, the a, b and c resonances attributed to the alkyl group are readily identified, and the d resonance overlaps with glycoside resonances. In the glycoside part of the structure for X > 0, the polydispersity of the glycoside chain length and its isomeric variability complicate and broaden the structure. However, as X increases the spectral broadening of its resonances becomes greater and their intensity ratio to the alkyl resonances becomes larger. The spectra in Figure 88 have been arranged such that those corresponding to fractions soluble the less polar solvent are placed immediately below the spectrum of the unfractionated Glucopon 225DK, and spectra of those fractions precipitated from the more polar solvents are at the bottom. The trend of higher glycoside signal resolution and higher alkyl resonance intensity correlates with the shorter chain lengths (lower value of X) of the organic solvent soluble fractions.

Another diagnostic for the polyglycoside chain length is gel permeation chromatography. This method separates molecules according to size by using a gel that has a pore size that retards the passage of small molecules through the column. Most GPC columns use organic solvents, most often THF as is the case at NRL. As indicated above Glucopon 225DK is 70% soluble in THF. While the insoluble fraction may include the longer chain polyglycosides, such an analysis of this APG and its fractions can provide useful characterization information. The chromatograms of the THF soluble portions of the unfractionated Glucopon and its CH3CN-sol, Acetone-sol and Acetone-ppt fractions (the EtOH-ppt fraction was insoluble in THF) are depicted in Figure 89. The distribution of mono-, di- and triglycoside contents is clearly indicated by the intensities of the chromatographic peaks. It clearly shows that the content CH3CN-sol fraction relative to that of the unfractionated Glucopon 225DK is significantly enriched in monoglycoside, strongly diminished in diglycoside and depleted of triglycoside. The Acetone-sol fraction is also enriched in monoglycoside, slightly enhanced

In diglycoside and slightly diminished in triglycoside content. The Acetone-ppt fraction is strongly diminished in monoglycoside, has a near equivalent quantity of diglycoside and a greater

quantity of triglycoside. This correlates well with the glycoside composition variation indicated by the NMR characterization. By extrapolation, the EtOH-ppt fraction is to be more enriched in the triglycoside content.

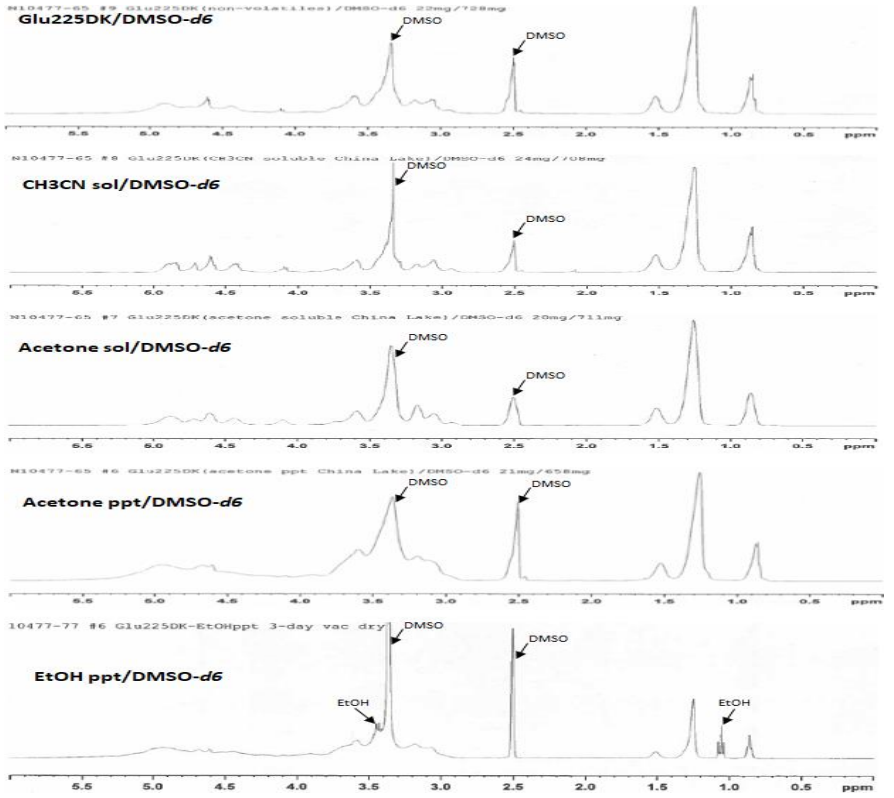

Figure 88. NMR spectra of the unfractionated Glucopon 225DK and CH3CN-sol; Acetone-sol; Acetone-ppt and EtOH-ppt fractions depicted in order of increasing fractioning solvent polarity.

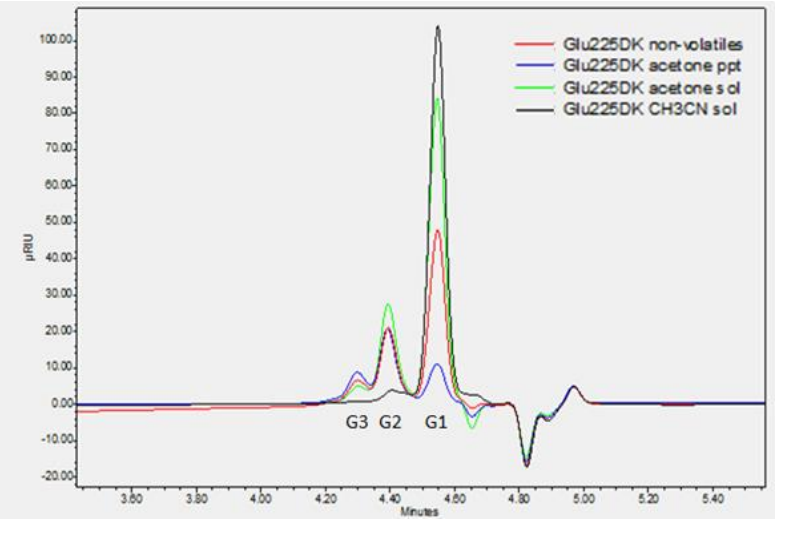

Figure 89. GPC chromatogram of the unfractionated Glucopon 225DK and CH3CN-sol; Acetone-sol; Acetone-ppt fractions. The G1, G2 and G3 indicate retention times that correspond to mono-, di- and triglycoside size molecules as calibrated by the analytical glycoside compounds (ANATRACE Inc.).

4.8.3. Commercial Monodispersed Glycoside Structures

A number of analytical grade monodispersed alkylglycoside surfactants with well-defined chemical structures were purchased from ANATRACE Co., Maumee, OH [66]. They are used to replace Glucopon225DK in formulations shown in column 1 of Table 17. Their chemical structures are shown in Figure 90.

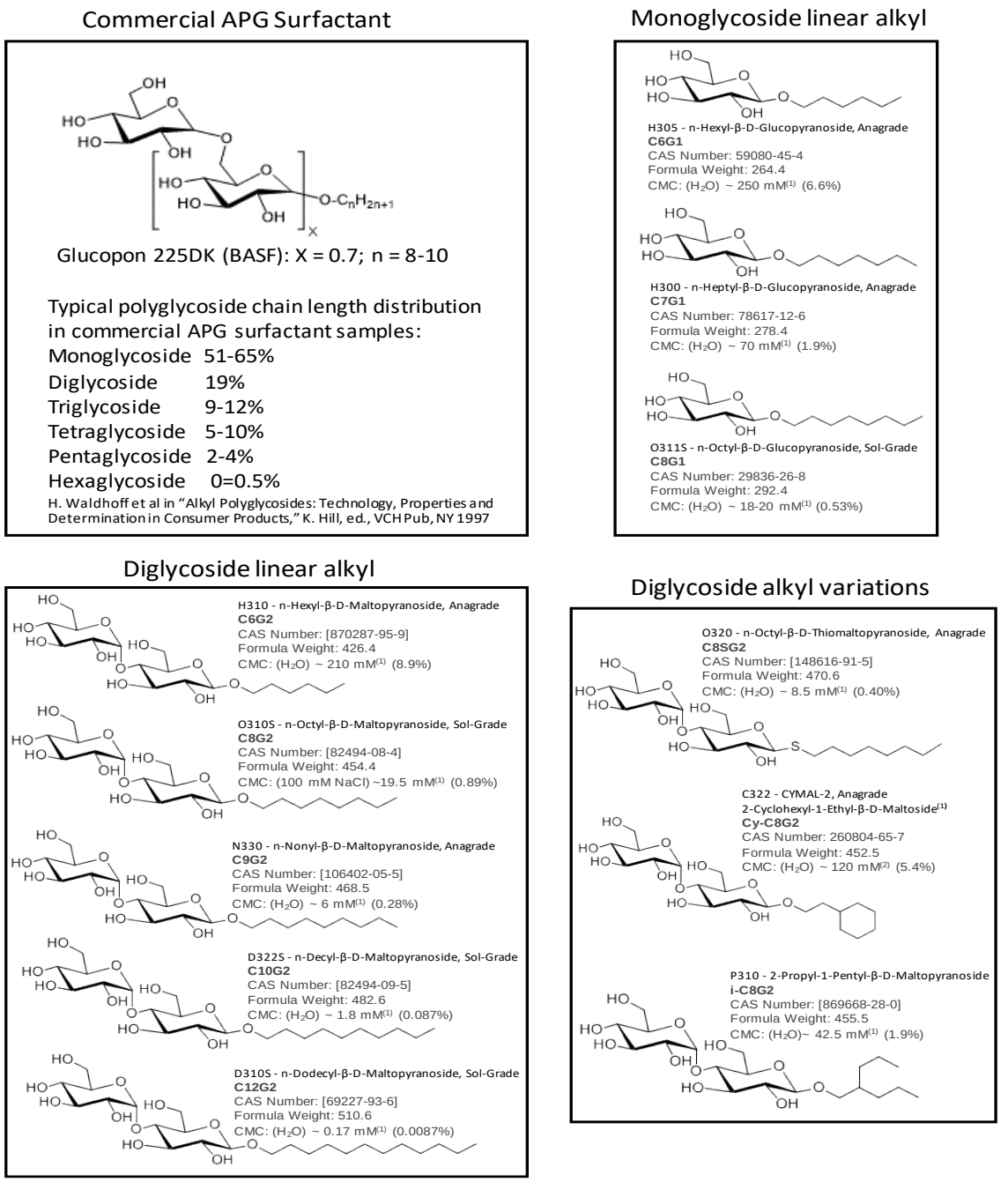

Figure 90. Chemical structures [66] of monodispersed alkyl glycosides used to replace Glucopon225DK as shown in column 1 of Table 17.

While the fractionation of Glucopon225DK yielded polydispersed fractions, monodispersed glycosides can be used both as references for analytical characterizations but also can enable well-defined, systematic, variations of the glycoside structure to provide insights into how they affect fire extinction. They enable variation of alky tail length with head size fixed and variation of glycoside head with the alky tail length fixed. Their effects on solution and foam properties, and fire extinction can also be quantified. In addition to the commercial glycosides, Dr. Matthew Davis kindly provided us with monodispersed alkyltriglycosides, which he synthesized at NAWC, China Lake, CA for foam and fire suppression evaluations.

4.8.4. Surface tension and CMC measurements

Table 19 shows the measurements of surface and interfacial tensions for formulations containing the commercial glycosides (ANATRACE Co., Maumee, OH) as shown in column 3 of Table 17. Increased alkyl length of the alkylglycoside appears to increase the surface tension slightly. Figure 91 shows the surface tension of siloxane formulation with hexyldiglycoside C6G2 as a function of total surfactant concentration in water. The critical micelle concentration (cmc) is 0.009 wt% as determined from the plot.

Table 19. Interfacial properties of siloxane-glycoside formulations shown in column 3 of Table 2.

Formulation	Surface Tension mN/m (± 0.5 mN/m)	Int Tension Hept mN/m (± 0.5 mN/m)	Int Tension Gasoline mN/m (± 0.5 mN/m)
502W+C8G1	21.5	3.0	2.7
502W+C8G2	21.6	4.0	4.3
502W+C10G2	23.8	3.9	2.1
502W+C12G2	24.1	3.3	1.5

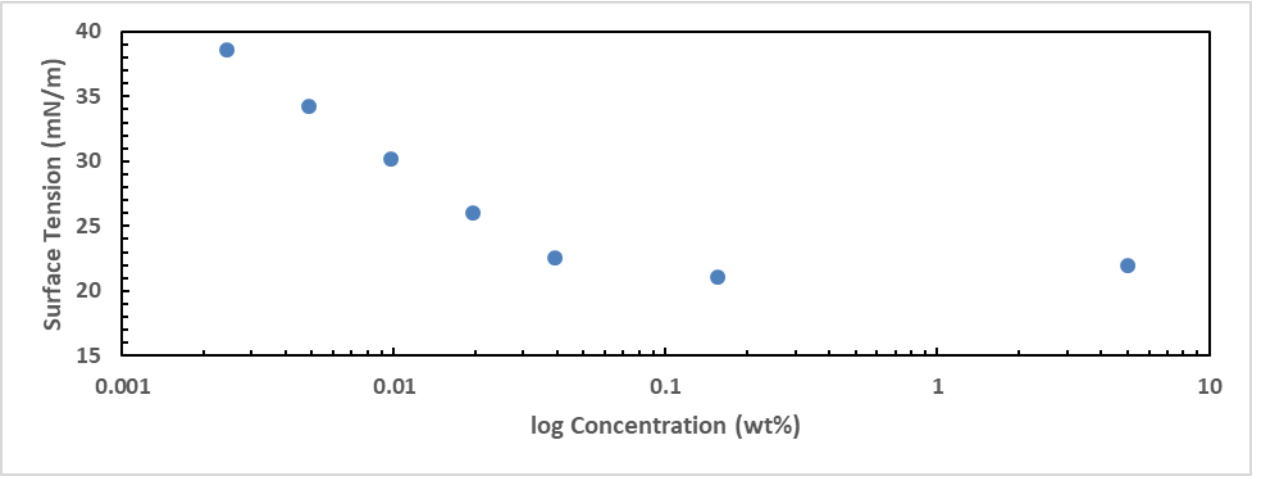

Figure 91. Critical micelle concentration (cmc) for siloxane formulation with C6G2 replacing Glucopon225DK as shown in column 3 of Table 17.

Figure 92 shows cmc as a function of alkyl tail length for solutions of alkylglycoside surfactants. These are aqueous solutions of individual surfactants rather than formulations

containing surfactant mixtures. Log of cmc decreases linearly with increasing tail length, number of carbon atoms n, for both mono and di- glycosides. Thioglycoside has lower cmc than iso and cyclic glycosides.

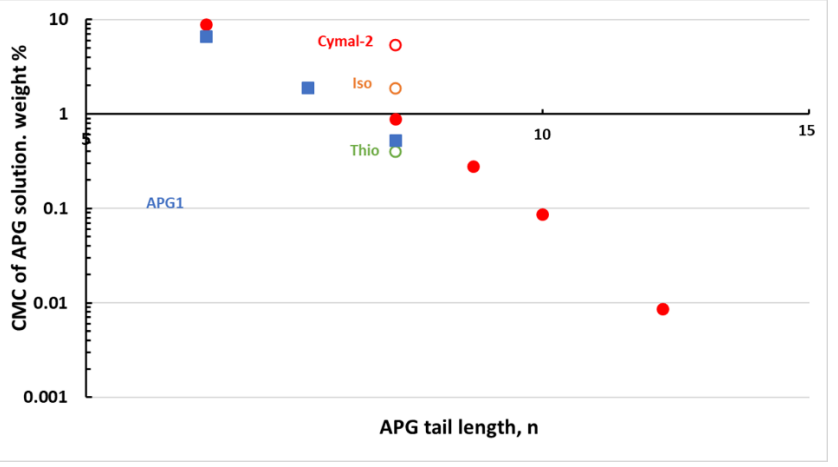

Figure 92. Critical Micelle Concentration (CMC) as a function of alkyl tail length for individual monodispersed alkyl glycoside solutions in water.

4.8.5. Foam generation and Expansion ratio

Foams were generated using sparging method. The expansion ratio (volume of foam/volume of liquid) was calculated by measuring the weight and volume of the foam and it represents water content of the foam. Figure 93 shows the expansion ratio versus foam generation rate using formulations containing different fractions of Glucopon225DK replacing Gucopon225DK as shown in column 2 of Table 17.

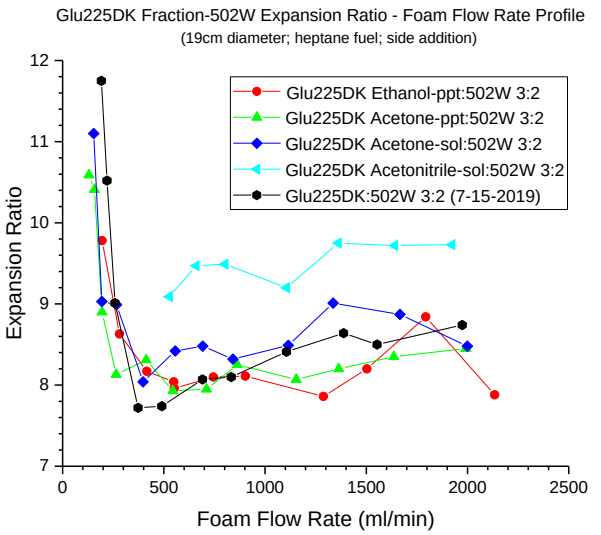

Figure 93. Foam expansion ratio with foam generation rate through the sparger disc for the formulations shown in column 2 of Table 17; different glycoside fractions varying in monoglycoside content (shown in Figure 89).

Figure 93 shows relatively constant expansion ratio at foam flow rates higher than 500 mL/min and an increase in expansion ratio when foam flow rate is below 500 mL/min. This is due to increased liquid drainage from the foam before it exits the generator outlet at low foam flow rates; liquid drains from foam collected above the solution in foam generation cup for longer times at low foam flow rates. Among different fractions, acetonitrile fraction that is enriched in monoglycoside content has higher expansion ratio than other fractions.

Figure 94 is similar to Figure 93 but for the monodispersed alkylglycosides shown in Figure 90. Figure 94 shows that the expansion ratio is relatively independent of foam generation rate with the exception RefAFFF, which exhibits a decrease in expansion ratio with increased generation rate. Figure 95 shows that expansion ratio relatively independent of alkyl tail length of alkyldiglycosides shown in Figure 90.

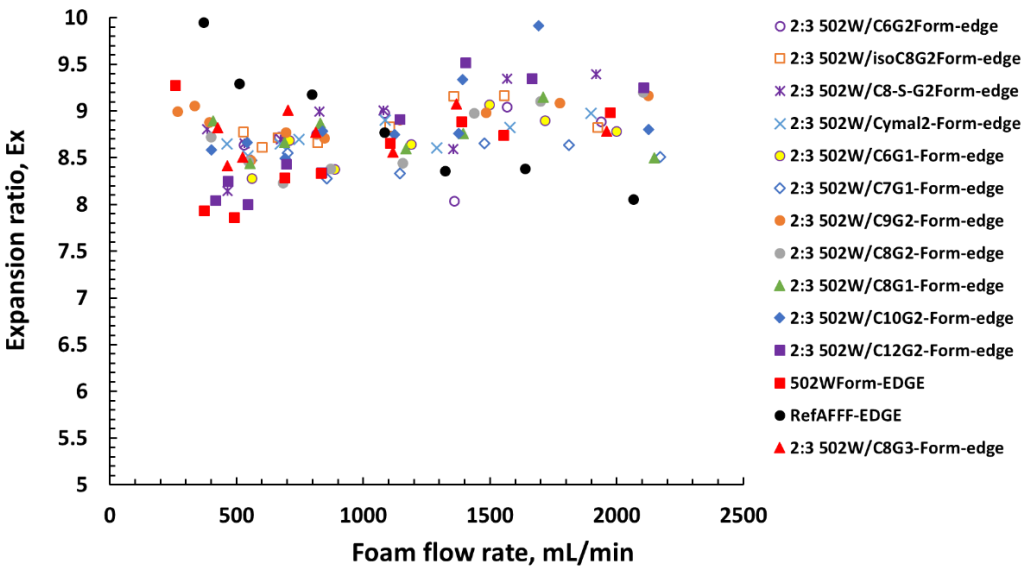

Figure 94. Foam expansion ratio with foam generation rate through the sparger disc for formulations shown in column 3 of Table 17.

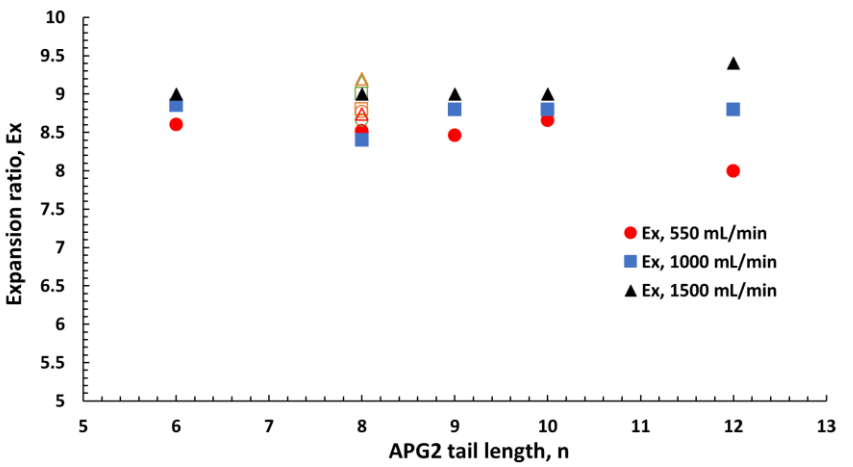

Figure 95. Foam expansion ratio versus alkyl tail length for formulations shown in column 3 of Table 17 generated at different foam flow rates, 550 mL/min to 1500 mL/min.

4.8.6. Foam Degradation by Fuel and Fuel Transport

The foams derived from formulations containing each of the three Glucopon 225DK fractions substituted into the 502W shown in column 2 of Table 17 were characterized by degradation measurements and compared with analogous data for the unfractionated Glucopon 225DK formulation. This characterization involves monitoring the time-dependent reduction of a 4cm layer of foam deposited onto a 60 mL volume of 60ºC preheated fuel in a 150 mL beaker and results are depicted in Figure 96.

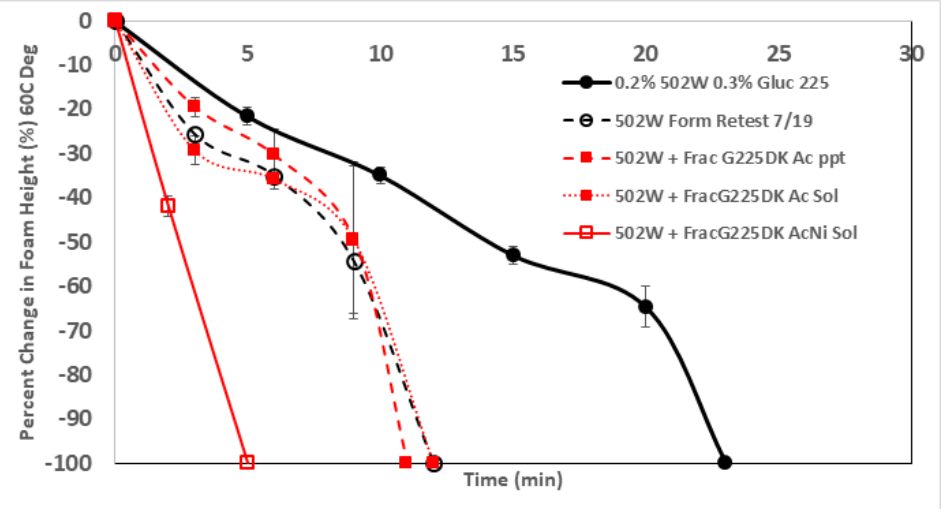

(a)

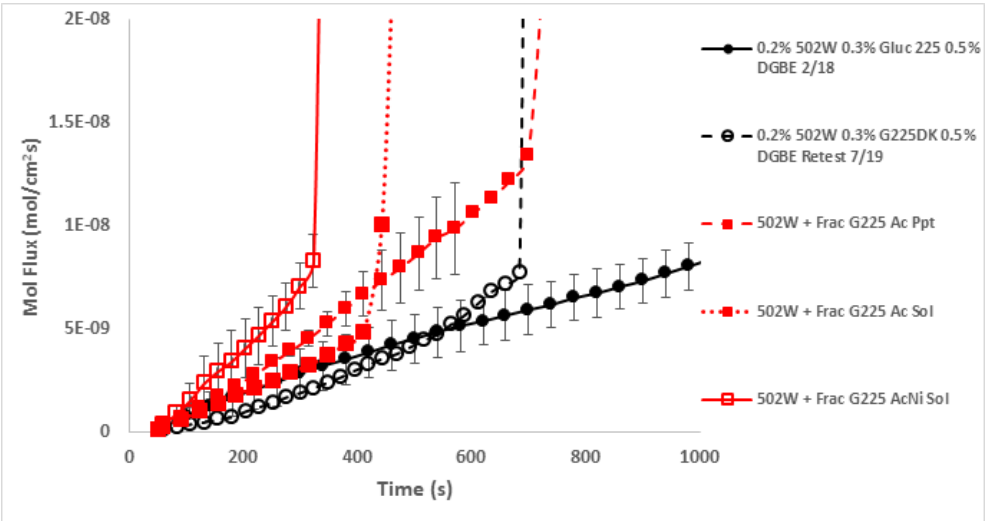

(b)

Figure 96. (a) Foam degradation measurements, (b) fuel vapor flux from the foam covered heptane pool at 60 ºC for foams generated from formulations in column 2 of Table 17; the solvent-separated 225DK fractions (Acetone-ppt; Acetone-sol; CH3CN-sol).

This result displayed in Figure 96(a) shows that substitution of the CH3CN-sol fraction in the formulation results in the most rapidly degraded foam. This correlates with the extinction data in

that the associated monoglycoside content of this fraction is associated with both the lesser extinction performance and the more rapid foam degradation. The degradation data for the foams associated with the Acetone-sol and Acetone-ppt fractions' formulations shows little difference between the foams. Comparison with degradation of the foam derived from the unfractionated Glucopon 225DK will require more testing as results in one run indicate little difference and another run indicate the unfractionated 225DK derived foam to be more degradation resistant.

These foams were also characterized by heptane fuel vapor transport measurements where the heptane content in the headspace above an initial 4 cm foam layer laid over a 60ºC heptane pool is monitored as a function of time via an infrared gas cell and slow moving carrier gas. Results are presented in Figure 96(b). The foam derived from CH3CN-sol fraction exhibited the highest permeability which would also correlate with the lowest extinction activity. The foams derived from the Acetone-sol and Acetone-ppt fractions' formulations show moderately divergent behavior with the former being less permeable but both being slight more permeable to heptane vapors than foam derived from the formulation with the unfractionated Glucopon 225DK.

Fuel transport and foam degradation data was also collected for a set of monoglucoside materials that were fire tested in a formulation containing 502W siloxane as shown in column 3 of Table 17. The set included 11 monoglucosides with variation in glucoside value (G1 or G2), tail length (C6, 7, 8, 9, 10, 12) and additional variation on the C8G2 (cymal, i-C8G2, C8SG2).

Figure 97 plots fuel transport rates for all 11 in comparison to 0.5% 502W alone and 502W in a 2:3 formulation with Glucopon 225DK and 0.5% DGBE. Little difference in transport rates were seen for all of the monoglucosides tested. Most had worse transport performance than the 502W surfactant individually, and none compared to the performance of the formulation containing 502W and Glucopon 225DK (column1, Table 17). Figures 98 to 100 are monoglucosides separated to identify potential trends in glucoside size, tail length, or variations on C8G2. Differences in transport are very minor, but the best two performers from the group for transport were C6G1, C8G2, and C12G2.

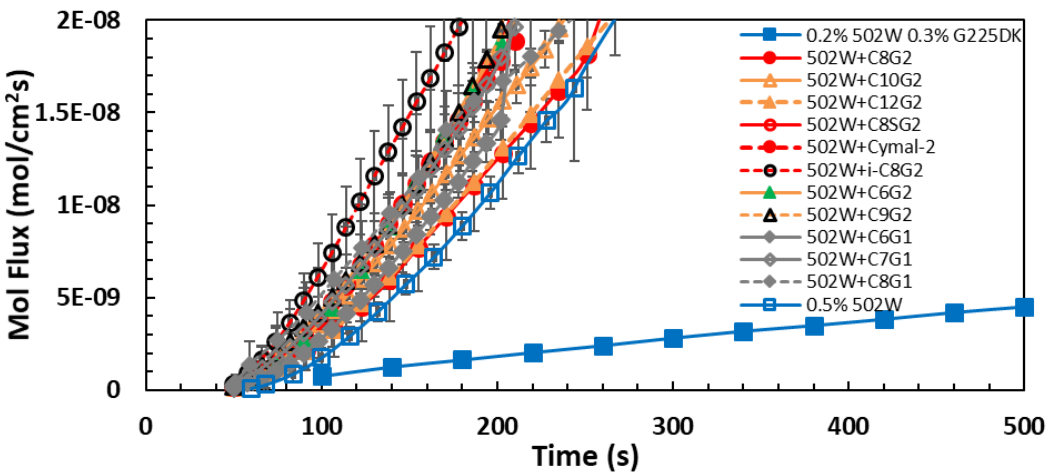

Figure 97. Heptane fuel transport rate through a 4-cm foam layer covering hot (60 ºC) heptane pool with time. All foams are generated by sparging method with formulations shown in column 3, Table 17.

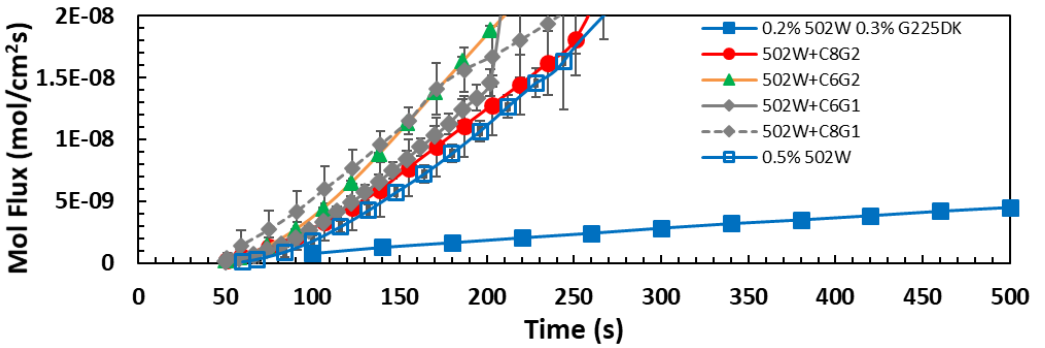

Figure 98. Trends in G1 vs G2: No clear trend, C8G2 has better transport than C8G1, however, C6G1 has better transport than C6G2 and might be due to different degrees of amphiphilicity.

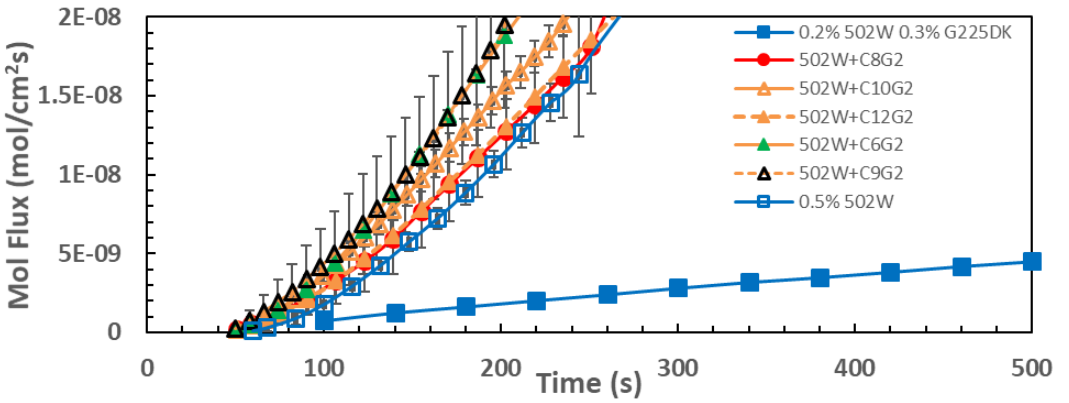

Figure 99. Trend in length: No clear trend, transport rate order from fast to slow C9G2=C6G2 > C10G2 > C8G2=C12G2.

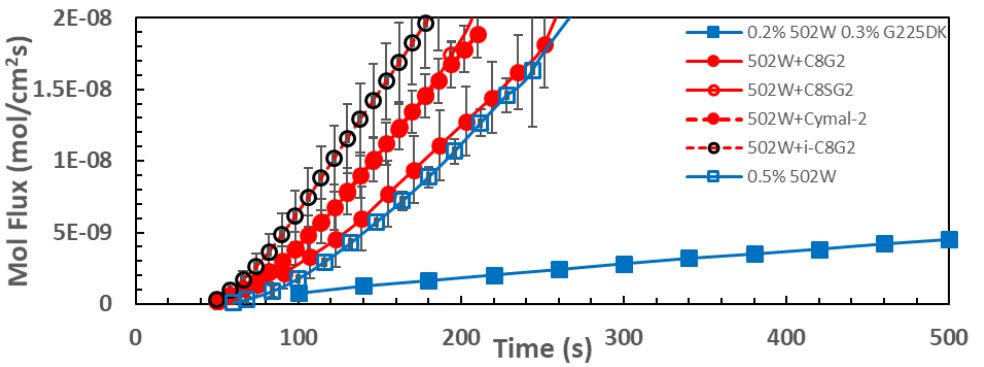

Figure 100. Variations in C8G2 showed some differentiation. C8G2 performed better than the other 3. Cymal and C8SG2 performed similarly, and i-C8G2 performed the worse. C8G2 containing 502W and DGBE performed as well as 502W alone with the other formulations showing faster (worse) transport despite 502W being in the formulation with the monoglucoside.

Degradation data in an open beaker was also collected for this series and the data is plotted in Figure 101. Little variation seen in degradation performance. Foam lifetimes are slightly longer than the 3 minutes of the 0.5% 502W surfactant alone, but do not match the 23 minute performance of the 502W formulation with Glucopon 225DK and DGBE. Figure 101 plots the 11 variations

together. Figures 102 to 104 separate degradation profiles based on glucoside value, tail length, and variations in C8G2. Foams with the longest lifetimes were 502W+Cymal-2 and 502W+C9G2, this does not trend with transport performance which showed these two foams having marginal transport performance: not the worst or the best.

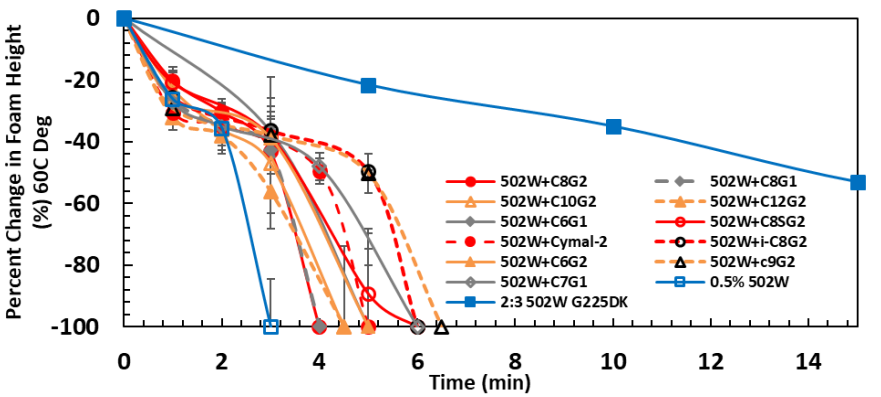

Figure 101. Change in foam layer thickness with time due to degradation by hot heptane (60 ^{o}C)

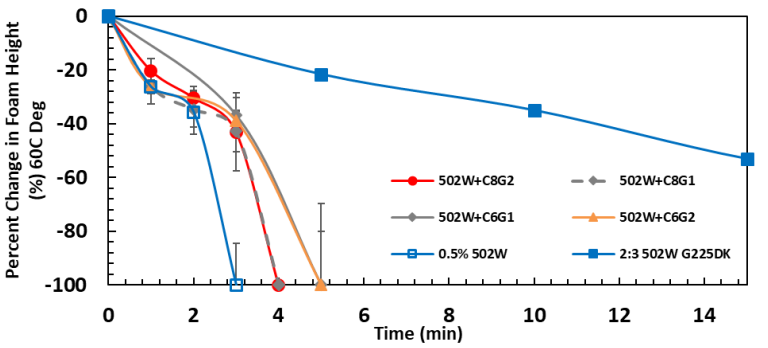

Figure 102. Trends in G1 vs. G2: change from G1 to G2 does not appear to effect degradation performance for tail lengths of C6 and C8 significantly. C6G1 and C6G2 have the same foam lifetime with small differences in degradation profile. Similarly, C8G1 and C8G2 have the same foam lifetime and small differences in degradation profile.

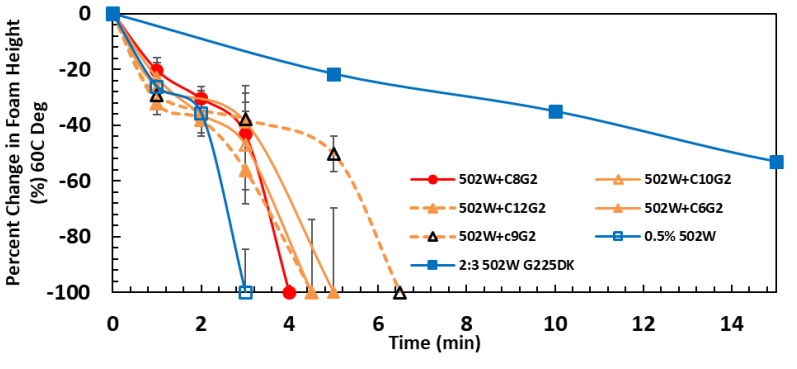

Figure 103. No clear trend in degradation performance due to tail length. Foam lifetimes are in the order C8G2 < C10G2 = C12G2 < C6G2 < C9G2. All are an improvement in lifetime over 502W alone, but do not compare to the performance of 502W with Glucopon 225DK.

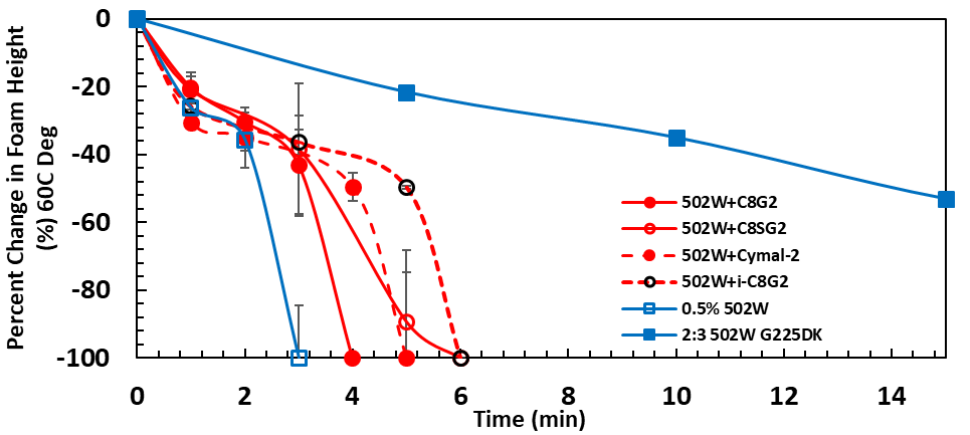

Figure 104. Trends in C8G2 variation: exhibit similar foam lifetimes and profiles. Slight variations, foam lifetime in the order of C8G2 < Cymal-2 ≈ C8SG2 ≈ i-C8G2.

4.8.7. Bench Scale Fire Extinction with Glycosides

Benchtop fire extinction testing of the four fractionated compositions of Glucopon 225DK in a formulation shown in column 2 of Table 17 (502W:fractions of Glucopon225DK:DGBE) was conducted 19cm heptane pool using the edge deposition of foam. The extinction time versus foam flow rate and time for full coverage of the pool surface versus foam flow rate profiles data are illustrated in Figures 105 and 106. Using the unfractionated Glucopon 225DK in the 502W formulation as a reference, the formulations using the Acetone-sol and Acetone-ppt fractions as the APG component very closely track this reference. The CH3CN-sol fraction containing formulation has a profile displaced to longer extinction times and faster foam flow rates making it significantly less effective compared to the unfractionated Glucopon225DK. Use of the EtOH-ppt fraction in place of Glucopon 225DK in the formulation results in a profile moderately displaced to longer extinction times and faster flow rates. These results indicate that the monoglucoside component in Glucopon 225DK does not contribute as much as the di- and triglucoside surfactant components to the fire extinction. However, substitution of the acetone-sol and acetone-ppt fractions with their diminished monoglycoside and enhanced di- and triglycoside contents did not improve extinction performance beyond that of the formulation with the unfractionated Glucopon 225DK. The presumably triglycoside rich EtOH-ppt fraction containing formulation also did not improve but diminished fire suppression effectiveness. This result appears to indicate that simply increasing the glycoside chain length beyond a certain threshold does not result in an enhanced fire suppression capability. One of the reason is that tail length can have significant effect on fire suppression; the GPC shown in Figure 89 could only resolve glycoside head size but not the tail sizes. Second reason has to do with the polydispersity. One must also keep in mind that there are a multitude of glycoside isomers and other components in the complex Glucopon 225DK. Also, 502W siloxane is a polydispersed mixture leading to a geometrical fit among different sized molecules in NRL's siloxane formulation (column 1, Table 17) mixture resulting in synergism to increase fire suppression. The siloxane has wide tail and skinny head of different sizes and vice a versa for the Glucopon that could fit geometrically, and increase surfactant packing density at the interface. The fractions from Glucopon225DK would have shifted that polydispersity one way or another from Glucopn225DK that could have a deteriorating effect on the synergisms and the degree of fire suppression.

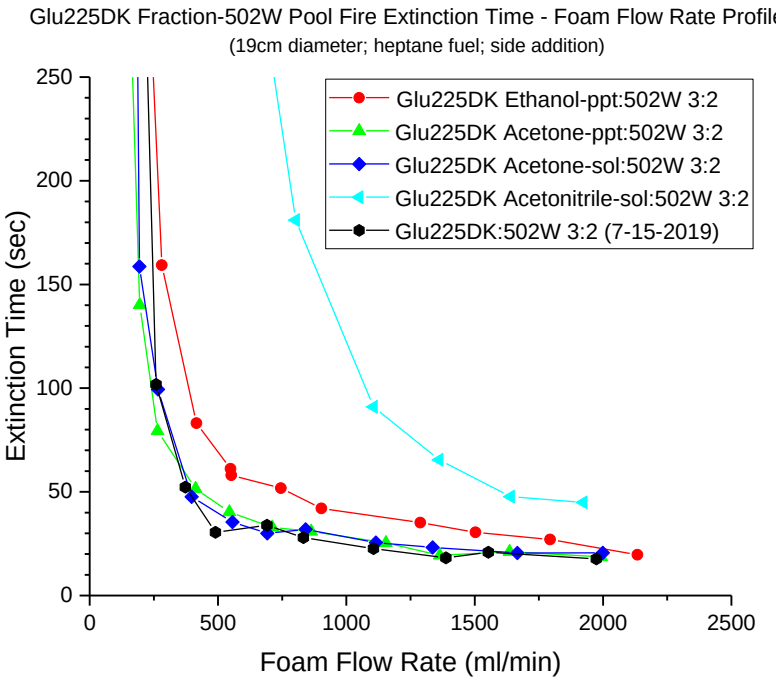

Figure 105. Heptane pool fire extinction time at different foam application rates for different fractions of Glucopon225DK as shown in column 2 of Table 2, replacing the unfractionated Glucopon225DK in NRL formulation. Foam was deposited at the edge of the pool and was allowed to spread to cover the pool.

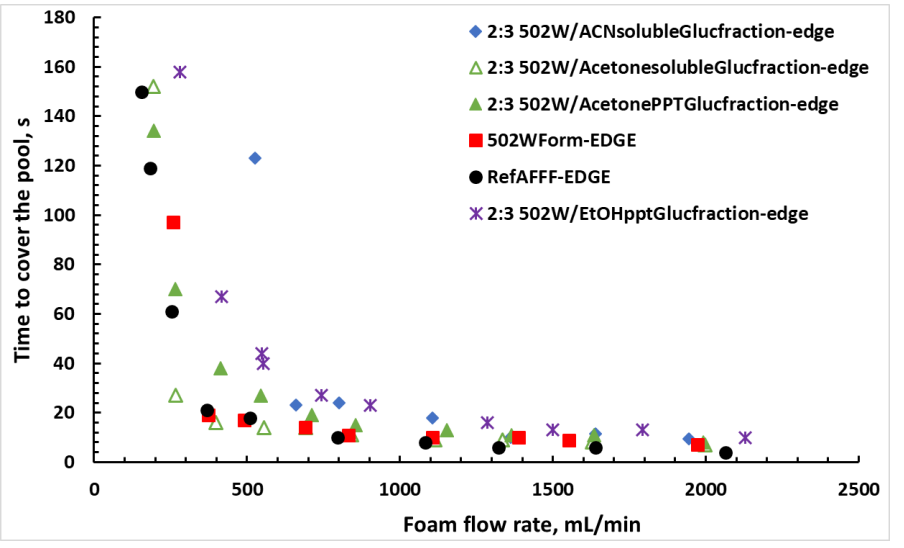

Figure 106. Time for foam to completely cover the pool surface measured at different foam application or generation rates for different fractions of Glucopon225DK as shown in column 2, Table 17. All foams are generated using sparging method and deposited at the edge of the pool.

The time for full coverage of the pool surface was also measured during the fire extinction experiment and are shown in Figure 106. The coverage time data appear to follow the extinction time data especially at low foam flow rates. It is interesting that the expansion ratio data shown in

Figure 93 indicate that only the CH3CN-sol fraction (value of 9.5) is consistently outside of the 7.5-8.5 range of the other fractions and unfractionated Glucopon 225DK.

A 19 cm benchtop extinction test is also conducted on a burning heptane pool fire by foam formulations shown in column 3 of Table 17. These are based on the 502W polyoxyethylene-trisiloxane and Glucopon 225DK APG surfactants wherein the ANATRACE analytical APG compounds are substituted for the Glucopon 225DK surfactant. Fire extinction times are measured as a function of foam flow rate to correlate with the analytical APG compound chemical structure.

An initial experiment involved extinction testing the series of alkyl diglycoside analytical compounds to determine the effect of the carbon chain length in the alkyl group. The extinction profile plot is presented in the left side in Figure 107. While none of the substitutions out-performed the 502W-Glucopon 225DK formulation, it appears that there is an optimum in extinction effectiveness near the C8 alkyl chain length with a very large drop in effectiveness as the alkyl chain length increased to 10 and 12 carbon atoms.

We varied the position where the foam is delivered onto the pool surface from center to the edge of the pool to examine how it affected fire extinction time and its sensitivity to glycoside structure as shown in Figure 108. The foam, generated by air sparging, has to travel through a relatively long glass tube to a point above the center of the burning pool where it exits the tube, drops to the center of the burning pool surface and spreads to the edges. The glass tube is positioned over the burning pool and becomes quite hot especially at low foam flow rates where extinction times are long. As the foam travels through the hot tube, the foam can undergo thermal degradation before it exits the delivery tube. That can reduce the delivery rate and change properties of the foam that is actually delivered to the pool center be different from the foam that is generated. The adjustment in protocol involved positioning the end of the foam delivery tube just over the edge of the burning pool instead of the center of the pool. Very little heating of the foam delivery tube occurs at the edge position. But, after being deposited on the edge of the burning pool, the foam must spread to the opposite side of the pool before extinction can occur. This is referred to an “edge deposition,” and its results are presentedin Figure 108. The disparity be extinction time versus foam flow rate profiles becomes much smaller with the C10 and C12 members becoming much more effective. This may indicate that C10 and C12 members may actually be more effective in a MilSpec tests where the nozzle and foam do not get hot because the foam travels through the fire very quickly in time significantly less than the extinction time. This may also indicate that foams derived from these longer chain APG compounds have a greater susceptibility to thermal degradation. With respect to the C6 to C8 chain length data, the performance is much less effected by the center vs edge foam deposition. With respect to higher performance formulations such as 502W-Glucopon 225DK and the RefAFFF (Capstone 1157-Glucopon215UP), the difference in profiles derived from the center vs edge foam depositions is very small as shown in Figure 108.

A result of particular importance in Figure 109 is the very significant effect of alkyl tail length on fire extinction profile. At a fixed foam flow rate, the extinction time decreases as the tail length is increased from C6G2 to C9G2 and increases slightly with further increase in the tail length to C12G2. C9 tail length appears to have the optimum fire extinction profile among the different tail lengths examined. This appears to be consistent with Figure 103, which also shows slowest foam degradation for C9G2 among different tail lengths. But, Figure 99 shows no clear trend; both C8G2 and C12G2 have the slowest fuel transport rates among different tail lengths. Figure 109

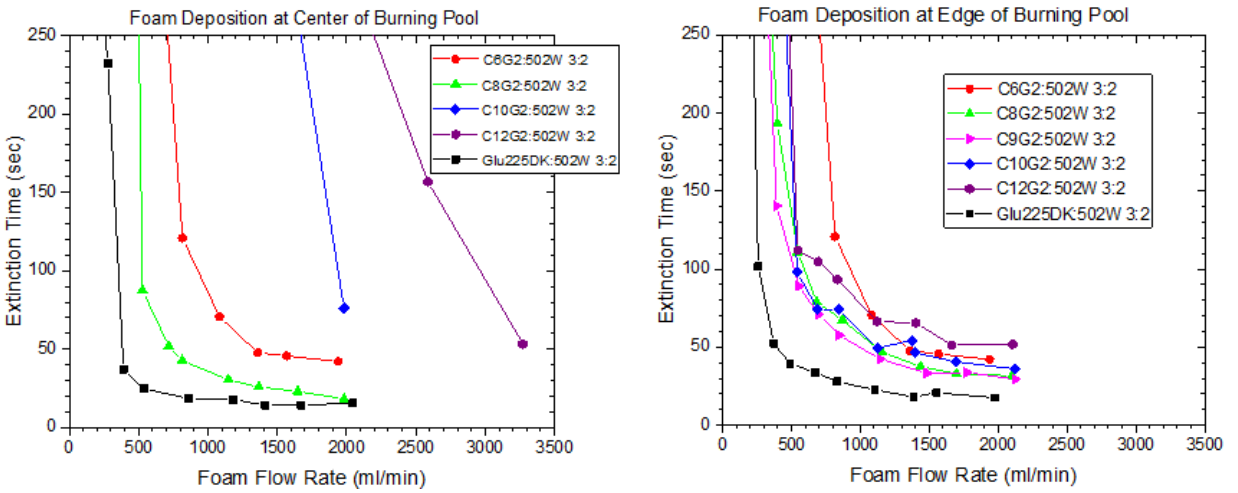

Figure 107. Fire extinction testing of foams from solutions where the CnG2 analytical APG compounds have been substituted for Glucopon 225DK as shown in column 3, Table 17.The effect of a foam deposited at center (left) and at the edge (right) of a burning heptane 19 cm pool.

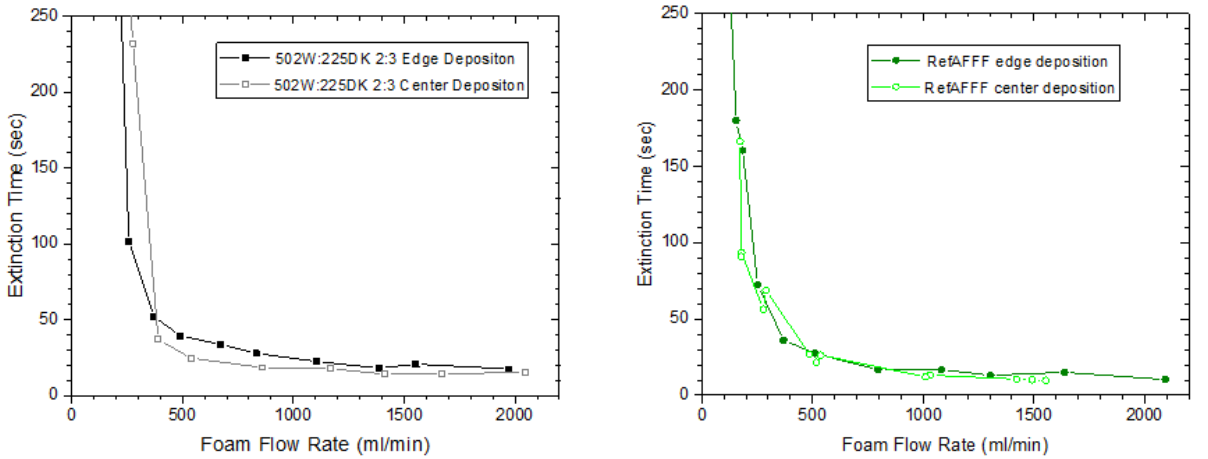

Figure 108. Fire extinction testing of 502W – Glucopon 225DK (left) and RefAFFF (right) foam formulations shown in columns 1 and 4 of Table 17 respectively. Center vs edge foam deposition effects on extinction time versus foam flow rate profiles.

shows that the effects of tail length on fire extinction time are less pronounced among the alkylmonoglycosides examined; C6G1, C7G1, and C8G1. No clear differences were seen in foam degradation and fuel transport rates with tail length for the monoglycosides in Figures 101 and 97 respectively. Figure 109 shows that increasing the tail length with the head size fixed did not improve the fire suppression performance over the 502W - Glucopon 225DK formulation.

In addition to the tail length, the polyglycoside has many structural features to vary. The simplest is the number linked glycoside rings forming the head. From Anatrace the analytical APG compounds are available as mono- and diglycosides as presented in Figure 90. Direct comparison between the pairs of C8G1 and C8G2 and of C6G1 and C6G2 are presented in Figure 110 and show that the diglycosides are more effective than the monoglycosides. However, the foam degradation and fuel transport rates shown in Figures 102 and 98 respectively do not show significant differences between the mono- and di- glycosides. Also, Figure 110 shows that neither

of the glycosides closes the fire extinction profile gap with the 502W-Glucopon 225DK formulation. Finally, within the diglycoside series C8 alkyl groups with a branched, cyclic and sulfur for oxygen linkage substitution were tested. Figure 111 shows the fire extinction times increase in the order n- < thio- < cyclic- < iso- at a fixed foam flow rate and is consistent with fuel transport rates shown in Figure 100. But, the degradation rates shown in Figure 104 are not significantly different among the tail variations.

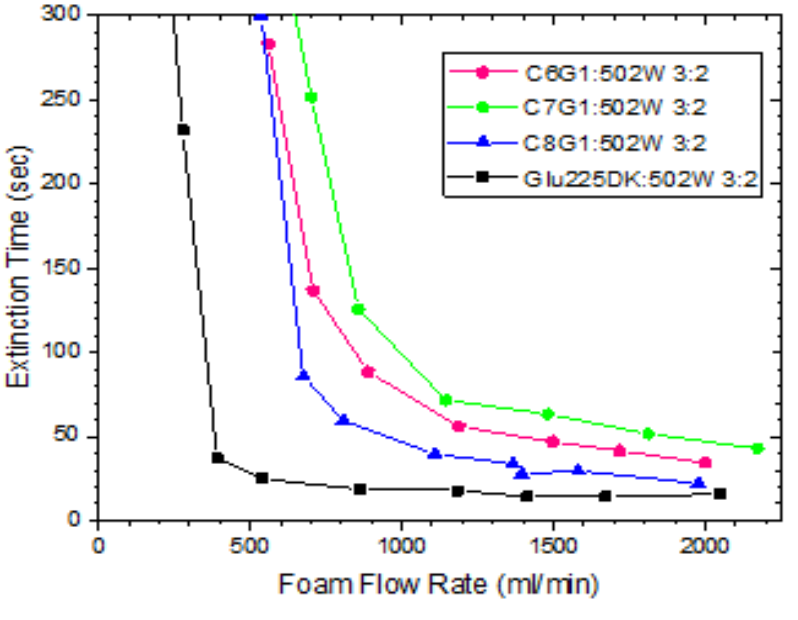

Figure 109. The effect of alkyl tail length of monoglycoside on fire extinction time versus foam application rate for formulations shown in column 3, Table 17. Foams were depoited at the pool edge.

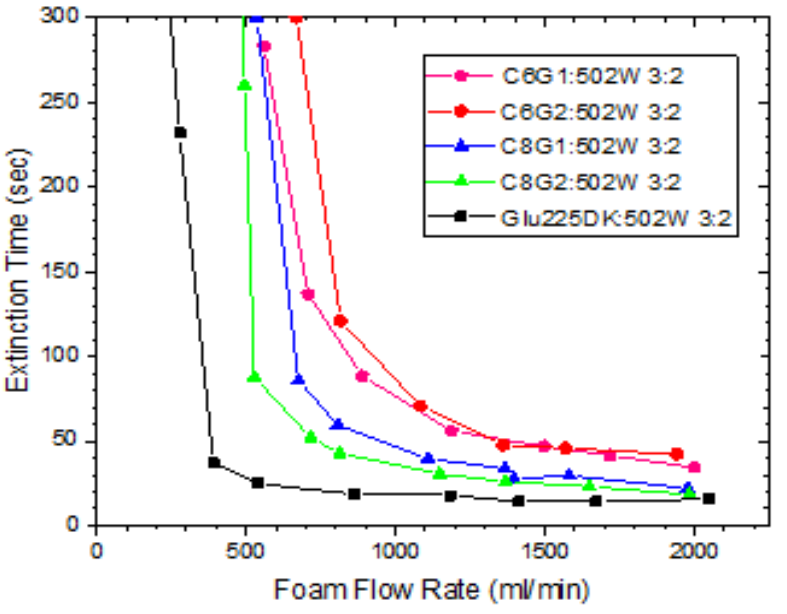

Figure 110. The effect of glycoside head size on fire extinction time versus foam application rate for formulations shown in column 3, Table 17 with edge deposition of the foam.

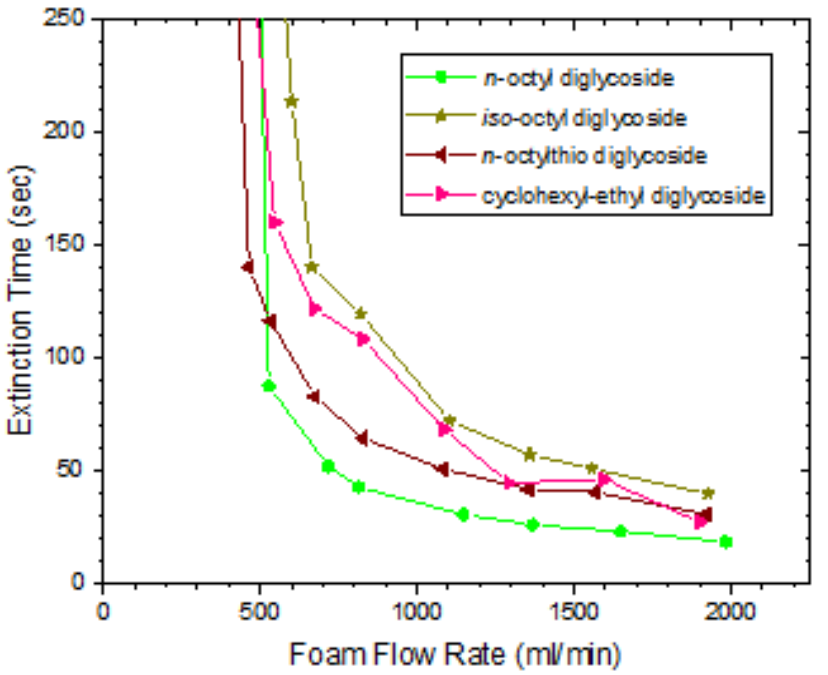

Figure 111. The effect of varying tail geometry of diglycoside compounds with linear, branched alkyl chain, cyclic, and sulfur atom substitution on fire extinction time versus foam application rate for formulations shown in column 3, Table 17 with edge deposition of the foam.

Figures 112 and 113 show quantitatively the effects of varying tail and head sizes of the alkylglycoside structure on extinction time using the monodisersed materials. They show that the extinction times for the monodispersed are higher than the polydispersed. The monodispersed octyltriglycoside was synthesized by Dr. Matthew Davis, NAWC, China Lake because it is not available commercially. With head size fixed, as the tail size increases, the extinction time goes through a minimum as shown in Figure 112. Similarly, the extinction time exhibits a minimum as the head size is varied, with the tail size fixed as shown in Figure 113. The tail and head size effects appear to be more pronounced at high and low foam flow rates respectively. For comparison the Glucopon225DK's extinction times at three foam application rates are represented as a rectangular box in Figures 112 and 112. Clearly, the Glucopon extinction times are significantly smaller than the monodispersed alkyl glycosides and some of the possible reasons are discussed below.

Amphiphilicity is necessary to make large foam volumes for a given amount of solution. For amphiphilicity, the hydrophobicity of tail should be in balance with the hydrophilicity of the head. As the tail size increases the balance shifts from head to tail and may be causing the minimum in extinction time. A similar phenomena could be happening when head size is increased with the tail size fixed. This suggests, both head and tail sizes should be changed simultaneously to maintain the amphiphilic balance rather than varying one at a time as was done in the current report.

A second reason for the difference between monodispersed glycosides and Glucopon225DK extinction times has to do with polydispersity of Glucopon225DK. Previously, we showed that there is synergisms between alkyl glycoside and trisiloxane polyoxyethylene (502W) surfactants that reduce the extinction time for the mixture relative to the individual components. There could

be a geometrical fit between these two surfactants because 502W is polydispersed molecules with fat tail and skinny heads of different sizes while Glucopon225DK has the opposite geometry (fat heads and skinny tails of different sizes). When a monodispersed alkylglycoside is mixed with the polydispersed 502W trisiloxane surfactant, a mismatch in geometry results and could lead to smaller degree of synergism compared to the mixtures with polydispersed Glucopon225DK. Further work should be performed to understand this by inducing polydispersity by mixing different monodispersed glycosides.

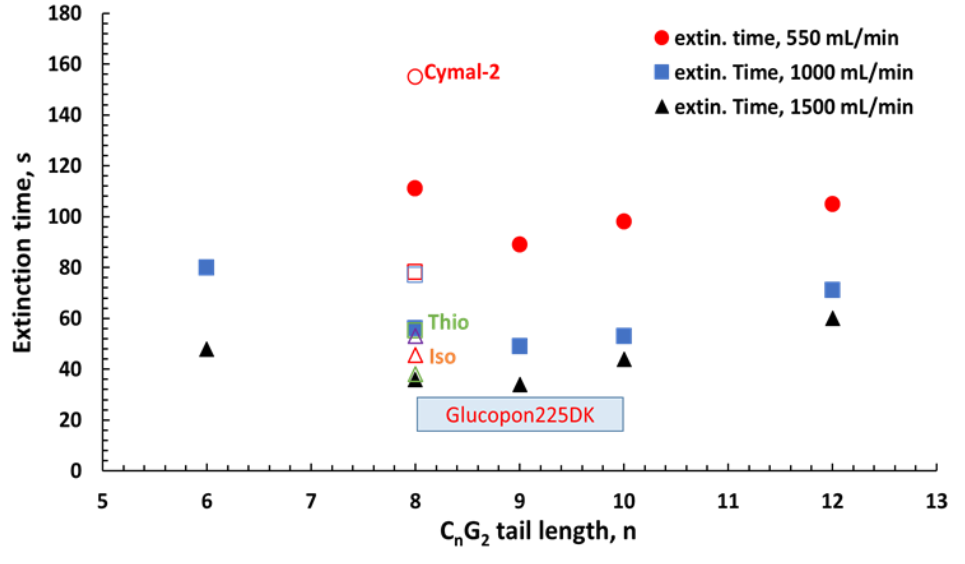

Figure 112. The effect of tail length of monodispersed alkylglycosides on heptane fire extinction time at different foam application rates relative to the polydispersed Glucopon225DK with edge deposition.

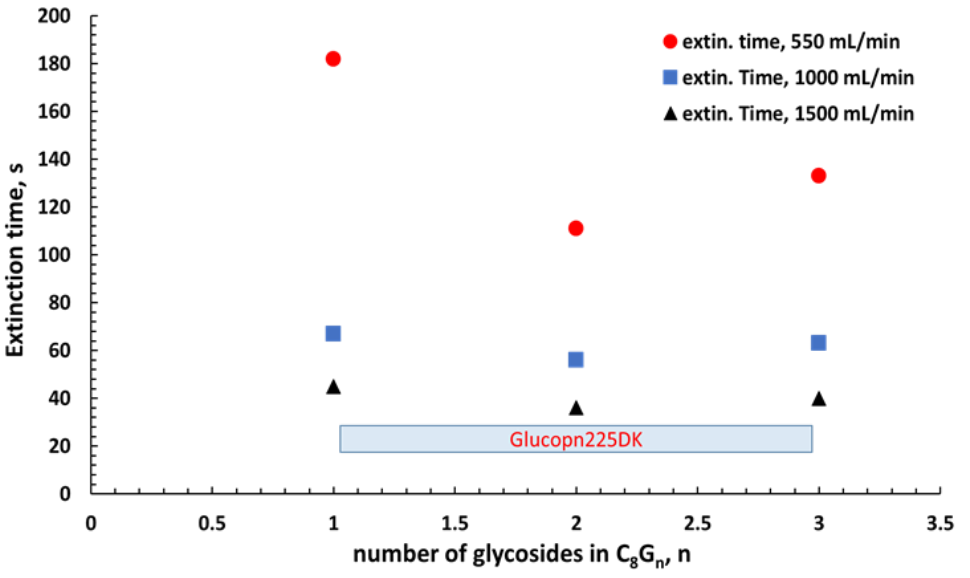

Figure 113. The effect of head size of monodispersed alkylglycosides on heptane fire extinction time at different foam application rates relative to the polydispersed Glucopon225DK with edge deposition.

During the fire extinction experiments discussed above, times for full coverage of the pool surface by foam were also recorded and are shown in Figure 114. They show a significant effect due to changes in alkylglycoside chemical structure. The polydispersed Glucopon225DK has the fastest spread relative to the monodispersed glycosides.

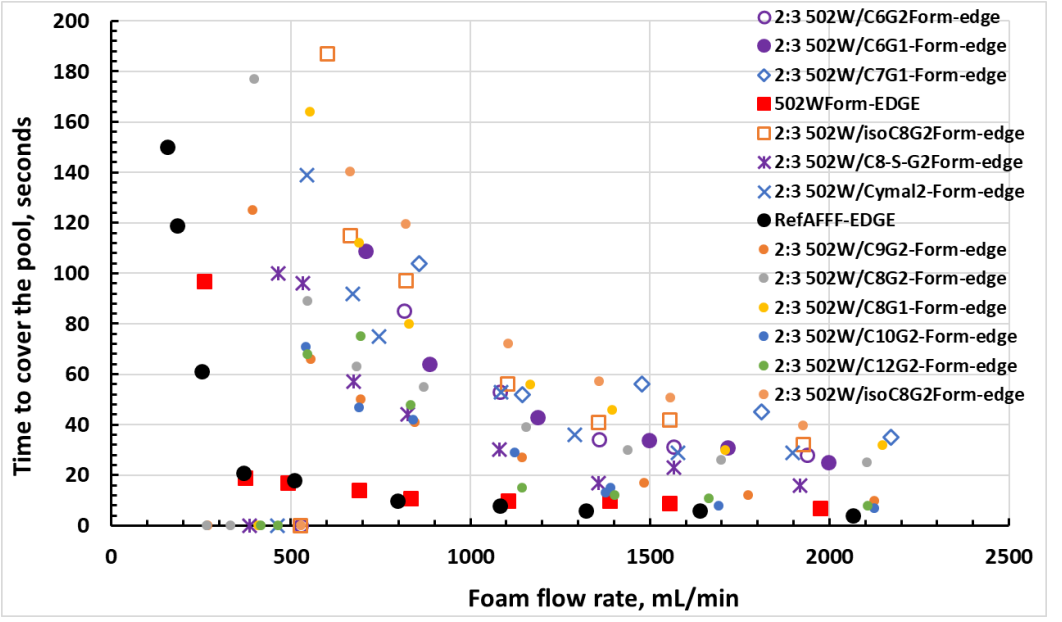

Figure 114. The effect glycoside head and tail variations on foam coverage time versus foam flow rate with edge deposition of the foam.

Figures 115 and 116 show that foam coverage times for the monodispersed alkylglycoside containing siloxane formulations are significantly longer compared to the polydispersed Glucopon225DK especially at low foam application rates.

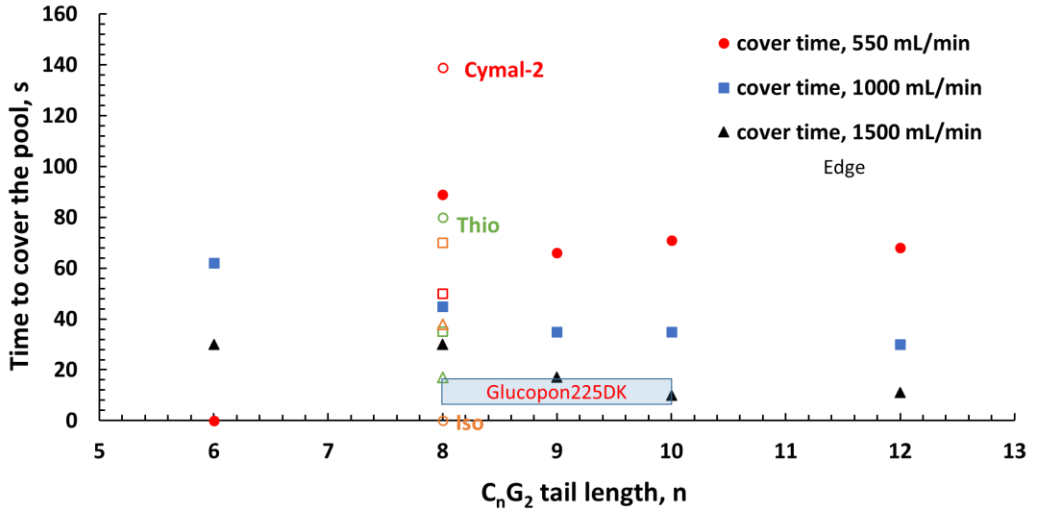

Figure 115. The effect alkylglycoside tail variations on foam coverage time versus foam flow rate relative to Glucopon225DK with edge deposition of the foam.

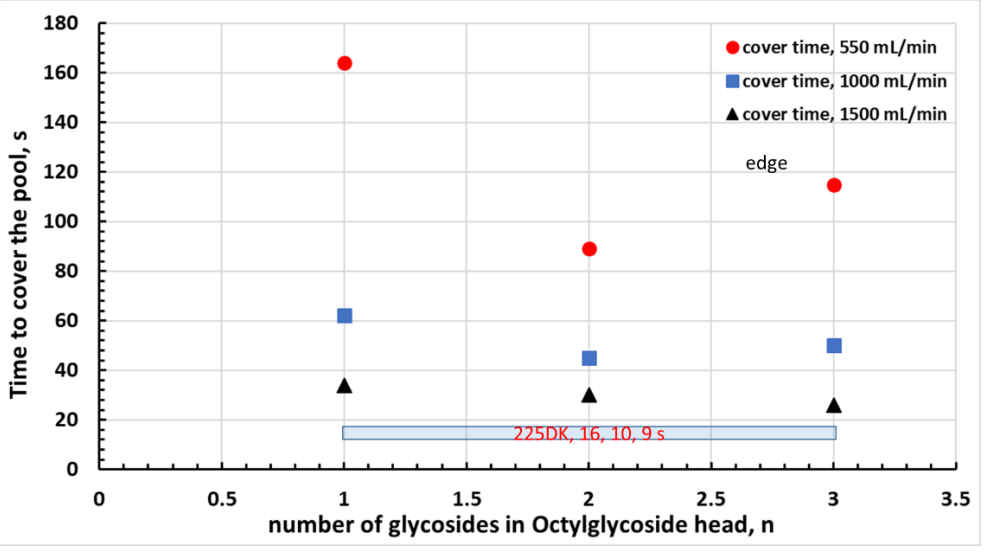

Figure 116. The effect alkylglycoside head size variations on foam coverage time versus foam flow rate relative to Glucopon225DK with edge deposition of the foam.

This could be due to differences in foam degradation rates and in foam expansion ratios which can affect rheological properties of spreading. Also, Figure 115 shows that there does not appear to be a minimum in coverage time as the tail size is increased, with head size fixed, unlike the minimum in fire extinction time shown in Figure 40. However, Figure 116 shows that there is a minimum with increased head size, with tail size fixed, similar to extinction time versus head size at low foam application rates shown in Figure 113. Figure 117 and 118 show the ratio of pool coverage time and fire extinction time. As one may expect, the ratio gets close to 1 at low foam application rates indicating the influence spreading on fire extinction. At high foam application rates, foam spreading plays less significant role.

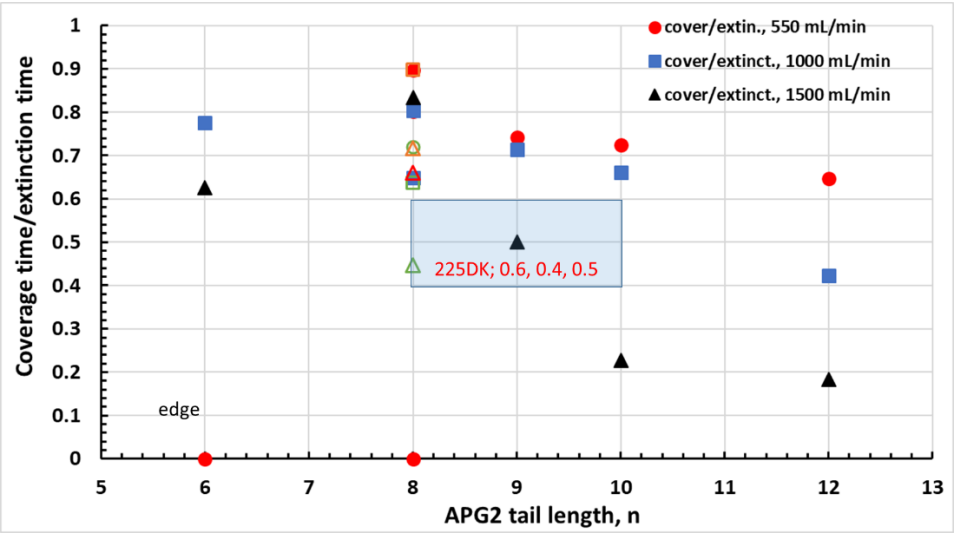

Figure 117. Coverage time as a fraction of extinction time and the effects alkylglycoside tail variations with edge foam deposition.

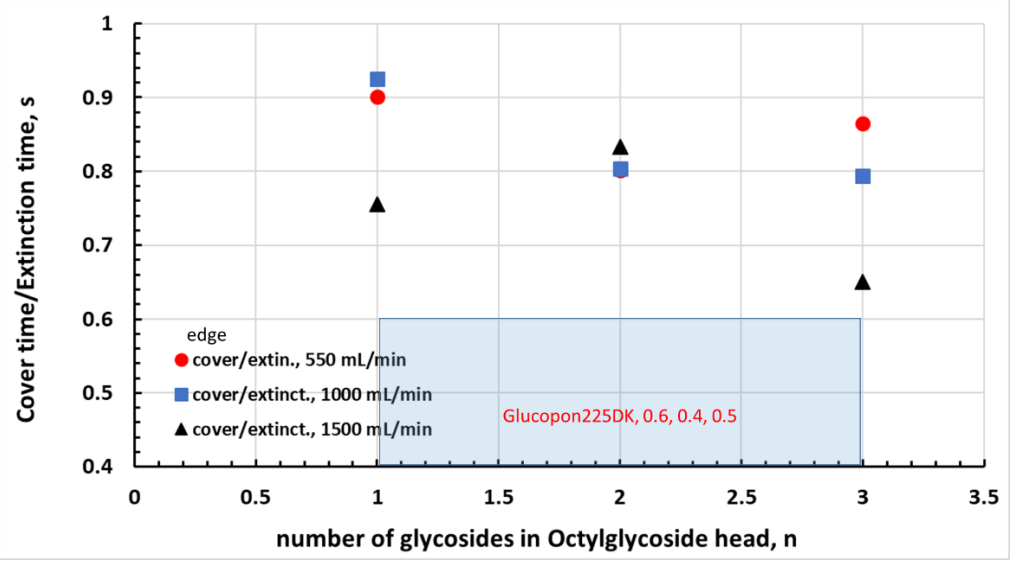

Figure 118. Coverage time as a fraction of extinction time and the effects alkylglycoside head size variation with edge foam deposition.

4.9. Siloxane Hydrolysis

Siloxanes are prone to undergo hydrolysis in dilute solutions. While that may be helpful in breaking it down in nature in aqueous environment, it can limit its shelf life, which is one of the MilSpec requirements.

4.9.1. Analytical Characterizations of Hydrolytic Susceptibility

A very important property and issue is the comparative hydrolytic susceptibility of the branched and linear trisiloxane functional groups of the surfactant tail. Hydrolyzed surfactants lose their ability to form foams and suppress fires. While the hydrolysis of the Si-O-Si bonds via combination with one water molecule to yield two Si-OH functionalities is very simple in concept, when it is incorporated into a surfactant system, it becomes somewhat complex for several reasons. This reaction is very pH sensitive being strongly catalyzed by acid and base. Micelle formation provides variable levels of hydrolysis protection depending on size, shape, surfactant diffusion rates and surfactant critical micelle concentration. The silicic acid decomposition products may condense into a complex mixture of other products. Silicone surfactant hydrolysis studies are mostly limited to correlations of solution surface tension changes with aging time of the solution and do not address the role the micelle plays. Finally, higher molecular weight surfactants (particularly those of commercial origin) involve dispersity in isomer and chain length structures and lower levels of purity. In this work, having synthesized, purified and characterized low molecular weight (oxyethylene chain length n = 2) representatives of the branched and linear trisiloxane and of the tetrasilane classes of silicon surfactant a technique more definitive hydrolysis observation than surface tension correlation is available. As a reaction diagnostic, methyl groups also bonded to the silicon nucleus can serve as a probe of cleavage of the Si-O-Si bond via their ^{1}H NMR chemical shifts of reagent and product.

To monitor the hydrolysis of the *B*-HMTS$(CH_2)_3(OE)_2$-OH, *L*-HMTS$(CH_2)_3(OE)_2$-OH surfactants by the Si-CH_3 proton resonances conditions (solvent, concentration, pH, temperature and observation time) need to be designated so that the result is physically meaningful and within

the operational capability of the NMR technique. To be physically meaningful from the perspective fluorine-free foam concentrate for use in fire suppression, a concentration corresponding to that used in a 1 to 6% proportioning rate is a range to target. This concentration is higher than the CMC of practically all surfactants designed for foams meaning that most of the surfactant will reside in micelles in a water medium. This concentration is well within the NMR sensitivity limits, but surfactants residing in micelles display resonances that are somewhat broadened and displaced in chemical shift compared with spectra of the unimolecular dissolved surfactant. Also, some surfactants lack this level of micelle solubility in water form opaque emulsions or two phase systems. This limited micelle solubility is observed with the short (n = 2) oxyethylene chain length surfactants in that these three surfactants form hazy to opaque mixtures in D_2O in the 1-6% concentration range. Recording spectra of such mixtures is complicated by broad overlapping peaks originating from suspended droplets and micelles superimposing on low intensity narrow peaks from dissolved surfactant. To obtain a comparative analysis for the *B*- and *L*-HMTS$(CH_2)_3(OE)_2$-OH surfactants, it was found that switching to an organic solvent into which a small quantity of water was added. Water saturated $CDCl_3$ was observed to provide ^1H NMR spectra of these molecularly dissolved surfactants identical to those in Figure 77 without the broad resonances attributed to micelle formation.

Concentrating on the $–SiCH_3$ region (0.2 to -0.1 ppm) of the spectrum, the spectra as a function of time were recorded as depicted in Figure 119. The initial spectra consist of three $-SiCH_3$ resonances for *L*-HMTS$(CH_2)_3(OE)_2$-OH and of two resonances $-SiCH_3$ for *B*-HMTS$(CH_2)_3(OE)_2$-OH with assignments indicated in Figure 77. After 9 hr, the first indication of hydrolysis for *L*-HMTS$(CH_2)_3(OE)_2$-OH is observed with the appearance and growth of a new resonance at 0.08 ppm and several more in the range 0.06 to 0.03 ppm between the second and third initial resonances at 0.07 and 0.01 ppm respectively. These new hydrolysis-associated resonances grow rapidly in intensity as the successive spectrum at 27.5 hr indicates. By comparison, the *B*-HMTS$(CH_2)_3(OE)_2$-OH 9 hr spectrum exhibits a very weak new resonance at 0.6 ppm which increases in intensity much more slowly. After 231 hr, the spectral change has subsided. To determine whether hydrolysis was complete as 100 µl volume of HCl vapor from head space of concentrated HCl container was transferred to and mixed in the NMR cell solution. This resulted in little change in the *L*-HMTS$(CH_2)_3(OE)_2$-OH spectrum but an appreciable change particularly after 12 hr in the *B*-HMTS$(CH_2)_3(OE)_2$-OH spectrum. This experiment demonstrates that the linear trisiloxane surfactant is significantly more susceptible to hydrolysis than the branched trisiloxane surfactant. This susceptibility appears to correlate with a protective steric hindrance of the branched isomer.

Conducting this NMR hydrolysis assessment in the aqueous phase is more complicated and is also illustrated in Figure 120 for the short and long chain (n = 2 and 12.3) oxyethylene-B-HMTSF surfactants. The n = 2 surfactants are less water-soluble, and the 1% solution preparation results in a fine hazy suspension rather than a clear solution. The initial spectrum reflects the micelle/microdroplet effect. For the *B*-HMTS$(CH_2)_3(OE)_2$-OH surfactant it consists of the two $–SiCH_3$ resonances being broadened and shifted up field to 0.28 and 0.20 ppm. Over the 400 hr period the *B*-HMTS$(CH_2)_3(OE)_2$-OH undergoes a gradual hydrolysis with it spectral features resembling those of the hydrolysis depicted in Figure 119.

The n = 12.3 long chain surfactants are water-soluble at 3% composition forming clear transparent solutions. The freshly prepared *B*-HMTS$(CH_2)_3(OE)_{12.3}$-OH solution yields a spectrum composed of two somewhat broadened signals corresponding to the two types of $-SiCH_3$

groups residing in a micelle. Over the 450 hr aging time these initial signals slowly diminish with the appearance of other resonances which correlate with a complex hydrolysis process.

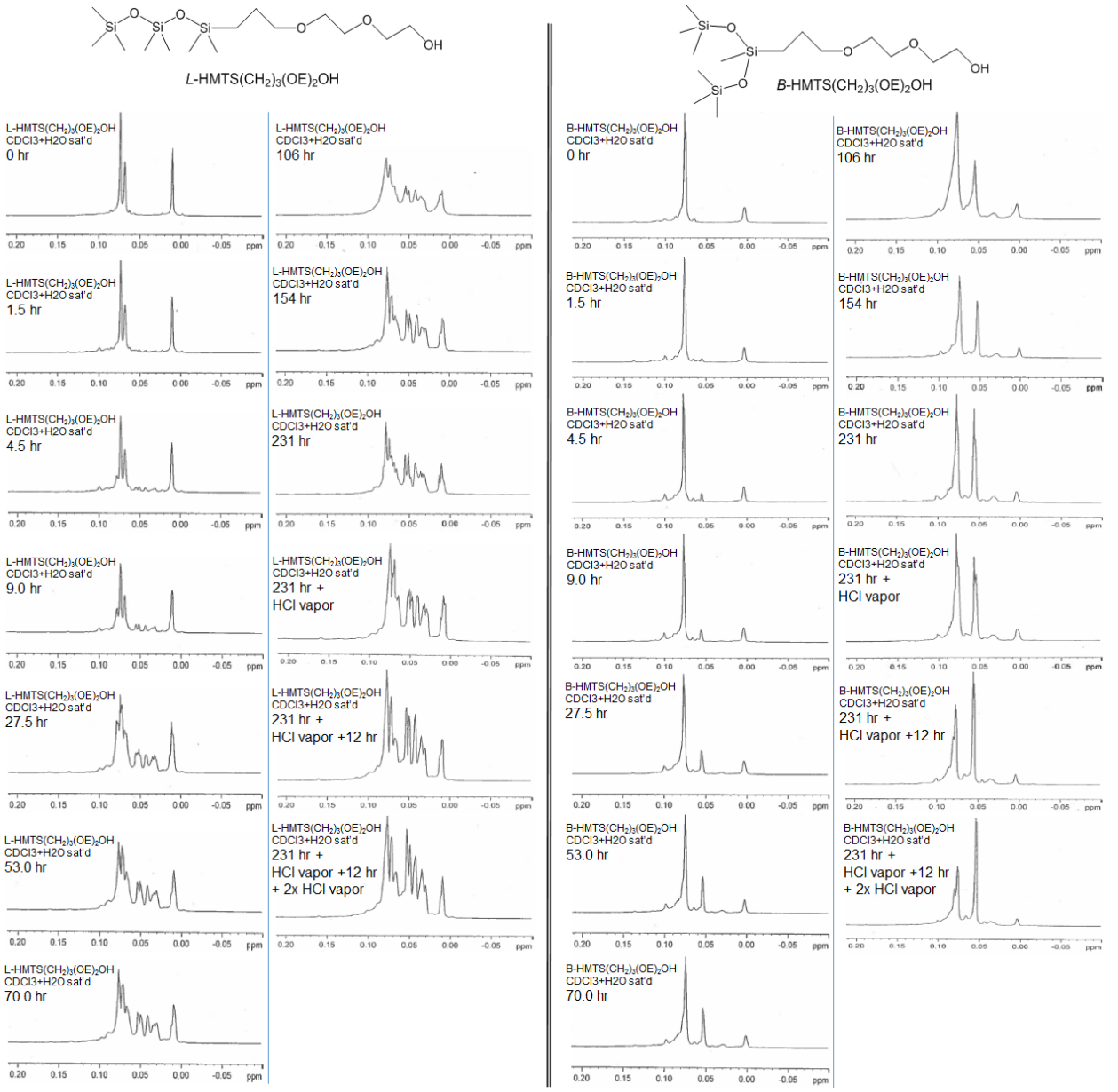

Figure 119. ^{1}H NMR spectra (–$SiCH_3$ region) of *L* and *B*-$HMTS(CH_2)_3(OE)_2$-OH, and polydispersed *B*-$HMTS(CH_2)_3(OE)_{12.3}$-OH dissolved in H_2O-saturated $CDCl_3$ as a function of time illustrating hydrolysis of the trisiloxane group.

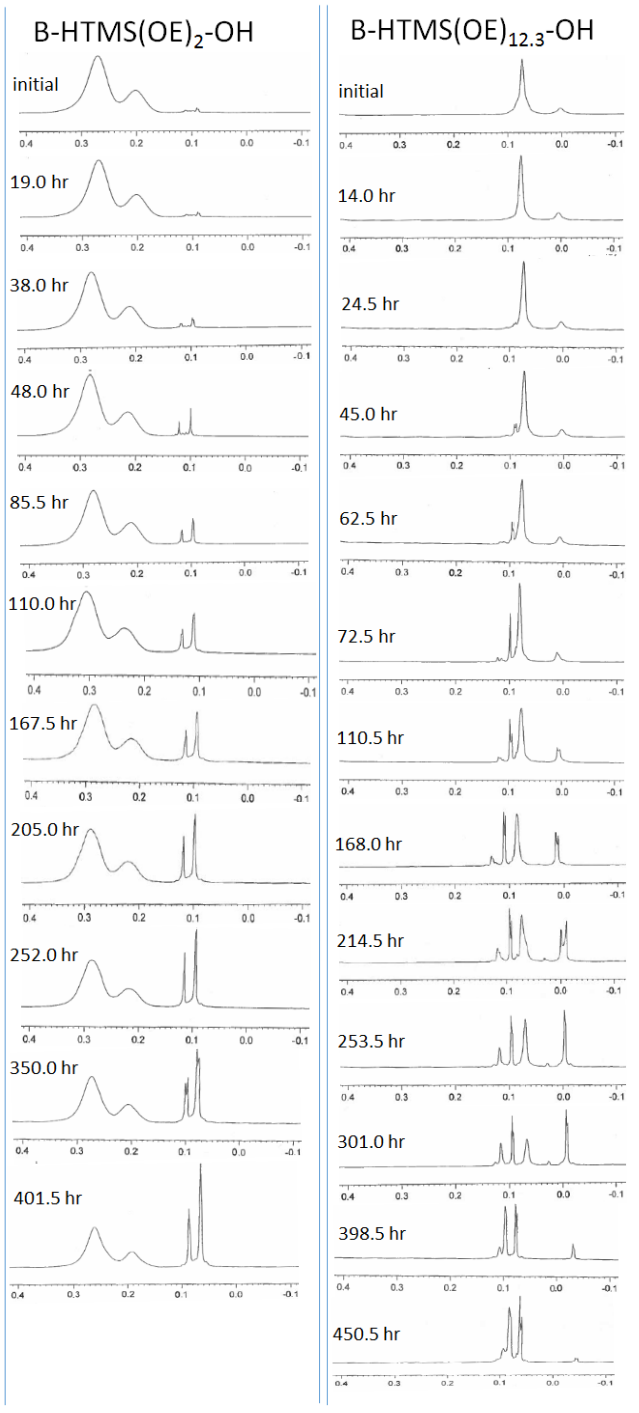

Figure 120. ^{1}H NMR spectra (–$SiCH_3$ region) of *B*-HMTS$(CH_2)_3(OE)_n$-OH, n = 2, 12.3, dissolved in D_2O as a function of time illustrating hydrolysis of the trisiloxane group and micelle effect.

4.9.2. Accelerated Age Testing

We conducted accelerated aged test listed in MIL-F-24385F by subjecting 3% concentrate of the surfactant formulations (column 1, Table 10). The accelerated aging was performed on the concentrates rather than the premix solutions. The surface and interfacial tensions were measured on the premix solutions prepared by diluting the aged and fresh concentrates at 3% proportioning with distilled water and are listed in Table 20.

Table 20. Surface and Interfacial Tensions of 502W-Gluc225 and RefAFFF formulations listed in column 1, Table 10 after subjecting the 3% concentrates to accelerated aging test by holding the concentrate at 60 ºC for 10 days in an oven as listed in MIL-F-24385F

Foam Solution	Surface Tension (mN/m)	Interfacial Tension with Heptane (mN/m)
Ref AFFF	15.2	1.00
Ref AFFF Aged	15.4	1.60
NRL's silxoane502W-Gluc225 formulation	22.4	2.29
NRL's Siloxane502W-Gluc225 Form Aged	25.1	3.80

Table 20 shows that the 502W-Gluc225 formulation's surface tension increased only slightly by 2.7 mN/m before and after the concentrate was subjected to the accelerated aging. As expected, the surface tension of the RefAFFF containing the fluorocarbon surfactant was unchanged by the accelerated aging test.

Foams were generated using aqueous solutions of surfactant formulations listed in Table 20 using sparging method. The expansion ratio (volume of foam/volume of liquid) was calculated by measuring the weight and volume of the foam. Table 21 shows that the expansion ratio decreased slightly after subjecting the 3% concentrates for the 502W-Gluc225 and RefAFFF formulations.

Table 21. Expansion Ratio Results

Foam Solution	Expansion Ratio
Ref AFFF Unaged	9.4
Ref AFFF Aged	9.30
502W Form Unaged	8.2
502W Form Aged	7.60

Figure 121 shows that the liquid drainage with time are comparable among different formulations after the concentrates were subjected to the accelerated aging test.

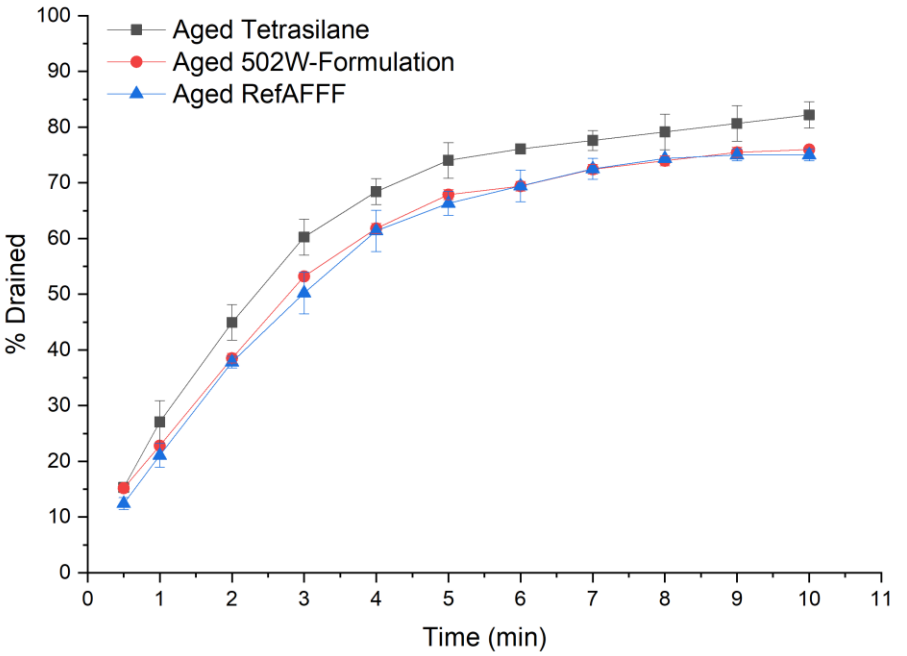

Figure 121. Liquid drainage from foams generated from premix solutions of different formulations after the concentrates were subjected to aging.

Figure 122 shows that the life time (time for 100% degradation of foam) foam generated from 502W-Gluc225 formulation reduced by a factor of 2 when subjected to the accelerated aging test, Similarly, the fuel transport rates of foams generated from 502W-Gluc225 and RefAFFF are unaffected by the accelerated aging as shown in Figure 123. The fuel transport rate is suppressed for a shorter time after the accelerated aging for foams generated from 502W-Gluc225 formulation consistent with shorter foam life time seen in Figure 122.

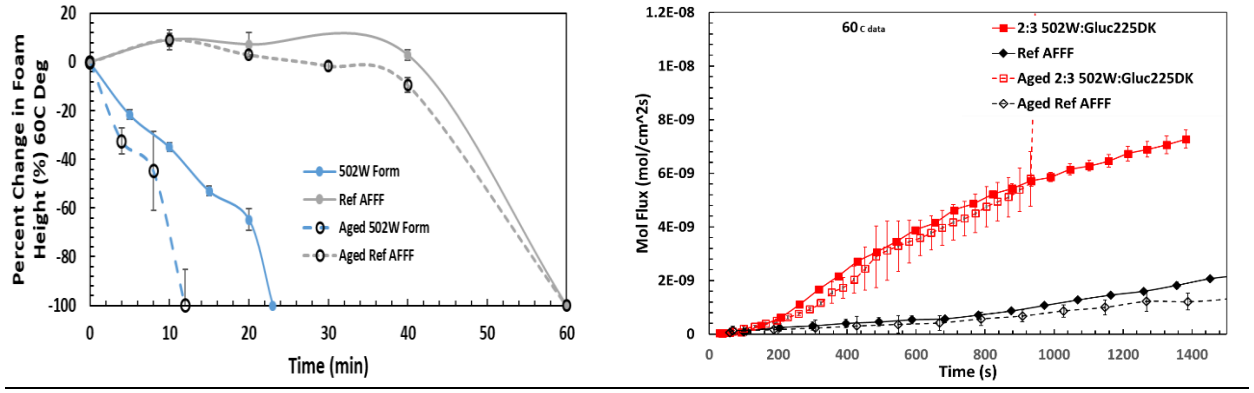

(a) (b)

Figure 122. The effect of accelerated aging on foams generated from 502W-Gluc225 and RefAFFF formulations shown in column 1, Table 10, on (a) foam degradation, (b) heptane fuel transport through a 4-cm thick (initial thickness) foam layer covering a hot (60 ^{o}C) heptane pool.

Figure 123 shows bench scale 19-cm heptane fire extinction times for the 502W-Gluc225 (shown in column 1, Table 10) and RefAFFF formulations before after subjecting the 3%

concentrates to accelerated aging by holding the concentrates at 60 ᵍC for 10 days and performing fire extinction with foams generated from the premix solutions. It shows that the extinction times are not changed significantly after accelerated aging.

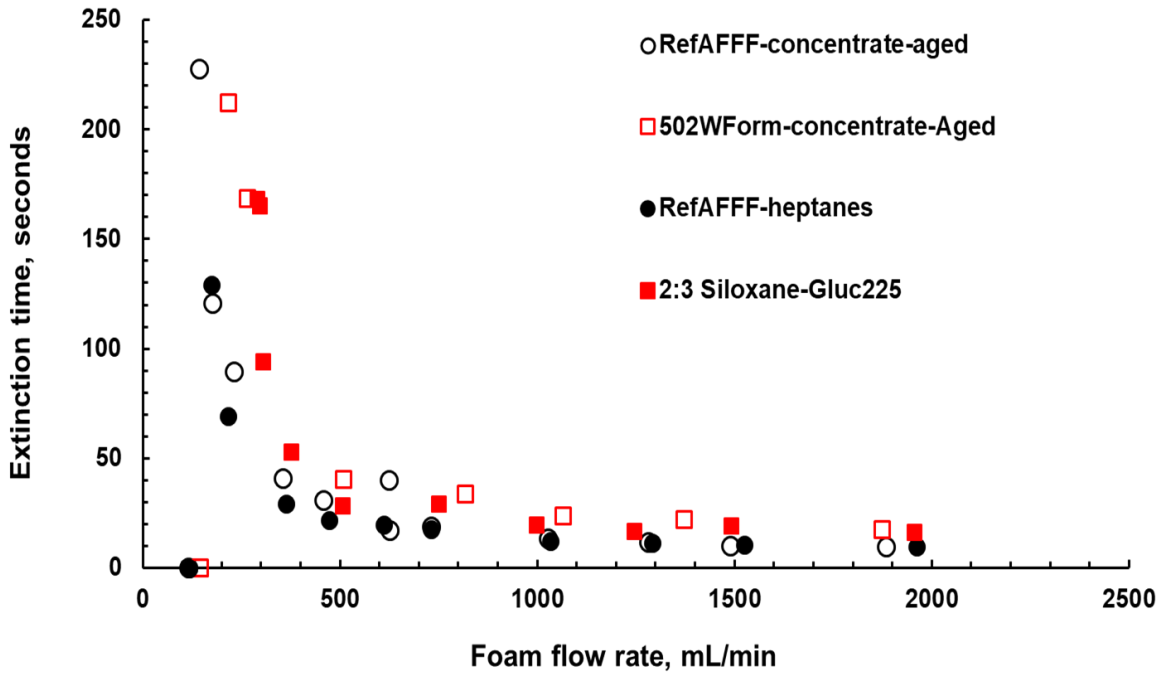

Figure 123. 19-cm heptane pol fire extinction before and after subjecting the 3% concentrates to accelerated aging. Data points along the x-axis represent no extinction in 5 min of foam application.

4.10. Dow Silicones Co. Collaboration to Develop Novel Siloxane Formulations

Dow Silicones Co. makes Dowsil 502W Additive surfactant as an intermediate used in a process to make poluurethane foams. Dow Chemical Co. makes alkylpolyglycosides (e.g., Triton CG425). Both the surfactants are key players in NRL's siloxane formulation that showed potential for making firefighting foams to replace AFFF [67]. So, Dow is a natural choice for a collaboration on research and development of novel siloxane surfactants for firefighting purpose. Dow has synthesized more than 50 different formulations and used NRL published screening methods to downselect several samples for foam and fire suppression evaluations, which are performed at NRL. To date we found, foam stability on warm gasoline and 19-cm gasoline fire extinction improved significantly in the bench scale evaluations.

5. CONCLUSIONS

The chemistry of surfactants and oleophobicity play a very important role in controlling pool fires. A reference AFFF formulation containing a fluorocarbon surfactant, a hydrocarbon surfactant (alkylpolyglycoside, APG), and a solvent was shown to extinguish heptane and gasoline pool fires as quickly as a commercial AFFF at bench (19-cm diameter pool) and large (28 ft^2 pool) scales. The RefAFFF and the bench scale measurements enabled direct comparison of solution and foam properties and fire suppression performance of a fluorine-free substitute component in

the three component formulation at different foam application rates. By substituting different fluorine-free surfactants for the fluorocarbon and different hydrocarbon surfactants for APG in the RefAFFF, we found that varying the composition significantly affected the fire suppression. By ranking the heptane-fire suppression performance of numerous commercial siloxane and hydrocarbon surfactants relative to RefAFFF, a trisiloxane-polyoxyethylene (Dowsil 502W) was selected for further development.

To understand how a surfactant affects fire extinction, we examined the surfactant's effect on three different contributing mechanisms; (1) aqueous film formation by measuring the spreading coefficients, (2) fuel-foam layer interactions by measuring foam layer degradation by fuel, fuel transport rate through a foam layer, and foam spread rate, and (3) foam structure by measuring bubble diameters, bubble coarsening, and liquid drainage from the foam. The three mechanisms were quantified independently in the absence of a fire. Trends in fire extinction among the surfactant formulations followed the trends in foam degradation, fuel transport, and foam spread rates, but not the trends in aqueous film formation and foam's structural properties.

Synergism between surfactants at a bubble surface can affect fire suppression significantly. The bench scale measurements revealed that synergism between the siloxane and APG surfactants reduced foam degradation and fuel transport which caused the observed higher fire suppression performance. We hypothesized that the skinny oxyethylene head and large trisiloxane tail fits geometrically with the large head size and skinny alkyl tail of the APG to form a bi-layer at the bubble surface preventing fuel vapor permeation through the foam. This is based on our molecular dynamics (MD) simulations, which revealed that the packing density at heptane-water interface is increased when APG is added to a trisiloxane surfactant. Further work is needed to confirm the hypothesis of geometrical fit and understand the mechanisms of synergism so that it could be increased by manipulating the surfactant structures and pairing different surfactants.

In addition to the synergism, surfactant's amphiphilicity and polydispersity can affect fire suppression significantly. We synthesized trisiloxane polyoxyethylene surfactants with different distributions of oxyethylene head sizes with the average values ranging from 0 to 50. We quantified the effects of varying the oxyethylene head size of the trisiloxane surfactant on the degree of synergism, solution and foam-structure properties, foam degradation rate, fuel transport rate, foam spread rate, and heptane-fire suppression. Both the fuel transport rate and fire extinction time exhibited minima possibly due to competition between the increased synergism and decreased amphiphilicity as the head size is increased. Similarly for the co-surfactant, APG, we varied the average head size of the polydispersed surfactant (Glucopon) from 1.5 glycoside units to 1.7 glycoside units and found a significant decrease in foam degradation and heptane-fire extinction time. To obtain even larger improvement, we varied the glycoside head size with the tail size fixed, and varied the alkyl tail size with the head size fixed using monodispersed APGs. We found slight minima in fire extinction time as the head or tail size is varied. Even though a slight minima was found in foam degradation rate with tail size variation, no clear trends were found in fuel transport either with the head size or tail size variations. In addition to the amphiphilicity effects, the lack of polydispersity of APG could have decreased the degree of synergism between the trisiloxane and APG molecules because a single size, monodispersed, APGs might not match geometrically with a distribution of head sizes in the polydispersed trisiloxane-polyoxyethylene surfactant (Dowsil502W). A fundamental understanding of how molecular structures of surfactants and their distributions affect synergism, foam degradation, foam spread, and fuel transport mechanisms, and fire suppression is needed.

By varying the fuel composition, we found that the siloxane surfactant formulation and other commercially available fluorine-free foams had much higher fire extinction times for gasoline compared to heptane due to the aromatic components in gasoline. Indeed, the degree of gasoline fire suppression was reproduced by using a mixture of trimethylbenzene and heptane as the surrogate fuel. This discovery from the bench scale measurements lead to further analytical measurements of surfactant-fuel interactions to establish the cause. The analytical measurements showed that the aromatics extracted the trisiloxane surfactant from the aqueous solution that could have caused larger foam degradation by gasoline and higher fire extinction time for the gasoline fires. In contrast, the fire suppression performance and foam degradation of AFFF were found to be less sensitive to fuels (aliphatic, aromatic, branched) possibly because the perfluorocarbon tail of fluorosurfactants is oleophobic as well as hydrophobic. A fundamental understanding of a surfactant's oleophobicity, amphiphilicity, and how molecular structure affects surfactant-fuel interaction mechanisms is needed.

The bench scale tests reported in this work enabled variation of each parameter (e.g., foam application rate, foam expansion ratio and bubble size, surfactant composition, fuel composition, preburn time) individually in well-controlled conditions. Detailed bench scale measurements were essential to establish and understand cause-and-effects needed for designing new surfactant formulations unlike the large scale tests, where the ability to control parameters and make detailed measurements was limited. Furthermore, the ranking of surfactants' performance by the bench scale measurements (fire extinction, fuel transport, and foam degradation) were confirmed qualitatively by 28 ft^2 large scale fire extinction and burnback tests, relative to AFFF's fire performance. But, the fire extinction time for a given formulation was longer at the large scale than at the bench scale for the same solution flow rate per unit pool area, likely due to differences in the foam generation methods used. Therefore, the bench scale tests are good screening tools but not replacements for the large scale tests, similar to the fact that a 28 ft^2 extinction test is not expected to be a replacement for a field scale test (1200 ft^2 pool or a flight deck extinction test) when developing new formulations.

While foam degradation, fuel transport, and foam spread were found to explain trends in fire extinction for the siloxane and APG surfactants examined in this report, the controlling mechanism may differ significantly for other types of surfactants and foams. For instance, foam spread may have a larger effect on fire suppression for formulations containing thickening agents (Xanthan gums) used to control liquid drainage. Similarly, fuel surface or bulk cooling may play a larger role for wetting agents. Quantitative relationships among different mechanisms and fire suppression need to be established by developing theoretical models so that fire suppression performance can be predicted from the bench scale measurements made in the absence of a fire.

Finally, the current modeling tools are not well-suited for designing surfactants because they cannot predict fire suppression from surfactant structures. Surfactant synthesis/experimentation are too slow to explore a large and diverse number of surfactant. Future works should develop new modeling approaches to design surfactants and use synthesis/experimentation more efficiently to explore a range of surfactant structures.

6. ACKNOWLEDGEMENTS

We would like to thank the US Office of Naval Research for funding this work through the Naval Research Laboratory 6.2 Base Program. We would like to thank the DOD for providing High Performance Computational resources. We like to thank Dr. Matthew Davis, NAWC, China Lake, CA for providing us Glucopon fractions. We also like to than Mr. Clarence L. Whitehurst and Stanley Karwoski Jr for helping to conduct the large scale tests. We also would like to thank Dr. Robin Nissan of the Strategic Environmental Research and Development Program (SERDP), U.S. Department of Defense (DOD) for supporting this work via projects WP2739, WP18-1592, and WP20-1507.

7. REFERENCES

[1] R.L. Tuve. and E.J. Jablonski, “Compositions and Methods for Fire Extinguishment and Prevention of Flammable Vapor Release”, U.S. Patent 3258423, June 28, 1966

[2] H.W. Carhart, J.T. Leonard, R.L. Darwin, R.E. Burns, J.T. Hughes, E.J. Jablonski, “Aircraft Carrier Flight Deck Firefighting Tactics and Equipment Evaluation Tests”, NRL Memorandum Rpt., 5952, February, 1987

[3] E. Houtz, C.P. Higgins, J.A. Field, D.L. Sedlak, "Persistence of Perfluoroalkyl Acid Precursors in AFFF-Impacted Groundwater and Soil, *Environmental Science & Technology*, 47(15) (2013).

[4] "Military Specification: Fire Extinguishment Agent. Aqueous Film-Forming Foam (AFFF) Liquid Concentrate, For Fresh and Sea Water" MIL-F-24385F, Naval Sea System Command, 1992.

[5] R.L. Tuve, H.B. Peterson, E.J. Jablonski, and R.R. Neill, “A New Vapor-Securing Agent for Flammable-Liquid Fire Extinguishment”, Naval Research Laboratory Report 6057, DTIC Document No. ADA07449038, .Washington DC, March 13, 1964

[6] E.C. Norman and A.C. Regina, "Alcohol Resistant Aqueous Film Forming Firefighting Foam", U.S. Patent 5,207,932, May 4, 1993

[7] R.A. Falk, “Aqueous Wetting and Film Forming Compositions”, U.S. Patent 4,042,522, August 16, 1977

[8]E.K. Kleiner. and R.A. Falk, “Aqueous Based Fire Fighting Foam Compositions Containing Hydrocarbyl Sulfide Terminated Oligomer Stabilizers”, U.S. Patent 4,439,329, March 27, 1984

[9] J.T. Martin, “Fire-Fighting Foam Technology,” in *Foam Engineering: Fundamentals and Applications*; P. Stevenson, Ed.; Ch.17, pp. 411-457; Wiley-Blackwell, West Sussex, UK; 2012

[10] A.D. Harkins and A. Feldman, "Films, the spreading of liquids and the spreading coefficient", J Am. Chem. 44, 2665 (1922).

[11] J.T. Leonard and J.C. Burnett, "Suppression of evaporation of hydrocarbon liquids and fuels by films containing aqueous film forming foam (AFFF) concentrate FC-196", U.S. Naval Research Laboratory Memo Report 7842, Washington, DC, December 31, 1974.

[12] M. Pabon M and J.M. Copart, "Fluorinated Surfactants: Synthesis, Properties, Effluent Treatment". J. Fluorine Chem. 114, 149-156 (2002)

[13] K.P. Clark and E.K. Kleiner, “Synergistic surfactant compositions and firefighting concentrates thereof”, U.S. Patent 5,616,273 April 1, 1997.

[14] K. Shinoda and T. Nomura, "Miscibility of Fluorocarbon and hydrocarbon surfactants in micelles and liquid mixtures; Basic studies of oil repellant and fire extinguishing agents", *Journal of Phys. Chem.*, 84, 365-369 (1978).
[15] E. Kissa, "Fluorinated surfactants and repellants", Surfactant Science Series, 97, New York, Marcel Dekker Inc, 2001.
[16] B.A. Williams, "Properties and performance of model AFFF formulations", Workshop on Firefighting Foams in the Military, U.S. Naval Research Laboratory, December 16-17, 2004.
[17] R. Hetzer, F. Kümmerlen, K. Wirz, D. Blunk, 'Fire Testing a New Fluorine-free AFFF Based on a Novel Class of Environmentally Sound High Performance Siloxane Surfactants', *Fire Safety Science*, 11, p.1261-1270. 2014
[18] X. Jia, Y. Luo, R. Huang, H. Bo, Q. Liu, X. Xhu., "Spreading kinetics of fluorocarbon surfactants on several liquid fuels surfaces", *Colloids and Surfaces A*, 589, (2020) 124441; https://doi.org/10.1016/j.colsurfa.2020.124441.
[19] T. Briggs and B. Abdo, "Emphasis on spreading qualities of AFFF could mislead fire-fighters", *FIRE*, p. 37 (1988).
[20] M.K. Bernett, L.A. Halper, N.L. Jarvis, T.M. Thomas, "Effect of Adsorbed Monomolecular Films on the Evaporation of Volatile Organic Liquids", *I&EC Fundamentals*, 9, 150-156 (1970).
[21] H.E. Moran, J.C. Burnett, J.T. Leonard, "Suppression of Fuel Evaporation by Aqueous Films of Fluorochemical Surfactant Solutions", Naval Research Laboratory Memo Report 7247, Washington DC, April 1, 1971.
[22] J.T. Leonard and J.C. Burnett, "Suppression of Hydrocarbon Liquids and Fuels by Films Containing Aqueous Film Forming Foam (AFFF) Concentrate FC-196", Naval Research Laboratory Memo Report 7842, Washington DC, December 31, 1974.
[23]H.L. Hardy, C.J. Purnell, "Use of Foam for Emergency Suppression of Vapor Emissions from Organic Isocyanate Liquid Surfaces", *Am. Oxxup. Hyg.*, 21, 95-98 (1978).
[24] J.A. Pignato, Jr., "Evaluation Test for Foam Agent Effectiveness" *Fire Eng.*, 46-48 (1984).
[25] C.P. Hanauska, "The Suppression of Vapors from Flammable Liquids with Stabilized Foams", Masters Thesis, Worcester Polytechnic Institute, 1988.
[26] M.L. Carruette, H. Persson, M. Pabon, "New Additive for Low Viscosity of AFFF/AR Concentrates – Study of the Potential Fire Performance", *Fire Tech.*, 40:367-384 (2001).
[27] T.H. Schaefer, B.-Z. Dlugogorski, E.M. Kennedy, "Vapour Suppression of n-Heptane with Fire Fighting Foams using Laboratory Flux Chamber", 7th Asia-Oceania Symposium on Fire Science and Technology, 2007.
[28] T.H. Schaefer, B.-Z. Dlugogorski, E.M. Kennedy, "Sealability properties of fluorine-free firefighting foams (FfreeF)", *Fire Technology*, 44, 297-309 (2008).
[29] K.M. Hinnant, S.L. Giles, Ananth, R., "Measuring Fuel Transport Through Fluorinated and Fluorine-free Firefighting Foams", *Fire Safety Journal*, 91, 653-661 (2017).
[30] K.M. Hinnant, M.W. Conroy, R. Ananth, "Influence of Fuel on Foam Degradation for Fluorinated and Fluorine-free Foams", *Colloids and Surfaces A*, 522, 1-17 (2017).
[31] K. Osei-Bonsu, N. Shokri, P. Grassia, Foam stability in the presence and absence of hydrocarbons: From bubble- to bulk-scale, *Colloids and Surfaces A*, 481, 514-526 (2015).
[32] K. Osei-Bonsu, P. Grassia, and N. Shokri, "Fundamental investigation of foam flow in porous media in the presence of oil", *J. Colloid and Interface Science*, 462, 288-296 (2016).
[33] M.W. Conroy, J.W. Fleming, R. Ananth, "Surface cooling of a pool fire by aqueous foams", *Combustion Science and Technology*, 189, 806-840 (2017).

[34] R. Ananth, S. Mott, M. Waheed, M. Epstein, J.M. Smith, "Bench-scale apparatus for studying pool fire extinguishment by class B fires", Paper 085FR-0045, Eastern States Section of the Combustion Institute Fall Technical Meeting, Clemson, SC, 2013
[35] X. Zhuang, K.M. Hinnant, R. Ananth, "Structures of fluorocarbon, hydrocarbon, and siloxane monolayers at air-water and heptane-water interfaces by molecular dynamics simulations", U.S. Naval Research Laboratory Memorandum Report, NRL/MR/6180-20-10,061, 26 May, 2020
[36] J.B. Klauda, R.M. Venable, J.A. Freites, J.W. O'Connor, C. Mondragon-Ramirez, I. Vorobyov, D.J. Tobias, A.D. MacKerell, R.W. Pastor, "Update of the CHARMM all-atom additive force field for lipids: Validation on six lipid types.", *Journal of Physical Chemistry B*, 114, 7830-7843 (2010).
[37] W.a.S.N.S.a.M.B.D. Shi, "Molecular simulations of CO2, H2, H2O, and H2S gas absorption into hydrophobic poly(dimethylsiloxane) (PDMS) solvent: solubility and surface tension", *Journal of Physical Chemistry C*, 119, 19253-19265 (2015).
[38] S.R. Durell, B.R. Brooks, A. Bennaim, "Solvent-induced forces between two hydrophilic group"s, *J. Phys. Chem.*, 98, 2198-2202 (1994).
[39] W.L. Jorgensen, J. Chandrasekhar, J.D. Madura, R.W. Impey, M.L. Klein, "Comparison of simple potential functions for simulating liquid water", *J. Chem. Phys.*, 79, 926-935) (1983.
[40] T.E. Oliphant, "Python for scientific computing", *Computing in Science & Engineering*, 9, 10-20 (2007).
[41] W. Humphrey, A. Dalke, K. Schulten, "VMD: Visual molecular dynamics", *Journal of Molecular Graphics*, 14, 33-38 (1996).
[42] T. Williams, C. Kelley, Others, "Gnuplot 4.2 an interactive plotting program", http://www.gnuplot.info/docs_4.2/gnuplot.html, (2009).
[43] X Zhuang, R. Ananth, "Surfactant monolayers at heptane-water interfaces," U.S. Naval Research Laboratory Memorandum Report, NRL/MR/6180-20-10,062, 26 May, 2020
[44] K.M. Hinnant, S.L. Giles, A.W. Snow, J.P. Farley, J.W. Fleming, R. Ananth, "An analytically defined fire-suppressing foam formulation for evaluation of fluorosurfactant replacement", *Surfactant and Detergents*, 21, 711-722, (2018)
[45] Company brochure “High Performance Substrate Wetting Agents: Dow Corning Brand Superwetter Family” by Dow Corning Inc. Catalog# 67674-67-3
[46] Company brochure, “Alkyl Polyglucosides” by Care chemicals, COGNIS, April 2005
[47] www.buckeyefire.com
[48] Fomtec Inc., https://www.fomtec.com
[49] S.L. Giles, A.W. Snow, K.M. Hinnant, R. Ananth, “Modulation of fluorocarbon surfactant diffusion with diethylene glycol butyl ether for improved foam characteristics and fire suppression”, *Colloids and Surfaces A*, 579, 123660 (2019).
[50] R. Ananth, A.W. Snow, K.M. Hinnant, S.L. Giles, J.P. Farley, “Synergisms between siloxane-polyoxyethylene and alkyl polyglycoside surfactants in foam stability and pool fire extinction”, *Colloids and Surfaces A*, 579, 123686 (2019).
[51] K.M. Hinnant, S.L. Giles, E.P. Smith, A.W. Snow, R. Ananth, *Fire Technology*, 56, 1413-1441 (2020)
[52] S.S. Jang, W.A. Goddard, "Structures and properties of newton black films characterized using molecular dynamics simulations", *Journal of Physical Chemistry B*, 110, 7992-8001 (2006).

[53] C.D. Vecitis, H. Park, J. Cheng, B.T. Mader, M.R. Hoffmann, "Enhancement of perfluorooctanoate and perfluorooctanesulfonate activity at acoustic cavitation bubble interfaces", *Journal of Physical Chemistry C*, 112, 16850-16857 (208).
[54] J.R. Lu, E.A. Simister, E.M. Lee, R.K. Thomas, A.R. Rennie, J. "Penfold, Direct determination by neutron reflection of the penetration of water into surfactant layers at the air/water interface", *Langmuir*, 8 1837-1844 (1992).
[55] A.S. Aronson, V. Bergeron, M.E. Fagan, C.J. Radke, "The influence of disjoining pressure on foam stability and flow in porous-media", *Colloids and Surfaces A*, 83, 109-120 (1994).
[56] V. Bergeron, "Disjoining pressures and film stability of alkyltrimethylammonium bromide foam films", *Langmuir*, 13, 3474-3482 (1997).
[57] E. Gorodinsky, S. Efrima, "Surface-tension studies of perfluorooctanoate anion in one-component, 2-component, and 3-component systems", *Langmuir*, 10, 2151-2158 (1994).
[58] M.J. Rosen, Y.F. Wu, "Superspreading of trisiloxane surfactant mixtures on hydrophobic surfaces. 1. Interfacial adsorption of aqueous trisiloxane surfactant-N-alkyl pyrrolidinone mixtures on polyethylene", *Langmuir*, 17, 7296-7305 (2001).
[59] O. Sonneville-Aubrun, V. Bergeron, T. Gulik-Krzywicki, B. Jonsson, H. Wennerstrom, P. Lindner, B. Cabane, "Surfactant films in biliquid foams", *Langmuir*, 16, 1566-1579 (2000).
[60] O. Belorgey, J.J. Benattar, "Structural-properties of soap black films investigated by x-ray reflectivity", *Physical Review Letters*, 66, 313-316 (1991).
[61] X. Zhuang, E.M. Dávila-Contreras, A.H. Beaven, W. Im, J.B. Klauda, "An extensive simulation study of lipid bilayer properties with different head groups, acyl chain lengths, and chain saturations, BBA", *Biomembranes*, 1858, 12 (2016).
[62] A.I. Rusanov, V.V. Krotov, "Manifestation of Gibbs elasticity in thin films", *Colloid Journal*, 66, 204-207 (2004).
[63] S. Achilefu, C. Selve, M.J. Stebe, J.C. Ravey, J.J. Delpuech, "Monodisperse perfluoroalkyl oxyethylene nonionic surfactants with methoxy capping - synthesis and phase-behavior of water surfactant binary-systems", *Langmuir*, 10, 2131-2138 (1994).
[64] L. Hsiao, H.N. Dunning, P.B. Lorenz, "Critical micelle concentrations of polyoxyethylated non-ionic detergents", *Journal of Physical Chemistry*, 60, 657-660 (1956).
[65] A.W. Snow, S.L. Giles, K.M. Hinnant, J.P. Farley, R. Ananth "Fuel for firefighting foam evaluations: Gasoline versus heptane", U.S. Naval Research Laboratory Memorandum Reprot, NRL/MR/6123-19-9895, June 15, 2019
[66] ANATRACE Co., Maumee, OH 43537, www.anatrace.com
[67] R. Ananth, A.W. Snow, K.M. Hinnant, S.L. Giles, "Siloxane and glucoside surfactant formulation for firefighting foam applications", US Patent Application, US20190321670A1, October 24, 2019..

APPENDIX A

Foam degradation and fuel transport rate with time were measured for numerous commercial siloxanes and hydrocarbon surfactants as discussed in Figures 35 to 38 in section 4.3.3. Figures shown below include more data and additional surfactants.

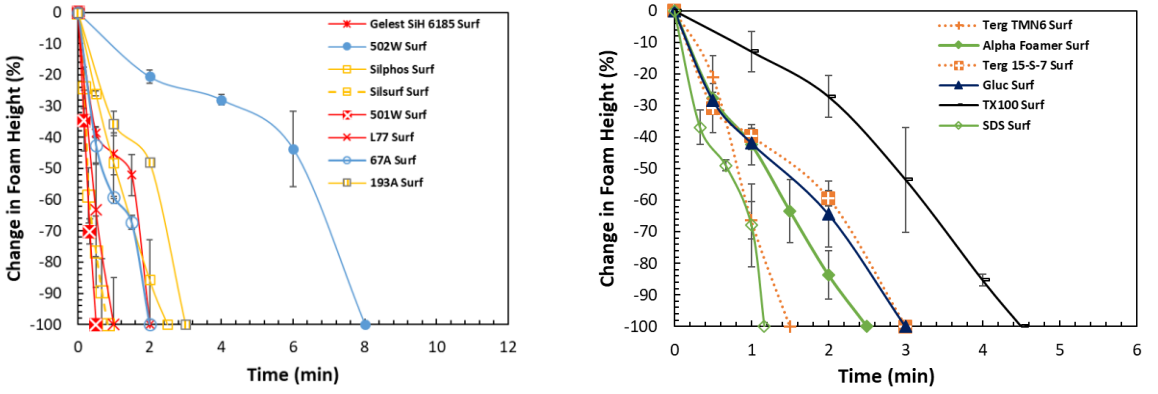

(a) (b)

Figure A1. Percent change in foam height for foams generated using (a) individual siloxane surfactants and (b) individual hydrocarbon surfactants.

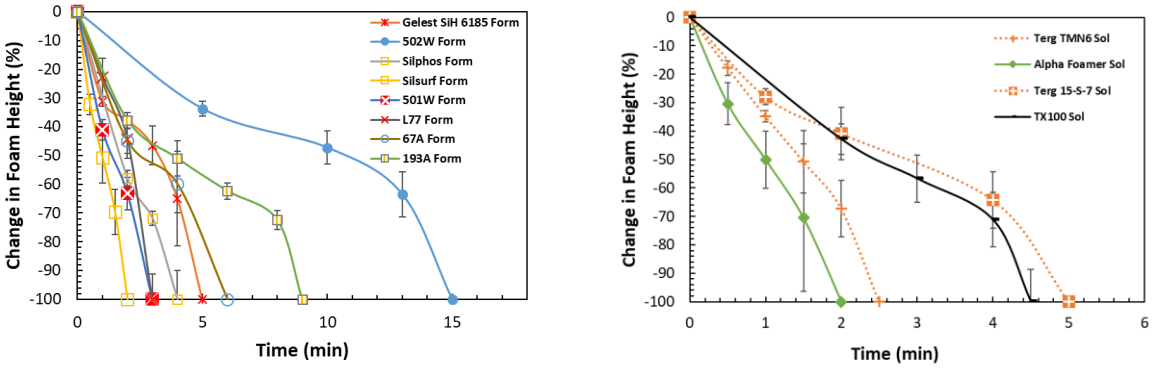

(a) (b)

Figure A2. Percent change in foam height for foams generated using (a) siloxane surfactants in a formulation with Gluc215, and (b) hydrocarbon surfactants in a formulation with Gluc215. SDS formulation not plotted. Alphafoamer was prepared as a 6:2 ratio with Gluc215 unlike the others which are at a 3:2 ratio.

Gluc215 has a lifetime of 3 minutes and many of the siloxanes have lifetimes below that as well in Figure A1. However, the formulations show longer lifetimes than the individual components in Figure A2 due to synergism between siloxane surfactants and Gluc215. The highest degree of synergism is seen with the 502W:G215 mixture.

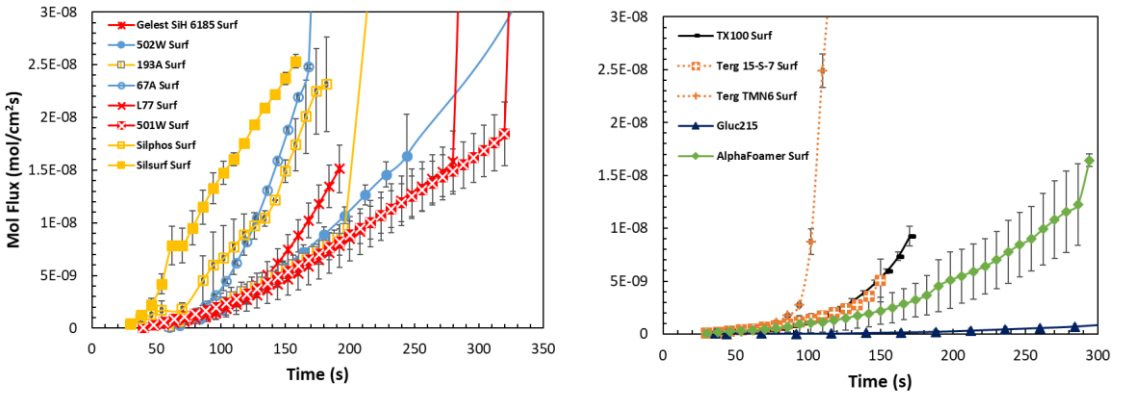

(a) (b)

Figure A3. Fuel vapor flux with time for foams generated with different surfactants (a) individual siloxane surfactants and (b) individual hydrocarbon surfactants. SDS surfactant is not plotted.

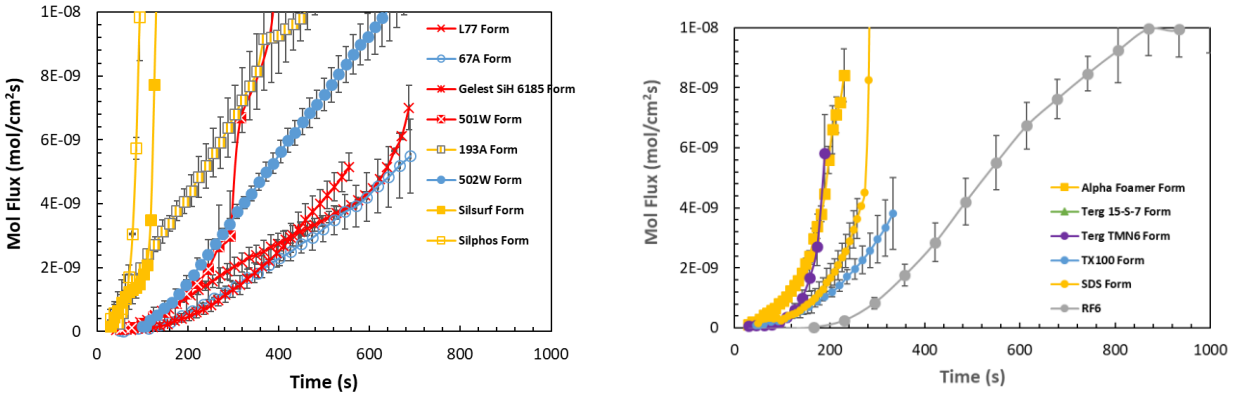

(a) (b)

Figure A4. Fuel vapor flux with time for foams generated with different surfactant formulations (a) siloxane surfactant formulations with Gluc215 and (b) hydrocarbon surfactant formulations with Gluc215. Alphafoamer formulation is in a 6:2 ratio with Gluc215 while all others are in a 3:2 ratio.

Figures A3 shows that Glucopon 215 CS UP of BASF has the smallest fuel transport rate among the commercial foams and 502W did not. The hydrocarbon surfactants alone appear to have slower fuel transport than the siloxane surfactants. However, when put in a mixture with Gluc215, the siloxane formulations have slower transport than the hydrocarbon formulations. Figure A4 shows that the 502W formulation and RF6 have the smallest transport rates. While synergism was seen in foam lifetime, none of the formulations have comparable or reduced fuel transport rates compared to the Gluc215 surfactant individually. This is surprising as the Capstone surfactant showed synergistic fuel transport with Gluc215. However, the data is promising as the 502W formulation has a long foam lifetime compared to other siloxane surfactants and a fuel transport rate comparable to RF6, a commercially available product.